Photoprotection from Ultraviolet and Visible Radiation Induced Damage to the Skin

Lawrence, Karl Perry

Awarding institution:
King's College London

Photoprotection from Ultraviolet and Visible Radiation Induced Damage to the Skin

Thesis submitted to the Faculty of Life Sciences and Medicine of the University of London for the degree of Doctor of Philosophy

By
Karl P. Lawrence

Photobiology Group
St John's Institute of Dermatology
Division of Genetics and Molecular Medicine
Faculty of Life Sciences and Medicine
King's College London
University of London

November 2017

Total word count (excluding references): 57,035

Abstract

Solar radiation has numerous effects on the skin. Some are beneficial, however the majority are negative and contribute to development of skin cancer. Most studies have focused on ultra violet radiation (UVR ~290-400nm), however there is growing evidence to suggest that visible light (400- 700nm) also causes skin damage. The main way of preventing solar damage is with the use of sunscreens, however these absorb in the UVR region with poor protection in the UVA/visible boundary waveband. There is growing evidence to suggest that synthetic UVR filters damage fragile marine environments, causing bleaching of corals and hormonal changes in fish. There is also evidence that some filters may damage human health, acting as exogenous oestrogens and inducing oxidative stress.

The aim of this thesis was to assess biomarkers of skin damage with a range of *in vitro* and *in vivo* endpoints: DNA photodamage, inflammation/ immunoregulation, photoageing, oxidative stress and pigmentation. The focus was on broadband solar simulated UVR and its boundary with visible radiation (385-405nm). It was determined whether current sunscreen formulations provided adequate protection in this region, and if the addition of a new synthetic filter, could improve photoprotection. Furthermore, the ability of naturally occurring marine UVR filters, mycosporine-like amino acids (MAAs) was assessed, with a view to the development of a new generation of biocompatible alternatives to eco-toxic synthetic UVR filters.

The results demonstrate that there is substantial damage in the UVR/visible boundary region for all biomarkers tested, and sunscreens using currently available filters do not provide sufficient protection; however the addition of the new filter significantly improved the protection offered. The MAA provided significant protection against all endpoints induced by solar simulated UVR. Furthermore, it demonstrated anti-oxidant capacity when added post UVR exposure. These results demonstrate that further investigation into the effects of visible radiation on the skin is required and the importance of improving sunscreens from an efficacy and environmental standpoint.

Contribution

I hereby declare the work presented in this thesis was performed exclusively by me, with the following exceptions. Formulation and absorbance spectroscopy of sunscreens was carried out by BASF GmbH, Grenzach-Wyhlen, Germany. The HPLC analysis of DNA photoproducts was carried out Dr. Thierry Douki, CEA-Grenoble, Grenoble, France.

Table of Contents

Abstract **2**
Contribution **4**
Figures **8**
Tables **12**
Abbreviations **15**
Acknowledgements **18**

Chapter 1: Introduction **19**
1.1 Ultraviolet and Visible Radiation **20**
1.1.1 Solar Radiation 20
1.1.2 UVR 21
1.1.3 Measurement of Solar Radiation 22
1.1.4 Variability of Solar Exposure 24
1.2 Molecular Effects of UV and Visible Radiation on the Skin **27**
1.2.1 Skin Structure 27
1.2.2 Chromophores 28
1.2.3 Oxidative Stress 30
1.2.4 DNA Damage 33
1.3 Clinical Effects of UVR **39**
1.3.1 Skin Type Classification 39
1.3.2 Erythema 40
1.3.3 Pigmentation 41
1.3.4 Immunoregulation 43
1.3.5 Photoageing 44
1.3.6 Skin Cancer 46
1.3.7 Photodermatoses 49
1.3.8 Benefits of UVR 50
1.4 Clinical Effects of Visible Radiation **53**
1.4.1 Benefits of Visible Light 53
1.4.2 Negative Health Effects of Visible Light 55
1.5 Endogenous Photoprotection **63**
1.5.1 Pigmentation 63
1.5.2 Stratum Corneum Thickening 64
1.5.3 DNA Damage Repair 64
1.5.4 Antioxidants 67
1.6 Exogenous Photoprotection **68**
1.6.1 Sunscreens 68
1.6.2 Visible Light Filters 79
1.6.3 Antioxidants 80
1.6.4 Topical DNA Repair Enzymes 84
1.6.5 Iron Chelators 86
1.7 Issues with Sunscreen Use **88**
1.7.1 Behavioural Issues 88
1.7.2 Health Issues 90
1.7.3 Environmental Damage 93
1.8 Mycosporine-like Amino Acids **98**
1.8.1 Background 98
1.8.2 MAA Structure and Biosynthesis 99
1.8.3 Structural Evidence for Photoprotection 104
1.8.4 Circumstantial Evidence for Photoprotection 105
1.8.5 Biological Evidence for Photoprotection 107

1.8.6 Additional Protective Roles of MAA in Nature....108
1.8.7 Photoprotection of the Skin....110
1.8.8 Potential Human Use of MAAs....119
1.9 Aims of Thesis....121

Chapter 2: Materials and Methods....123
2.1 UVR & Light Sources....124
2.2 Dosimetry....126
2.3 Absorbance Spectroscopy....127
2.4 Photoprotective Compounds....128
2.4.1 Palythine....128
2.4.2 BASF Compounds....129
2.5 Photostability....132
***2.6 In Vitro* Protection Factor Tests....133**
2.7 Cell Culture....135
2.8 *In Vitro* Irradiation Procedures....136
2.8.1 Palythine Studies....136
2.8.2 Filters in Formulation....137
***2.9 In Vitro* Assays....138**
2.9.1 Cell Viability....138
2.9.2 Neutral Red Assay....138
2.9.3 Alamar Blue Assay....139
2.9.4 Single Cell Gel Electrophoresis Assay (Comet assay)....140
2.9.5 Immunohistochemistry – CPD Imunnofluorscence *In Vitro*....142
2.9.6 Reactive Oxygen Species Assays....143
2.9.7 Gene Expression....145
***2.10 In Vivo* Studies....151**
2.10.1 Ethical Approval & Volunteer Recruitment....151
2.10.2 Methodology....151
2.10.3 385nm/405nm *in vivo* studies....151
2.10.4 Pigmentation Assessment....156
2.10.5 Biopsy Procedure....157
2.10.6 Tissue Processing....158
2.10.7 HPLC DNA Damage Assessment....158
2.10.8 Gene Expression....160
2.11 Statistical Analysis....161

Chapter 3: Molecular Photoprotection by the Naturally Occurring Mycosporine-Like Amino Acid (MAA) Palythine in a Human *In Vitro* Skin Model....162
3.1 Results....163
3.1.1 Photostability of Palythine....163
3.1.2 Photoprotection Against Cell Viability Reduction by Palythine....165
3.1.3 Photoprotection against DNA Damage by Palythine....167
3.1.4 Photoprotection Against Induction of Reactive Oxygen Species by Palythine....172
3.1.5 Anti-Oxidant and Radical Quenching Effects of Palythine....175
3.1.6 Photoprotection Against Gene Expression Changes by Palythine....177
3.1.7 Molar Extinction Coefficient, SPF, UVA-PF and Critical Wavelength Test of Palythine....180
3.2 Discussion....183
3.3 Summary of Chapter....195

Chapter 4: The Cellular and Molecular Effects of the UV/visible Border Region (385-405nm) on Human Skin *in vitro* and *in vivo*.....197
4.1 Results.....198
4.1.1 Cell Viability Reduction *In Vitro*.....198
4.1.2 Reactive Oxygen Species Induction *In Vitro*.....200
4.1.3 DNA Damage.....202
4.1.4 Gene Expression.....206
4.1.5 Pigmentation and Erythema Induction *In Vivo*.....216
4.1.6 Spectral Dependence of Endpoints.....230
4.2 Discussion.....234
4.3 Summary of Chapter.....245
Chapter 5: The Photoprotection of UV/visible Border Radiation Induced Damage of the Skin *In Vitro* and *in Vivo*.....246
5.1 Results.....247
5.1.1. Comparison of Spectra and Photostability of Sunscreen Formulations.247
5.1.2 Photoprotection Against Cell Viability Reduction *In Vitro*.....249
5.1.3 Photoprotection Against Induction Reactive Oxygen Species *In Vitro*.....251
5.1.4 Photoprotection Against delayed CPD induction *In Vivo*.....253
5.1.5 Photoprotection Against Gene Expression Changes.....255
5.1.6 Photoprotection Against Pigmentation Changes *In Vivo*.....265
5.1.7 Transmitted Spectra and Photostability.....274
5.2 Discussion.....277
5.3 Summary of Chapter.....287
Overall Conclusions.....288
Future Perspectives.....290
Development of Chapter 3: MAA Photoprotection.....290
Development of Chapter 4: UVR/visible border region induced damage...291
Development of Chapter 5: Photoprotection of UVR/visible border region induced damage.....292
References.....293
Appendix.....321

Figures

Figure 1.1: The spectral breakdown of solar radiation..... 20

Figure 1.2: The spectral differences at the Earth's surface compared to the top of the atmosphere..... 24

Figure 1.3: The structure of human skin and the *ex vivo* transmission of UV radiation..... 27

Figure 1.4: Routes of excitation and dissipation of photochemical excitation of electrons..... 30

Figure 1.5: The mechanisms for the generation of oxidative stress by UVR radiation..... 33

Figure 1.6: The CPD action spectra in different layers of the skin..... 34

Figure 1.7: The routes of formation of UVR induced CPD, 6-4PP and Dewar isomer formation..... 36

Figure 1.8: The routes of formation of 8-oxodGua..... 37

Figure 1.9: The structure of extracellular matrix proteins in young, old and photoaged skin..... 46

Figure 1.10: The spectral dependence of ROS formation measured *in vivo*..... 57

Figure 1.11: The NER pathway of DNA repair..... 66

Figure 1.12: The routes of excess energy dissipation in UVR filters..... 70

Figure 1.13: The general structures of mycosporines and MAA..... 99

Figure 1.14: The proposed route of MAA biosynthesis..... 102

Figure 2.1: The spectral outputs of the radiation sources..... 125

Figure 2.2: The chemical structure and absorbance spectrum of palythine..... 128

Figure 2.3: The chemical structure and absorbance spectrum of C1332..... 129

Figure 2.4: The absorbance spectra of BASF compounds..... 130

Figure 3.1: The MAA palythine is extremely photostable when exposed to high doses of solar simulated radiation…… 164

Figure 3.2: SSR significantly induced cell death in HaCaT keratinocytes in a dose dependent manner…… 165

Figure 3.3: HaCaT keratinocytes were significantly protected by palythine from SSR induced cell death…… 166

Figure 3.4: SSR significantly induced CPD in a dose dependent manner when measured by IHC-IF…… 167

Figure 3.5: The effects of SSR and UVA on the formation of DNA lesions assessed by comet assay…… 168

Figure 3.6: HaCaT keratinocytes were significantly protected from SSR induced CPD by palythine at a range of concentrations when measured by IHC-IF…… 170

Figure 3.7: HaCaT keratinocytes were significantly protected from SSR and UVA induced CPD, 8-oxoGua and ALS by palythine at a concentration of 0.3% as measured by the comet assay…… 171

Figure 3.8: SSR significantly induced the formation of ROS in a dose dependent manner in HaCaT keratinocytes when measured using the H_2DCFDA assay…… 172

Figure 3.9: Palythine provided significant protection from SSR induced ROS induction and exhibited anti-oxidant properties in HaCaT keratinocytes…… 174

Figure 3.10: The DPPH radical scavenging ability of known anti-oxidant compared with palythine……175

Figure 3.11: The oxygen radical scavenging ability of known anti-oxidant and palythine…… 176

Figure 3.12: SSR induced gene changes in HaCaT keratinocytes…… 178

Figure 3.13: Palythine provided significant protection from SSR-induced gene changes in HaCaT keratinocytes…… 179

Figure 3.14: The absorbance of palythine at λmax for a range of concentrations…… 180

Figure 4.1: Wavelengths at the UV/visible border (385-405nm) significantly reduced cell viability *in vitro* in a dose dependent manner…… 199

Figure 4.2: 385nm and 405nm significantly induced the formation of ROS in a dose dependent manner *in vitro* when measured with the H_2DCFDA assay…… 201

Figure 4.3: The ability of wavelengths at the UV/visible border (385-405nm) to induce CPD *in vitro* when measured by IHC-IF…… 203

Figure 4.4: The ability of wavelengths at the UV/visible border (385-405nm) to induce CPD over time *in vivo* assessed by HPLC-MS/MS…… 205

Figure 4.5: 385nm and 405nm induced gene expression changes *in vitro*…… 207

Figure 4.6: 385nm and 405nm induced gene changes *in vivo*…… 210

Figure 4.7: Individual responses of 385nm and 405nm induced gene changes *in vivo*. Gene expression responses were assessed on an individual-by-individual basis…… 212

Figure 4.8: Pooled response of 385nm and 405nm induced gene expression changes *in vivo*…… 213

Figure 4.9. Comparison of *in vitro* and *in vivo* 385nm and 405nm induced gene changes…… 215

Figure 4.10: Study layout for pigmentation/erythema studies…… 217

Figure 4.11: Images representing typical responses for each skin and time point tested…… 218

Figure 4.12: The effects of 385nm and 405nm wavelengths on skin pigmentation assessed visually…… 219

Figure 4.13: The effects of 385nm and 405nm wavelengths on skin % pigmentation values measured using the Optimize device…… 221

Figure 4.14: The effects of 385nm and 405nm wavelengths on skin % redness values measured using the Optimize device…… 223

Figure 4.15: The effects of 385nm and 405nm wavelengths on skin L* values (pigmentation) measured using the Minolta device…… 225

Figure 4.16: The effects of 385nm and 405nm wavelengths on skin a* values (redness) measured using the Minolta device…… 227

Figure 4.17: The spectral dependence of solar radiation induced cell viability reduction *in vitro*…… 231

Figure 4.18: The spectral dependence of solar radiation induced ROS production *in vitro*…… 232

Figure 4.19: The spectral dependence of solar radiation induced CPD production *in vitro*…… 233

Figure 5.1: The spectral properties of the sunscreen formulations…….. 248

Figure 5.2: Sunscreen prevention of 385nm and 405nm induced cell viability reduction *in vitro*…… 250

Figure 5.3: Sunscreen prevention of 385nm and 405nm induced ROS *in vitro*…. 252

Figure 5.4: The photoprotection of 385nm induced delayed CPD *in vivo*…….. 254

Figure 5.5: The photoprotection of 385nm and 405nm induced gene changes *in vitro*…… 257

Figure 5.6: The photoprotection of 385nm and 405nm induced gene changes *in vivo* in human volunteers…… 260

Figure 5.7: Pooled response of 385nm and 405nm induced gene changes *in vivo* with different formulations…… 263

Figure 5.8: Study layout for pigmentation photoprotection studies…… 266

Figure 5.9: Typical response of one volunteer over time for pigmentation studies…… 267

Figure 5.10: Photoprotection against pigmentation by different sunscreen formulations scored visually…… 268

Figure 5.11: Photoprotection against pigmentation by different sunscreen formulations scored with the Optimizer device…… 270

Figure 5.12: Photoprotection against pigmentation by different sunscreen formulations scored with the Minolta device…… 272

Figure 5.13: Spectral transmission through each formulation and their photodegradation for 385nm and 405nm sources…… 275

Figure 5.14: The transmission of radiation through conventional low SPF (SPF15) and high SPF (SPF 50+) sunscreens compared to the solar spectrum and the sources used in this study…… 278

Tables

Table 1.1: The Fitzpatrick scale of skin type classification…… 39

Table 1.2: The four-gene cluster found in *Anabaena variabilis* ATCC 29413 linked to the pentose phosphate pathway synthesis of MAA…… 101

Table 2.1: The spectral waveband analyses of the radiation sources…… 125

Table 2.2: Properties and protection factors of the BASF compounds…… 131

Table 2.3: The Boots Star rating sunscreen test method…… 134

Table 2.4: Assays used for *in vitro* studies…… 138

Table 2.5: cDNA synthesis master mix…… 148

Table 2.6: cDNA synthesis thermocycler schedule…… 148

Table 2.7: qPCR master mix…… 149

Table 2.8: qPCR analysis schedule…… 149

Table 2.9: Assays used for *in vitro* studies…… 151

Table 2.10: Volunteer Demographics for *in vivo* studies…… 155

Table 2.11: Grading and corresponding score for pigmentation assessment…… 156

Table 3.1: The doses of SSR used and percentage reduction in absorbance for palythine photostability study…… 164

Table 3.2: The molar extinction coefficient of palythine…… 180

Table 3.3: The *in vitro* SPF and UVA-PF of Palythine…… 181

Table 3.4: The critical wavelength test and Boots star rating result…… 182

Table 4.1: Volunteer demographics for *in vivo* DNA damage studies…… 204

Table 4.2: Results of the statistical analysis of differential gene expression *in vitro*…… 208

Table 4.3: Volunteer demographics for *in vivo* gene expression studies…… 209

Table 4.4: The statistical analysis of pooled gene expression changes using two-way ANOVA with Sidak's multiple comparisons test…… 213

Table 4.5: Volunteer demographics for in vivo pigmentation/erythema studies…… 216

Table 4.6: Linear regression analysis of pigmentation change scored visually… 220

Table 4.7: Linear regression analysis of pigmentation change scored with the Optimize device…… 222

Table 4.8: Linear regression analysis of redness change scored with the Optimize device…… 224

Table 4.9: Linear regression analysis of pigmentation change scored with the Minolta device…… 226

Table 4.10: Linear regression analysis of redness change scored with the Minolta device…… 228

Table 4.11: Comparison of wavelength differences in pigmentation induction.. 229

Table 4.12: Comparison of skin type differences in pigmentation induction…… 229

Table 4.13: The spectral breakdown of solar radiation…… 235

Table 4.14: The time required for equivalent dose of 385nm or 405nm radiation in world cities of varying latitude…… 236

Table 5.1: Statistical analysis for in vitro gene expression photoprotection studies…… 258

Table 5.2: Volunteer Demographics for in vivo photoprotection gene expression studies…… 259

Table 5.3: Statistical analysis for in vivo gene expression photoprotection studies…… 261

Table 5.4: Statistical analysis for pooled *in vivo* gene expression photoprotection studies…… 264

Table 5.5: Volunteer Demographics for *in vivo* pigmentation/erythema photoprotection studies…… 265

Table 5.6: Linear regression analysis of pigmentation photoprotection scored visually…… 269

Table 5.7: Linear regression analysis of pigmentation photoprotection scored with the Optimizer device…… 271

Table 5.8: Linear regression analysis of pigmentation photoprotection scored with the Minolta device…… 273

Table 5.9: The total irradiance, percentage of maximum dose and percentage degradation of each treatment group…… 276

Abbreviations

4-MBC	4-methylbenzylidene camphor
6-4 PP	(6-4) pyrimidone photoproducts
8oxoGua	8-oxo 7,8 dihydro-2-deoxyguanosine
AK	Actinic keratosis
AP	Apurinic/apyrimidic
APC	Antigen presenting cells
APPH	2,2'-azobis-2-methyl-propanimidamine dihydrochloride
BCC	Basal cell carcinoma
BER	Base excision repair
BSA	Bovine serum albumin
BZ-3	Benzophenone-3
C1332	2-(4-(2-(4-Diethylamino-2-hydroxy-benzoyl)-benzoyl)-piperazine-1-carbonyl)-phenyl)- (4-diethylamino-2-hydroxyphenyl)-methanone
CAT	Catalase
CFC	Chlorofluorocarbon gases
CIE	International Commission on Illumination
CoRAP	Community rolling action plan
COX2	Cyclooxygenase-2
CPD	Cyclobutane pyrimidine dimer
CRCE	Centre for Radiation, Chemical and Environmental Hazards
CRY61	Cysteine-rich 61 protein
DAHP	3-dehydroquinate
DAHPS	3-dehydroquinate synthase
DAPI	4', 6-diamidino-2-phenylindole
DHC	7-dehydrocholestrol
DHQ	3-dehydroquinate
DHQS	3-dehydroquinate synthase
DMEM	Dulbecco's Modified Eagle Medium
DMSO	Dimethyl sulfoxide
DPPH	1 ,1-Diphenyl-2-picryl-hydrazyl
DT	Delayed tanning
DTH	Delayed-type hypersensitivity
ECHA	European Chemical Agency
EC	European commission
EEAP	Environmental Effects Assessment Panel
EGF	Epidermal growth factor
EPP	Erythropoietic protoporphyria
EVS	2-epi-5-epi-valiolone synthase
FAM	6-carboxyfluorescein

FDO	2-furlidioxime
FPG	Formamidopyrimidine DNA glycosylase
FWHM	Full width at half maximum
GAPDH	Glyceraldehyde 3-phosphate dehydrogenase
GG-NER	Global genome nucleotide excision repair
GM-CSF	Granulocyte-macrophage colony-stimulating factor
GPx	Glutathione peroxidase
GSH	Glutathione
H2DCFDA	6-carboxy-2',7'-dichlorodihydrofluorescein
HaCaT	Human adult low calcium temperature
HMOX	Hemeoxygenase
hOGG1	Human 8-oxoguanine DNA N-glycosylase 1
HPLC	High performance liquid chromatography
IC	Internal conversion
IL	Interleukin
IPD	Immediate pigment darkening
IR	Infrared
ISC	Intersystem crossing
ISO	International Organization for Standardization
JCIA	Japanese Cosmetic Industry Association
JNK	c-Jun amino terminal kinase
KC	Keratinocyte cancers
KEAP1	Kelch-like ECH-associated protein 1
LED	Light emitting diode
LIP	Labile iron pool
MAA	Mycosporine-like amino acid
MAP	Mitogen-activated protein
MBBT	Bis-Benzotriazolyl Tetramethylbutylphenol
MED	Minimal erythemal dose
MM	Malignant melanoma
MMP	Matrix metalloproteinase
MMR	Mismatch repair
NADPH	Nicotinamide adenine dinucleotide phosphate
NER	Nucleotide excision repair
NFκB	Nuclear factor kappa-light-chain-enhancer of activated B cells
NMSC	Non-melanoma skin cancer
NQ01	NAD(P)H quinone dehydrogenase 1
NRF2	Nuclear factor erythroid-2-related factor 2
OCT	Octocrylene
ODC	Ornithine decarboxylase
OMT	*0*-methyltransferase
ORAC	Oxygen Radical Absorbance Capacity
PBS	Phosphate buffered saline

PCOLCE	Procollagen C proteinase enhancers
PCR	Polymerase chair reaction
PDT	Photodynamic therapy
PEP	Phosphoenolpyruvate
PHE	Public health England
PI	Propidium iodide
PLE	Polymorphic light eruption
PMMA	Poly (methyl methacrylate)
PON-2	Paraoxonase 2
PPD	Persistent pigment darkening
qPCR	Quantitative - polymerase chair reaction
ROS	Reactive oxygen species
RQ	Relative quantification
RT-PCR	Reverse transcription – polymerase chair reaction
SAD	Seasonal affective disorder
SCC	Squamous cell carcinoma
SCCS	Scientific Committee on Consumer Safety
SCN	Suprachiasmatic nucleus
SED	Standard erythemal dose
SPF	Sun protection factor
SRB1	Scavenger receptor class B member 1
SSB	Single strand break
SSR	Solar simulated radiation
T4N5	T4N DNA repair endonuclease V
TBT	Tris-biphenyl triazine
TC-NER	Transcription coupled - nucleoside excision repair
TEAA	Triethylammonium acetate solution
TGF-β	Transforming growth factor-β (
TIMP	Tissue inhibitor of metalloproteinases
TLS	Translesion synthesis polymerases
TNF	Tumour necrosis factor
UNEP	United Nations Environment Programme
UV	Ultraviolet
UVR	Ultraviolet radiation
VEGF	Vascular endothelial growth factor
VIC	4,7,2'-trichloro-7'-phenyl-6-carboxyfluorescein
WSpA	Water stress protein
XP	Xeroderma pigmentosum

Acknowledgements

I would like to express my sincere gratitude to my primary supervisor, Professor Antony Young, firstly for providing me with the opportunity to join his group and to undertake a PhD, and for his continued support and encouragement. I could not have asked for a better supervisor and appreciate all of the contributions, time and effort he has put into my studies to make the experience enjoyable, rewarding and ultimately a success. I would also like to thank my secondary supervisors, Professor Paul Long for allowing me to work on his MAA project, for all his helpful input into my research and exposing me to areas of research that are not usually part of a PhD studentship and Dr Robert Sarkany for his clinical support with *in vivo* studies.

I am extremely grateful for the financial support provided by BASF GmbH, Germany and the Photodermatology Charitable Trust, UK. I would also like to thank BASF for their technical support, particularly Professor Bernd Herzog for all his help throughout my studentship.

Completing my PhD would not have been possible without the help and encouragement of all past and present members of the Photobiology Department, particularly Kylie Morgan, Damilola Fajuyigbe, Dr Mieran Sethi and Graham Harrison, and all members of the 9th floor. They have always been there for me when I have needed them, most importantly when I have needed a break from work, and have become very close friends.

Finally I would like to thank my friends, and most importantly my family for supporting me in everything I have ever done. Without them I would not be where I am today and for that I will be forever grateful.

Chapter 1: Introduction

1.1 Ultraviolet and Visible Radiation

1.1.1 Solar Radiation

Solar radiation consists of a wide range of wavelengths that are split up into defined wavebands. The three of the most abundant on earth are ultraviolet (UV), visible and infrared (IR) radiation, which are further separated into sub categories, shown in Figure 1.1. Ultraviolet radiation (UVR) is divided into UVA, UVB and UVC. Similarly, IR is split up into IR-A, IR-B and IR-C. Visible radiation, as the name suggests, is the light that can be detected by the eye, and is split up according to its colour. Each type of radiation has different properties: including energy, tissue penetration depth, biological and physical effects (Diffey, 1982; Tewari *et al.*, 2013a).

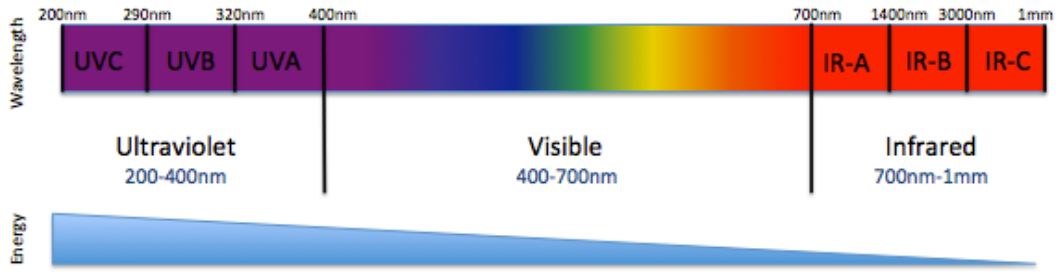

Figure 1.1: The spectral breakdown of solar radiation.

Solar irradiance from 200nm-1mm is the total radiation energy that is emitted from the sun, with a value of around 1.351kW/m^2 at the edge of the earth's atmosphere on a surface normal to the suns direction. Of this,

approximately two thirds reaches the earth's surface due to attenuation by many factors such as ozone (O_3), Mie and Rayleigh scattering. Ozone absorbs wavelengths at 330nm and below with increasing effectiveness with decreasing wavelength, with almost no wavelengths of 295nm or lower passing through to the earth's surface (Diffey, 1982).

1.1.2 UVR

UVR is defined as wavelengths between 100-400nm and is subdivided into three categories defined by the Commission Internationale de l'Eclairage (CIE) (International Commission on Illumination - http://www.cie.co.at/) – the commission responsible for the coordination of lighting related technical standards:

UVC - 100-280nm

UVB - 280-315nm

UVA - 315-400nm - UVA1 – 340-400nm,

UVA2 – 340-315nm.

However, most skin related photobiological studies use 320-400nm as the definition of UVA as the biological effects are better separated from UVB this way. Around 5% of total solar radiation that reaches the earth's surface is UVR. UVC has not been greatly studied on human skin *in vivo* as it is completely attenuated by the earth's stratospheric ozone layer, although it can be produced artificially. Although UVB only makes up a maximum of around 5% of the UVR

that reaches the earth's surface, historically it was thought to be the most damaging due to being the highest energy of the terrestrial UVR wavelengths. UVA accounts for around 95% of which over 70% is UVA1 and more recently studies have shown the damage caused by UVA may be almost as important as UVB. Thus, it is essential to study the damage UVA has on human health, as we are greatly exposed to this waveband throughout life.

1.1.3 Measurement of Solar Radiation

The biological effects of solar range radiation depend greatly on the wavelengths present in a given source, so the measurement of these sources is of great importance, especially to determine the specific part of the spectrum causing a given biological effect. This involves recording the spectral irradiance on a wavelength-by-wavelength (nm) basis ($W/m^2/s$), and is measured by a spectroradiometer. The sum of all wavelengths emitted gives the spectral irradiance (W/m^2), which can be used to calculate the exposure time for a given dose (J/cm^2) given by that source.

Spectroradiometers contain four main components:

I. Input optics
II. Monochromator
III. Detector
IV. Logging System

The input optics gather the electromagnetic radiation from its source and deliver it to the monochromator. These optics can be in many forms from glass quartz, fibre optics and barium sulphate coated integration spheres. The selection of input optics is dependent on the use of the spectroradiometer – some are better for UVR measurements for example. Next is the monochromator, which is responsible for separating the radiation into its constituent wavelengths. Usually, a spectroradiometer contains two monochromators to give greater resolution. The electromagnetic radiation is usually split using either a prism or a diffraction grating, with gratings typically used as they have a number of advantages such as reduced attenuation of UVR. After the radiation has been sufficiently divided it is focused onto the detector, where the intensity of each wavelength is measured. Again, depending on the spectrum of interest there are different options for detectors such as photoemissive detectors, semiconductors and thermal detectors. Photoemissive detectors (photomultipliers) and semiconductors act by freeing electrons from a photocathode surface by direct absorption of a photon, allowing the electron to flow and form a current which can be measured. These only work for a given waveband dependent on the material used. Thermal detectors measure the temperature rise caused by absorption of the photons and are not waveband specific. Finally, the control and logging system usually contains amplifiers to increase the signal and convertors to convert the detector's signal into a format that can be processed by computer. This can then log the intensity on a wavelength-by-wavelength basis. It is vital to note the importance of calibration when using a spectroradiometer to measure electromagnetic radiation as many different factors can affect the reading (Bentham, 2014).

1.1.4 Variability of Solar Exposure

Solar radiation can undergo attenuation or enhancement by many different atmospheric, temperate and geographical factors that can have a large effect on the composition of the radiation received by an individual.

The atmospheric gases present in the air have a large effect on the spectral distribution of the radiation. As previously mentioned, UVC is almost entirely filtered out by the ozone layer and by the strong absorption of UVC by oxygen. UVB is also attenuated to a degree by the ozone layer although some still reaches the earth, and UVA is only slightly absorbed; this is demonstrated in Figure 1.2 below. The depletion of the ozone layer by chlorofluorocarbon gases (CFC) can change the relative components of solar radiation leading to an increased UVB portion (McKenzie *et al.*, 2007; Norval *et al.*, 2007).

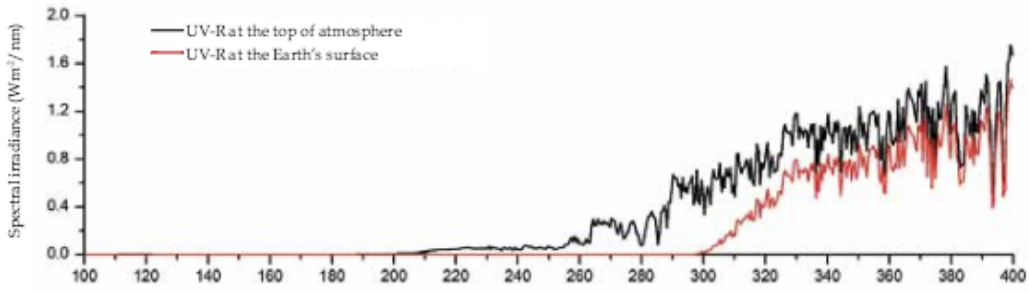

Figure 1.2: The spectral differences at the Earth's surface compared to the top of the atmosphere (Correa Mde, 2015).

In addition to absorption by O_3 in the stratosphere, the scattering of radiation by aerosols plays a large part in its irradiance. The scattering of photons is dependent on the size of the molecules. Mie scattering is scattering by particles of similar or larger size than the wavelength of the radiation and Rayleigh scattering

is the diffuse scattering of electromagnetic radiation by particles smaller than the wavelength of light, and is responsible for the colour of the sky. Scattering of UVB is responsible for the ability to be able to get a sunburn in the shade (Diffey, 1982). The scattering of radiation can be even larger on days of high pollution as there are more particles present in the air, with pollution in some areas leading to a decrease in the UV Index (UVI), a linear scale related to the intensity of sunburn producing UVR at a given place and time, by 1 (Correa Mde, 2015). Another major factor causing the attenuation of radiation is cloud cover. This can halve or even completely eradicate UVR exposure at the earth's surface. Water in the clouds is more effective at attenuating the heat of IR than UVR, which is why it is possible for cloud cover to make people underestimate their UVR exposure (Bais *et al.*, 2015).

The biggest influencing factor on solar exposure is the latitude. The poles receive the lowest yearly irradiance, which increases towards the equator. This is determined by the distance from the sun. This can change with the time of day, month and year as well as latitude and altitude. With the sun directly overhead, the atmosphere has a mass of value 1. When this angle changes to 60^{o} the mass changes to a value of 2, meaning the radiation has twice the thickness of atmosphere to penetrate, along with more scattering. An increase of 1500m will increase the irradiance of UVB by 20% (Correa Mde, 2015; Diffey, 1982).

The final important factor in the received irradiation from the sun is the albedo. Different surfaces of the earth can reflect vastly different amounts of UVR. Snow can reflect up to 80% of UVR upwards leading to greatly increased risk of

sunburn. Other surfaces will reflect much less for example: grass (4%), water (5%) and sand (10%) (Correa Mde, 2015; Diffey, 1982).

1.2 Molecular Effects of UV and Visible Radiation on the Skin

1.2.1 Skin Structure

The skin is the body's largest organ and serves many different functions, most importantly as a barrier to the outside environment – preventing infections, chemicals and solar radiation damaging the rest of the body. As well as protection, the skin has a role in regulating body temperature, retaining water and sensing pain and other external stimuli. Human skin is composed of three main layers, each with different cell types: the epidermis, dermis and subcutaneous layer, displayed in Figure 1.3.

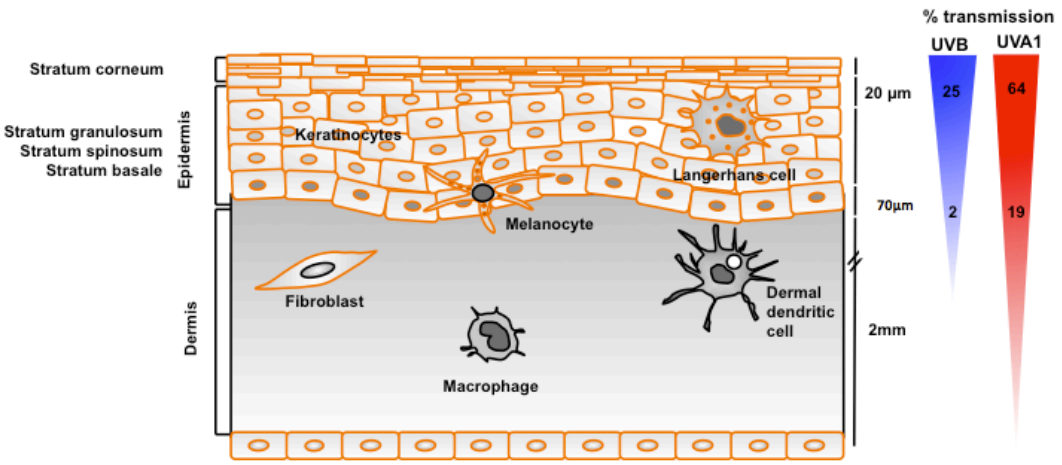

Figure 1.3: The structure of human skin and the *ex vivo* transmission of UV radiation (Bruls *et al.*, 1984).

The epidermis is the outer layer containing keratinocytes, Langerhans cells and melanocytes and is about 100-150µm thick. The vast majority of the cells in this layer are keratinocytes (95%), which actively divide on the basal layer (the deepest epidermal layer). The cells migrate externally towards the outermost *stratum corneum* in a process known as terminal differentiation, which takes

around 4 weeks. Corneocytes forming the *stratum corneum* are keratinocytes that have lost their nuclei and other organelles, and are dehydrated and flattened to form a protective barrier. Dispersed throughout the basal epidermal layer are the melanocytes, which produce the melanin pigments (eumelanin and pheomelanin) responsible for skin colour and attenuation of solar radiation. Melanocytes produce melanins, which are packaged and transported to keratinocytes via melanosomes. Finally, the Langerhans cells play a role in the skin's immune system as antigen presenting cells (APC), detecting antigens to present to the lymphatic ganglia to stimulate immune responses for the removal/inactivation of foreign bodies.

The dermis acts mainly as a structural connective tissue matrix layer composed largely of collagens and elastins known collectively as the extracellular matrix (ECM), giving the skin strength and elasticity. This layer also contains fibroblasts, some blood vessels, nerve endings, dendritic cells and macrophages and has functions including nourishment of the skin, sensory roles, ECM remodelling and immune response. Finally the subcutaneous layer is mainly composed of fatty tissue, nerves and the majority of the blood vessels and serves as an energy store and insulating layer.

1.2.2 Chromophores

When solar radiation reaches the skin a number of outcomes can occur, resulting in either direct damage to DNA, proteins or lipids, such as in the formation of DNA photoproducts (Young *et al.*, 1998), and indirect damage via

the generation of reactive oxygen species (ROS) (Bickers and Athar, 2006; Wolfle *et al.*, 2014). A small percentage of the radiation is reflected, with the remaining being scattered or absorbed by molecules in the skin. Molecules that absorb the radiation are known as chromophores and each chromophore has a characteristic wavelength dependent absorption profile. The number and location of chromophores in the skin for a given waveband determines the penetration depth of the radiation. There are numerous chromophores in the skin, many of which are still unknown, and when they absorb radiation there can be a variety of different reactions. The most important endogenous chromophore is DNA, but aromatic amino acids such as phenylalanine, tryptophan and tyrosine, as well as melanins and porphyrins also absorb UVR and visible radiation. There are also exogenous chromophores that are important to consider such as sunscreens (discussed later), drugs such as tetracycline antibiotics and psoralens, which have important clinical significance.

When a chromophore absorbs a photon, it can enter a singlet or triplet excited state. Singlet states last only a few nanoseconds and return to the ground state emitting the absorbed energy as either a longer wavelength of radiation (fluorescence), or heat by an internal conversion mechanism. A third mechanism can occur by which the excited electron can be transferred to the triplet-excited state by a system known as intersystem crossing. This state can last much longer, in the order of 10^{-8} to 10^{-3} s and dissipates the energy as phosphorescence or by reacting with other molecules. The process by which either of these mechanisms occurs is dependent on the electron spin state, with singlet states having

opposing spin directions and triplet states having the same spin direction. This is displayed in the below Jablonski diagram (Figure 1.4)

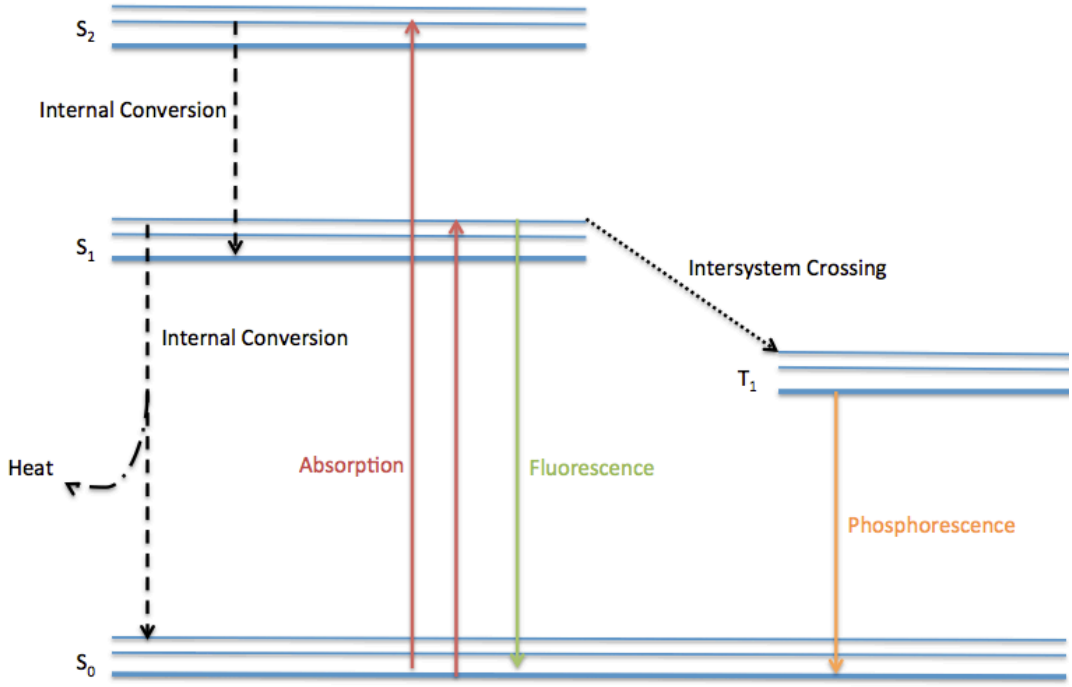

Figure 1.4: Routes of excitation and dissipation of photochemical excitation of electrons.

1.2.3 Oxidative Stress

An excited chromophore can be effective or ineffective at dissipating the excess energy. Chromophores that are ineffective at dissipating the excess energy are known as photosensitizers. These are molecules that populate the triplet state and are poor at dissipating this absorbed energy in a controlled way by phosphorescence and are highly reactive with oxygen molecules. Photosensitzers can undergo either type I or type II photosensitisation reactions and can cause damage to cellular molecules and are the source of many of the adverse events

that exposure to solar radiation induces. The first step is the excitation of the photosensitizer to an excited triplet state (Sen*). In type I reactions, the excited state sensitizer reacts directly with the target molecule, known as the substrate (this can be any cellular molecule), transferring an electron to produce radical ions in both the substrate (substrate^{+}) and sensitizer (Sen^{-}). When in an aerobic environment, both radicals can react with oxygen to produce oxidised products. This can lead to another reaction that involves the direct transfer of an electron to produce a superoxide radical ion (0_2-), regenerating the sensitizer without damage.

For type II reactions the first steps are the same, however the Sen* transfers the excess energy to oxygen ($^3O_2$) to produce singlet oxygen $^1O_2$, which then reacts with the substrate to form oxidised products. This damage can lead to change of structure or loss of function in proteins, with recent work showing this can lead to loss of function in DNA repair proteins (McAdam *et al.*, 2016), exacerbating the effect of UVR induced DNA damage (Gueranger *et al.*, 2014). It is this process that is thought to be the cause of UVR induced cell cycle arrest, which potentially results in cell death. This is due to the photosensitization of tubulin, resulting in the inhibition of its formulation and the arrest of cell cycle at the m-G_1 phase preventing cell division. This is a useful effect for cancer treatment by photodynamic therapy (PDT) (McMicken *et al.*, 2014). These reactions cause oxidative stress in the skin.

1.2.3.1 Fenton Reaction

A process closely related to this is the Fenton reaction, which has been demonstrated to induce oxidative stress, by the generation of reactive oxygen species (ROS), in the presence of H_2O_2:

$$Fe^{2+} + H_2O_2 \rightarrow OH + OH^- + Fe^{3+}$$

Equation 1.1: The Fenton reaction.

In this reaction, iron catalyses the reduction of hydrogen peroxide to the highly reactive oxidant hydroxyl radicals (•OH). Under normal conditions this process does not occur due to the iron binding proteins ferretin, and transferrin sequestering free iron, however under oxidative stress (for example by exposure to UVR) this iron is released from these proteins, allowing the free iron to participate in the production of hydroxyl radicals. The •OH can then react with other molecules such as lipids and proteins to cause damage (Bissett *et al.*, 1991).

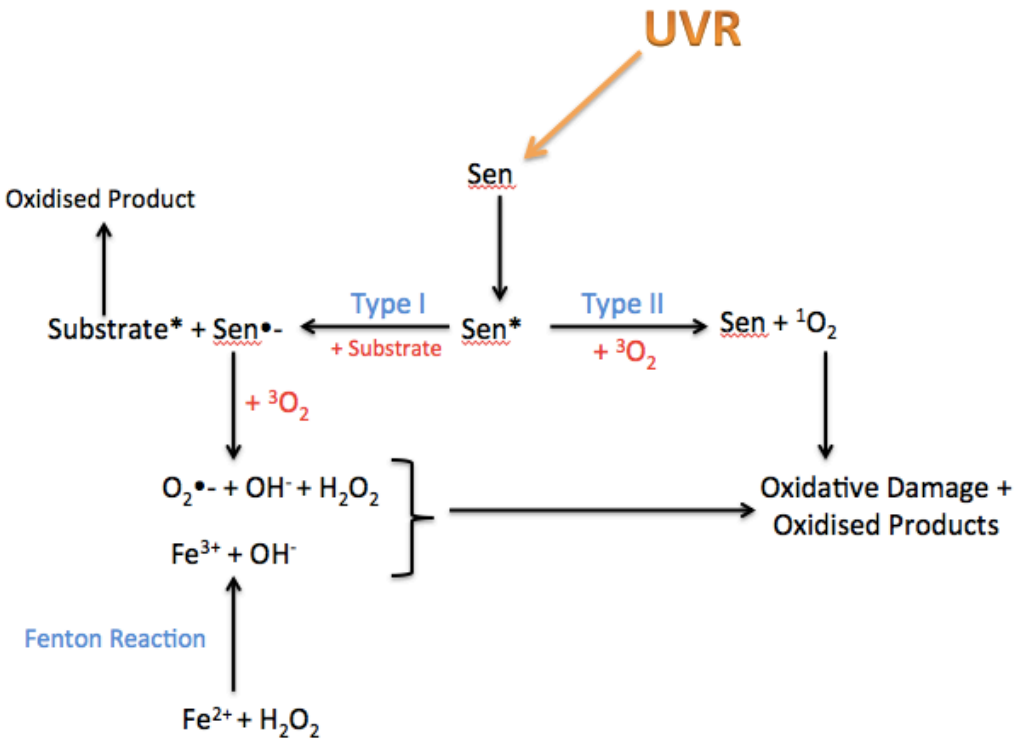

Figure 1.5: The mechanisms for the generation of oxidative stress by UVR radiation.

A summary of the process involved in oxidative stress is shown in Figure 1.5. These processes are vitally important in many of the photobiological responses in the skin after irradiation.

1.2.4 DNA Damage

1.2.4.1 CPD, 6-4PP and Dewar Isomers

DNA photodamage can occur in many different forms, by differing mechanisms and is wavelength dependant (Kielbassa and Epe, 2000; Kielbassa *et*

al., 1997; Kuluncsics *et al.*, 1999). The DNA lesion thought to have the biggest impact on health is the cyclobutane pyrimidine dimer (CPD). CPDs are formed mainly by a direct absorption of UVR photons, although recent evidence suggests these may also form through photosensitisation mechanisms, most likely due to melanin excitation (Premi *et al.*, 2015). The *in vitro* peak for CPD production is around 260nm, which matches the absorption profile of DNA, however *in vivo* in human skin the peak is in the UVB region (peak at 300nm), due to competing chromophores that alter the optical properties of skin. The action spectrum also extends into the UVA region (Figure 1.6), matching the erythema action spectrum very closely, suggesting DNA is an important chromophore for this endpoint (Young *et al.*, 1998).

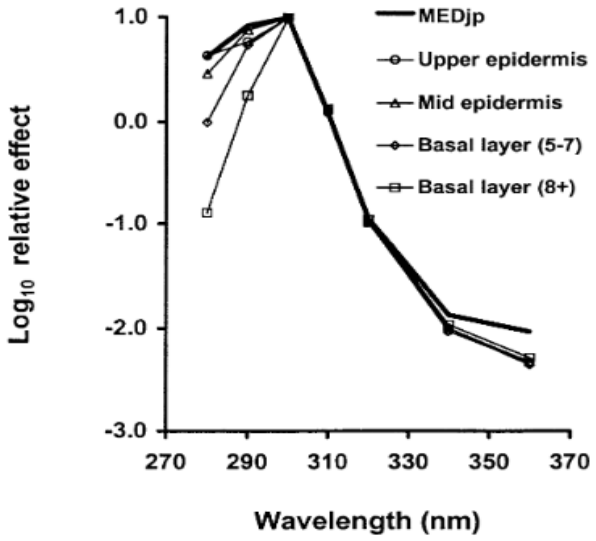

Figure 1.6: The CPD action spectra in different layers of the skin (Young *et al.*, 1998).

The majority of CPDs form after the direct absorption of UVA and/or UVB photons and subsequent excitation of DNA bases, mostly thymine. UVC is more efficient in forming CPDs, but as previously mentioned this spectral region does

not reach the earth's surface. CPDs form when the C5=C6 double bond of two adjacent pyrimidine bases, cytosine (C) or thymine (T) is split forming new bonds, linking the pyrimidines at these positions, forming a 4 carbon cyclobutane ring (shown in Figure 1.7). This damage, if left unrepaired, can lead to incorrectly recognised bases and cause a characteristic C > T transition mutation in key genes such as p53. There is overwhelming evidence to show that CPDs induce keratinocyte cancers, and more recently melanoma (Brash, 2014; Pfeifer and Besaratinia, 2012). CPD formation may also initiate cytokine release, which can induce immunosuppression important in the development of squamous cell carcinomas (SCC) and basal cell carcinomas (BCC) (Nishigori *et al.*, 1996).

In addition to CPD formation, (6-4) pyrimidone photoproducts (6-4PP) and its Dewar photoisomers are also formed. The action spectrum for the 6-4PP is similar to that of CPDs, but its formation is 5-10 times less abundant (Rosenstein and Mitchell, 1987). Dewar isomers are formed after UVA exposure of 6-4 PP (peak formation at 320nm). During the formation of 6-4PP, the C5=C6 double bond breaks and rotates around one of the pyrimidine rings which then forms a new bond at C4 and C6 of adjacent bases (Ichihashi *et al.*, 2003). As 6-4PP and Dewar isomers have a more distorted confirmation compared to DNA and CPD lesions, it is thought that they are identified and repaired much more quickly (Young *et al.*, 1996), although 6-4PP have also been shown to cause C>T mutations (Brash, 2014).

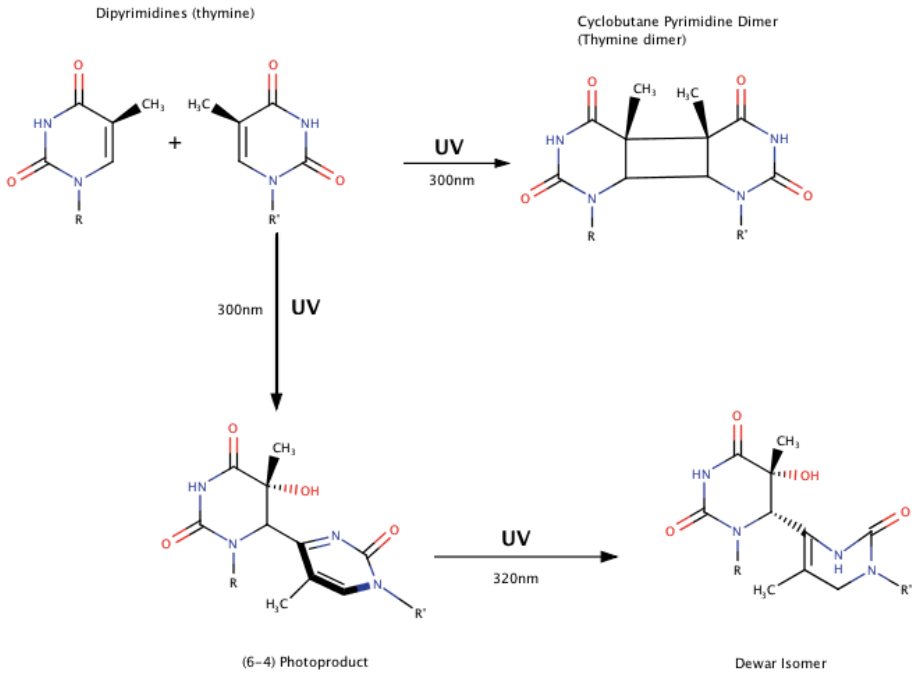

Figure 1.7: The routes of formation of UVR induced CPD, 6-4PP and Dewar isomer formation.

1.2.4.2 Oxidative Damage to DNA

Oxidative stress can lead to oxidative damage to various cellular molecules including DNA. The most predominant subunit to be oxidised in DNA is the base Guanine (G), forming 8-oxo 7,8 dihydro-2-deoxyguanosine (8-oxodGua), mostly by UVA irradiation (although CPDs are still the predominant DNA lesion after UVA exposure) (Courdavault *et al.*, 2004). There is also evidence that the formation of 8-oxodGua spans into the visible radiation region (Kvam and Tyrrell, 1997; Pflaum *et al.*, 1994). There are thought to be more than 20 oxidatively damaged base lesions as well as single strand breaks (SSB) formed due to oxidative damage (Cooke *et al.*, 2003). The mechanism of formation is thought to

be via both type I and II photosensitization reactions from endogenous or exogenous photosensitizers (Figure 1.8), leading to signature T>G mutations (Drobetsky *et al.*, 1987).

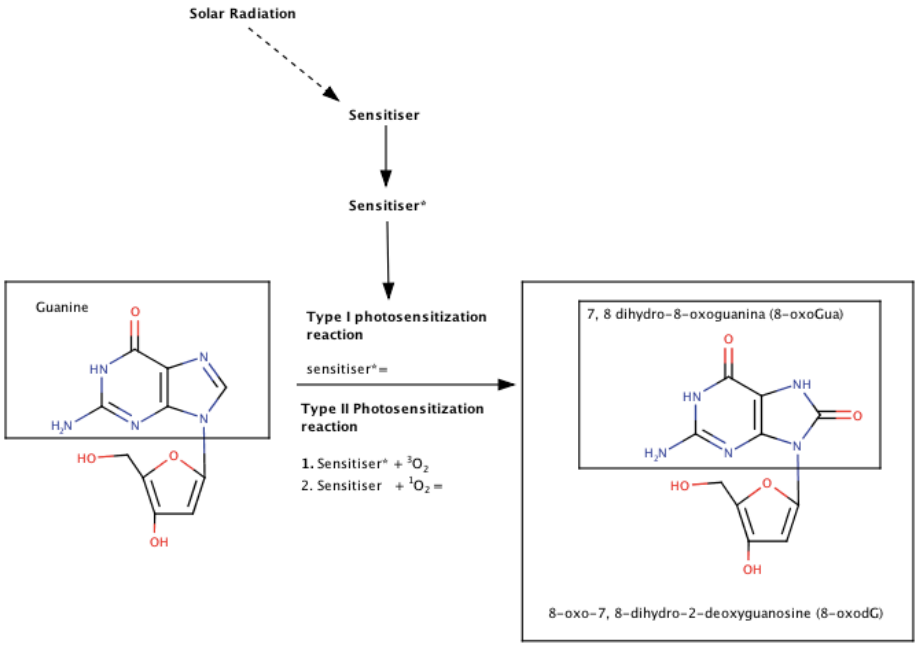

Figure 1.8: The routes of formation of 8-oxodGua.

The link of 8-oxodGua to skin carcinogenesis is much less well defined than for CPDs and 6-4PPs. Increased levels of 8-oxodGua are linked with increased oxidative stress and cancer, however this may be due to changes in gene expression rather than DNA structural change (Valavanidis *et al.*, 2013). A mouse model lacking 8-oxoguanine DNA N-glycosylase 1 (OGG1) (oxidative DNA damage repair enzyme) showed an increase in skin tumour development, although this study used a UVB irradiation source so the effects cannot be attributed to 8oxoGua alone (Kunisada *et al.*, 2005). *Xiphophorus* fish models show a peak in the action spectra of melanoma induction in the UVA/visible region suggesting a

contribution due to oxidative damage (Setlow *et al.*, 1993; Wood *et al.*, 2006), however this has recently been disputed (Mitchell *et al.*, 2010).

1.3 Clinical Effects of UVR

1.3.1 Skin Type Classification

The biological and clinical responses to solar radiation vary with skin phototype. The most widely used system currently employed to define skin types' reactions to UVR is the Fitzpatrick scale, which uses a I-VI ranking (Fitzpatrick, 1988). The classification is based on a subject's report on how their skin reacts to acute UVR exposure, in relation to erythema and pigmentation. The classification and criteria are listed in Table 1.1:

Classification	Definition	Skin phenotype (sun protected)
I	Always burns, never tans	Pale white; blond or red hair; blue eyes; freckles
II	Usually burns, tans minimally	White; fair; blond or red hair; blue, green, or hazel eyes)
III	Sometimes mild burn, tans uniformly	Cream white; fair with any hair or eye colour
IV	Burns, always tans well	Moderate brown
V	Very rarely burns, tans	Dark brown
VI	Never burns, never tans	Deeply pigmented dark brown to darkest brown

Table 1.1: The Fitzpatrick scale of skin type classification.

1.3.2 Erythema

Erythema (sunburn) is the cutaneous inflammation that is identified by redness and sometimes warmth of the skin. This is a consequence of vasodilation leading to increased blood flow. Erythema is caused by the release of many pro-inflammatory cytokines after UVR exposure such as TNFα, IL-1, IL-6, IL-8 and IL-12. This release is most like most likely triggered by DNA damage, as DNA damage (CPDs) and erythema in the skin share similar action spectra (Matsumura and Ananthaswamy, 2002; Young *et al.*, 1998). However there is also evidence that ROS can induce erythema (Auletta *et al.*, 1986). UVR, particularly UVB, is well known to cause erythema, usually peaking 6-24 hours after exposure (Sklar *et al.*, 2013). UVA wavelengths (in particular the shorter wavelengths) are also erythemogenic, but UVA is around 1000 times less effective than UVB per unit dose (Sklar *et al.*, 2013). Erythema is used to assess individual sensitivity to UVR by the determination of the minimal erythema dose (MED), which is the minimum UVR dose required to induce a just perceptible reddening of the skin. MED is a subjective measure and the dose required to induce an MED varies depending on the individual and the UVR spectrum being tested. The MED is the endpoint used to measure the protection offered by sunscreens discussed later in the 'Exogenous Photoprotection' section. Another objective measure is used known as the standard erythemal dose (SED), which is independent of individual or spectrum and is an erythemally weighted dose of 100J/m^2 (Diffey *et al.*, 1997).

1.3.3 Pigmentation

1.3.3.1 Constitutive Pigmentation

Constitutive pigmentation of the skin provides protection against UVR induced damage due to the absorption properties of melanin. Melanins are produced by melanocytes in the epidermal basal layer, after which they are transferred to the keratinocytes (Tran *et al.*, 2008). There are two main types of melanin in the skin: eumelanin and pheomelanin. Eumelanin is an insoluble brown-black coloured molecule and pheomelanin is a yellow-red colour, responsible for red hair. A third melanin, neuromelanin, is found in the brain but its function remains unclear (Fedorow *et al.*, 2005). Skin colour is determined by the relative amounts of several epidermal and dermal chromophores – melanins, carotenoids and haemoglobins. The level of constitutive skin pigmentation determines a range of outcomes, many of which appear more beneficial for darker skin types. The numbers of melanocytes in light and dark skin are very similar. The large differences in skin colour are largely due to the production of different amounts of melanin, the different forms of melanin and its distribution within the epidermis. Lighter skin tends to have less melanin that is found in melanosomes clustered in keratinocytes and is made up mainly of pheomelanin. Darker skin has more melanin, of which there is a higher ratio of eumelanin, which is more evenly dispersed between the keratinocytes rather than in clusters (Miyamura *et al.*, 2007; Thody *et al.*, 1991). There is evidence that pheomelanin may be a photosensitizer, leading to the increased skin cancer risk in the skin type I population (Vincensi *et al.*, 1998).

1.3.3.2 Acquired Pigmentation

Acquired pigmentation or 'tanning' is the process whereby exposure to solar or artificially produced radiation leads to darkening of the skin above the levels of the person's constitutive pigmentation. There are three distinct types of acquired tanning: immediate pigment darkening (IPD), persistent pigment darkening (PPD) and delayed tanning (DT).

IPD occurs within minutes of exposure to solar radiation, lasting for a few hours. It is thought to occur due to the rapid oxidation and polymerisation of melanin and its precursors (e.g. DHI, DHICA), and appears as a black/grey colour. The effect is more efficient in the UVA range than in the UVB range, probably a consequence of the greater oxidising potential of UVA. There is disputed evidence that in addition to oxidation, there is a re-dispersion of melanin (Honigsmann *et al.*, 1986; Lavker and Kaidbey, 1982). IPD is closely associated with PPD, which is seen as the second phase of IPD. PPD occurs within two hours and can persist for several days and appears tan/brown in colour. Studies have shown that in the process of IPD and PPD, there is no significant increase in the amount of melanin present (Miyamura *et al.*, 2007; Sklar *et al.*, 2013).

The third acquired pigmentation process is DT. This results from the synthesis of new melanin and is a process that has a action spectrum peak in the UVB region around 290nm (Parrish *et al.*, 1982), however high doses of UVA will also induce DT (Maeda and Hatao, 2004). DT generally takes several days to develop, peaking at 3-7 days post exposure as the new melanin is synthesized

and transported into the upper layers of the epidermis, and lasts for around 7 weeks at which point the melanin containing keratinocytes are shed. Melanin is produced in response to UVR by inducing an increase in tyrosinase activity. Tyrosinase catalyses the conversion of L-Tyrosine to L-DOPA. This is the precursor of DOPA-quinone that is used to make eumelanin and pheomelanin (Brenner and Hearing, 2008; Miyamura *et al.*, 2007).

1.3.4 Immunoregulation

Numerous studies have shown that irradiation with both UVA and UVB suppresses the skin's acquired immunity. This can lead to the immune system not responding to tumour formation (Kripke, 1974). The mechanisms for such effects are thought to be local and systemic. Locally, Langerhans APC are depleted. After UVR exposure (even at sub-erythemal exposure); these cells migrate to the lymph nodes, die, or have loss of function. Additionally, epidermal skin cells themselves can influence the immune response by their production of cytokines such as IL-10, TNF-α, and many other immunoregulatory factors (Luger *et al.*, 1985). Systemically, an increased blood flow to the skin at erythemal doses causes cytokines and other signalling molecules, aimed at regulatory T-cells, to enter the circulation, suppressing the immune response (Halliday and Rana, 2008; Schwarz, 2008). In contrast, UVR may enhance innate immunity of the skin as it stimulates the production of antimicrobial peptides such as β-defensin (Navid *et al.*, 2012).

1.3.5 Photoageing

Ageing of the skin is a result of two processes: intrinsic chronological ageing, which is natural ageing due to the passing of time, and extrinsic ageing as a result of external factors such as the chronic exposure to solar radiation leading to molecular changes that result in changes in the cutaneous appearance and function of the skin.

The production of ROS in the skin induces the inhibition of protein-tyrosinase phosphatase-κ, triggering the activation of many cell surface receptors such as epidermal growth factor (EGF), the interleukins, and tumour necrosis factor (TNF-α). This leads to intracellular signalling through the mitogen-activated protein (MAP) kinase pathway stimulating p38 and c-Jun amino terminal kinase (JNK) inducing the transcription of nuclear transcription complex AP-1, which is activated even at sub-erythemal doses of UVB exposure (Fisher *et al.*, 1996), with a peak upregulation at around 9 hours (Quan *et al.*, 2009). Increased AP-1 activity inhibits transforming growth factor-β (TGF-β) leading to the reduced synthesis of structural proteins such as collagens and elastins. AP-1 is also triggered by another UVR induced protein, cysteine-rich 61 protein (CRY61) that triggers the upregulation of matrix metalloproteinases (MMP). UVR also induces nuclear factor κB (NFκB) that promotes the expression of inflammatory cytokines (IL-1, IL-6), vascular endothelial growth factor (VEGF) and TNF-β, which again stimulates the expression of MMP (Yaar and Gilchrest, 2007). ROS have been demonstrated to inactivate the tissue inhibitor of metalloproteinases (TIMP), enhancing the effect of MMP upregulation (Scharffetter-Kochanek *et al.*, 2000).

The MMP are a large group of extracellular matrix metalloproteinases consisting of a zinc-containing binding site, which are produced as pro-enzymes. In healthy skin their role is in the regulation of tissue remodelling in response to various physiological and pathological processes. The MMP are responsible for the breakdown of many different extracellular structural proteins such as collagens, elastins, gelatin, laminin and fibronectin. MMP-1 is the major enzyme for breakdown of collagen and is expressed in response to both UVA and UVB damage, with a link of expression due to both ROS and DNA damage (Dong *et al.*, 2008; Tewari *et al.*, 2012a). Other MMP may have different wavelength dependence, for example MMP-12 is selectively upregulated by UVA1 (Tewari *et al.*, 2013b). The breakdown of the extracellular matrix proteins results in a modification to the organization of the proteins into a less uniform, disorganised structure compared to intrinsic ageing (Figure 1.9), resulting in a change of appearance of sun exposed skin to becoming dyspigmented, wrinkled, dry, rough and sagging.

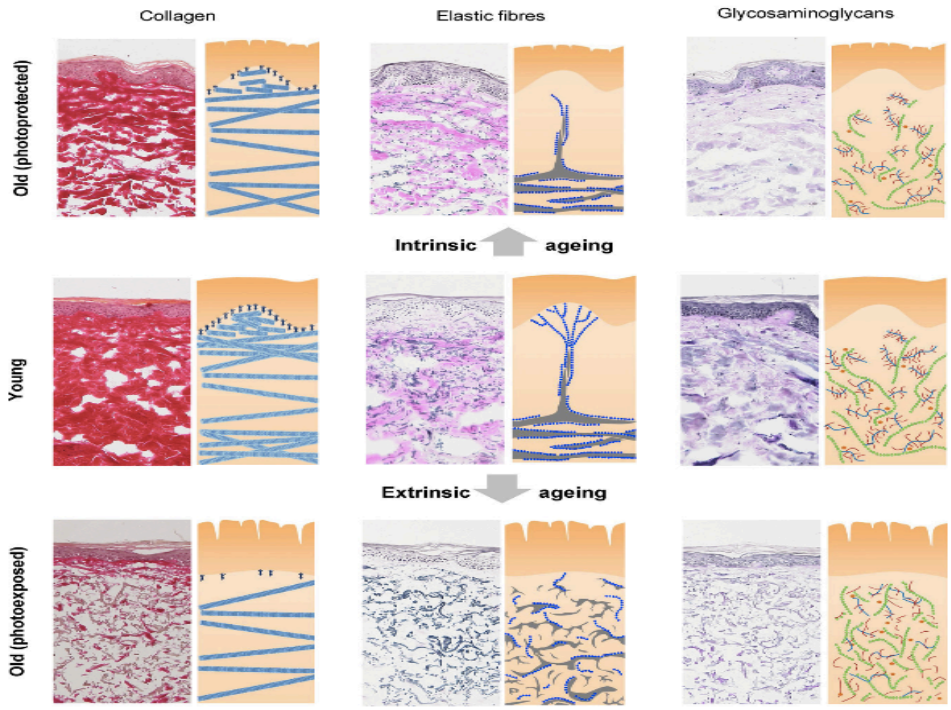

Figure 1.9: The structure of extracellular matrix proteins in young, old and photoaged skin (Naylor *et al.*, 2011).

1.3.6 Skin Cancer

There are three main types of skin cancer: SCC, BCC and MM, each with different rates of occurrence and prognosis. SCC and BCC are derived from keratinocytes at differing locations in the epidermis and were known collectively as non-melanoma skin cancer (NMSC) but are now called keratinocyte cancers (KC), and MM is derived from melanocytes. KC are extremely common, with 72,100 new cases in the UK in 2013, although this underestimates true occurrence as it is estimated that around 30% go unreported. The prognosis for KC is extremely good, with around 90% of cases successfully treated, and only around 2-5% of cases undergo distal metastasis, and even in this case there is still a good response rate to treatment. MM is the fifth most common cancer in the UK,

accounting for 4% of all new cases, with 14,500 new cases in 2013. Over the past 30 years, MM has been the fastest growing cancer of the 10 most common cancers. There are several different stages of MM, categorized by the amount of invasion into surrounding tissue and its depth. The prognosis is highly dependent on the stage. For stage 1 MM, almost all those diagnosed will survive. For stage 2, 80-90% will survive, stage 3 around 50% and for stage 4, which has metastasized into other parts of the body, the survival rates are only 10-25%.

UVR exposure has been unequivocally linked to the induction of skin cancer and is categorised by the International Agency for Research on Cancer (IARC) as a complete carcinogen i.e. it induces initiation and promotion. The initiation is via UVR-induced mutation in the genome, but UVR also inhibits tumour rejection by its immunosuppressive properties (Gjersvik, 2001; Kripke, 1974)

Genome sequencing technologies have demonstrated there are UVR signature mutations, with C>T, CC>TT and G>A mutations accounting for around 90% of total mutations in skin cancers (Leiter and Garbe, 2008; Pfeifer *et al.*, 2005). In the initiation phase DNA damage causes mutation in genes important for normal cellular function, and prevention of cancer via programmed cell death (apoptosis) (e.g. BCL2) and tumour suppressor genes, such as TP3, which codes for the tumour suppressor p53 protein. During the promotion stage, a mutated cell undergoes other changes leading to its proliferation to form a visible lesion, and eventually, under the correct conditions, to invasion into local and distal tissue via metastases. The p53 protein is a vitally important in the response to UVR exposure. It is activated in response to DNA damage via its phosphorylation by a

signal cascade, and directs the cell's response to UVR exposure. This leads to transcription of DNA repair enzymes, cell cycle arrest and apoptosis, with the aim of preventing carcinogenesis (Harris and Levine, 2005). Mutations in this gene therefore lead to impaired response to UVR damage; it has been shown that 90% of SSC have a mutation in p53, with 60% being a UVR characteristic C>T mutations (Brash *et al.*, 1991). There is also a link between extracellular matrix breakdown and an increase in tumour formation, as elastase deficient mice showed a significant decrease in UVR-induced tumour formation (Starcher *et al.*, 1996).

There is a large difference in skin cancer rates depending on the skin type. Lighter skin (skin type I/II) has a much higher incidence compared to darker skin (V/VI) individuals (Leiter and Garbe, 2008). This is thought to be mainly due to the presence of eumelanin because of its UVR absorption properties. At the same dose of 2-3 SED it has been demonstrated that that there is significantly more CPD formation in skin types II than IV (Mouret *et al.*, 2011). It has also been found that white Americans have a 70-fold higher risk of KC than in comparison to the black African-American equivalent, and around a 22 fold increase for MM (Lea *et al.*, 2007). There is evidence however this difference could be due to behavioural and social factors i.e light skinned people tend to seek sun and have a desire to tan, whereas darker skinned individuals tend to avoid the sun and do not want to become darker.

1.3.7 Photodermatoses

The photodermatoses are skin disorders in which there is an abnormal reaction to solar radiation. These are wavelength dependent and can be caused by UV or visible radiation (discussed later in visible light section). There are two main categories of photodermatosis – genetic or acquired.

Polymorphic light eruption (PLE) is the most common solar sensitivity condition affecting around 15% of the UK population. This is usually UVA induced and is characterised by an itchy erythema like papulo-vesicular rash which can occur within a few hours of exposure and last up to two weeks. Xeroderma pigmentosum (XP) is a much less common genetic disorder with only around 80 patients in the UK but has been vitally important in the study of DNA repair. In this condition there is loss of function in one of the XP proteins, which responds to, and repairs DNA damage induced by UVR. XP patients have a dramatically increased risk of skin cancer and a life expectancy of only around 32 years of age (Cleaver, 2005). Different conditions are induced by different wavebands of radiation for example PLE and XP symptoms are induced by UVR exposure, whereas erythropoietic protoporphyria (EPP) symptoms are triggered by visible light. This condition is discussed later in the 'visible light' section. Drug induced photosensitivity can be brought on by a number of different drugs and can have minor effects, such as a mild rash as with doxycycline which affects 4-40% of users depending on the dose, to a hugely increased risk of skin cancer in users of the anti-fungal voriconizole (Goyal, 2015). The first line of defence for these conditions is with the use of sunscreens or phototherapy.

1.3.8 Benefits of UVR

1.3.8.1 Vitamin D Production

The main beneficial effect of UVR on health is the production of vitamin D. This is a fat-soluble hormone that is acquired through the diet and from UVR exposure, with a peak production at around 300nm. The first step in the production of cholecalciferol (vitamin D_3) is the absorption of UVB photons by 7-dehydrocholestrol (DHC) to form previtamin D, which is followed by its thermal conversion to cholecalciferol, which mainly occurs in the epidermis. This is then transported by vitamin D binding protein where it is transported to the liver and kidneys to be metabolised to 25-hydroxyvitamin D and 1,25-dihydroxyvitamin D (calcitriol) respectively (Webb and Holick, 1988). Sufficient levels of vitamin D have been shown to be produced by short and limited UVR exposure (Dale Wilson *et al.*, 2012).

Vitamin D has numerous consequences on human health and is becoming of interest to many fields of research (Grant *et al.*, 2003). It was originally thought to be solely linked to bone health and conditions such as rickets (Shore and Chesney, 2013), but in recent years has been linked to a wide variety of diseases such as HIV (Spector, 2011), cancer (Nemazannikova *et al.*, 2013; Stubbins *et al.*, 2012) and immune system disorders (Hewison, 2011). Recently vitamin D receptors have been located in human skin that can be linked to different processes such as melanin production, which is thought to offer some natural protection to the skin from UVR (Kim *et al.*, 2013). Insufficient vitamin D levels

have been linked to rickets in children and osteoporosis and fractures in the elderly (Dale Wilson *et al.*, 2012). There is some conflicting evidence that vitamin D deficiency is linked to personal and lifestyle characteristics that are also determinants of disease (Autier, 2016).

1.3.8.2 Phototherapy

UVR can effectively be used to treat numerous skin conditions in a process known as phototherapy. Psoriasis is an autoimmune condition that manifests itself as a localised inflammation leading to inflamed scaly patches of skin. UVB phototherapy has been proven to be effective as it reduces cell proliferation and has anti-inflammatory effects leading to down regulation of T-cell response, improving the patient's symptoms. Psoriasis can also be treated with UVA in combination with a drug called psoralen that induces photosensitivity in a process known as PUVA therapy. A similar process has also shown to be effective in the treatment of vitiligo and cutaneous T-cell lymphoma (Dale Wilson *et al.*, 2012).

1.3.8.3 Blood Pressure Reduction

Finally, there is new evidence that UVR exposure can lead to a reduction in blood pressure. This is important because high blood pressure and associated cardiovascular disease is one of the leading causes of mortality. This is thought to occur by the conversion of the rich nitrogen oxide stores of the skin into nitric

oxide (NO) by UVA1. Controversially it has been suggested that this benefit outweighs the damaging effects of solar UVR on the skin (Weller, 2016).

1.4 Clinical Effects of Visible Radiation

Visible radiation, accounts for around 40% of the solar radiation that reaches the earth (Mahmoud Bh Fau - Ruvolo *et al.*, 2010) and until very recently, was not widely studied as a damaging agent to skin, mainly due to not being of as high energy as UVR. However as solar radiation is a continuum, its effects do not stop at the boundary of UVA and visible radiation. The mechanisms of effects caused by light are thought to be similar as those for UVR. Additionally, visible radiation also has longer wavelengths than UVR and can penetrate much deeper into the skin, potentially coming into to contact with a greater number of chromophores. In the past few years increasing research has been carried out, and it has been demonstrated that visible radiation can cause damage and undesirable effects. It is an area that is becoming of increasing interest of research, particularly to pharmaceutical companies who are interested in the development of visible light sunscreens.

1.4.1 Benefits of Visible Light

Visible light affects many aspects of life. It is vital for vision as different wavelengths of light activate different photoreceptors (rods and cones) in the retina to produce a neural impulse that the brain uses to produce vision (Palczewski, 2012). Light from vision is closely related to the maintenance of the circadian rhythm, which is thought to be regulated by a third type of photoreceptor, the retinal photosensitive ganglion cell. This sends a signal to the suprachiasmatic nucleus (SCN) in the brain which sets the body to a cycle of

around 24 hours, by the hormone melatonin (Munch and Bromundt, 2012). This cycle controls many different processes and it is thought that about 10% of all genes are controlled by the circadian cycle. Disruption of the circadian rhythm has been linked to many negative health effects such as renal complications, cardiovascular disease (Martino *et al.*, 2008), metabolic disease, psychiatric diseases (Desotelle *et al.*, 2012) and even cancer (Straif *et al.*, 2007). Melatonin release is also thought to contribute to immunomodulation (Haldar and Ahmad, 2010) with conditions such as seasonal affective disorder (SAD) being prevalent during winter when there are low levels of ambient light. SAD is effectively treated with bright light therapy (Kurlansik and Ibay, 2012; Pail *et al.*, 2011). There is also evidence that the circadian rhythm can affect the rate of repair of DNA photodamage in the skin, with greater repair occurring at some points of the cycle (Gaddameedhi *et al.*, 2014).

1.4.1.1 Photodynamic Therapy (PDT)

PDT combines visible radiation and a photosensitizer – usually a tetrapyrrole. These are molecules that contain four pyrrole rings, usually around a metal ion core, and are the active molecules in haemoglobin and chlorophyll. They are also linked to photosensitivity diseases discussed in the '*Adverse skin reactions to visible light*' section. PDT can be used to treat cancers, including skin cancers. The treatment requires drug delivery to the cancerous tissue, which undergoes a type I photoreaction with oxygen to produce $^1O_2$ that results in cell death. Sensitizers are designed to accumulate in cancer cells, especially in the organelles that most effectively cause death. This is a highly targeted strategy designed to cause

damage to cancer cells without systemic effects or to cause unwanted damage to healthy cells. The main considerations with PDT are drug and light delivery, light penetration and an adequate oxygen supply. Cancers in tissues that are hard to reach with fibre optics are not suitable for PDT, which is also being developed for use in other applications such as acne, photorejuvination and inactivation of bacteria (Agostinis *et al.*, 2011; MacCormack, 2008).

1.4.2 Negative Health Effects of Visible Light

1.4.2.1 Pigmentation

Much of the work of light on skin is based on its pigmentary properties, especially in darker skin types (III-VI). This is very evident in Asian skin types that pigment heavily, lasting many weeks (Duteil *et al.*, 2014; Mahmoud Bh Fau - Ruvolo *et al.*, 2010). In the study by Mahmoud et al, such pigmentation did not occur in a skin type II volunteer, however this was only a single volunteer so demonstrates limited value. Both UVA and visible light induced pigmentation, but visible irradiation gave 'darker and more sustained pigmentation' than UVA, present even 2 weeks post irradiation. However, the dose of visible radiation needed to cause pigmentation was many times higher than that for UVR (Mahmoud Bh Fau - Ruvolo *et al.*, 2010). This confirms work by Porges et al, who found that visible light induced pigmentation that lasted for around 10 days in skin types II-IV (Porges *et al.*, 1988) and Rosen et al (Rosen *et al.*, 1990) who found that IPD occurs up to wavelengths of 470nm in skin types IV-VI. Pigmentation has also been confirmed histologically by the significant increase in

melan-A positive cells (a melanocyte differentiation antigen) (Kleinpenning *et al.*, 2010). More recently repeated exposure to visible light has been shown to increase pigmentation more than that of a single exposure, with an increase in tyrosinase activity suggesting a response similar to the DT mechanism (Randhawa *et al.*, 2015). This is an area of particular interest to some Asian populations for which pigmentation is an undesired effect.

1.4.2.2 Erythema

Solar radiation can cause erythema with wavelengths longer than UVA1, but with much higher doses. Porges *et al*, reported erythema in skin types II-IV with doses of 40-80 J/cm^2 (400-700nm). This presented immediately, along with IPD, and faded within 24 hours of exposure (Porges *et al.*, 1988). Mahmoud et al found that erythema in melanocompetent skin (skin types IV-VI) presented in a dose dependent manner, after visible light (400-700nm) exposures with doses of 150-500J/cm^2 and erythema faded within 24 hours. This erythema was found as a halo surrounding the IPD response, which confirmed Porges et al findings of visible light-induced erythema, although the source used in this study had significant UVA1 contamination, which could account for the different doses required. (Mahmoud Bh Fau - Ruvolo *et al.*, 2010).

1.4.2.3 Reactive Oxygen Species

Some studies have investigated ROS produced by light. An *in vivo* method has been used to produce an action spectrum of ROS production in human skin across

UVR, visible light and IR (Figure 1.10). This reported that of the total ROS produced by solar radiation, 50% are produced in response to visible light and IR, demonstrating the importance of studying this region (Zastrow and Lademann, 2016).

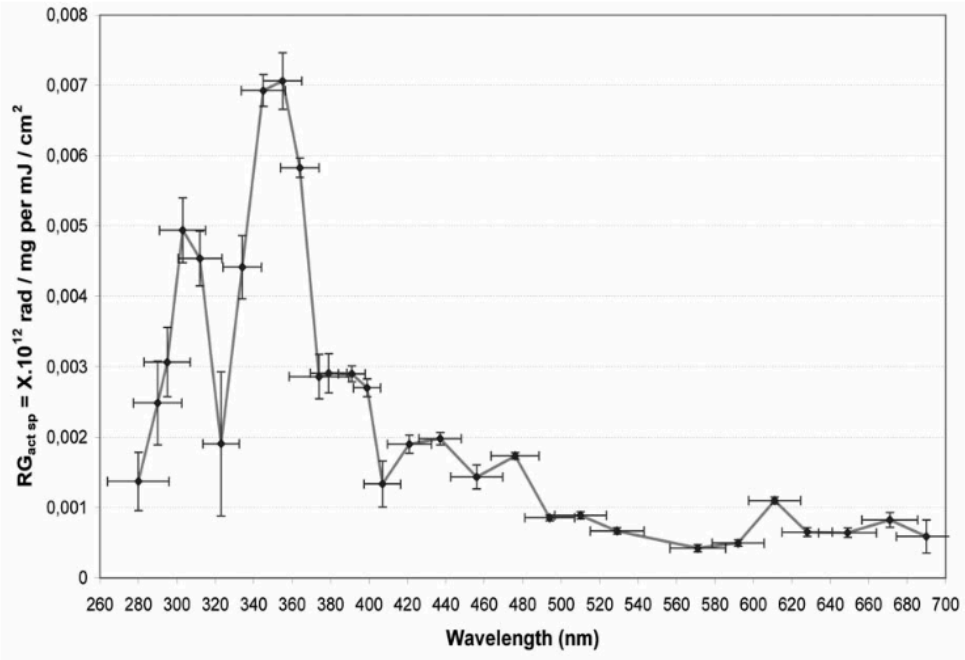

Figure 1.10: The spectral dependence of ROS formation measured *in vivo*.

ROS production has been confirmed by various methods in a range of cell types *in vitro* (Kushibiki *et al.*, 2013) and *in vivo* (Arndt *et al.*, 2013), particularly at the near visible wavelengths (400-500nm). A study by Liebel *et al* assessed the production of ROS by visible light using an *in vitro* epidermal equivalents model and *in vivo* on human volunteers. The visible light doses used were equivalent to 20-90 minutes of summer sun in Texas, USA. It was shown that light produced a dose dependent increase in ROS *in vitro*, which could be significantly reduced by anti-oxidants. A broad spectrum UVA/UVB sunscreen had no effect on the results. These findings were confirmed *in vivo*, which found an increase of 85%

in ROS production over background levels, which was also reduced by treatment with anti-oxidants (Liebel *et al.*, 2012). This confirmed the findings of previous work from Oplander et al, who used light emitting diodes (LED) that produced blue light at different wavelengths to test the oxidative stress produced. Wavelengths at 410nm and 420nm produced a dose dependent induction of ROS, which was not observed at 453nm or 480nm (Oplander C Fau - Hidding *et al.*, 2011). The Zastrow et al action spectrum, showed that production of ROS extended to 480nm (Zastrow *et al.*, 2009), but other studies have shown an effect up to 532nm in pigmented skin (Chiarelli-Neto *et al.*, 2014), so there is some conflict as to how far into the visible spectrum this effect is observed. There is growing evidence that the level of pigmentation is linked to the production of ROS, with an increase in pigmentation leading to an increase in ROS production after exposure (Chiarelli-Neto *et al.*, 2014). A *Xiphophorus* fish model of melanoma has also shown a link between melanin-photosensitzed oxidant production and melanoma production, with the action spectrum extending into the visible region (Setlow *et al.*, 1993; Wood *et al.*, 2006). This however is disputed in another study (Mitchell *et al.*, 2010).

1.4.2.4 Gene Expression

Differential expression of mRNA for MMP and inflammatory cytokines has been demonstrated. Liebel *et al* exposed human epidermal equivalents to different doses of light and assessed cytokine and MMP upregulation (Liebel *et al.*, 2012). There was a significant increase in IL-1α, IL-1 receptor agonist, IL-6, GM-CSF and IL-8 but not TNFα, unlike UVA. Additionally MMP-1 and MMP-9

production increased significantly and were also shown to be up regulated *in vivo* in response to visible and infrared radiation combined (Cho S Fau - Lee *et al.*). However, this is disputed in another study that found no significant change in MMP-1 expression *in vivo* after exposure to blue light (Kleinpenning *et al.*, 2010).

1.4.2.5 DNA Damage

As light induces ROS, it would be expected that it would have similar DNA damaging effects as UVA1, however there is limited research on this. Kvam and Tyrell produced an action spectrum for production of 8-oxodGua in human primary fibroblasts by UV and visible radiation. This showed a peak at 360nm, but production was still high at 405nm and some damage was detected at 434nm (Kvam and Tyrrell, 1997). Kuluncsics et al produced action spectra for formamidopyrimidine DNA glycosylase (FPG) sensitive sites (8-hydroxyguanine and formamidopyrimidines), CPDs and single strand breaks. FPG sensitive sites showed a second peak between 400-450nm. CPDs were still detected up to around 420nm, however other studies by Liebel shows that no CPDs, specifically thymine dimers, were induced by visible light, so it is unclear if these are produced (Kuluncsics *et al.*, 1999; Liebel *et al.*, 2012). Chiarelli-Neto et al investigated the effect of visible light (532nm) induced DNA damage in a cell line that could be induced to produce melanin. Endonucleases were used to identify specific lesions, FPG that recognises 8-oxoguanine, 8-hydroxyguanine and formamidopyrimidine, and Endo III which recognises strand breaks, abasic sites and additional oxidative pyrimidine modification (Chiarelli-Neto *et al.*, 2014).

They found that DNA damage was detected by the comet assay in the melanin-induced cell lines but not in the same cell line without pigment. Another recent study by Premi et al reported that UVA-induced melanin photosensitization produced delayed CPD with a peak around 4 hours after exposure in a murine melanocyte model, which could explain the effect seen by Chiarell-Neto (Premi *et al.*, 2015). IR has recently been linked to survival of cells containing UVR-induced DNA damage, demonstrating the importance to investigate effects outside of the UVR spectrum (Kimeswenger *et al.*, 2016).

1.4.2.6 Other Damage

Investigation into cell viability and apoptosis by visible light is limited. Induction of p53 has not been convincingly shown in studies *in vivo* in lighter skin types (II-III), although there was a slight induction 24 hours after the first irradiation, but this diminished with subsequent irradiations (Duteil *et al.*, 2014; Kleinpenning *et al.*, 2010). A decrease in cell viability and caspase-3 activation was shown *in vitro* in pigmented cells exposed to light that was not seen in cells lacking pigment. Membrane damage occurred, in addition to activation of caspase-3, suggesting cell death by necro-apoptosis - cell death that induces inflammation (Chiarelli-Neto *et al.*, 2014).

Other outcomes of light exposure have been observed in studies but these are much less well defined than the above effects. Denda and Fuziwara et al found that blue light (430-510nm) delayed epidermal permeability barrier recovery rate, where as red light (550-670nm) accelerated the recovery rate *in vivo* and *ex*

vivo in mice (Denda and Fuziwara, 2007). Blue light (412-426nm) in particular has been shown *in vitro* to induce toxic effects at high irradiances; dose dependently reducing proliferation, which leads to differentiation of the cells. Longer wavelengths of light had no effect (Liebmann *et al.*, 2010). This response could help explain the delayed epidermal barrier recovery rate in the previously mentioned study. Finally perinuclear vacuolisation was noted after visible exposure of keratinocytes, which decreased after irradiations had ended (Kleinpenning *et al.*, 2010).

1.4.2.7 Adverse Skin Reactions to Visible Light

There are a number of genetic and drug induced conditions, known as the porphyrias, which are linked to the dysfunction of the haem biosynthetic pathway enzymes. A number of different drugs such as sulphonamides, sulfonylureas and barbiturates can also induce porphyria. There are two main skin disorders that are initiated by visible radiation. These are EPP and solar urticaria. EPP is a condition in which the haem biosynthetic pathway is deficient because the final enzyme in the biosynthesis, ferrochelatase, has poor activity. This leads to a build up of the metabolite, and the UVA1 and visible light photosensitizer (λ_{max} 415nm), protoporphyrin IX. The photosensitivity is usually immediate and painful causing stinging and burning sensations (Lecha *et al.*, 2009). Patients are usually treated by the use of a high concentration zinc oxide based sunscreen which blocks some visible radiation reaching the skin, but these are cosmetically undesirable and are not very effective. The main advice given to

patients is to avoid sunlight exposure (Sarkany, 2002), however there is research currently being carried out on the use of alpha-melanocyte stimulating (MSH) analogues to treat photosensitivity disorders, by increasing melanin production which reduces solar penetration (Haylett *et al.*, 2011).

Solar urticaria is a disease in which patients are sensitive to UV and sometimes, visible radiation. This may cause a break out in hives in exposed and unexposed areas of the skin. The photosensitizer for this condition is not yet known but there are treatments available in the form of anti-histamines and phototherapy to desensitise the patients and lessen the allergic response (Lugovic Mihic *et al.*, 2008). Sunscreens are also used to better tolerate solar exposure (Faurschou and Wulf, 2008).

1.5 Endogenous Photoprotection

The skin's exposure to solar radiation has benefits in certain circumstances, however prolonged and high exposure to this radiation must be reduced to prevent skin cancer, photoageing and symptoms of photosensitivity. Photoprotection strategies advocated in public health messages include shade seeking, avoiding sun when it is high in the sky, and the use of clothing and sunscreens. The skin has several mechanisms to protect itself against solar radiation induced skin alterations. These include pigmentation, *stratum corneum* thickening, DNA repair and antioxidant capacity. These mechanisms provide protection by preventing the damaging UVR from reaching the epidermal cells, and dermal structural proteins, immune cells and fibroblasts.

1.5.1 Pigmentation

As previously mentioned, exposure to UVR, and in some skin types visible light, induces different forms of facultative pigmentation from IPD, PPD and DT. There is a wide range of constitutively pigmented skin types and both facultative and constitutive pigmentation offer photoprotection to the skin. This is demonstrated by the formation of melanin caps over epidermal basal cell nuclei, especially in skin types V and VI that have evolved to live in climates of high insolation, and are resistant to skin cancer. A light skinned individual may have a UVR tolerance of 1-3 SED before they sunburn compared to heavily a pigmented individual who could be able to withstand up to 20 times this dose. Other studies have demonstrated that pigmentation acquired over the spring/summer months

can increase the dose required to form sunburn by a factor of 2, and UVR exposures over a 4-week period increase the dose by a factor of 1.5 (Wulf *et al.*, 2004).

1.5.2 Stratum Corneum Thickening

Stratum corneum thickening has been demonstrated in numerous studies to be a consequence of UVR exposure (Gambichler *et al.*, 2005). This is believed to be a protective mechanism of the skin as the *stratum corneum* alone offers a base protection of preventing around 0.8 SED of UVR reaching the cells, which increases with thickness (Gniadecka *et al.*, 1996). UVR phototherapy is used to thicken the *stratum corneum* and to increase the levels of acquired pigmentation to increase the tolerance to UVR, in many photodermatoses (Honigsmann, 2003).

1.5.3 DNA Damage Repair

Damage to DNA is the most significant cellular consequence of solar exposure. In humans and other species, the damaged DNA bases are excised from the genome by three main mechanisms: nucleotide excision repair (NER), base excision repair (BER) and mismatch repair (MMR). MMR corrects post replicative erroneous insertions, deletions and mis-incorporations in the DNA strand and is not relevant to UVR induced DNA damage (Stojic *et al.*, 2004). Much of the understanding of DNA repair comes from studying patients with XP who have defects in their DNA repair enzymes (Cleaver, 1968). This leads to a 1000-10000-fold increase in the occurrence, and the early onset, of skin cancer

demonstrating the importance of repairing DNA photolesions (Grampurohit *et al.*, 2011).

The NER pathway is divided into two subgroups: global genome repair (GG-NER) and transcription coupled repair (TC-NER). GG-NER is responsible for most repair of CPDs and 6-4PPs in non-transcribed regions and prevents somatic mutations that could potentially be passed on to daughter cells by mitosis. TC-NER is similar but is selectively directed at the actively transcribing strands in the genome, with the two subgroups of repair only differing in the DNA damage recognition step (Cleaver, 2005; Cleaver *et al.*, 2009). DNA damage in GG-NER is recognised by the XPC and/or XPE proteins (also known as DDB2), which bind to the lesion in a hetrodimeric complex with DDB1 or HR23B respectively. For TC-NER, CSA and CSB proteins recognise the lesion, initialising repair by stalling the RNA polymerase II. From this point on, both GG-NER and TC-NER are identical. Upon recognition of the damaged DNA, XPB and XPD proteins complex and gain helicase activity and unwind the DNA to expose the damaged base. XPA and RPA determine the cleavage sites to which XPG and nuclease complex XPF-ERCC1 bind, and cleave the damage site. The excised site is then replaced by synthesizing new DNA with the enzymes PCNA and Pol δ. This process is shown in Figure 1.11 (Shah and He, 2015).

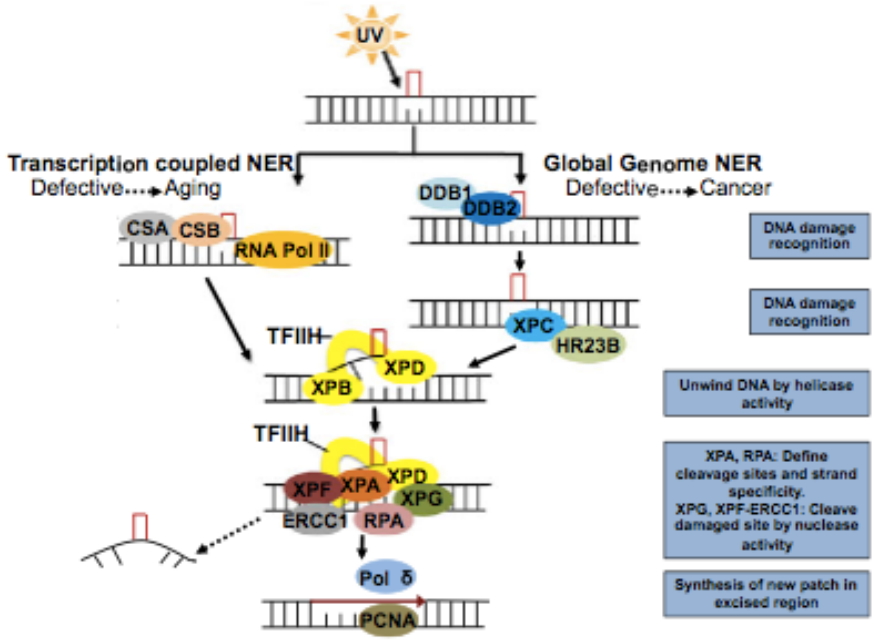

Figure 1.11: The NER pathway of DNA repair (Shah and He, 2015).

Unrepaired DNA damage can lead to genomic instability during cell division, as polymerases cannot synthesize DNA past the lesion, however special polymerases known as translesion synthesis polymerases (TLS) can allow replication to continue past the lesion. In general this is an error prone process compared with regular polymerases, but some are highly effective with minimal or no incorporated mutations. TLS across thymine-thymine CPDs is carried out by Pol η, which effectively places an A opposite the lesion, ensuring error free replication (Shah and He, 2015). TLS across 6-4PP is carried out error-free by Pol ζ, however the process can also be carried out in an error prone manner by Pol η or Pol ι (Jansen *et al.*, 2009).

The BER pathway repairs DNA damage caused by oxidative mechanisms, which produce lesions such as 8-oxoGua, FapyA and FapyG. The damaged bases

are excised by DNA glycosylases (mainly OGG1 and NTH1) that break the glycosylic bond between the deoxyribose sugar and base. The apurinic/apyrimidic (AP) site that is left in its place is removed by the enzyme AP endonuclease, and then replaced using Pol β, XRCC1 and DNA ligase III (Kozmin *et al.*, 2005; Moriwaki and Takahashi, 2008).

1.5.4 Antioxidants

Solar radiation can induce oxidative damage and the skin is equipped with antioxidant systems that act by preventing ROS from forming or by eliminating ROS. This defence includes numerous antioxidant enzymes such as: superoxide dismutase (SOD), hemeoxygenase 1 and 2 (HMOX-1, HMOX-2), catalase (CAT) and glutathione peroxidase (GPx) as well as non-enzymatic antioxidants such as vitamin C (ascorbic acid), vitamin E (α-tocepherol), carotenoids, ubiquinol and glutathione (GSH). These antioxidants eliminate the free radicals by electron sharing or elimination. For example SOD catalyses the conversion of O2□- to H_2O_2, which is then further converted into H_2O and O_2 glutathione peroxidase (Pandel *et al.*, 2013). These anti-oxidants can be quickly depleted by UVR exposure and the anti-oxidant defence system can be overcome.

1.6 Exogenous Photoprotection

Although endogenous methods of photoprotection attenuate the effects of solar radiation, they are often insufficient to prevent the clinical outcomes of exposure – erythema and tanning in the short term and skin cancer and photoageing in the long term. This has led to the development of exogenous photoprotection to complement the endogenous systems. The main form of protection is by sunscreens, however the future of this field involves a number of additional strategies including the use of visible light filters, antioxidants, iron chelators, DNA repair enzymes and systemic photoprotection.

1.6.1 Sunscreens

1.6.1.1 History of Sunscreens

The first recorded use of a sunscreen comes from the Egyptians who used formulations containing rice bran, jasmine and lupine to prevent tanning, rather than the other harmful effects of sun exposure, as lighter skin was more cosmetically desirable. It was only later discovered that these compounds filter UVR, enhance DNA repair and lighten the skin (Aldahan *et al.*, 2015).

After the discovery of UVR in 1801, its effects were investigated throughout the 1800s, until the early 1900s where it was decided that something was needed to protect the skin from UVR damage. The first 'modern' sunscreen filter was acidified quinine sulphate. Later a natural product called aesculin, which

was extracted from chestnuts, was sold under the brand name 'Zeozon' as a 3% mixture (Urbach, 2001). From this point to the current day, new sunscreens and formulations are continuously being developed to improve their absorption profiles, photostability, cosmetic appearance and many other characteristics.

1.6.1.2 Modern Sunscreens

Modern sunscreens are formulations that are applied to the skin. They contain a range of different sunscreen filters, with different absorbance profiles to provide broad-spectrum protection across the solar UVR spectrum. Sunscreens are usually classified as organic, inorganic or organic particulate filters.

1.6.1.3 Organic Filters

The organic chemical filters contain a chromophore, which is typically an aromatic molecule conjugated to carbonyl groups. In general, increasing the number of conjugated double bonds (and so generally the size of the molecule) and number of resonance structures (bringing importance to the substitution groups and their position around the aromatic ring) stabilizes the excited state and shifts the absorption spectrum to longer wavelengths and a larger absorption cross section – leading to UVB absorbers having typically smaller molecular weights compared to UVA and broad spectrum filters (Herzog, 2012; Osterwalder *et al.*, 2014).

The energy of UVR photons lies in the same magnitude as the energy of the filters' electrons, and allows for the absorption of UVR photons. Once absorbed, this causes a photochemical excitation of the electrons to a higher energy (π*) state (excited singlet state), the electrons then return to the ground state emitting the excess energy, which can occur by a number of different processes shown in (Figure 1.12).

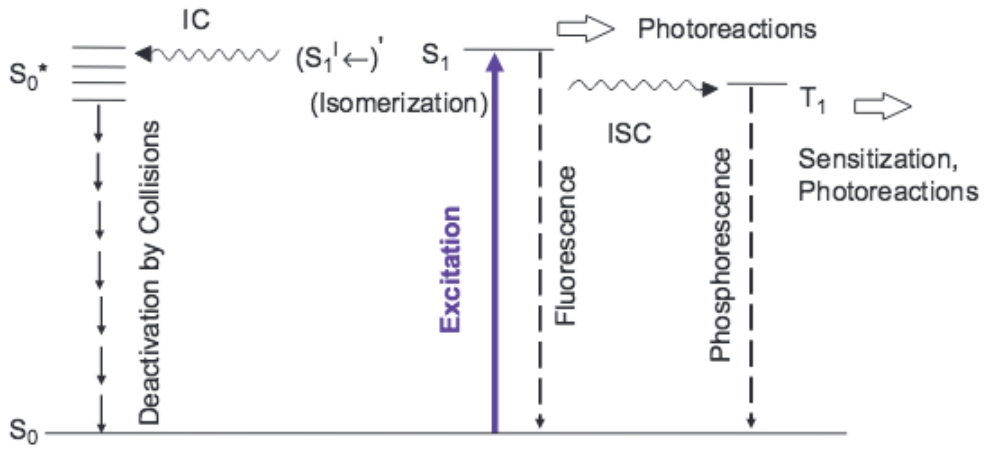

Figure 1.12: The routes of excess energy dissipation in UVR filters (Herzog, 2012).

The preferable route to dissipate the energy returning the excited molecule to the ground state is by internal conversion (IC), leading to dissipation by heat, or reversible isomerisation. When this is not possible, the remaining energy can be converted into photons as fluorescence, corresponding to the difference in energy between the two levels, as the energy released is lower than the energy initially absorbed. This energy can be emitted in either the visible, infrared or long wave UVR region (Lowe *et al.*, 1997). Finally, through intersystem crossing (ISC), the singlet excited state can cross to the triplet state which can lead to phosphorescence and potentially photosensitisation reactions. These reactions

can result in the transfer of the excess energy to oxygen molecules to form ROS, or to cause bonds to break (Herzog, 2012). This is highly undesirable for a sunscreen molecule; as the molecules need to be stable enough to prevent further damage, not potentially inducing increased damage.

1.6.1.4 Inorganic Filters

The inorganic filters that are commonly used in sunscreen formulations are titanium dioxide (TiO_2) and zinc oxide (ZnO), and despite popular belief also act by absorption of UVR, with only a minimal effect by reflection or scattering. A recent study demonstrated that the average reflection range of UVR by TiO_2 and ZnO was around 4-5%, equating to an SPF of less than 2 (Cole *et al.*, 2015). The UVR is absorbed by excitation of the electrons from the valence band to the conduction band. These molecules do not absorb in the visible range but being particles (due to their insolubility) causes the scattering and reflecting effect, which accounts for the white appearance on the skin. Clearly this is highly undesirable for a sunscreen, so these molecules are increasingly micronized to improve their cosmetic properties (Herzog, 2012; Lowe *et al.*, 1997).

1.6.1.5 Organic Particulate Filters

Some organic filters have limited solubility in the oil and water phases, which can cause difficulties in the formulation of consumer products. Producing these filters as aqueous particulate dispersions has solved this issue. This formulation is obtained using a wet milling method. In two examples of these filters,

Methylene Bis-Benzotriazolyl Tetramethylbutylphenol (MBBT) and Tris-biphenyl triazine (TBT), the organic particulate formulation has a slight UVA shift compared to the dissolved form but the specific extinction coefficients are comparable (Osterwalder *et al.*, 2014).

1.6.1.6 Formulation

Generally sunscreen preparations contain a mix of the above active ingredients with different absorption spectra to cover the different wavebands of the solar UVR spectrum (Tuchinda *et al.*, 2006). Sunscreens can be formulated for different needs, with some aimed at allowing more vitamin D producing wavelengths (Kockott *et al.*, 2016) through the filter and some prioritising UVB protection for example; however many argue that the 'ideal' sunscreen would act as a neutral density filter and uniformly protect against UVA and UVB (Osterwalder and Herzog, 2010).

1.6.1.7 Measurements of Photoprotection

The measurement of the efficacy of sunscreens is extremely important. There are a number of different methods that have been developed for this task, which employ *in vivo* and *in vitro* techniques.

1.6.1.8 Extinction Coefficients

The Beer-Lambert law, states the absorbance of a sample is directly proportional to its thickness (path length) and concentration. This law is used to calculate the molar extinction coefficient of a filter and determine the relative absorption of a compound at a given wavelength. This is usually calculated at its maximal absorption wavelength (λ_{max}). The extinction measures the UVR attenuation properties of filters but does not take into consideration the full spectrum, and is mainly useful for testing how different conditions affect the absorption such as the solvent used (Agrapidis-Paloympis and Nash, 1987).

1.6.1.9 The Sun Protection Factor (SPF)

The SPF was introduced in 1962 and is the most important and well-known metric for quantifying sunscreen efficacy. It is a simple biological test measured *in vivo* in human volunteers (test method is described by ISO 24444). This first measures the volunteers' minimal erythemal dose (MED) using incremental doses of solar simulating radiation (SSR) on the lower back (as this is generally an unexposed area). The MED is the threshold SSR dose at which erythema occurs without any protection (MED_u). This process is then repeated with the application of the sunscreen at $2mg/cm^2$ skin to determine the MED with protection (MED_p). The SPF is the obtained by the following equation (Equation 1.2):

$$SPF = \frac{MED_p}{MED_u}$$

Equation 1.2: The calculation for determination of the SPF of a sunscreen.

The SPF is more biologically relevant than the extinction coefficient as it measures the formulated sunscreens' *in situ* efficacy under laboratory conditions, rather than the optical proprieties of the active filters. This test is agreed upon around the world as defined by ISO. There are very detailed criteria for this test. For example, the SSR spectrum must comply with rules that dictate the spectral composition. There is a common misconception that the SPF is solely a measure of UVB protection, however this is not the case. UVA also induces erythema, although it is much less effective at doing so compared to UVB.

Work has been carried out *in vitro* to determine the transmittance of UVR through formulations of differing SPF. An SPF 60 sunscreen transmits half as much UVR as an SPF 30 sunscreen ie 1.7% compared to 3.33%. Another study using SPF 15, 30 and 60 sunscreens demonstrated that after 10 minutes of SSR exposure, 80% of a sunburn dose is reached with an SPF 15 sunscreen compared with 40% for an SPF 30 and 20% for an SPF 60 (Osterwalder *et al.*, 2014; Sambandan and Ratner, 2011). There is however an incorrect widespread belief that this is not the case that stems from the looking at the amount of UVR that is blocked, for example SPF 30 sunscreens blocks 96.67% and SPF 60 blocks 98.3%, but the important number is the amount of photons that are transmitted.

The determination of SPF requires *in vivo* measurement in human volunteers. Despite many attempts to establish an *in vitro* method, none has been able to accurately replicate the *in vivo* technique. An *in vitro* determination of SPF is a high priority of the sunscreen industry, as this will reduce the time and costs of testing, as well as solving the ethical implications of using human volunteers (Osterwalder and Herzog, 2010).

1.6.1.10 UVA Protection Measurements

There are a number of methods to measure the ability of sunscreens to prevent UVA damage. These involve *in vivo* and *in vitro* approaches with the primary method varying from country to country. The *in vivo* UVA-PF (ISO 24442) method was developed in France by L'Oreal, and is based on the prevention of PPD. This method is now accepted in Europe and the U.S.A., and soon to be worldwide. This method is much like the SPF, but PPD is used as the endpoint instead of erythema. In Australia, Europe, and in particular the U.K, an *in vitro* method is preferred (ISO 24443) as this reduces the cost and removes the ethical issues associated with using volunteers. The *in vitro* method is based on the transmission of the UVR through the sunscreen, the PPD action spectrum and the *in vivo* SPF value and provides a relative measurement of the protection offered. The issue with UVA protection comes with the recommended amount of protection relative to the SPF and the labelling of this, which varies from country to country. This is largely based on the ratio of UVA to UVB and/or SPF. The UK-Boots star rating recommends a UVA/UVB protection ratio of >0.9 for the highest 5* rating and is independent of the absorbance values, just the shape of the

curve. The US proposed a UVA-PF of >12, and/or UVA-1/UV ratio of >0.95 and a critical wavelength of ≥370nm for the highest 4* rating. The agreed European Commission recommendation suggests a UVAPF/SPF ≥1/3, with the critical wavelength above 370nm. In the critical wavelength test, the absorbance of the sunscreen is integrated from 290nm to 400nm, until the sum reaches 90% of the total absorbance, and the wavelength this falls on must be above 370nm (critical wavelength). This system does not use a rated system and is just the requirement for being labelled as UVA protective, and the requirements are designed to ensure that formulations are shifted more towards the 'ideal' sunscreen (Osterwalder and Herzog, 2009). Although this ensures broadband protection, it also means that a sunscreen will provide less protection in the UVB region for a given SPF (Young *et al.*, 2010).

1.6.1.11 Efficacy of Sunscreens Against Non-erythema Endpoints

Sunscreen use is widely advocated to prevent solar UVR induced damage and ultimately skin cancer and photoageing. There have been many studies exploring the efficacy of sunscreens measuring numerous endpoints.

Prospective studies have shown a direct protective effect of sunscreen use against AK (Naylor *et al.*, 1995; Thompson *et al.*, 1993) and SCC (Green and Williams, 2007). A large randomised trial (the Nambour trial) over 4.5 years in Australia demonstrated that sunscreen (daily SPF 16 application) users had 39% fewer SCC on sun exposed areas compared with the control group, with an 8 year follow-up showing a further 40% reduction in SCC (Green *et al.*, 1999; van der

Pols *et al.*, 2006). The ability of sunscreens to protect against BCC is unclear. In the above study there was no effect on BCC in the sunscreen group compared to control after 4.5 years. In the 8-year follow up trial BCC rates tended to decrease but this was not statistically significant. There is some criticism of this work as the results may have been skewed by the fact that 26% of the non-intervention group regularly applied sunscreen, and with the intervention group applying the sunscreen poorly. Although this would better reflect real world conditions (Iannacone *et al.*, 2014), it means the two groups sunscreen use would be more similar than intended. In addition this study does not take into consideration other confounding factors like phenotype, previous sunscreen use and exposure and frequency of sunscreen use (Lautenschlager *et al.*, 2007). It is also important to note that sunscreen formulations have vastly improved since these studies were carried out.

Photoprotection by sunscreens against MM is even less clear. Several studies have indicated that sunscreens are associated with increased nevus density, which is used as a predictor of melanoma. Other studies have shown a decrease in nevus development (Lautenschlager *et al.*, 2007). A review of 18 heterogeneous case controlled studies found no association between sunscreen use and melanoma (Dennis *et al.*, 2003), but a recent randomized follow up to the Nambour trial found that 10 years after the trials end, the sunscreen group had 11 new primary melanomas compared to 22 in the discretionary group, with a substantial reduction in invasive melanomas (3 vs 11) (Green *et al.*, 2011). Another population based study found use of sunscreens of SPF 15 and above prevented melanoma (Ghiasvand *et al.*, 2016). This indicates the uncertainty in

sunscreen's prevention against cancer, but again in these studies there are many confounding factors, many of which are discussed in the *'Behavioural Issues'* section. Again, a major limitation of this study is that sunscreens have improved massively, particularly in protection against UVA damage. This is highly significant, as fish models of melanoma (although disputed) have implicated UVA as an inducer of melanoma (Wood *et al.*, 2006). Most of the understanding into cancer prevention by sunscreens comes from only one trial, so much more work needs to be done to understand fully.

There is good evidence to show that sunscreen use is effective in preventing photoageing. Studies in mice, as a model of human skin, have demonstrated the ability to prevent photoageing, with even a UVB sunscreen with an SPF of 2 showing some benefit, with the addition of a UVA filter showing even greater benefit (Young, 1990). Another study in humans over 24 months revealed that the application of sunscreen prevented solar elastosis compared with a placebo group. The same study found other photoageing markers measured, including epidermal thickening and organisation, and dermal inflammatory infiltrate found no difference between intervention and placebo groups (Boyd *et al.*, 1995). The Nambour skin cancer trial also evaluated photoageing in the younger participants (to measure the effect of photoageing rather than natural ageing) by measuring the presence and severity of photoageing on the back of the hand at baseline, 4.5 years and 8 years. After 4.5 years there was no detectable increase in photoageing in the intervention group and when compared to the control group they were 24% less likely to show an increase (Hughes *et al.*, 2013).

Broad-spectrum sunscreens have been demonstrated to be significantly effective in preventing solar radiation induced immunosuppression, with a repeat exposure study finding delayed-type hypersensitivity (DTH) was significantly reduced compared to unprotected volunteers, however a UVB sunscreen failed to protect effectively, signifying the importance of broad spectrum protection (Moyal and Fourtanier, 2008).

Many of the photodermatosis show peak sensitivity in the UVA and visible ranges and sunscreens have poorer protection in this region; so many sunscreens are ineffective in providing protection to patients, particularly in EPP. For some conditions broad-spectrum sunscreens with high UVA protection can provide some protection for example against rash formation in PLE, and in actinic dermatitis. In other conditions like XP, a high SPF sunscreen with a UVB bias has proven to be effective (Deleo, 2006; Lenane and Murphy, 2001).

1.6.2 Visible Light Filters

As visible light becomes increasingly studied as a damaging agent to the skin, the interest in protecting against the damage has grown with a recent study suggesting the importance of visible light photoprotection (Zastrow and Lademann, 2016). The first logical step in protecting the skin will be to mimic the strategies used in photoprotection against UVR – with the use of filters to absorb the damaging wavelengths. This however has its own issues, as filters blocking wavelengths of visible light will appear coloured on the skin, a problem not relevant in UVR photoprotection, as the eye cannot recognise this spectral

region. As this is a relatively new area of research there is currently only one known visible light sunscreen formulation known as the "Dundee cream", which is used by patients with visible light allergies and only provides minimal protection. This takes advantage of the reflective properties of titanium dioxide and zinc oxide, with the addition of colouring agents. This only provides minimum protection and is also very unpleasant to use – it is very thick and sticky, and is mainly used by EPP patients. Visible photoprotection is of particular interest to photodermatoses patients, as many of the conditions have an action spectrum peak in the long wave UVA and visible regions, in which there is much less protection currently (Lenane and Murphy, 2001).

1.6.3 Antioxidants

Although the skin has its own antioxidant systems, these can be quickly overcome by ROS, with cell cultures and mouse models having demonstrated that both enzymatic and non-enzymatic antioxidants are greatly reduced after exposure to UVR (Shindo *et al.*, 1993). This can lead to DNA damage, lipid peroxidation and protein oxidation (Pandel *et al.*, 2013; Sander *et al.*, 2002). This has led to research into topically applied and orally supplemented antioxidants to enhance the skin's capacity to cope with oxidative stress. Along with using endogenous antioxidants such as carotenoids and vitamin C (ascorbic acid) and vitamin E (α-tocepherol), many natural antioxidant polyphenol products, such as green tea polyphenols (Elmets *et al.*, 2001) and grape seed extracts (Ageeva *et al.*, 2015) have been examined in their effectiveness to reduce solar radiation

induced oxidative stress. Despite some evidence of their benefit, their use has not been fully proved as effective.

1.6.3.1 Carotenoids

The carotenoids are a large group of plant lipids, present in fruits and vegetables that tend to have radiation absorbing, provitamin and antioxidant properties. They are composed a long chain of conjugated double bonds with acyclic or cyclic substituents and occasionally functional oxygen groups.

There are thought to be three modes of action of the carotenoids, (i) absorption of radiation, (ii) quenching of $^1O_2$ and other ROS produced during oxidative damage and (iii) the production of retinoic acid, required for cell growth, development and immune function. These compounds are absorbed by the gut from dietary intake and transported in the blood stream via lipoproteins to the skin by where they are deposited in the epidermal layer, most likely through interaction with cholesterol transporters such as scavenger receptor class B member 1 (SR-B1) (Goralczyk and Wertz, 2009).

There have been several studies *in vitro* and *in vivo* in various different cell types and models to examine the effects of carotenoids, reporting the ability to prevent lipid peroxidation (Goralczyk and Wertz, 2009; Lomnitski *et al.*, 1997), $^1O_2$ (Ranadive *et al.*) and photo-inactivation of enzymes (O'Connor and O'Brien, 1998). There have also been human intervention studies with carotenoid rich diets to assess protection. These have shown a decreased sensitivity to UVR-induced erythema, with one study reporting an equivalent of 16mg of lycopene a

day for 10 weeks (acquired through tomato paste), reduced erythema by 40%, measured by chromatometry (Stahl *et al.*, 2001). These results have been confirmed in other studies, however no protection has also been demonstrated, possibly due to the fact that these studies were carried out for a shorter time periods, so the effectiveness remains unclear (Fernandez-Garcia, 2014). β-carotene, apigenin and chrysin has recently been linked to photoprotection against UVA and visible light induced damage (Freitas and Gaspar, 2016).

1.6.3.2 Vitamin E

Vitamin E refers to 8 different compounds, of which α-tocopherol is the most abundant. They are acquired from the diet mainly in vegetables, oils cereals and nuts, and are absorbed by the same method at the carotenoids. Vitamin E is thought to act mainly by radical scavenging but there is also some evidence of UVR absorbing and cellular response modification by the arachadonic acid cascade. α-tocopherol has been the subject of many different anti-oxidant studies. UVB induced cell toxicity was reduced in fibroblasts, and additionally in supplemented mice, lipid peroxidation was cut by one third compared with mice without supplementation (Fernandez-Garcia, 2014). In studies in humans much of the evidence has shown no protective effect of supplementation (McMillan *et al.*, 2002; Werninghaus *et al.*, 1994), unless in combination with other antioxidants such as vitamin C, which resulted in an increased MED (Fuchs and Kern, 1998), and with carotenoids, which showed reduced erythema (Stahl *et al.*, 2000).

1.6.3.3 Vitamin C

Vitamin C is acquired mainly from citrus fruits, however other fruits and vegetables are also a source, and is absorbed by active transport. It is required for many different enzymatic reactions in the body in addition to its anti-oxidant capacity. Both vitamin C and vitamin E have higher levels in the epidermis than in the other layers of the skin (Fernandez-Garcia, 2014). The protective effect of vitamin C has been demonstrated *in vitro* in keratinocytes which showed a significant decrease in UVB induced oxidative DNA damage (Stewart *et al.*, 1996), Protection against UVA-induced lipid peroxidation and inhibition of secretion of pro-inflammatory cytokines (Tebbe *et al.*, 1997) has also been demonstrated. As with vitamin E, *in vivo* studies have only demonstrated a protective effect in combination with other antioxidants (Fuchs and Kern, 1998; Placzek *et al.*).

1.6.3.4 Polyphenols

Polyphenols are a large family of UVR absorbing anti-oxidant molecular pigments that are responsible for the colour of many plants. They consist of many different subgroups: flavanones, isoflavones, proanthocyanidins, anthocyanidins, flavenols and catechins. The beneficial effects of consuming fruits are thought to be due to the polyphenols, but they are poorly absorbed by the gut. The molecules that are absorbed conjugate to glucuronide, sulphate and methyl groups in tissues (Fernandez-Garcia, 2014).

Much of the work into their benefit has been carried out on green tea polyphenols and grape skin extracts. Green tea polyphenols have resulted in a reduction of erythema, skin tumour development and pro-inflammatory cytokine release in UV irradiated hairless mice (Nichols and Katiyar, 2010). They are protective against UVB-induced DNA damage in keratinocytes and human skin equivalents (Schwarz *et al.*, 2008). Red grape wines have also shown anti-oxidant and radical scavenging properties (Ageeva *et al.*, 2015). The protective effect in human studies of green tea polyphenols is less well defined with one study with supplementation over a four-week period finding no effect in reducing erythema, although participants reported less severe sunburn (Chow *et al.*, 2003). Flavanol studies have shown more promise with high dose supplementation over 6-12 weeks, which showed a significant reduction in erythema and an improvement in skin condition (Greul *et al.*, 2002; Heinrich *et al.*, 2006).

1.6.4 Topical DNA Repair Enzymes

Topically application of DNA repair enzymes is one of the emerging fields of photoprotection. Originally they were developed to treat XP patients by applying the bacterial T4N DNA repair endonuclease V (T4N5) to remove CPD photolesions, and they are believed to act in a similar way in the BER repair pathway (Zahid and Brownell, 2008). Application of this enzyme to the skin of XP patients resulted in a decrease in the formation of precancerous AK by over 68% and a 38% reduction in BCC (Yarosh *et al.*, 2001). In a more recent, 6 month long randomised clinical trial, two sunscreens were tested in AK patients, one was a

traditional formation alone, and another that contained the sunscreen plus DNA repair enzymes. Both regimes provided a significant decrease in the formation of hyperkeratosis, with no marked difference between the two; however when measuring occurrence of CPDs, there was a 35% reduction in the sunscreen group, compared with a 61% reduction in the sunscreen plus repair enzymes group (Carducci *et al.*, 2015). Plant derived OGG1 is also used in a similar manner, although no clinical benefit was demonstrated recently (Emanuele *et al.*, 2014).

Another class of DNA repair enzymes are the photolyases. These enzymes use the energy in differing wavelengths of light to 'photoreactivate' and repair the lesion. These are found throughout nature but are not thought to occur in placental mammals. Photolyases are lesion specific, with enzymes specific to CPDs (class I and II) and 6-4PPs (class III) (Weber, 2005). Class I, CPD photo-reactivating enzymes can be further be subdivided according the light-harvesting co-factor present: a folate, with 5,10-methenyltetrahydrofolyl-polyglutamate (MTHF) as the second chromophore or a deazaflavin, with 8-hydroxy-5-deazaflavin (8-HDF) as the second chromophore. MTHF for example has an absorbance maximum at 384nm, so exhibits the greatest catalytic ability in the range of 377-410nm, meaning exposure to less damaging wavelengths are effective in repairing the damage (Weber, 2005).

There are few clinical studies on the effectiveness of photolyase, though two recent studies have demonstrated efficacy, with photolyase in addition to a sunscreen providing significant protection against cell death and CPD formation

compared to sunscreen alone (Berardesca *et al.*, 2012). A more recent study measured a cocktail of filters, DNA repair enzymes (photolyase, endonuclease and OGG1) and powerful anti-oxidants (carnosine, atrazine and ergothionine) and found improved genomic and proteomic integrity of skin cells, with a synergistic reduction in CPDs. However as this was a cocktail its hard to distinguish the effect of photolyase alone (Emanuele *et al.*, 2014).

1.6.5 Iron Chelators

The prevention of UVR induced free iron release by iron chelators is an increasingly studied area. These act by forming a stable complex with iron to prevent the Fenton reaction (*'Fenton Reaction'* section) from taking place, and usually have a low redox potential to reduce the number of Fe^{2+} compared to the less damaging Fe^{3+} ion (Kitazawa *et al.*, 2006).

There is some evidence that topical iron chelators can be effective, with a study indicating a 5% solution of 2-furlidioxime (FDO) provided a 90% reduction against induction of ornithine decarboxylase (ODC), and a 3.5 fold protection against erythema, reduction in SBC, epidermal thickening and infiltration of inflammatory cells (Bissett *et al.*, 1994). The second generation of iron chelators is currently being developed, with the goal of activation in response to solar radiation exposure. This would reduce the risk of side effects due to differential iron homeostasis in the unexposed state. A collection of these second-generation caged iron chelators has been evaluated *in vitro* and it was found that intracellular labile iron pool (LIP) and necrotic cell death is significantly reduced

when fibroblasts were exposed to UVA radiation, but no difference was observed without irradiation (Yiakouvaki *et al.*, 2006).

1.7 Issues with Sunscreen Use

The discussion above has shown that sunscreen use has many beneficial effects on human health in reducing skin cancer incidence, immune suppression and photoageing. However, there are still many unresolved issues with their use.

1.7.1 Behavioural Issues

Many of these issues are not directly related to the sunscreens themselves but more to do with the attitude, lack of understanding and behaviour associated with their use. The SPF is tested at very carefully controlled conditions, with a uniform application at 2mg/cm^2, and these conditions are required by the user to achieve the labelled SPF. In reality only 0.39-1mg/cm^2 is applied, meaning a sunscreen labelled as SPF 30 could actually only provide an SPF of 15 or in some cases around SPF 6 (Petersen and Wulf, 2014). Uniformity of the application is also a major issue affecting the level of protection received, along with the number of applications and when the sunscreen is applied and reapplied (for example after swimming or sweating) (Diffey, 2001).

Many argue that sunscreen use actually increase the users exposure to UVR, giving them a false sense of security and leading to increased time spent in the sun, especially when the sun is at its highest. A study of students on summer holiday found participants in an SPF 10 group tending to have less sun exposure than the SPF 30 group (52.8 vs 72.6 hours respectively) (Autier *et al.*, 1999). This is corroborated by a more recent study that concluded that UVR exposure

doses were considerably higher on days where sunscreen was used and on days where sunburn occurred, and that sunscreen application showed no link with days without risk behaviour (Thieden *et al.*, 2005).

In addition to the lack of understanding in how to apply sunscreen correctly and the behaviour their use encourages, there is also a problem with the attitude to sunscreens, which affects their use. Numerous studies have been carried out investigating why different groups do not use sunscreens regularly or at all in some cases, but many of them come to the same conclusions:

- Cost
- Unpleasant to use (greasy, sticky)
- Adverse reaction (acne, stinging of the eyes)
- Forgetfulness
- Time taken to apply sunscreen
- Inhibits ability to tan
- Safety concerns (Nanoparticles)

(Lee *et al.*, 2015; Wang and Dusza, 2009; Wysong *et al.*, 2012).

The safety concerns also link with a desire by the public to use more natural products as they are perceived to be safer, which could increase their use among a section of the population (Kim and Seock, 2009). These issues lead to ineffective use of sunscreens and lack of compliance. This may result in the assumption that sunscreens are ineffective in preventing sunburn, or that they may cause more damage than they prevent, when it is actually the poor level of understanding/compliance that is the problem. It is almost certainly these

factors that contribute to the lack of evidence for sunscreens to prevent cancer, as there are many confounding factors influencing their intended use.

1.7.2 Health Issues

There is much debate into the negative health effects of sunscreen use. A number of studies have reported that sunscreens and filters cause allergic reactions. An Australian study in 1993 found that adverse reactions from sunscreens are reported in 19% of users, including allergic and contact dermatitis, phototoxic and photoallergic reactions and it some cases anaphylaxis (Foley *et al.*, 1993). Octocrylene (OCT) has been studied extensively and has been shown to be a contact and photocontact allergen on UVR exposure, possibly caused by its interaction with the amino acid lysine (de Groot and Roberts, 2014; Karlsson *et al.*, 2011). This is not the only filter to have caused an allergic response; numerous other sunscreen filters have also been shown to induce responses in the skin (Burnett and Wang, 2011; Heurung *et al.*, 2014; Saraswat, 2012). These reactions are relatively rare and are disputed (Osmond-McLeod *et al.*, 2016), and many allergic reactions associated with sunscreens are actually caused by preservatives and other "inactive" chemicals in the formulations, but this needs to be considered with continued monitoring.

Another concern of sunscreens is with their potential for systemic absorption and accumulation in the body. Oxybenzone has been extensively studied and there is some evidence that it can be absorbed and accumulated in the body. After topical application, oxybenzone was found systemically intact, and with

some metabolites, in urine (Hayden *et al.*, 1997). Other studies have shown similar results with different filters, all found in the plasma and urine after topical application (Janjua *et al.*, 2004). A study in rats by Okereke *et al* showed a peak plasma level at 2.5 hours and that the expulsion of the filters from blood plasma was biphasic. It was shown that there was an accumulation of the compound metabolites in the liver, kidneys, spleen and testes (Okereke *et al.*, 1994). This work has not been confirmed in humans but the presence of some filters has been reported in other bodily fluids such as faeces, semen, breast milk and placental tissues (Chisvert *et al.*, 2012).

The concern with UVR filters being absorbed by the skin and taken into systemic circulation is that they may act as endocrine disruptors. Some filters have demonstrated estrogenic or anti-androgenic properties, however much of this work as been focused *in vitro* and *in vivo* in mice rather than in humans. The *in vitro* work has mainly been carried out on human breast cancer cells or in receptor assays, which have shown that oxybenzone and its metabolites compete with estradiol to bind estrogen receptors, which can activate estrogen-regulated gene expression (Burnett and Wang, 2011; Schlumpf *et al.*, 2001; Schreurs *et al.*, 2005). Another study in mice tested endocrine activity of filters by the oral route and a dose dependent increase in uterine weight was observed suggesting a hormonal effect, however the doses in this study were unrealistically high (Schlumpf *et al.*, 2001). After a full body application of sunscreen in human volunteers at the recommended application density of $2mg/cm^2$, plasma levels of the filters and numerous different hormones were measured (FSH, LH, testosterone, estradiol and inhibin B) and it was found that only a slight

difference in the levels occurred. It was concluded that these difference were not due to the sunscreen absorption but due to variation of the volunteers (Janjua *et al.*, 2004). More recent work on mouse and human liver microsomes has revealed numerous metabolites of benzophenone-3 (BZ-3), which have differing levels of estrogenic activity in addition to BP-3 itself (Watanabe *et al.*, 2014). This shows there may be an endocrine disruptive effect that requires further investigation.

The above problems with sunscreens relate to organic filters, but the inorganic filters TiO_2 and ZnO have their own concerns. These are micronised to nanoparticles (sizes between 1-100nm) to reduce the white colour on skin, which is undesirable to users, and to improve UVR protection. However, this can also change the properties of the particles, giving rise to concerns about toxicity and absorption. The absorption of filters through the skin has been extensively studied and nanoparticles have not been shown to penetrate the *stratum corneum* when applied topically to intact, healthy skin. Less is known about diseased skin or through other administration routes. The suggested toxicity of nanoparticles is more complicated. It has been hypothesised that these filters can be toxic to skin by generating ROS upon UVR exposure. There are conflicting reports with many *in vitro* studies demonstrating this may be the case but more recently this has been disputed (Burnett and Wang, 2011; Dufour *et al.*, 2006; Wang and Tooley, 2011). Zinc oxide nanoparticles have recently shown a significant increase in oxidative DNA damage upon exposure to UVB radiation *in vivo* in hairless mice suggesting much more research is needed (Pal *et al.*, 2016).

Due to the overlap in the absorbance spectra of sunscreens and the action spectra for vitamin D production, there is concern that sunscreens will inhibit vitamin D production. Numerous studies seem to have shown this to be the case (Matsuoka *et al.*, 1987; Matsuoka *et al.*, 1988), but unpublished work by our group and other field studies have shown this to be incorrect (Marks *et al.*, 1995). One important factor in these studies is that sunscreen is not used as in test conditions (Burnett and Wang, 2011) and there have been efforts to formulate sunscreens with increased potential for vitamin D production (Kockott *et al.*, 2016) .

1.7.3 Environmental Damage

In addition to behavioural and health issues, there are a number of negative environmental impacts with synthetic sunscreens use, particularly to coastal and marine environments. As sunscreens are particularly stable molecules by design, they are not readily broken down and so accumulate in the environment. This can lead to a wide variety of environmental impacts.

UVR filters have been found in many different environmental samples but their impact to the environment has been less well studied (Fent *et al.*, 2010; Zenker *et al.*, 2008). Levels of filters found in the sea water around beaches and costal areas can be high but these can be higher in lakes and rivers as they are in a closed system (Fent *et al.*, 2008). In a 2013 study, Tovar-Sanchez investigated the potential effect of sunscreen filter release in near shore waters by beachgoers in Majorca. They found the presence of four main filters: 4-

methylbenzylidene camphor (4-MBC,) BZ-3, TiO2, ZnO in the surface microlayer of samples in concentrations up to 38±7μg/L. The amount found varied throughout the day but peak times were between 14:00 and 18:00. Two of the filters were even found in waters along the coast of pristine beaches showing alongshore connectivity, meaning the impact of these chemicals would be on the whole island, not just the source areas. This study also investigated the effects of sunscreen on inorganic nutrient release. It was found that PO_4^{-3} was the nutrient with the greatest increase. The authors conservatively estimated that sunscreen use could lead to a 55% increase in the PO_4^{-3} concentration in offshore waters which is enough to have a significant impact on phytoplankton by increasing algal growth resulting in various negative effects (Landsberg, 2002). Conversely the concentrations of filters found in the samples were several magnitudes lower than for toxicity to phytoplankton, but were thought to be high enough to cause growth inhibition (Tovar-Sanchez *et al.*, 2013). A later study by Sanchez-Quiles studied the inorganic UVR filters TiO_2 and ZnO and their ability to produce H_2O_2 under UVR exposure. They calculated that the amount of sunscreen released per day on a beach could lead to around a 270nM/day increase in H_2O_2. This causes high levels of oxidative stress on marine phytoplankton affecting their growth (Sanchez-Quiles and Tovar-Sanchez, 2014; Zepp *et al.*, 2007). A decrease in phytoplankton can have significant adverse effects on food trophic levels and the carbon cycle (Ferreyra *et al.*, 2006).

As many sunscreens are lipophilic molecules, they are highly likely candidates to be bioaccumulated in the aquatic food chain, and research into this area is growing. Filters have been found to be bioaccumulated in a vast range of

aquatic biota from invertebrates, fish (Balmer *et al.*, 2005) and even fish eating birds (Fent *et al.*, 2010), all at similar levels. Most recently filters have been found in *Franciscana* dolphins, which are under special conservation protection methods. OCT levels in the livers were measured in dolphins accidentally caught or washed ashore, and was frequently found at concentrations of between 89-782ng.g^2 of lipid weight. OCT was also found in the placenta of one of the pregnant animals suggesting that these compounds are passed on to the young (Gago-Ferrero *et al.*, 2013b).

The effects of this accumulation in mammals is relatively unknown and there were no sex differences determined in this study, but it is well documented that UVR filters particularly impact females due to acting as environmental hormones (Gago-Ferrero *et al.*, 2013a). In particular many UVR filters act as environmental oestrogens which has been demonstrated *in vitro* and *in vivo* (Fent *et al.*, 2008). As well as acting as oestrogens, UVR filters have been tested for additional hormonal activities, with many of the compounds exhibiting androgenic, antiestrogenic and antiandrogenic activities with some displaying multiple activities (Kunz and Fent, 2006b).

These endocrine disrupting effects lead to a number of different consequences for the species that they affect. Firstly they can reduce the frequency of reproduction and even lead to it ceasing completely at higher concentrations, in a dose dependent manner. UVR filters also cause demasculinisation of male fish that leads to secondary sex characteristics being altered, such as males producing vitellogenin, which is a yolk protein usually

only produced by females. The gonads of both males and females were also altered so that spermatocyte and oocyte development was inhibited (Kunz *et al.*, 2006; Weisbrod *et al.*, 2007). In some cases the concentrations at which these activities are shown are several magnitudes higher than those found environmentally, but additive/synergistic effects from different compounds are shown to occur, with some filter combinations (Kunz and Fent, 2006a, 2009).

Not only have there been negative effects in plankton, fish, birds and sea mammals; the use of sunscreens has been linked to the bleaching of corals that can lead to a dramatic effect on reef ecosystems. Coral bleaching occurs with the expulsion of the symbiotic photosynthetic algae *Zooxanthellae*. This effect has been demonstrated and appears to occur due to several different sunscreen filters, promoting viral infection leading to 'the rapid and complete bleaching of hard corals, even at extremely low concentrations' (Danovaro *et al.*, 2008). Another study has also confirmed coral bleaching activity, phototoxic and genotoxic effects and necrosis by the sunscreen benzophenone-2 (BP-2) (Downs *et al.*, 2014).

The Environmental Effects Assessment Panel (EEAP), that answers to the United Nations Environment Programme (UNEP), recently expressed concern about sunscreen damage to fragile marine ecosystems (United Nations Environment Programme, 2017). One approach to this concern, especially for marine environments, is to develop natural biocompatible compounds as alternative sunscreens. The European Chemicals Agency (ECHA) recently (2012-2016) published its Community Rolling Action Plan (CoRAP) list that contained

eight UVR filters that are at risk of becoming banned due to the environmental and health concerns associated with their use. If banned these would leave a gap in the market that would need to be filled by safer alternatives.

1.8 Mycosporine-like Amino Acids

1.8.1 Background

Microorganisms, plants and animals have evolved complex DNA repair and antioxidant pathways to mitigate UVR-induced damage. It is also advantageous to attenuate UVR before it reaches critical cellular targets; consequently animals have also evolved photoprotective mechanisms such as melanogenesis. Another such mechanism is the biosynthesis of a family of UVR-absorbing molecules called mycosporine-like amino acids (MAAs), which are thought to provide photoprotection to marine species and terrestrial fungi. Many marine species are exposed to very high levels of solar radiation, particularly in shallow clear waters. Solar UVR can penetrate to depths of between 0.5-47m depending on the water clarity. DNA is very susceptible to UVR-induced damage and wavelengths that readily damage DNA can reach depths of 16.4m (Tedetti and Sempere, 2006).

These compounds are synthesized or acquired by the diet in a taxonomically diverse range of marine organisms, including protozoa, algae, seaweed, corals, invertebrates and fish (Shick and Dunlap, 2002). The first MAAs were discovered in fungi species in 1965 (Leach, 1965) and a recent study found a terrestrial alga containing MAAs (Hartmann *et al.*, 2015b). The cellular concentration of MAAs varies depending on the species, location and environment in which they are found, with concentrations of 1-6913ng/L (0.09-0.84% of dry weight) reported (Garcia-Pichel and Castenholz, 1993; Llewellyn and Airs, 2010).

Research on the photoprotective potential of these compounds has largely been focused on the species in which they are produced or found, but more recently there has been more work investigating their possible role as photoprotective agents in human skin models. In addition to their UVR absorption characteristics, MAAs appear to have other protective properties, such as antioxidant activity.

1.8.2 MAA Structure and Biosynthesis

MAAs are typically small (<400 Da) colourless, water-soluble compounds, of which over 20 are currently known. They have a similar general structure based on 4-deoxygadusol, containing cyclohexenone or cyclohexenimine rings conjugated to the nitrogen substituent of an amino acid or imino alcohol. These can undergo further carboxylation or demethylation, which changes their UVR absorption properties (Singh *et al.*, 2008b). Displayed in Figure 1.13 are the general structures for mycosporines and MAAs.

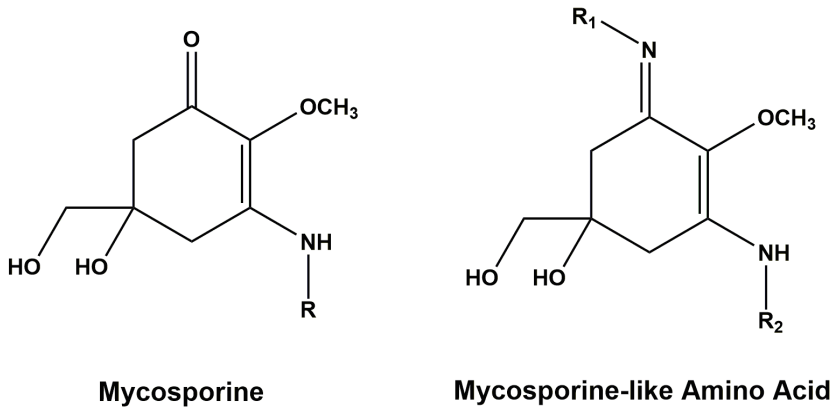

Figure 1.13: The general structures of mycosporines and MAAs.

The route of MAA biosynthesis is a contentious area. Historically it was believed that MAAs were synthesised via the shikimate pathway. This pathway is found in many microorganisms including bacteria, algae, fungi and plants and is responsible for the biosynthesis of the essential aromatic amino acids phenylalanine, tyrosine and tryptophan. This pathway is not found in animals and these amino acids must be acquired by diet. The shikimate pathway was first implicated because the addition of the radiolabeled precursor [U-^{14}C]3-dehydroquinate to the fungus *Trichothecium roseu* produced labelled glutamicol. Furthermore, the cyanobacterium *Chlorogloeopsis* successfully synthesised the MAAs shinorine and mycosporine-glycine when ^{14}C-pyruvate was added to the culture (Favre-Bonvin *et al.*, 1987; Portwich and Garcia-Pichel, 2003). The use of the shikimate pathway inhibitors glyphosate and tyrosine has also demonstrated the ability to inhibit the production of MAAs in the cyanobacteria *Nostoc commune* and the coral *Stylophora pistillata* (Shick *et al.*, 1999; Sinha *et al.*, 2003).

Further investigation has also implicated the pentose phosphate pathway in MAA synthesis. A four-gene cluster, linked to the pentose phosphate pathway in *Anabaena variabilis* ATCC 29413, was able to produce the MAA shinorine when inserted in to E. coli (Balskus and Walsh, 2010). The genes in this cluster have been identified as shown in Table 1.2:

Designation	Name	Product
Ava_3858	2-epi-5-epi-valiolone synthase (EVS)	2-epi-5-epi-valiolone
Ava_3857	*O*-methyltransferase (OMT)	4-deoxygadusol
Ava_3856	ATP-grasp amino acid ligase	Mycosporine-glycine
Ava_3855	NRP-like synthase	Shinorine

Table 1.2: The four-gene cluster found in *Anabaena variabilis* ATCC 29413 linked to the pentose phosphate pathway synthesis of MAAs.

This finding has also been confirmed in other cyanobacteria such as *N. punctiforme,* which shares homologues of the first three genes of *Anabaena variabilis* (NpR5600, NpR5599 and NpR5598), and produced mycosporine-glycine after treatment with the 2-epi-5-epi-valiolone precursor sedoheptulose 7-phosphate (SH-7P) (Gao and Garcia-Pichel, 2011). The incubation of the first two proteins of this cluster (NpR5600 and NpR5599) with SH-7P has also demonstrated the production of 4-deoxygadusol (Gao and Garcia-Pichel, 2011). Typically the EVS gene is found in genome mining of species that produce MAAs and is absent in those without this ability (Rosic, 2012; Singh *et al.*, 2010). There is however one known exception, in *Synechocystis* sp. PCC6803, which lacks EVS but produces three novel MAAs after exposure to UVR. These are mycosporine-tau, dehydroxylusujirene and M-343 (Zhang *et al.*, 2007) and suggests that MAAs are not solely produced from 3-dehydroquinate (DAHP) of the shikimate pathway as many other studies have claimed.

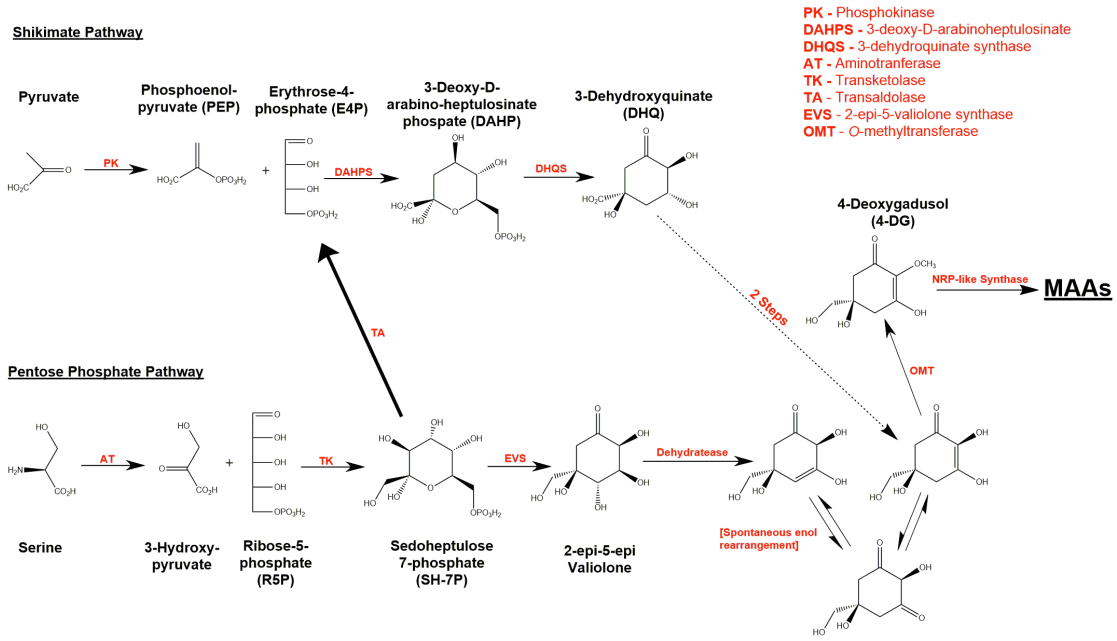

Figure 1.14: The proposed route of MAA biosynthesis.

Despite experimental data that support the pentose phosphate pathway, there is evidence that this is not the major route of MAA synthesis. *A. variabillis* ATCC 29413 still produced shinorine, at levels equivalent to the wild type exposed to UVR, after a deletion of the gene encoding the enzyme EVS (a key pentose phosphate pathway gene). This eliminates the role of the pentose phosphate pathway as the only mechanism for MAA synthesis (Spence *et al.*, 2012). Another proteomic study of the same cyanobacterium found that UVA exposure led to an increase in expression of the enzymes DAHPS and DHQS (part of the shikimate pathway) after irradiation. There was no increase in any enzymes associated with the pentose phosphate pathway, and when shikimate inhibitors were used there was only minimal shinorine produced, suggesting any activity from the pentose phosphate pathways was minimal. Overall, this implies

the shikimate route of production as the most predominant for MAA synthesis in sufficient quantities to provide photoprotection. This is confirmed in studies with shikimate inhibitors, which found expression of shinorine after UVR exposure was very low, at levels equivalent to no exposure (Pope *et al.*, 2015). Quantities of MAAs produced by the pentose phosphate pathway are likely to have other biological functions, for example in *Anabaena* there is evidence of a possible phycobillosome trimming role (Spence *et al.*, 2012).

There are however clear links between the pentose phosphate and shikimate pathways. SH-7P, an intermediate of the pentose phosphate pathway is easily converted to the shikimate intermediate erythrose-4-phosphate by a transaldolase enzyme. The enzymes 3-dehydroquinate synthase (DHQS), from the shikimate pathway, and EVS, from the pentose phosphate pathway, are both part of the sugar phosphate cyclase family of enzymes. These enzymes also have remarkably similar amino acid sequences and carry out very similar reactions (Asamizu *et al.*, 2012). A knockout of the gene encoding the enzyme O-methyltransferase (OMT) (linked to the pentose phosphate pathway) in A. variabillis ATCC 29413 completely prevented shinorine synthesis (Pope *et al.*, 2015) implying that both pathways must be linked at this point.

Evaluating this evidence, one proposed scheme for MAA synthesis is that SH-7P of the pentose phosphate pathway is fed into the shikimate pathway to form erythrose-4-phosphate (which is also formed from the earlier stages of the shikimate pathway). This then reacts with phosphoenolpyruvate (PEP) to form 3-deoxy-D-arabinoheptulosinate phosphate (DAHP) and 3-deyhdroquinate

(DHQ). This explains the upregulation of the enzymes DAHPS and DHQS. The involvement of OMT implies that DHQ cannot be the direct precursor of 4-deoxygadusol, and it must feed back into the pentose phosphate pathway and undergo conversion to an intermediate (by an unidentified enzyme(s)), which is then converted by OMT into 4-deoxygadusol. A suggested biosynthesis scheme is depicted in Figure 1.14, which incorporates both pathways.

The synthesis of mycosporine-glycine from 4–deoxygadusol has been shown to occur via ligase, and shinorine through NRP-like synthase of mycosporine-glycine. The biosynthesis routes of many other MAAs are yet to be established (D'Agostino *et al.*, 2016). Recently however, a new five-gene cluster was discovered in the soil dwelling cyanobacteria *Cylindrospermum stagnale* sp. PCC 7417, which when cloned into *E. coli* produced mycosporine-ornithine and mycosporine-lysine, giving insight into the synthesis of other MAAs and a possible route to large scale production (Katoch *et al.*, 2016).

1.8.3 Structural Evidence for Photoprotection

The UVR protective properties of MAAs are largely inferred from their absorption spectra and high molar extinction coefficients. Typically, they have a peak absorption wavelength (λmax) between 268-362nm, covering much of the spectral range of UVR (~295-400nm) that that reaches the earth's surface (Shick and Dunlap, 2002).

The photochemistry of MAAs is poorly understood, with only a select few compounds having been investigated. The MAAs that have been most studied are porphyra-334, shinorine and mycosporine-glycine. The photo-excited states of these molecules have been shown to relax by intersystem crossing from the singlet excited state to the triplet excited state and by subsequent non-radiative decay, resulting in a controlled dissipation of the energy as heat without the production of ROS (Conde *et al.*, 2007). Porphyra-334 and shinorine dissipate 96-98% of absorbed energy in this way (Conde *et al.*, 2000, 2004). This pathway is consistent with the strong photostability of MAAs. Palythine in particular has been shown to be extremely photostable in a saturated aqueous solution (Conde *et al.*, 2007), as well in the presence of seawater and the strong photosensitising agents riboflavin and rose Bengal (Whitehead and Hedges, 2005). The increased photostability of palythine over other MAAs (such as shinorine and asterina-330) has been attributed to the substitution of the nitrogen atom R group (R1=H), in relation to the geometrical isomerisation around the C=N double bond (Conde *et al.*, 2007). Many synthetic filters rely upon additional filters to provide photostability; this demonstrates that this is not necessary with MAAs.

1.8.4 Circumstantial Evidence for Photoprotection

In addition to the optical properties of MAAs, there is also a large body of circumstantial evidence to suggest a photoprotective role in their natural environments. This has been extensively reviewed by Shick and Dunlap (Shick and Dunlap, 2002), but the key conclusions are summarised below.

MAAs appear to be preferentially accumulated in tissues that receive the greatest UVR exposure – the epidermis of coral reef holothuroids, sea urchin eggs and the eggs and lenses of freshwater and marine teleosts (Chalker *et al.*, 1983; Mason *et al.*, 1998; Shick and Dunlap, 2002). In other circumstances, such as with corals, the MAAs are transferred through symbiosis with algae (e.g. *zooanthellae*). In this relationship, the host also receives organic carbon in the form of carbohydrates, lipids and amino acids and the symbiont is nourished by the host's waste products such as nitrogen, phosphorus, sulphur and carbon dioxide for photosynthesis (Starcevic *et al.*, 2008; Starcevic *et al.*, 2010).

The MAA concentration of a species is directly related with its UVR exposure level that is dependent on latitude and altitude. Zooplankton sampled from lakes at different altitudes showed increasing MAA concentration with increasing altitude (Tartarotti *et al.*, 2001). Species found in tropical waters have a greater concentration of MAAs than those found in cooler climates. High levels of MAA are also found in species in the Antarctic Ocean, possibly due to high irradiances from the ozone layer hole (Dunlap and Shick, 1998). Species show seasonal variation in MAA concentration. In winter months, species have a lower concentration compared to summer months when UVR exposure is highest as demonstrated in plankton growing in lake environments (Ha *et al.*, 2015; Tartarotti and Sommaruga, 2006). There is also a strong negative correlation between the coral depth and MAA concentration that reflects the attenuation of UVR by water. This has been demonstrated experimentally by Dunlap *et al*, who relocated corals, with low MAA concentration, from deep to shallow waters (Dunlap *et al.*, 1986). This resulted in an increased in MAA content that supports

a role in photoprotection. An increase in extracellular nitrogen concentration has also demonstrated an increase in MAA production, suggesting a potential role in intracellular nitrogen storage (Peinado *et al.*, 2004).

1.8.5 Biological Evidence for Photoprotection

The role of MAAs in protecting marine species from UVR damage is a widely researched area. One study has shown an inverse relationship between the production of DNA photolesions, especially the CPD, and total MAA concentration in the coral *Montipora verrucosa* (found in Kaneohe Bay, Oahu, Hawaii) which contains mycosporine-glycine, shinorine and porpyra-334 (Torregiani and Lesser, 2007). Reduction of CPDs and 6,4 pyrimidine-pyrimidone photoproducts by MAA has also been demonstrated, acting by attenuating the UVR before it reaches critical cellular targets in addition to quenching effects (discussed in DNA Damage section) the photo-excited state thymine base (Misonou *et al.*, 2003). Photoprotection has also been demonstrated in green sea urchin embryos by preventing UVB induced abnormalities (Adams and Shick, 1996; Adams and Shick, 2001). There are numerous studies investigating the effect of increased MAA content on UVR resistance for a range of species and environmental stressors such as UVR and desiccation (Bhatia *et al.*, 2011; Feng *et al.*, 2012; Olsson-Francis *et al.*, 2013; Oren and Gunde-Cimerman, 2007; Wright *et al.*, 2005).

Initially it was thought that MAAs acted solely by absorbing UVR before it could reach the critical cellular targets, but they also appear to have antioxidant

properties. This is an extremely desirable characteristic for a photoprotective molecule, as much of the damaging effect of UVR is due to ROS. This has been demonstrated with different MAAs from a large variety of species (Matsui *et al.*, 2012; Nazifi *et al.*, 2013; Rastogi and Incharoensakdi, 2013; Takamatsu *et al.*, 2003). MAA have also been shown to block specific consequences of oxidative damage preventing lipid peroxidation and superoxide radicals (de la Coba *et al.*, 2009b). An extensive review of MAA antioxidant abilities has been carried out by Wada et al (Wada *et al.*, 2015).

1.8.6 Additional Protective Roles of MAA in Nature

Apart from their photoprotective properties, MAAs exhibit additional protective effects, particularly to other environmental stressors. These roles are summarised below and are reviewed in more detail by Oren and Gunde-Cimerman (Oren and Gunde-Cimerman, 2007).

1.8.6.1 Osmotic Stress

MAAs appear to regulate osmotic stress, where a change in the solute concentration surrounding an organism, causes a loss or gain of cellular solvents. One halotolerant unicellular cyanobacterium, inhabiting in a gypsum crust in a hypersaline saltern pond, has an extremely high concentration of MAAs (≥98mM), accounting for >3% of its mass. A reduction of the salinity of its surroundings was accompanied with a rapid expulsion of MAAs, suggesting a role in osmotic stabilisation (Oren, 1997). This hypothesis has since been

investigated and the role of MAA in prevention from osmotic stress supported (Kogej *et al.*, 2006; Oren and Gunde-Cimerman, 2007; Portwich and Garcia-Pichel, 1999; Singh *et al.*, 2008a; Waditee-Sirisattha *et al.*, 2014).

1.8.6.2 Desiccation Stress

There is also evidence that MAAs can protect against desiccation. Cyanobacteria under desiccation stress contain high concentrations of water stress protein (WSpA) and MAAs in a 1:1 ratio (around 4-5% of dry mass each), along with other compounds including scytonemin (another UVR filter), superoxide dismutase and glycan. This group of compounds is thought to act by modifying the structure of the extracellular matrix. Upon rehydration there is an expulsion of MAAs. Overall, this supports a role for MAAs comparable to that for osmotic stress (Wright *et al.*, 2005). Another study found that cyanobacteria, experimentally stressed by desiccation, increased their total MAA content. When these pre-stressed cells were placed under desiccation conditions, they had better viability compared to control cyanobacteria (with a lower MAA content) (Olsson-Francis *et al.*, 2013). Many different bacteria have shown this property in a range of environments (Oren and Gunde-Cimerman, 2007).

1.8.6.3 Thermal Stress

In the above mentioned desiccation study, cyanobacterium survival was also measured under different temperatures. Pre-stressed cells had a higher survival rate than the controls between -20°C and 40°C, but this difference was lost at

50°C (Olsson-Francis *et al.*, 2013). There are also other examples of thermal stress protection by an increase in MAA production in a range of species (Oren and Gunde-Cimerman, 2007).

1.8.6.4 Photosynthesis Accessory Pigments

There are other reported properties of MAAs but these are much less researched. There is evidence that porphyra-334 may act as a photosynthetic accessory pigment due its UVA absorption and subsequent production of small amounts of fluorescence in the Soret band of chlorophyll. This has been debated due to the relatively low amount of fluorescence that is produced in this way and that MAAs are produced in environments of significant irradiance, suggesting photosynthetic wavelengths are in abundance (Oren and Gunde-Cimerman, 2007; Sivalingam *et al.*, 1976).

1.8.7 Photoprotection of the Skin

Despite the evidence that MAAs are prime candidates for use as biocompatible photoprotective molecules for human use, there has been surprisingly little work carried out in skin models to demonstrate potential for human use. The reported effects in skin models are described below.

1.8.7.1 Cell Viability and Proliferation

Cell viability and toxicity are critical endpoints for MAA assessment. One study, done according to ISO 'extracted media' recommended short-term toxicity assay (ISO 10993-12), showed no toxicity of MAAs including shinorine, porphyra-334 and mycosporine-glycine in murine fibroblasts. This was confirmed in a second longer-term direct incubation assay in the same cell line. After 14 and 21 days of incubation, with the different MAAs, there was no significant toxicity and only minor effects on cell morphology for some of the MAAs tested (Fernandes *et al.*, 2015). The same three MAAs were shown to be non-toxic in human TIG-114 lung fibroblast cells at concentrations between 0-100μM at 48 hours, and actually increased cell proliferation (Oyamada *et al.*, 2008); an effect confirmed by Kim et al studying cell viability (Kim *et al.*, 2014). Porphyra-334 has also shown to have no effect on cell viability of human skin fibroblasts at concentrations up to 200μM (Ryu *et al.*, 2014). In contrast with these findings, is work by Choi et al who found shinorine, porphyra-334 and mycosporine-glycine all significantly reduced cell viability in HaCaT keratinocytes, to differing extents, at concentrations from 0.1-mg/ml (around 0.301mM for shinorine) and above (Choi *et al.*, 2015). As mentioned MAAs have demonstrated cell proliferation properties and have potential wound healing applications (Choi *et al.*, 2015).

There are several studies that show that MAAs prevent UVR induced toxicity. This protective effect has also been demonstrated in other MAAs such as collemin A (a compound with a structure related to MAA), where UVB exposure

of HaCat keratinocytes through a collemin A coated quartz plate produced an increase in cell viability, demonstrating a filtering effect (Torres *et al.*, 2004). Post 20J/cm^2 UVA exposure, application of poryhyra-334 at concentrations 10-40μM to skin fibroblasts also prevented reduction in cell viability and induction of senescence (Ryu *et al.*, 2014), confirmed with UVB irradiation with a greater effect with increasing MAA concentration (Oyamada *et al.*, 2008). Application of MAAs post exposure contributing to increased cell viability compared to control suggests a significant effect outside of UVR filtering.

1.8.7.2 Oxidative Stress

Oxidative stress is a major consequence of UVR exposure (Bickers and Athar, 2006; Wolfle *et al.*, 2014). This results from photosensitization reactions, which can produce highly reactive molecules (such ROS). UVR-induced ROS may also be generated post-UVR exposure (Valencia and Kochevar, 2008). As previously mentioned, oxidative DNA damage can lead to mutations, and recently oxidative damage to proteins has shown to inhibit DNA repair, exacerbating the effect of UVR induced DNA damage (McAdam *et al.*, 2016).

Many studies using non-biological chemical assays have shown that MAAs are antioxidants (Andreguetti *et al.*, 2013; Nazifi *et al.*, 2013; Rastogi and Incharoensakdi, 2013; Rastogi *et al.*, 2015). A DPPH radical scavenging assay demonstrated that mycosporine-glycine had significant, dose dependent radical scavenging ability, but that porphyra-334 and shinorine had no effect. The authors concluded that this was because mycosporine-glycine has an oxo-

carbonyl structure whereas porphyra-334 and shinorine have an imino structure (Suh *et al.*, 2014). However, many other chemical and biological studies have reported that porphyra-334 and shinorine have antioxidant properties, and it is possible that MAAs act in multiple ways.

Studies have also been carried out in biological models. Porphyra-334, the most widely studied MAA, has also demonstrated a dose dependent reduction in oxidative stress in skin fibroblasts, when added post exposure, again suggesting antioxidant capability (Ryu *et al.*, 2014). These studies measured oxidative stress immediately post irradiation suggesting a ROS quenching role of MAAs. The results from the biological and chemical assays are not always in agreement suggesting the further investigation is required to elucidate the mechanism of the anti-oxidant effects. Catalase and SOD showed reduced post-irradiation activity over time in unprotected mouse skin. However, the application of a reference sunscreen, or a porphyra-334 and shinorine formulation offered complete protection, along with a decrease in the expression of 70 kilodalton heat shock (stress) protein (Hsp70) (de la Coba *et al.*, 2009a). For the most part, studies demonstrate that MAAs efficiently prevent oxidative stress though filtering, direct and indirect quenching mechanisms, however the exact mechanism are yet to be elucidated.

1.8.7.3 Nrf-2 Activation

Closely linked to prevention of environmental damage to the skin is the Kelch-like ECH-associated protein 1 (Keap1) and nuclear factor erythroid-2-

related factor 2 (Nrf2) complex. Under conditions of stress (particularly oxidative stress), this complex dissociates to release Nrf-2 which subsequently binds to the antioxidant response element (ARE), leading to the transcription of over 200 cytoprotective genes linked to DNA repair, inflammation anti-oxidant response (among others). This is an area of emerging interest for photoprotection, using Nrf2 activators to boost the skin's natural responses to UVR damage (Saw *et al.*, 2011; Tao *et al.*, 2013).

Recently, a bioinformatics based protein modelling and virtual screening approach has been applied to investigate potential compounds that interact with Keap1-Nrf2 complex. This approach identified 75 promising compounds that activated Nrf2, of which 25 were experimentally known to be potent activators. Eleven of these compounds were known to have anti-oxidant activities but had not been previously linked to Nrf2 activation, of which three were MAAs: mycosporine-glycine, mycosporine-glycine-valine and porphyra-334 (Gacesa *et al.*, 2015). This *in silico* approach has been confirmed experimentally with porphyra-334, which demonstrated potent Nrf2 activation activity through the prevention of UVA induced markers of inflammation and cell death. Skin fibroblasts were incubated with increasing concentrations of porphyra-334 (0-40μM) after UVA irradiation. This resulted in a significant reduction of gene and protein expression of IL-6, IL-1β, TNF-α and nuclear expression of NF-κB. In addition there was sustained Nrf2 activation, leading to the expression of a number of cytoprotective genes such as (HMOX-1), glutathione (GSH) and NAD(P)H dehydrogenase [quinone] 1 (NQO1) and the direct scavenging of

reactive oxidative entities and their conversion to less harmful and inert products (Ryu *et al.*, 2015).

1.8.7.4 Accumulation in Human Skin Models

A key property of MAAs is their accumulation in the food chain in marine species. This is a poorly researched area in non-marine species. In one study, investigators fed SKH-1 hairless mice a standard daily diet or the same diet with a freeze-dried red alga that contained a mixture of MAAs that was known to accumulate in medaka fish. They found no MAA accumulation in the eyes, skin or liver after 14-130 days, apart from small amounts in the small intestine, suggesting no route for accumulation in mammals (Mason *et al.*, 1998). As part of the same study, the uptake of the MAA shinorine by human skin cancer A431 cells was also investigated. A dose dependent increase in shinorine (1-1.5mM) was observed after 48 hours of incubation, but saturation occurred at concentrations from 1.5-2.5mM. Raman confocal spectroscopy has shown that MAAs incorporated into polymer gels applied to the skin *in vivo* penetrate and accumulate at depths of 2μm in the *stratum corneum* at a concentration 103.4% higher than at the surface. These results suggest that MAAs may accumulate in the skin, if not through the diet but further research is needed (Tosato *et al.*, 2014).

1.8.7.5 DNA Damage and Erythema

It is generally accepted that the most damaging consequence of UVR exposure to the skin is the formation of DNA photoproducts, which can subsequently lead to genomic mutations (Pfeifer and Besaratinia, 2012). The CPD is the predominant and most important photoproduct induced by both UVA and UVB radiation, however oxidative photoproducts such as 8-oxo-7,8-dihydroguanine (8-oxoGua) are proving to be of increasing importance (Huang *et al.*, 2012). Closely related to the formation of DNA photoproducts, particularly the CPD, is the development of erythema in the skin, with DNA absorption and erythema sharing very similar action spectra (Young *et al.*, 1998).

In terms of photoprotection, the most widely used metric of the efficacy of sunscreen products is the SPF, which is a measure of their ability to prevent erythema (and presumed causal DNA damage). Despite this, the investigation of MAAs to prevent DNA damage and/or erythema in human models is hugely under researched.

Collemin A significantly reduced UVB-induced CPDs in HaCat human keratinocytes cells *in vitro* compared to an irradiated control (Torres *et al.*, 2004). In the same study, a crude formation of collemin A was made by mixing with olive oil and then applied to the skin (6μg/cm2) of one volunteer. This formulation was estimated to have an SPF of at least 4. Little can be concluded from this pilot study other than it requires confirmation (Torres *et al.*, 2004). A more robust study in SKH-1 hairless mice, with a galenic formulation of 2%

porphyra-334 and shinorine (ratio of 88:12) applied to the dorsal skin, prevented solar simulated UVR induced erythema, *stratum corneum* thickening, edema and sunburn cell (apoptosis) formation comparable with a reference sunscreen (the reference sunscreen is the standard used in sunscreen testing according to Cosmetics Europe guidelines). The calculated SPF was 3.71±0.78 (de la Coba *et al.*, 2009a). One criticism of this study is the formulation was applied at a thickness of 4mg/cm2, double the thickness at which sunscreens are tested suggesting that the real SPF would be at least half of this value, and used at a concentration significantly thicker than sunscreens are typically applied in real life situations (Petersen *et al.*, 2013).

Studies in a chemical model have shown that UVR-induced CPDs can be inhibited by an MAA extract containing porphyra-334, shinorine and palythine. Thymine monomers were irradiated through the MAA extract with, no direct contact (in manner theoretically similar to a sunscreen application to the surface of the skin), and also irradiated with the extract and monomers mixed together. There was a greater protective effect in the mixed samples than those with no contact, suggesting an effect beyond the absorption properties of MAAs. Further investigation established this was through quenching of the triplet state of UVR-excited thymine (Misonou *et al.*, 2003). This shows MAAs may have even greater potential for photoprotection over current filters, especially with the recent discovery of delayed (also know as 'dark') CPD formation, which suggests that CPDs can form for hours after exposure through a triplet photoexcitation mechanism (Premi *et al.*, 2015).

1.8.7.6 Inflammation

The ability of MAAs to inhibit biomarkers of skin inflammation is poorly studied. Over expression of these markers is linked to a range of inflammatory skin conditions such as psoriasis. Expression of cyclooxygenase-2 (COX-2) mRNA, widely associated with inflammation, was also prevented by topical application of mycosporine-glycine to HaCat keratinocytes at the highest concentration tested (0.3mM) and with only the lowest concentration of shinorine (0.03mM) having a statistically significant effect (questioning the validity of the result), and with porphyra-334 having no effect (Suh *et al.*, 2014). This study used a broad-spectrum UVR source and the results could possibly be explained by the peak absorbance of each of the MAAs, with mycosporine-glycine (λmax =310nm) and shinorine (λmax =334nm) absorbing in shorter wavelengths and poryra-334 (λmax =344nm) absorbing at slightly longer wavelengths, suggesting COX-2 expression is linked to shorter wave UVR, however the lack of dose-response relationship is unclear.

1.8.7.7 Photoageing

Skin photoageing is a consequence of long-term solar UVR exposure. This is different from chronological skin ageing and is associated with deep wrinkles and sagging. It is generally accepted that photoageing is the consequence of UVR induced activation MMPs, which degrade the structural extracellular matrix proteins of the dermis such as elastins and collagens (Quan *et al.*, 2009).

The incubation of fibroblasts with porphyra-334 (0-40μM) after UVA exposure inhibited MMP-1 and MMP-8 gene expression, but had no effect on MMP-13. Elastase activity was dose dependently reduced by porphyra-334, with an increase in collagen and elastin mRNA and protein expression, and procollagen secretion (Ryu *et al.*, 2014). Shinorine, porphyra-334, and palythine significantly inhibited MMP-2 activity in an *in vitro* fluorogenic assay, which was hypothesised to be due to competitive inhibition by binding to the active site determined using computer modelling (Hartmann *et al.*, 2015a).

In addition to their photoprotective properties, mycosporine-glycine, porphyra-334 and shinorine have been shown to be procollagen C proteinase enhancers (PCOLCE) and induced elastin mRNA upregulation in a largely dose dependent manner after UVA exposure, whereas only porphyra-334 showed an upregulation of involucrin, another skin protein (Suh *et al.*, 2014).

Overall, relatively limited data suggest that MAAs have multiple actions in the prevention of photoageing.

1.8.8 Potential Human Use of MAAs

The evidence reviewed above demonstrates that MAAs have huge photoprotection potential in traditional optical ways as well as with new photomolecular strategies. Many studies have suggested the widespread use of MAAs as sunscreens (Cardozo *et al.*, 2007; M. Bandaranayake, 1998; Scheuer, 1990; Torres *et al.*, 2006), however they have yet to been exploited on a large

scale, with only a few products currently available. One MAA product currently available is called Helioguard 365, which contains the MAAs porphyra-334 and shinorine (11.5:1 ratio) extracted from the red alga *Porphyra umbilicalis* (Schmid *et al.*, 2003). This product however mainly provides protection in the UVA region with minimal protection in the more damaging UVB range, and the final concentration of MAAs in the product is extremely small when compared to the concentration of UVR filters in most sunscreen products. One product contains a final MAA concentration of 0.0005%, whereas most sunscreen formulations contain filters at 0.5-10% w/v. This suggests the addition of a very low MAA concentration to a formulation will have a negligible influence on the SPF claims of the product.

There are numerous reasons for the lack of widespread use of MAAs, one of which is the poor understanding of biosynthesis pathways involved to make specific MAAs in an industrially economic manner. This makes the production process more complex, for example the need to farm vast amounts of seaweed. Further understanding of these pathways could lead to easier large-scale commercial biosynthesis, for example in a heterologous bacterial host e.g. *E. coli*, which is easier to cultivate. The chiral centres of MAA compounds make them highly difficult to synthesise chemically; again meaning large-scale synthesis is difficult, with unrealistic costs associated to production.

1.9 Aims of Thesis

Skin cancer rates in the UK and worldwide, especially in those with light skin, continue to rise year on year and most of this is attributed to damage caused by solar exposure. The importance of preventing damage by solar radiation, with the aim of reducing skin cancer rates, is greater than ever. Sun protection by sunscreens is the main preventative strategy. There are however a number of unresolved problems with their efficacy, safety and environmental impacts, which can lead to reduced compliance. Furthermore, most sunscreens do not afford protection in the UV/visible border (380-420nm) region that is increasingly shown to have adverse effects on skin.

The main aim of this project was to investigate new approaches to photoprotection. These included the photoprotective properties of a biocompatable natural marine sunscreen, which may address concerns about the environmental impact of synthetic sunscreens. Furthermore, the photoprotective properties of a new sunscreen that offers protection in UV/visible border region were determined.

The specific goals of the thesis were to:

a) Develop methods to measure solar radiation damage in HaCat keratinocytes *in vitro* and in human skin from volunteers *in vivo.* This includes specific DNA photolesions, gene expression associated with adverse UVR effects, and oxidative damage.

b) Evaluate the capacity of the naturally occurring MAA palythine to act as an effective sunscreen against the previously identified markers *in vitro,* and to determine its antioxidant properties.

c) Investigate markers of solar simulated UVR (280-400nm), near visible UVA (385nm) and high-energy visible light (405nm) damage at environmentally relevant doses using invasive and non-invasive methods.

d) Test the ability of conventional sunscreen formulations to prevent near visible UVA and high-energy visible light damage and investigate the benefits of the addition of a new broad spectrum sunscreen filter (C1332) to formulations in preventing this damage *in vitro* and *in vivo.*

e) To generate data for patent applications for KCL and BASF (details in Appendix).

f) To write a review summarising the properties and photoprotection potential of naturally occurring MAA compounds. This has been accepted by Current Medicinal Chemistry

Chapter 2: Materials and Methods

2.1 UVR & Light Sources

For SSR and UVA studies, radiation was obtained from a Solar® Light 300W-16S xenon arc solar UV simulator (Solar Light, Glenside, USA) with full solar spectrum UVR and UVA settings, complying with the International Organisation for Standardisation (ISO) Standard 24444 and Cosmetics Europe 2006 for SSR, and the Japanese Cosmetic Industry Association (JCIA) for UVA for the assessment of sunscreen photoprotection. A quartz beam splitter filter was used to filter out heat/IR. A 3mm WG335 filter was used as an optional UVB cut off filter to give the UVA spectrum. The UVR was delivered through a liquid light guide with an exit diameter of 7mm.

The 385nm and 405nm sources were Loctite LED flood systems (Loctite, Henkel Ltd, UK) using either the UVA array head (385nm ± 5nm – i.e. 10nm at full width at half maximum (FWHM)) or 405nm array head (405nm ± 8.5nm, FWHM = 17nm). Each head has an irradiation surface of 97mm x 96mm consisting of 144 LEDs. The spectral irradiances of all sources are shown in Figure 2.1 and outputs described in Table 2.1. Spectra for SSR and UVA were measured at distance of 0cm, and 385nm and 405nm were measured at a distance of 40cm. Irradiation distances were based on the output of the source being measured and were selected to be within the working range of the spectroradiometer.

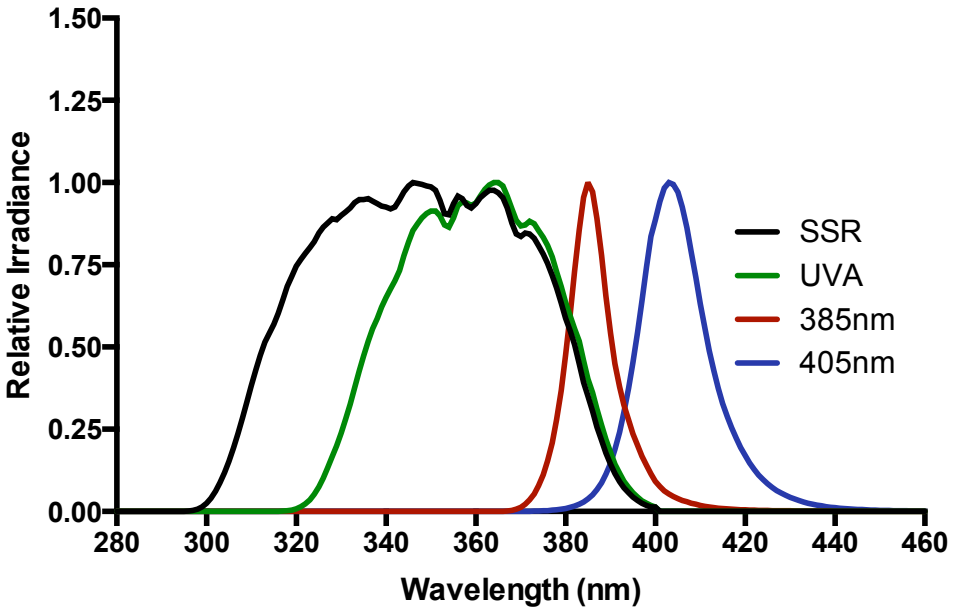

Figure 2.1: The spectral outputs of the radiation sources. The spectral output of the sources used in all the studies as measured with a Bentham spectroradiometer (details below in *Dosimetry* section) from 280-460nm.

Source	Region	Wavelengths (nm)	% of Total Irradiance
SSR	**UVC**	250-280	0.00
	UVB	280-320	12.00
	UVA	320-400	88.00
	Visible	400-500	0.00
	Total	**280-500**	**100.00**
UVA	**UVC**	250-280	0.00
	UVB	280-320	0.00
	UVA	320-400	100.00
	Visible	400-500	0.00
	Total	**280-500**	**100.00**
385nm	**UVC**	250-280	0.00
	UVB	280-320	0.00
	UVA	320-400	94.82
	Visible	400-500	5.18
	Total	**280-500**	**100.00**
405nm	**UVC**	250-280	0.00
	UVB	280-320	0.00
	UVA	320-400	23.60
	Visible	400-500	76.40
	Total	**280-500**	**100.00**

Table 2.1: The spectral waveband analyses of the radiation sources. The spectral breakdown of each of the sources used in all the studies as measured.

2.2 Dosimetry

The spectral irradiances of the sources were measured using a DM120BC double-monochromator spectroradiometer (Bentham Instruments, Reading, UK) with an integration sphere, calibrated by the Centre for Radiation, Chemical and Environmental Hazards (CRCE), Public Health England (PHE) against a UK national standard. Irradiance of the sources was routinely measured with a hand-held radiometer. Spectra from the Solar Light solar simulator were measured using a Solar® Light PMA 2100 radiometer (Solar® Light, Glenside, Pennsylvania) after calibration against the spectroradiometric readings, and gave a typical reading of 1120μW/cm^2 or 18s for an MED. For studies with the 385nm or 405nm sources, a Loctite UVA/Vis radiometer (Loctite, Henkel Ltd, UK) was used, with a typical irradiance of 125mW/cm^2 for 385nm and 320mW/cm^2 for 405nm.

2.3 Absorbance Spectroscopy

The UVR and visible absorbance properties of each studied compound (in solution) were measured with a Jenway 7315 UV/Vis spectrophotometer (Jenway, Staffordshire, UK) for wavelengths between 250-500nm. Absorbance profiles of the BASF sunscreens in formulation were provided by BASF, and were calculated using the BASF Sunscreen Simulator (Figure 2.4). Details of the formulations are provided in Table 2.2. The *in vitro* measurements for BASF compounds were assessed from 290 to 450 nm using a Labsphere UV-2000S device with SB6-plates (Helioscreen, Creil, France). 1.3 mg/cm^2 of the sunscreens were applied to the plates used for the measurements (see section *Filters in Formulation* below). The spectra are averages of measurements on three plates at five spots on every plate. These measurements were carried out by BASF GmbH, Grenzach-Wyhlen.

2.4 Photoprotective Compounds

2.4.1 Palythine

The MAA palythine was extracted to analytical grade purity from the red algae *Chrondus yendoi* as previously described (Tsujino *et al.*, 1978), and diluted at different concentrations (0-10 % w/v) (0-0.004M) in PBS. The molecular structure and UVR absorbance of palythine are shown in Figure.2.2. Absorption is primarily between 280-340 nm (UVB and UVA 2) with a peak at 320 nm. The molecular mass of palythine is 245.17.

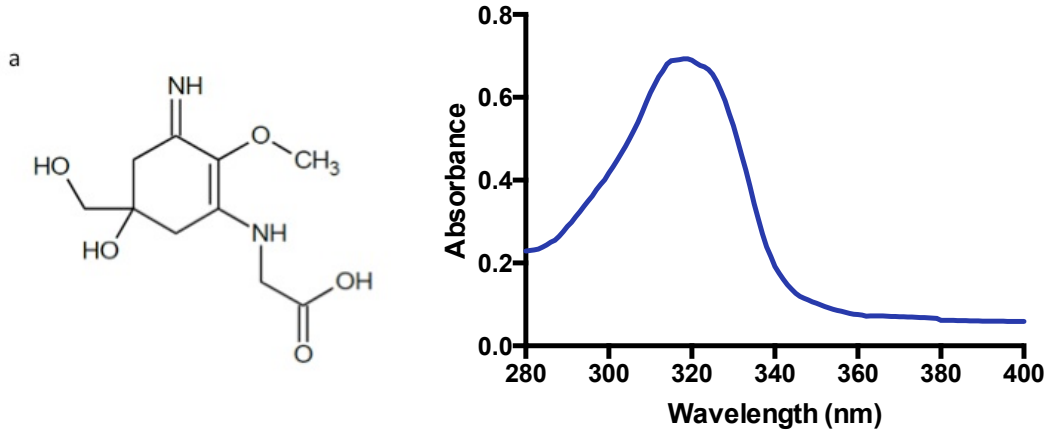

Figure 2.2: The chemical structure and absorbance spectrum of palythine. (a) The chemical structure of the MAA amino acid palythine. (b) The absorbance spectrum of 0.0001% w/v palythine extracted from red algae *Chondrus yendoi* in PBS. There is strong absorbance in the UVA and UVB regions with a peak absorbance at 320 nm.

2.4.2 BASF Compounds

2.4.2.1 2-(4-(2-(4-Diethylamino-2-hydroxy-benzoyl)-benzoyl)- piperazine-1-carbonyl)-phenyl)- (4-diethylamino-2- hydroxyphenyl)-methanone (C1332)

The experimental UVR/visible filter 2-(4-(2-(4-Diethylamino-2-hydroxy-benzoyl)-benzoyl)- piperazine-1-carbonyl)-phenyl)- (4-diethylamino-2-hydroxyphenyl)-methanone (identified as C1332) was tested to assess the benefits of attenuating the longwave UVA, and shortwave visible light wavelengths, and is used in the formulations described below. The molecular structure and UVR absorbance of C1332 are shown in Figure.2.3. Absorption is primarily between 330-425 nm with a peak at 394 nm. The molecular mass of C1332 is 676.33.

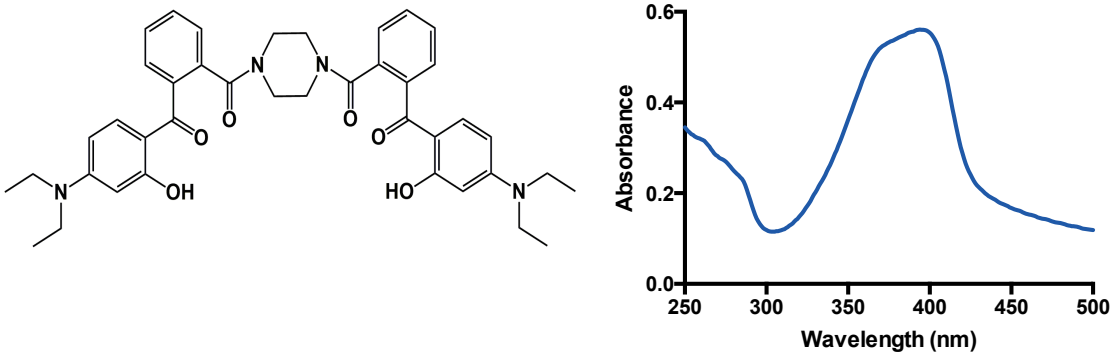

Figure 2.3: The chemical structure and absorbance spectrum of C1332. (a) The chemical structure of the experimental UVR/visible light filter C1332. (b) The absorbance spectrum of a 2.25×10^{-2} M solution of C1332. There is strong absorbance in the UVA and into the visible region with a peak absorbance of 394 nm.

2.4.2.2 Formulations

Two formulated sunscreens were provided BASF (BASF GmbH, Grenzach-Wyhlen, Germany) with their absorbance spectra shown in Figure. 2.4. Characteristics of each formulation are shown in Table 2.2. Filters Uvinul T150, PBSA and Uvinul A Plus are EU approved UVR filters used in many commercial sunscreen formulations. Formulations were designed to have the same SPF, and used the same filters, but one contained C1332. This led to different UVA-PF and UVA/UVB ratios.

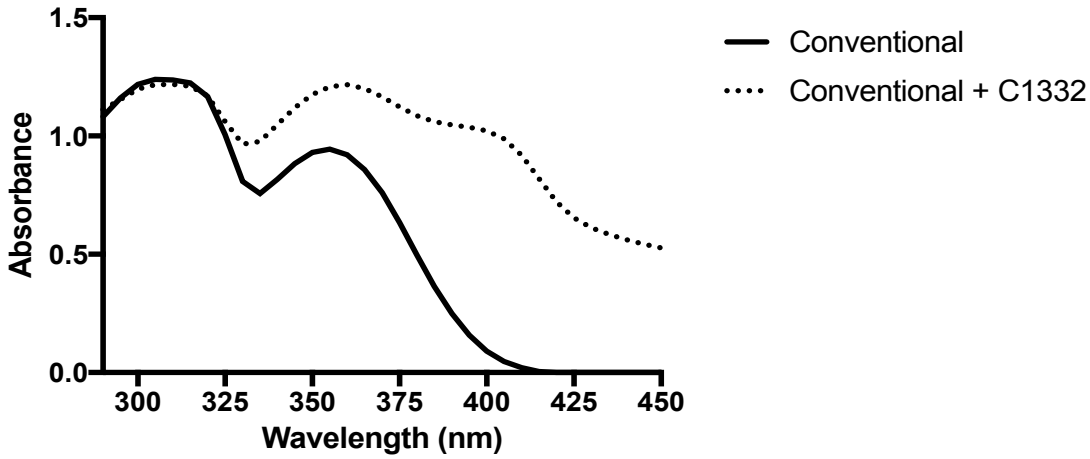

Figure 2.4: The absorbance spectra of BASF compounds. The simulated absorbance spectra of sunscreen formulations used for the UV/visible radiation border region photoprotection studies. Spectra were simulated using the BASF sunscreen simulator.

Formulation	Vehicle (UV13129-1-1)	Conventional (UV13129-1-2)	Conventional + C1332 (UV14189-2-2)
Concept	Vehicle base cream	SPF/UVA-PF > 1/3	Same SPF/Same Uvinul A Plus conc. + 5% C1332
Composition	No UVR Filters	1.5% Uvinul T150 2.0% PBSA 2.0% Uvinul A Plus	1.0% Uvinul T150 1.5% PBSA 2.0% Uvinul A Plus 5.0% C1332 (active)
SPF Calc.	-	15.0	15.8
UVA-PF Calc.	-	5.2	12.6
Ratio Calculation. (UVB:UVA)	-	2.91	1.19

Table 2.2: Properties and protection factors of the BASF compounds. The details of the UVR filters contained within each formulation are described, along with their respective SPF, UVA-PF and UVA/UVB ratios.

2.5 Photostability

The photostability of the palythine was determined by absorbance spectroscopy. Filters were exposed to increasing doses of SSR and absorbance measured after each exposure. The absorbance spectrum was measured between 280-400 nm using a Jenway 7315 spectrophotometer, (Jenway, Staffordshire, UK).

2.6 In Vitro Protection Factor Tests

2.6.1 SPF/UVA-PF

In vitro protection factors of compounds were measured by BASF GmbH using the methods described by Herzog and Osterwalder (Herzog and Osterwalder, 2015). Briefly, this used the extinction coefficient at various wavelengths across the UVR spectrum (280-400nm) to calculate the SPF and UVA-PF.

2.6.2 Critical Wavelength Test

The absorbance of the UVR filter/sunscreen was integrated from 290nm to 400nm, until the sum reached 90% of the total absorbance. To pass this test the wavelength at the 90% target must be ≥370nm.

2.6.3 Boots Star Rating

The Boots Star rating is determined by calculating the UVA:UVB ratio from the absorbance profile before and after irradiation with 17.5J/cm^2 of SSR. The rating given is dependent on the values obtained as described in Table 2.3.

	Initial Mean UVA:UVB Ratio				
Post exposure mean UVA:UVB ratio		**0.0 - 0.59**	**0.60 - 0.79**	**0.80 - 0.89**	**≥ 0.90**
	0.0 - 0.56	No Rating	No Rating	No Rating	No Rating
	0.57 - 0.75	No Rating	***	***	***
	0.76 - 0.85	No Rating	***	****	****
	≥ 0.86	No Rating	***	****	*****

Table 2.3: The Boots Star rating sunscreen test method. The allocation of star ratings depends on the UVA:UVB ratios.

2.7 Cell Culture

The spontaneously transformed human keratinocyte cell line, human adult low calcium temperature (HaCaT) was the only cell line used in this project. This cell line has two p53 point mutations that are thought to make it immortalised. The cell line (purchased from ATCC, USA) was cultured in Dulbecco modified Eagle medium (DMEM; Life Technologies, Paisley, UK) supplemented with 10% foetal calf serum (Sigma-Aldrich, Pool, UK), 100U/ml penicillin, and 100μg/ml streptomycin (Life Technologies, Paisley, UK) maintained in a humidified incubator at 37^{o}C with 95% air and 5% CO_2. Cells were cultured to around 80% confluence in 75cm^2 plastic flasks (Corning, USA). Cells were plated into multiwell plates and left to reach a confluence of 70-80% before being used for experiments.

2.8 *In Vitro* Irradiation Procedures

In vitro studies were split into two sub-studies. One sub-study investigated the effects of the MAA compound palythine, which is highly water-soluble and so was used in solution. The other sub-study assessed the BASF filters, which are insoluble in cell culture media, and may have caused other unwanted effects if applied directly. For this reason the UVR filters were formulated into creams, which would also better mimic real life use. These were used on plates that simulated the structure of the epidermis (see below).

2.8.1 Palythine Studies

Cells were washed twice in PBS and different concentrations of palythine (0%-10%, in PBS) and were applied on top of the cell monolayer (150µl/well). Cells were irradiated, without the plate lid, with the use of a liquid light guide that was placed 2cm above the cells, one well at a time for SSR and UVA studies. Irradiation time was adjusted to account for the irradiation distance. Cells were kept on a cooling platform to keep them around 37^{o}C. Unirradiated controls, and samples with shorter irradiation times, were kept in the same conditions as the longest sample to ensure any differences observed were due to the UVR or visible light exposure rather than any confounding factors. After irradiation, the palythine solution was removed by washing twice in PBS and either processed immediately or media replaced and returned to the incubator.

2.8.2 Filters in Formulation

Cells were washed twice in PBS and left in fresh PBS (200μl/well) during irradiation. Sunscreens in formulation were applied to Poly(methyl methacrylate) (PMMA) plates at a concentration of 1.3mg/cm^2 and applied using a pre-coated finger cot and left to dry for 10 minutes. The sunscreen concentration used was advised by BASF, as it is known to give consistent results in their commercial tests. PMMA plates are routinely used by the sunscreen industry for different *in vitro* tests such as SPF and UVA-PF. They are made with sandblasted or moulded plastics to mimic the natural ridges that are found on the epidermis, and they also transmit UVR. The PMMA plates were then placed over each well of a 24 or 48 well plate (without their normal lids) and cells were irradiated through the plate with the sunscreen film and cooled to 37^{o}C with a cooling platform.

2.9 *In Vitro* Assays

Assay Name	Endpoint Measured
Neutral Red Assay	Cell Viability
Alamar Blue Assay	Cell Viability
Comet Assay	DNA damage (ALS, CPD, 8oxoGua)
Immunohistochemistry – CPD Imunnofluorscence	DNA Damage (CPD)
Reactive Oxygen Species Assay	Reactive oxygen species generation
DPPH Assay	Free radical quenching (Electron transfer)
ORAC Assay	Peroxyl Radical quenching (Hydrogen atom transfer)
Gene Expression	RNA expression

Table 2.4: Assays used for *in vitro* studies.

2.9.1 Cell Viability

Cell viability was assessed using two different techniques for the 385/405nm studies to validate the findings. The Neutral Red assay alone was used for palythine studies. The techniques used different methods to assess the viability and are described below.

2.9.2 Neutral Red Assay

The Neutral Red assay assesses the ability of cells to incorporate the dye into lysosomes. This dye is weakly cationic and penetrates the cell membrane by non-ionic passive diffusion, and then concentrates in lysosomes by forming electrostatic hydrophobic bonds with the lysosomal matrix. Loss of uptake of Neutral Red is indicative of decreased viability (Repetto *et al.*, 2008).

Cell viability was measured 24 hours post irradiation. Neutral Red solution (4μgml^{-1} in growth medium) (Sigma, UK) was added to the cells and they were incubated at 37°C, 5% CO_2 for 2 hours. Cells were then washed three times in PBS to remove excess Neutral Red solution and then the destain solution (50% v/v ethanol, 49% v/v ddH_2O, 1% v/v glacial acetic acid) was added. Optical density was measured at 540 nm with a Spectra Max 384 Plus spectrophotometer (Molecular Devices; California, USA). Each condition was tested in triplicate and the average calculated.

2.9.3 Alamar Blue Assay

The Alamar Blue assay assesses cellular energy to reduce resazurin to fluorescent resorufin, by measuring the reduction potential of the cell. Cell viability was measured 24 hours post irradiation. Alamar Blue solution (1/10th of total growth medium volume) (ThermoFisher, UK) was added to the cells and they were incubated at 37°C, 5% CO_2 for 4 hours and protected from light. Fluroescence was measured using an excitation wavelength of 540–570 nm (peak excitation is 570 nm) and reading the emission at 580–610 nm (peak emission is 585 nm) with a Spectra Max 384 Plus (Molecular Devices; California, USA) spectrophotometer. Each condition was tested in triplicate and the average calculated.

2.9.4 Single Cell Gel Electrophoresis Assay (Comet assay)

DNA damage was measured using the alkaline comet assay, with lesion specific enzymes to determine the type of damage produced (Singh *et al.*, 1988).

25 mm × 75 mm glass slides (Sigma, UK) were pre-coated with 1% agarose and allowed to dry. Cells were untreated or exposed to UVR. Positive controls were treated with ice cold 0.03% H_2O_2 for 5 minutes and negative controls were kept in the same conditions as the treatments without UVR exposure.

After treatment, cells were scraped gently with a cell scraper in EDTA solution to help dissociate cells and prevent clumping. The cells (40µl) were then added to low melting point (LMP) agarose (160µl) and gently mixed. The final concentration of cells in the LMP agarose was 10,000 cells/100µl of agarose. 100µl of the agarose-cell solution was pipetted onto the pre-coated slides and a cover slip placed onto the gel, which was left to set for 5-10 minutes before removal of the cover slip. Two replicates were placed on each slide. All steps were carried out on a cooled platform at 4°C. Slides were then placed into lysis buffer (2.5M NaCl, 100mM EDTA, 10mM TRIS, 1% sodium sarcosinate, 1% Triton x-100, 10% DMSO) left overnight at 4°C in the dark.

Following this, the slides were washed in ice-cold ddH_2O (2 x 5mins) in the dark and once in ice-cold enzyme reaction buffer (0.4mM HEPES, 1mMKCl, 0.005mM EDTA, 0.02mg/ml BSA) for 5 minutes. After this step, different lesions were detected using lesion specific enzymes.

Two specific DNA lesions were measured, 8-oxodGua and CPDs. 8-oxodGua, a form of oxidatively induced DNA damage, was measured using the hOGG1 enzyme whilst CPDs were measured using the T4endoV enzyme (both enzymes - New England BioLabs, Ipswich UK). After washing, 50µl of enzyme diluted in reaction buffer (hOGG1– 3.2U/ml, T4EndoV – 0.1U/ml) or reaction buffer alone was added to each gel, a cover slip placed on top and left in a humidity chamber in the dark at 37°C for 45 minutes. The comet assay, without lesion specific enzymes, measures DNA SSB and alkali labile sites.

After enzyme treatment, coverslips were removed and transferred into ice-cold electrophoresis buffer (10mM NaOH, 200mM EDTA, pH13 in ddH_2O) and incubated at 4°C in the dark for 20 minutes. Electrophoresis was then carried out in fresh electrophoresis buffer for 25 minutes at 25V (1V/cm) 300mA, at 4°C in the dark. Slides were washed in neutralisation buffer (0.4M TRIS, pH7.5) for 2x 10 minutes then in ddH_2O for 2 x 5 minutes before being left to dry overnight.

The DNA embedded in the slides was stained using propidium iodide (PI) solution (2.5ug/ml in PBS), 50µl PI was added to each gel and cover slip placed over. The slides were analysed on a Zeiss Axiophot epifluorescence microscope (Carl Zeiss, Germany), with a green excitation filter (536nm) detected with a red emission at 617nm. Pictures covering the whole gel were taken, avoiding the outer edges, using a Zeiss Axiocam MRm at a magnification of 10x. The images were analysed using Comet Score Pro software (Tritek Corp, Summerduck, VA), typically scoring 150 individual comets per condition. The percentage of DNA in

the tail compared to the total DNA present in the whole ((DNA in tail/Total DNA) x100) comet was the parameter used to determine the damage of each condition.

2.9.5 Immunohistochemistry – CPD Imunnofluorscence *In Vitro*

At different time points post irradiation, cells were washed and fixed in 2% (v/v) paraformaldehyde with 0.5 % (v/v) Triton X-100 in PBS for 30 mins at 4°C. DNA was then denatured by incubation in 2M HCl for 10 mins at 37°C. Non-specific sites were blocked using blocking buffer of 20% (v/v) goat serum and 0.1% (v/v) triton X-100 in PBS for 30 mins at room temperature. The primary antibody used was Anti-CPD (Clone TDM-2) (Cosmobio, Tokyo, Japan) at 1:1000 in blocking buffer for 1 hr at room temperature. Alexafluor 488 was diluted in blocking buffer (1:200 dilution) and incubated for 1 hr at room temperature and finally DAPI (a DNA stain) was added for 10 mins. Washing was carried out (3x5 mins) between each step.

2.9.5.1 Image Acquisition

Image capture of all stained sections was carried out using a Ziess Axio-Observer Z1 Microscope (Carl Zeiss, Cambridge, UK) with AxioVision V. 4.8 software (Carl Zeiss, Cambridge, UK). All fluorescent channel exposures were set at the beginning of each experiment and remained constant throughout each batch analysed. All pictures taken in the same experiment were captured on the same day.

2.9.5.2 Image Analysis

Image analysis was carried out using Cell Profiler v.2.1.1 software (Cell Profiler, Broad Institute, Cambridge MA, USA). A pipeline was created to gate around the nucleus of each cell (DAPI - blue channel) and the relative mean green intensity (CPD staining) of each gated nucleus was then measured. This allowed specific quantification of nuclear staining. The mean green intensity of every nucleus for each picture was averaged. The mean of the nine pictures was determined and used as the end point.

2.9.6 Reactive Oxygen Species Assays

2.9.6.1 H_2DCFDA ROS Assay

ROS were assessed using 6-carboxy-2',7'-dichlorodihydrofluorescein diacetate (carboxy-H_2DCFDA), which is a non-fluorescent molecule that is converted to a green-fluorescent form when the acetate groups are removed by intracellular esterases and oxidation (by the activity of ROS). HaCat cells were irradiated as above, with palythine also added post irradiation in some experiments. Cells were then incubated with 10μM carboxy-H_2DCFDA (Invitrogen, UK) in PBS for 30 mins in the dark at 37^{o}C, 5% CO_2. They were washed in PBS, trypsinized for 10 minutes at 37^{o}C, centrifuged at 1200 rpm for 5 minutes at room temperature then resuspended in PBS and counterstained with DAPI for analysis by FACS. This was carried out with a Becton Dickinson FACSAria II. Cells were gated to analyse live cells only (DAPI negative) and the

average mean green intensity (representitive of ROS intensity) per condition was then plotted from at least 10,000 measured events. Analysis was carried out using FlowJo 8.7 (Ashland, Oregon, USA).

2.9.6.2 1,1-Diphenyl-2-picryl-hydrazyl (DPPH) Assay

The DPPH assay was used to assess compounds for their ability to quench free radicals by electron transfer. A 100uM stock of DPPH was prepared in methanol and 187.5µl was added to the wells of a 96 well plate. Serial dilutions of test compounds were prepared in a solvent in which the test compound was soluble, and 12.5µl was added to each well and mixed. The plate was protected from light and placed on a shaker at room temperature for 30 minutes. Absorbance was measured at 517nm using a Spectra Max 384 Plus spectrophotometer (Molecular Devices; California, USA). Each condition was tested in triplicate and the average calculated. The percentage inhibition was calculated and a graph was plotted. Linear regression analysis was carried out to calculate the effective concentration for 50% inhibition (EC_{50}) for each compound.

2.9.6.3 Oxygen Radical Absorbance Capacity (ORAC) Assay

The ORAC assay quantifies the anti-oxidant properites of a compound in its ability to inhibit peroxyl radicals (ROO•) from oxidising fluorescein and consequently reducing fluorescence. The assay was carried out with the ORAC Antioxidant Assay Kit (Zenbio, North Carolina, USA) according to manufacturer's

instructions. Trolox standards were prepared in the assay buffer (100-0μM) along with serial dilutions of the test compounds. 150μl of the fluorescein working solution was added to the inner wells of a 96 well plate, with 25μl of each of the standards or test compound in duplicate, and the plate was incubated to 37°C for at least 15 minutes. The 2,2'-azobis-2-methyl-propanimidamine dihydrochloride (APPH) working solution was then added to each well (25μl) to start the reaction. Fluorescence was measured in a preheated incubation chamber (37°C) using a Spectra Max 384 Plus spectrophotometer (Molecular Devices; California, USA) with excitation/emission = 485/530nm immediately and then every minute for 30 minutes. Standard curves were generated for each compound and the area under the curve (AUC) calculated. Each compound tested was then expressed as a Trolox equivalent concentration.

2.9.7 Gene Expression

2.9.7.1 RNA Extraction

Total RNA isolation for real-time RT-PCR was isolated using the *mirVana* miRNA isolation kit with phenol (Life Technologies, Carlsbad, USA) according to the manufacturer's instructions. All extractions were carried out on ice. Cells were treated as in the previously described irradiation procedure and RNA extraction was performed at 3, 6, 12 and 24 hours post irradiation.

Media was removed from the wells and cells were washed twice in PBS before 200µl of lysis buffer was added. Cells were vigorously scraped using a cell scraper in the lysis buffer and transferred to an Eppendorf tube and vortexed for 1 minute to ensure samples were fully homogenised. 20µl of homogenate additive was added to each sample, inverted several times then left on ice. After 10 minutes, 200µl of acid-phenol:chloroform was added to the lysate and the tube was vortexed for 1 minute and centrifuged for 5 minutes at 10000 x g at room temperature to separate the aqueous and organic phases. After centrifugation, the upper aqueous phase was carefully removed without disturbing the lower phase and transferred into a fresh Eppendorf tube with the volume noted. Room temperature 100% ethanol, at a volume of 1.25x the volume of the transferred layer (usually 250µl), was then added to the aqueous phase and vortexed.

Following this, a filter cartridge was placed into a collection tube and the lysate/ethanol mixture was pipetted onto the filter cartridge and centrifuged at 10000 x g for 1 minute to allow the mixture to pass through, and the RNA to bind to the filter. Flow through was discarded and the collection tube was reused in the following washing steps. 700µl *miRNA* wash solution 1 was applied to the filter cartridge and centrifuged for 30 seconds. Again, flow through was discarded and the filter cartridge was replaced into the same collection tube. 500µl of wash solution 2 was then applied to the filter cartridge, centrifuged for 30 seconds and the process was repeated once more. Flow through was then discarded; the filter was replaced into the tube and further spun for 2 minutes to remove any residual fluid. The filter cartridge was transferred into a fresh

collection tube. 100µl of pre-heated nuclease-free water was applied to the centre of the filter. This was spun for 1 minute at 10000 x g and the elutant containing the RNA was collected.

The RNA yield was determined by quantifying the samples on a Nanodrop ND1000 UV-Vis spectrophotometer (Labtech, East Sussex, UK). RNA samples were stored at -20°C for up to one month or -80°C for longer-term storage until used for PCR.

2.9.7.2 cDNA Synthesis

cDNA synthesis was carried out using High Capacity cDNA Reverse Transcription kit (Applied Biosystems by Life Technologies, Carlsbad, USA). Kit components were thawed on ice and reverse transcriptions were carried out according the manufacturer's instructions. The following 2x master mix was made (Table 2.5) 20µl of the 2x master mix was then added to 20µl of RNA in a PCR tube on ice and mixed gently. The tubes were spun down on a micro centrifuge to remove air bubbles and loaded into a thermocycler (GeneAmp® PCR System 9700, Applied Biosystems by Life Technologies, Carlsbad, USA) and run on the following cycle (Table 2.6).

Component	Volume (µl)
10x RT buffer	4
25x dNTP Mix (100mM)	1.6
10x RT random primer	4
Multiscribe reverse transcriptase	2
Nuclease free H_2O	8.4
Total per reaction	**20.0**

Table 2.5: cDNA synthesis master mix. The details of the master mix used to synthesis cDNA from RNA.

	Step 1	Step 2	Step 3	Step 4
Temperature (°C)	25	37	85	4
Time (Min)	10	120	5	∞

Table 2.6: cDNA synthesis thermocycler schedule. The details of the thermocycler programme used to synthesis cDNA from RNA.

2.9.7.3 Real Time PCR

Gene expression was assessed by real time quantitative RT-PCR using TaqMan Gene Expression Assays (Thermoscientific, Waltham, USA) according to the manufacturer's instructions. cDNA samples within the same experimental run were diluted to be at the same concentrations. The volume of each component to make up the master mix is displayed in Table 2.7. 20µl of the master mix:probe:cDNA mix was added to a well of a 96 well plate, the plate was then sealed with an optical adhesive seal and spun down to remove air bubbles. Each sample was repeated in duplicate. The plate was analysed using an ABI prism 7900 HT sequence detection system (Applied Biosystems) under the following conditions (Table 2.8).

Reagent	Volume per Reaction (μl)
2x Gene expression master mix	10
Endogenous control	1
Probe of gene of interest	1
cDNA	1
ddH_2O	7

Table 2.7: qPCR master mix. The details of the master mix used to carry out qPCR from cDNA.

	Step 1	Step 2	Step 3
Temperature (°C)	95	95	60
Time	15 min	15s	1 min
		Repeated 40x	

Table 2.8: qPCR analysis schedule. The details of the programme used for qPCR.

The housekeeping gene was human glyceraldehyde 3-phosphate dehydrogenase (GAPDH) labelled with 4,7,2'-trichloro-7'-phenyl-6-carboxyfluorescein (VIC). This was chosen as previous work in our laboratory showed that three different housekeeping genes, including GAPDH, gave similar results and GAPDH is more commonly used than the others. The probes for the genes of interest were labelled with 6-carboxyfluorescein (FAM). All probes and housekeeping genes were purchased from Applied Biosystems (Applied Biosystems by Life Technologies, Carlsbad, USA).

2.9.7.4 Analysis of Real Time PCR data

The expression of genes of interest was normalised to that of the GAPDH housekeeping gene. Data analysis was performed using the ΔΔCycles threshold (Ct) method, which does not require the use of a standard curve. The ΔΔCt value

was determined using the formula: $\Delta\Delta Ct = (Ct_{GOI} - Ct_{HK})$, with Ct_{GOI} being the average Ct value for the gene of interest and Ct_{HK} the average Ct value of the housekeeping gene. The data were expressed as mRNA expression fold change, relative to a calibrator sample. Assuming a doubling of material during each PCR cycle, this relative quantification (RQ) was estimated according to the formula: $(RQ) = 2^{-\Delta\Delta Ct}$.

2.9.7.5 Gene Selection

The genes selected for the *in vitro* studies were based on the literature and a panel of genes that were differentially regulated by SSR, UVA or UVB *in vivo* in human studies in our laboratory (Dr Angela Tewari and Kylie Morgan). After analysing the data and literature, a panel of genes covering different responses was chosen.

2.10 In Vivo Studies

Assay Name	Endpoint Measured
qPCR	Gene expression
HPLC	DNA damage (CPD)
Pigmentation assessment	385 and 405nm induced pigmentation assessed visually and using two reflectance devices

Table 2.9: Assays used for *in vitro* studies.

2.10.1 Ethical Approval & Volunteer Recruitment

The study (coded Sunshield) was approved by the National Research Ethics Service (NRES) City and East (Ref 15/LO/0380) and the Guy's and St Thomas' NHS Foundation Trust Research and Development (R&D) department and conducted in accordance with the Declaration of Helsinki Principles. All volunteers gave written informed consent. There were several sub-studies within the Sunshield protocol.

2.10.2 Methodology

The *in vivo* studies investigated various different endpoints. These are described below with volunteer demographics described in Table 2.10.

2.10.3 385nm/405nm *in vivo* studies

The 385nm and 405nm sources were the same as those described in the *in vitro* section. 1cm^2 irradiation sites on the lower back or upper buttocks of

healthy young volunteers were exposed to increasing doses of 385nm or 405nm light ranging from 0-150J/cm^2 from a distance of 15cm from the source. These doses were selected based on a literature review (Randhawa *et al.*, 2015) and are environmentally achievable on a mid-summers day in a tropical climate (for example in Rio de Janeiro) (Diffey, 2015). A fan was used to cool irradiation sites to ensure the skin did not overheat. For studies involving BASF compounds (formulations described in *BASF Compounds* section), the area was cleansed with ethanol wipes and each formulation was applied with a finger cot or glove to an area of 2.5 x 10cm at a concentration of 2mg/cm^2 (total application area = 25cm^2, total sunscreen weight 50mg ± 1mg (SD)), as advised by BASF using a technique widely used by the sunscreen industry. The sunscreen was allowed to dry for 10 minutes before any irradiations were carried out.

2.10.3.1 Sunshield – Study ID: FIL-2a1: 385nm and 405nm Induced Pigmentation and Erythema Dose-Time Response

The time-dependent pigmentation and/or erythema response to irradiation at 385nm and 405nm was determined in different skin types (SPT II-IV). The lower back of volunteers was irradiated with increasing doses of 385nm and 405nm between 0-150J/cm^2, using 25J/cm^2 increments for each site. Pigmentation and erythema was measured immediately, 4-6 hours and 24 hours post irradiation.

2.10.3.2 Sunshield – Study ID: FIL-2a2: Prevention of 385nm and 405nm Induced Pigmentation and/or Erythema by Sunscreens

The volunteers with the greatest responses in study 'Sunshield Fil-2a1' were selected to determine the ability of a range of sunscreens (*BASF Compounds*) to inhibit 385nm and 405nm induced pigmentation and/or erythema. Sunscreens were applied, and the volunteers' lower backs were irradiated (at a site separate from the previous study) with doses of 0, 100, 125 and 150J/cm^2 385nm and 405nm radiation with or without sunscreen. The sunscreens were removed with ethanol wipes immediately after exposure, and pigmentation and/or erythema were assessed immediately and 6 and 24 hours post irradiation.

2.10.3.3 Sunshield – Study ID: FIL-2b1: 385nm and 405nm Induced DNA damage and Gene Expression Dose-Time Response

The ability of irradiation at 385nm and 405nm to induce DNA damage and differential gene expression over time was determined in fair skin types (SPT I-II). The upper buttock was unirradiated or exposed to 385nm and 405nm radiation at a dose of 150J/cm^2 and biopsies were taken at 0, 2, 4, 6 or 24 hours (as described in the section *Biopsy Procedure*) to assess DNA damage and differential gene expression.

2.10.3.4 Sunshield –Study ID: FIL-2b2: Prevention of 385nm and 405nm induced Differential Gene Expression by Sunscreens

Different sunscreens were tested for their ability to prevent 385nm and 405nm differential gene expression. Sunscreens were applied to the upper buttocks of volunteers and were irradiated with doses of 150J/cm^2 of 385nm or 405nm radiation with or without each sunscreen. Sunscreens were removed with ethanol wipes and biopsies were taken 24 hours post irradiation as described and differential gene expression assessed.

2.10.3.5 Sunshield –Study ID: FIL-2b3: Prevention of 385nm Induced Delayed CPD induction by Sunscreens

Different sunscreens were tested for their ability to prevent 385nm induced delayed CPD production. Sunscreens were applied to the upper buttocks of volunteers and were irradiated with a dose of 150J/cm^2 of 385nm radiation with or without each sunscreen. Sunscreens were removed with ethanol wipes and biopsies were taken 4 hours post irradiation as described and CPDs were measured by HPLC.

No.	Sub-study	ID	Age	Sex	Skin Type
1	FIL-2a1	003	21	M	II
2	FIL-2a1	004	23	F	III
3	FIL-2a1	005	19	F	III
4	FIL-2a1	006	26	F	II
5	FIL-2a1	007	30	M	IV
6	FIL-2a1	008	32	F	III
7	FIL-2a1	009	31	F	IV
8	FIL-2a1	010	25	M	II
9	FIL-2a1	011	33	F	IV
10	FIL-2a2	001	25	M	III
11	FIL-2a2	003	21	M	II
12	FIL-2a2	004	31	M	IV
13	FIL-2b1	002	21	M	II
14	FIL-2b1	003	32	F	II
15	FIL-2b1	004	26	M	III
16	FIL-2b1	005	27	M	II
17	FIL-2b1	006	21	F	III
18	FIL-2b1/FIL-2b3	007	28	F	I
19	FIL-2b1/FIL-2b3	008	23	M	II
20	FIL-2b1/FIL-2b3	009	27	M	II
21	FIL-2b1/FIL-2b3	010	18	M	II
22	FIL-2b2	001	27	M	II
23	FIL-2b2	002	27	F	II
24	FIL-2b2	003	27	M	II
25	FIL-2b2	004	25	F	II
26	FIL-2b2	005	28	M	II

Table 2.10: Volunteer demographics for *in vivo* studies.

2.10.4 Pigmentation Assessment

The skin's pigmentary responses to irradiation were measured in three ways: (i) visually (ii) Minolta CM-700d reflectance spectrometer (Konica Minolta Sensing Inc., Osaka, Japan) (iii) UV-Optimize 555 reflectance spectrometer. (Matic, Naerum, Denmarkl). Visual assessment was made and graded according to the scheme in Table 2.11.

Grading		Score
No Pigmentation	-	0
Just Perceptible Pigmentation	±	0.5
Moderate Pigmentation	+	1
Dark Pigmentation	++	2

Table 2.11: Grading and corresponding score for pigmentation assessment.

The Minolta chromameter measures reflectance over a wide spectral range (400-700nm) at 10nm increments and automatically generates the International Commission on Illumination (CIE) L* a* b* coordinates. The chromameter was calibrated before each use against a standard reference. Brightness (L*) was used to evaluate the degree of pigmentation ranging from totally black (0) to completely white (100) and a* was used a measure of redness/erythema.

The Optimize device was also used to objectively measure pigmentation. This is a reflectance spectrometer that uses wavelengths of 555nm and 660nm to independently determine pigmentation and redness on scale from 0% to 100%. These wavelengths represent the maximal spectral absorption discrimination

between melanin and haemoglobin, the main two chromophores of the skin. Three replicates were measured and the device was calibrated before each use.

2.10.5 Biopsy Procedure

An authorised clinician or research nurse with the relevant training carried out all biopsy procedures in a clinical setting (Clinical Research Facility (CRF), 15th floor, Tower Wing, Guy's Hospital). The area to be biopsied was cleaned with local antiseptic (Chlorhexidine gluconate 0.05%). Following this, a local anaesthetic (Xylocaine 1% with adrenaline [epinephrine] 1:200,000; Astra Zeneca, UK) was administered subcutaneously to each biopsy site using a sterile syringe and a suitably sized sterile needle. A 4mm punch biopsy was then taken from each site and the biopsied areas were each sutured with a single 4-0 prolene stitch. The areas were then cleaned with chlorhexidine and dressed with Tegaderm™+ Pad. Spare dressings were given to volunteers after the procedure and they were advised to keep the biopsied areas dry for 24-48hrs before changing the dressings and secondly to avoid extensive bathing or sporting activities. Volunteers then returned 7-10 days later to have the stiches removed.

2.10.6 Tissue Processing

2.10.6.1 DNA Damage Assessment

Skin to be analysed by HPLC was immediately snap frozen in liquid nitrogen and stored at -80°C until transport on dry ice (temperature logged) to Grenoble, France where it was also stored at -80°C.

2.10.6.2 Gene Expression Analysis

Biopsies were placed in RNA*later* and stored at 4°C for 24hrs before being stored at -80°C until they were processed. RNA was then extracted as described in the below.

2.10.7 HPLC DNA Damage Assessment

DNA damage was assessed by laboratory of Thierry Douki (CEA Grenoble, France) as described below. DNA extraction was done with a DNeasy Kit (Qiagen, Limburg, The Netherlands), according to the manufacturer's instructions. The biopsies were disaggregated in 360 µL of ATL buffer in a TissueLyser system (Qiagen, Limburg, The Netherlands) using steel beads shaken for 15 min at a frequency of 25 Hz. The beads were removed and 40 µL of a proteinase K solution was added. The samples were incubated for 3h at 55°C with mild stirring. This was followed by treatment with RNaseA for 2 min at room temperature. A second buffer (AL, 400 µL) and ethanol (400 µL) was added. The

resulting mixture was eluted through a DNeasy column and washed by the extraction kit buffers (AW1 and AW2). In a final step, DNA was eluted by the addition of 200 µL of water in the column. The resulting solution was concentrated to 50 µL, after which DNA was enzymatically hydrolysed. For this purpose, it was incubated first with phosphodiesterase II, DNase II and nuclease P1 at pH 6 for 2 h at 37°C. Tris buffer was then added (final pH 8), together with phosphodiesterase I and alkaline phosphatase. The resulting mixture was left 2h at 37°C.

The samples were then transferred into HPLC injection vials and freeze-dried. The resulting residues were suspended in 50 µl of a 20 mM triethylammonium acetate solution (TEAA). They were injected onto a HPLC system (series 1100, Agilent) equipped with a reverse phase column (2×150 mm ID, 5 µm particle size, Uptisphere ODB, Interchim, Montluçon, France). The HPLC elution was performed at a flow rate of 200 µL/min in the gradient mode. The solvent was aqueous 2 mM TEAA with an increasing concentration of acetonitrile that reached 20% at the end of the analysis. The outlet of the column was first connected to a UVR detector, which was used for the quantification of normal nucleosides. The flow was then directed to the inlet of a triple quadrupole electrospray mass spectrometer (API 300, SCIEX, Framingham, MA) operated in the negative mode. Pyrimidine dimers were detected as modified dinucleoside monophosphates, using the multiple reaction-monitoring mode. For this type of detection, a specific molecular ion is selected and fragmented and specific fragments are quantified. For both the UVR and mass spectrometry detections, an external calibration using solutions of authentic standards was performed.

Results were expressed as the number of thymine dimers (TT) photoproducts per million normal base pairs.

2.10.8 Gene Expression

The kit used for all RNA extraction during the study was the same as for the *in vitro* studies (mirVana™ miRNA Isolation kit with Phenol; Life Technologies).

Biopsies were defrosted on ice and briefly washed in ice cold PBS and dried on tissue. Tissue was then added to 1ml of lysis buffer in a gentleMACS M tube (Miltenyi Biotech Ltd., Surrey, United Kingdom). Tissue was homogenised using a gentleMACS dissociator (Miltenyi Biotech Ltd., Surrey, United Kingdom) running the pre-set programme for total RNA extraction. All subsequent steps are as the *in vitro* method.

2.11 Statistical Analysis

All data are expressed as the mean ± standard deviation (SD) where n ≥3 unless stated otherwise. Statistical analyses were carried out using Graphpad Prism 6.0 (Graphpad Software, San Diego, CA) and were evaluated using the student's t-test, ANOVA with multiple comparisons tests (Dunnet's, Tukeys, Kruskal-Wallis), linear and non-linear regression. Significance limits were set as: $* = p \leq 0.05$, $** = p \leq 0.001$, $*** = p \leq 0.0001$.

Chapter 3: Molecular Photoprotection by the Naturally Occurring Mycosporine-Like Amino Acid (MAA) Palythine in a Human *In Vitro* Skin Model

3.1 Results

3.1.1 Photostability of Palythine

The photostability of palythine was assessed by UV spectrometry. Palythine was diluted in PBS at a concentration of 0.0001% w/v (4.098E-06M) and exposed to increasing doses of SSR, and absorbance was measured between 280-400nm after each dose with results displayed in Figure 3.1. Doses used, total absorbance and percentage reduction absorbance are described in Table 3.1. Even at the highest dose of 50 SED there was only a 3% reduction in the total absorbance, implying palythine is an extremely photostable molecule.

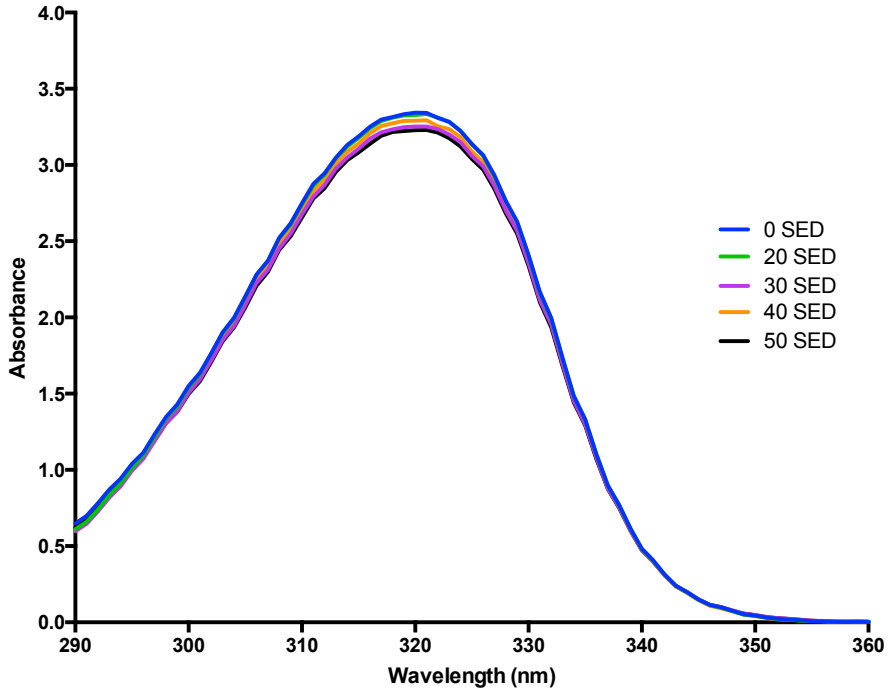

Figure 3.1: The MAA palythine is photostable when exposed to high doses of solar simulated radiation. Palythine at a concentration of 0.001% w/v was exposed to increasing doses of SSR and the absorbance subsequently measured by UV spectrometry between 280-400nm (n=3). There were very low levels of photodegradation as described in Table 3.1.

Dose (SED)	Dose (J/cm²)	Total Absorbance	Percentage Degradation
0 SED	0.00	114.3	0.00
20 SED	25.5	112.5	1.60
30 SED	37.8	110.4	3.42
40 SED	51.9	111.3	2.73
50 SED	63.3	110.3	3.63

Table 3.1: The doses of SSR used and percentage reduction in absorbance for palythine photostability study. The equivalent doses (J/cm²) for each dose (SED) used to test the photostability of palythine and the percentage degradation compared to 0 SED as measured by UV spectrometry between 280-400nm (n=3). There was only minimal degradation due to SSR exposure.

3.1.2 Photoprotection Against Cell Viability Reduction by Palythine

SSR is known to induce cell death. To select suitable doses for later experiments, the effect on cell viability of HaCat keratinocytes by a range of doses of SSR was assessed using the Neutral Red assay (Repetto *et al.*, 2008). Doses between 0-20J/cm^2 were selected based on previous work in our group, the literature and what was considered to be environmentally and biologically relevant. There was a significant SSR dose dependent reduction in cell viability (Figure 3.2)

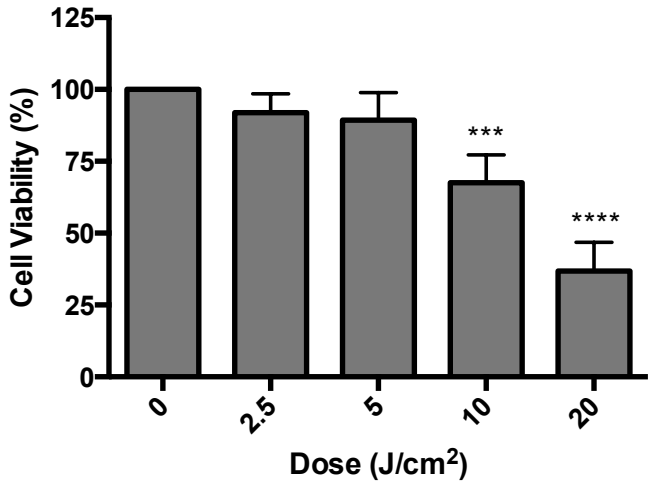

Figure 3.2: SSR significantly induced cell death in HaCaT keratinocytes in a dose dependent manner. HaCaT keratinocytes were untreated, or exposed to 2.5, 5, 10 or 20J/cm^2 of SSR. Cell viability was measured 24 hrs later by the Neutral Red assay. Columns represent the mean ± SD (n=3). There was a significant dose dependent decrease in cell viability by SSR ($p<0.0001$, One-way ANOVA with Dunnett's multiple comparisons test).

The toxicity of palythine, and its protection against SSR induced cell death was measured. Cells were exposed to SSR (20J/cm^2) with a range of palythine concentrations (0-10 % w/v (0-0.0041M)), and to palythine (10 % w/v) without SSR exposure. There was a significant decrease in viability when cells were exposed alone to SSR without palythine compared to unexposed cells. There was no significant difference found between unexposed cells and cells treated with palythine without SSR, which indicates that palythine is not cytotoxic and provides significant protection against SSR induced cell death at all concentrations tested (Figure 3.3).

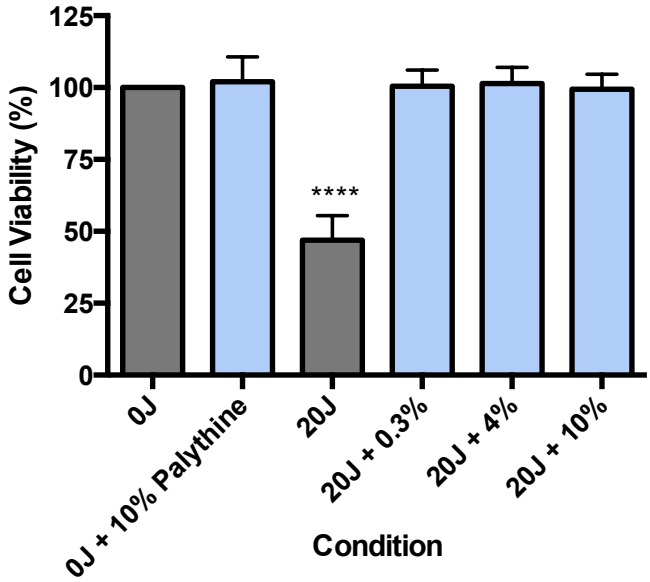

Figure 3.3: **HaCaT keratinocytes were significantly protected by palythine from SSR induced cell death.** HaCaT keratinocytes were untreated, exposed to 20J/cm^2 of SSR with PBS alone, 0.3 % (w/v), 4 % (w/v) or 10 % (w/v) of palythine or 10 % (w/v) palythine without exposure to UVR. Cell viability was measured 24 hrs later by the Neutral Red assay. Columns represent the mean ± SD (n=3). Palythine provided significant protection at all concentrations against cell death, without exposure and cells exposed without palythine had significantly reduced viability ($p<0.0001$, One-way ANOVA with Dunnett's multiple comparisons test).

3.1.3 Photoprotection against DNA Damage by Palythine

The most widely studied molecular endpoint measured when assessing UVR-induced damage is DNA lesions. Two methods of DNA damage assessment in HaCat keratinocytes were employed: IHC-IF and the single cell gel electrophoresis assay (comet assay). Firstly IHC-IF was used to assess the dose-response of increasing doses of SSR (0-20J/cm^2) on the induction of CPD lesions (Figure 3.4). There was a significant dose dependent increase in CPD production.

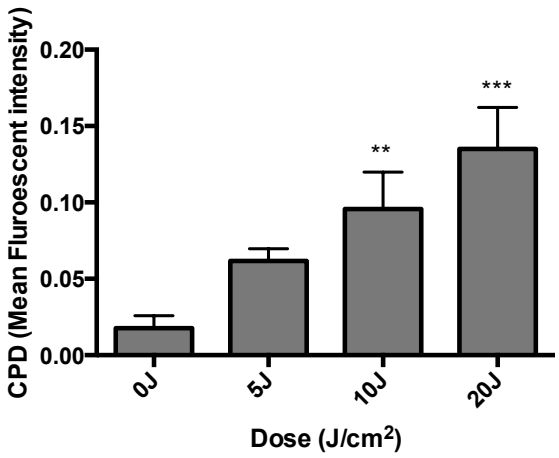

Figure 3.4: SSR significantly induced CPD in a dose dependent manner when measured by IHC-IF. HaCaT keratinocytes were untreated, or exposed to 5, 10 or 20J/cm^2 of SSR. CPDs were measured immediately post exposure using IHC-IF. Columns represent mean ± SD (n=3). There was a significant dose dependent increase in CPD formation by SSR (p=0.0004, one-way ANOVA with Dunnett's multiple comparisons test).

The second method used was the comet assay to measure ALS, CPD and 8-oxoGua by SSR and UVA radiation. HaCat keratinocytes were exposed to a dose of 5J/cm^2 of SSR or 20J/cm^2 UVA (based on previous work in the laboratory) and the three lesions were measured (Figure 3.5). Graphs are displayed as mean ± SD (n=3). There was significant increase in all lesions tested for both SSR and UVA.

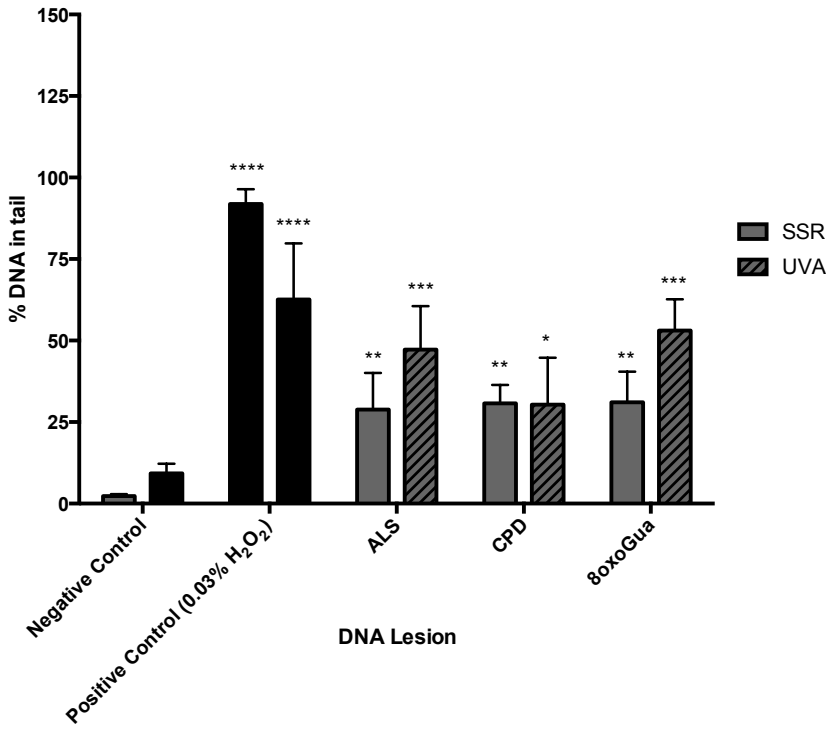

Figure 3.5: The effects of SSR and UVA on the formation of DNA lesions assessed by comet assay. HaCaT keratinocytes were untreated, or exposed to 5J/cm^2 of SSR or 20J/cm^2 UVA. DNA lesions (ALS, CPD, 8oxoGua) were measured immediately post exposure using the comet assay. Columns represent mean ± SD (n≥3). SSR and UVA experiments were independent so all control are plotted. There was a significant increase in all lesions when exposed to SSR or UVA (SSR: $p<0.0001$, UVA: $p<0.0001$ one-way ANOVA with Dunnett's multiple comparisons test).

Both detection methods were employed to assess the ability of palythine to reduce UVR induced DNA damage; IHC-IF to measure CPDs by SSR and the comet assay to measure ALS, CPD and 8oxoGua damage by SSR and UVA. HaCaT keratinocytes were irradiated with 20J/cm^2 SSR in PBS alone or 0.3-10% w/v palythine and measured by IHC-IF. UVR exposed cells showed a significantly increased number of CPD lesions (Figure 3.6) compared to the unirradiated control. In the samples irradiated with palythine, there was a significant decrease in CPD formation across all of the concentrations tested compared to without palythine.

a.

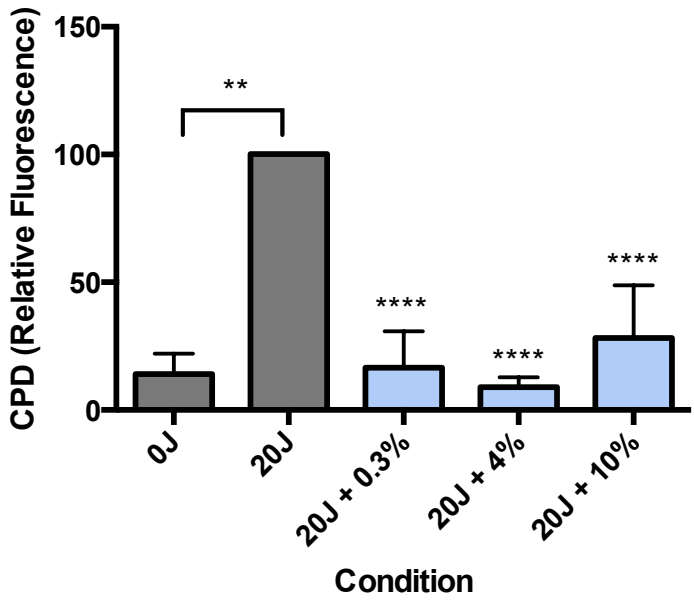

b.

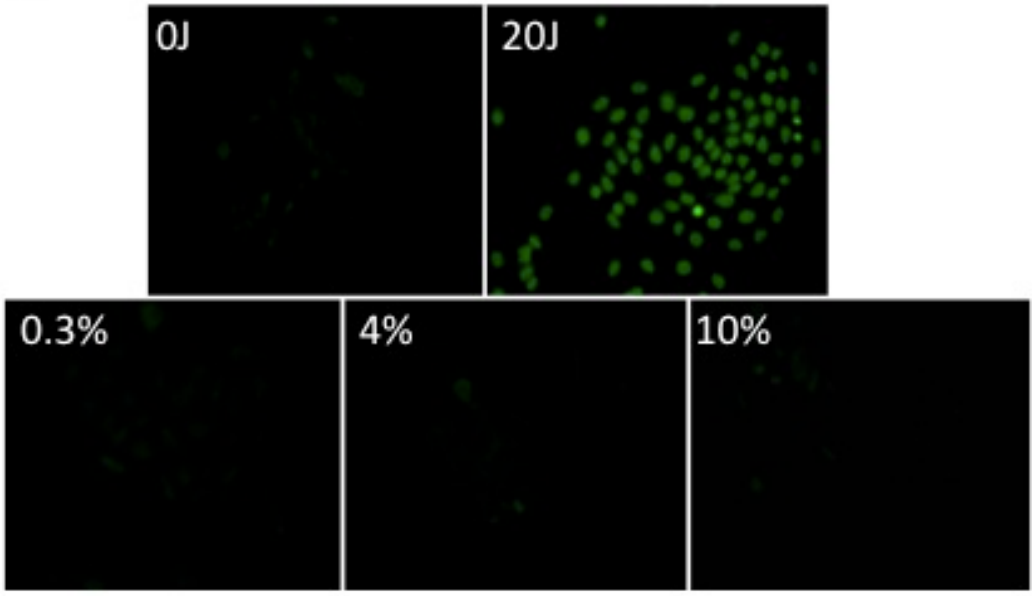

Figure 3.6: HaCaT keratinocytes were significantly protected from SSR induced CPDs by palythine at a range of concentrations when measured by IHC-IF. (a) HaCaT keratinocytes were untreated, exposed to UVR (20J/cm^2 SSR) with 0%, 0.3, 4 or 10% w/v palythine. CPD were measured immediately post exposure using IHC-IF. Columns represent mean ± SD (n=3). Cells irradiated without palythine showed a significant increase in CPD ($p=0.0029$, paired t test) compared to the unirradiated control. Palythine at 0.3-10%w/v showed a significant reduction in CPDs compared to irradiated control ($p<0.0001$, one-way ANOVA with Dunnett's multiple comparisons test). (b) Typical fluorescent images for each condition.

This result was confirmed using the comet assay (Figure 3.7), which showed a significant reduction in ALS, CPDs and 8oxoGua when exposed to 5J/cm^2 with 0.3% palythine compared to PBS alone, measured with unpaired t-test. UVA induced DNA damage reductions were also measured. Cells were exposed to 20J/cm^2 of UVA radiation in PBS alone or with 0.3% w/v palythine and there was a significant reduction in ALS, CPDs and 8oxoGua. These data suggest that palythine provides significant protection in reducing different types of UVR induced DNA damage.

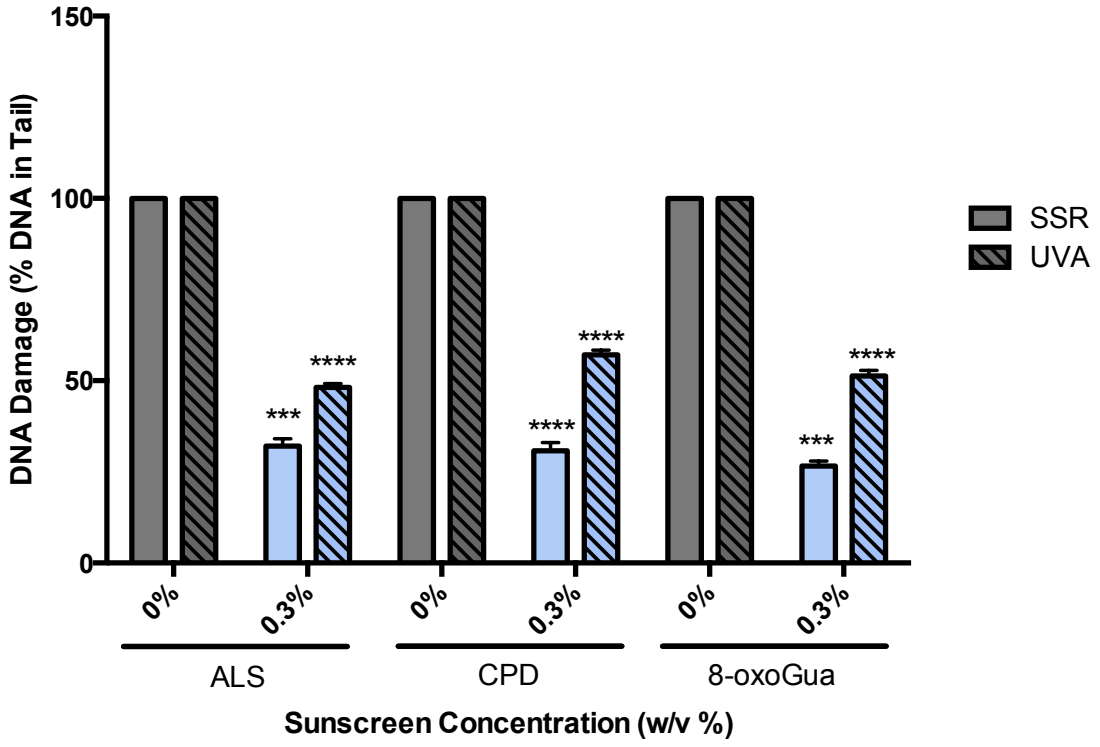

Figure 3.7: HaCaT keratinocytes were significantly protected from SSR and UVA induced CPD, 8-oxoGua and ALS by palythine at a concentration of 0.3% as measured by the comet assay. Cells were irradiated with 5J/cm^2 SSR or 20J/cm^2 of UVA radiation with or without 0.3% w/v of palythine and ALS, CPDs or 8oxoGua production were measured by the comet assay. There was a significant reduction for all legions measured for both spectra tested (SSR- ALS ($p=0.006$; n=3,), CPD ($p<0.0001$; n=3, 8oxoGua ($p=0.0004$; n=3); UVA - ALS ($p<0.0001$; n=3,), CPD ($p<0.0001$; n=3,) 8oxoGua ($p<0.0001$; n=3); unpaired t-test).

3.1.4 Photoprotection Against Induction of Reactive Oxygen Species by Palythine

UVR is known to induce ROS. The effect of different doses of UVR on ROS production was assessed to determine optimal doses for the photoprotection experiments HaCat keratinocytes were exposed to increasing doses of SSR (0-40J/cm^2) (Figure 3.8). FACS was used to measured ROS levels immediately after exposure. There was a significant dose dependent increase in ROS production.

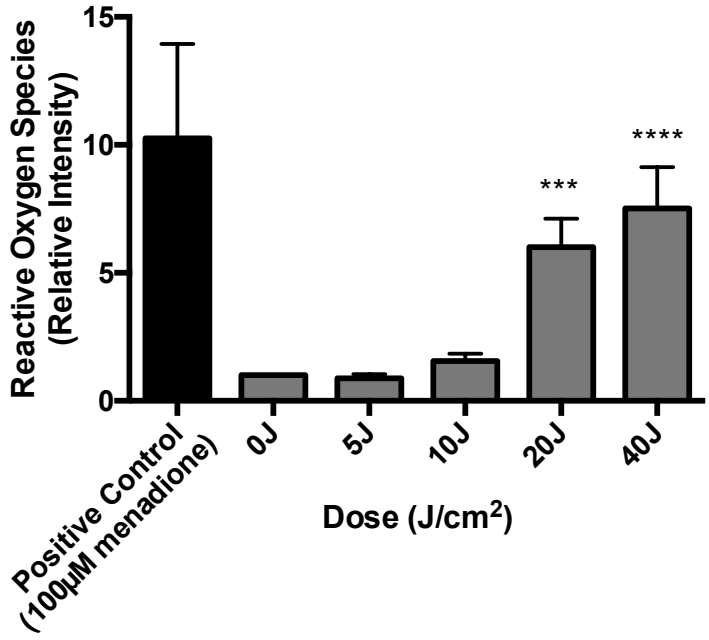

Figure 3.8: SSR significantly induced the formation of ROS in a dose dependent manner in HaCaT keratinocytes when measured using the H_2DCFDA assay. HaCaT keratinocytes were untreated, or exposed to 5, 10, 20 or 40J/cm^2 of SSR. The levels of ROS were measured using FACS, recording the mean fluorescent intensity for each condition after cells were treated carboxy-H_2DCFDA immediately post exposure. Columns represent the mean ± SD (n=3). SSR induced a significant dose dependent increase in ROS ($p<0.0001$, one-way ANOVA with Dunnett's multiple comparisons test).

The UVR filtering and anti-oxidant properties of palythine were assessed (Figure 3.9). HaCat keratinocytes were irradiated with 20J/cm^2 of SSR either in PBS alone, with 0.3-10% w/v of palythine or, to assess the anti-oxidant ability, irradiated in PBS and then incubated post SSR exposure with 4% palythine. After exposure ROS levels were measured as before. Cells irradiated with 20J/cm^2 SSR, after palythine incubation, demonstrated a significant increase in ROS production compared to unirradiated control. Palythine, when added post exposure at 4%, also showed significant protection against ROS induction.

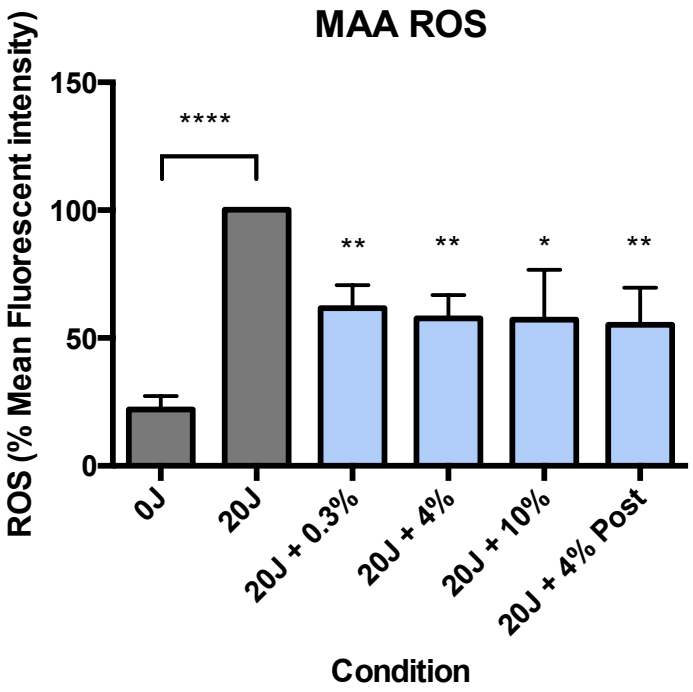

Figure 3.9: **Palythine provided significant protection from SSR induced ROS induction and exhibited anti-oxidant properties in HaCaT keratinocytes.** HaCaT keratinocytes were untreated, exposed to 20J/cm^2 of SSR with PBS alone, 0.3%, 4% or 10% palythine or 4% palythine post exposure. ROS levels were measured by FACS to record the mean fluorescent intensity for each condition after cells were treated carboxy-H_2DCFDA. Columns represent the mean ± SD (n=5). Cells irradiated without palythine showed a significant increase in ROS ($p<0.0001$, paired t test) compared to the unirradiated control. Palythine at 0.3-10%w/v showed a significant reduction in ROS production compared to irradiated control when added pre exposure or at 4% post exposure ($p<0.0001$, one-way ANOVA with Dunnett's multiple comparisons test).

3.1.5 Anti-Oxidant and Radical Quenching Effects of Palythine

The mechanisms behind the antioxidant effect displayed in the previous section were investigated further. Firstly the DPPH assay was used to assess the radical quenching activity of palythine compared to three widely used anti-oxidants: vitamin C, vitamin E and vitamin E phosphate. Vitamin E phosphate was assessed because it is water-soluble analogue of vitamin E which is believed to be more stable that vitamin E (which is insoluble in water and therefore unsuitable for this assay) (personal communication – Dr Stuart Jones). The results are displayed below in Figure 3.10. All compounds showed a significant inhibition of DPPH radicals demonstrating radical quenching ability.

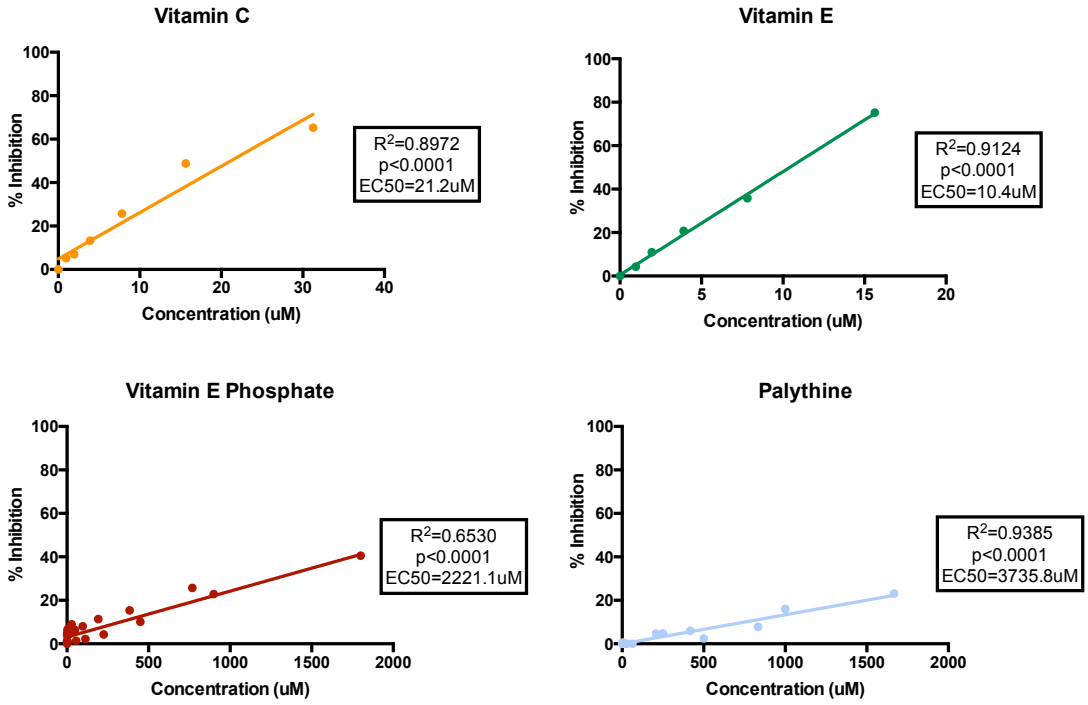

Figure 3.10: The DPPH radical scavenging ability of known anti-oxidants compared with palythine. Known antioxidants and palythine solutions of increasing concentration were analysed in their ability to quench the DPPH radical as a measure of radical scavenging activity. All compounds demonstrated significant activity (Linear regression analysis). Each data point represents the mean (n=3).

Another chemical anti-oxidant assay, the ORAC assay, was used to assess the hydrogen atom transfer ability of compounds by its ability to reduce peroxyl radical (ROO•) induced damage to fluorescein. The same compounds were used as in the previous assay, with the addition of Trolox, a water-soluble analogue of vitamin E, used as the standard compound for comparison with test molecules. All compounds demonstrated a significant anti-oxidant effect with exception of vitamin E, as displayed in Figure 3.11.

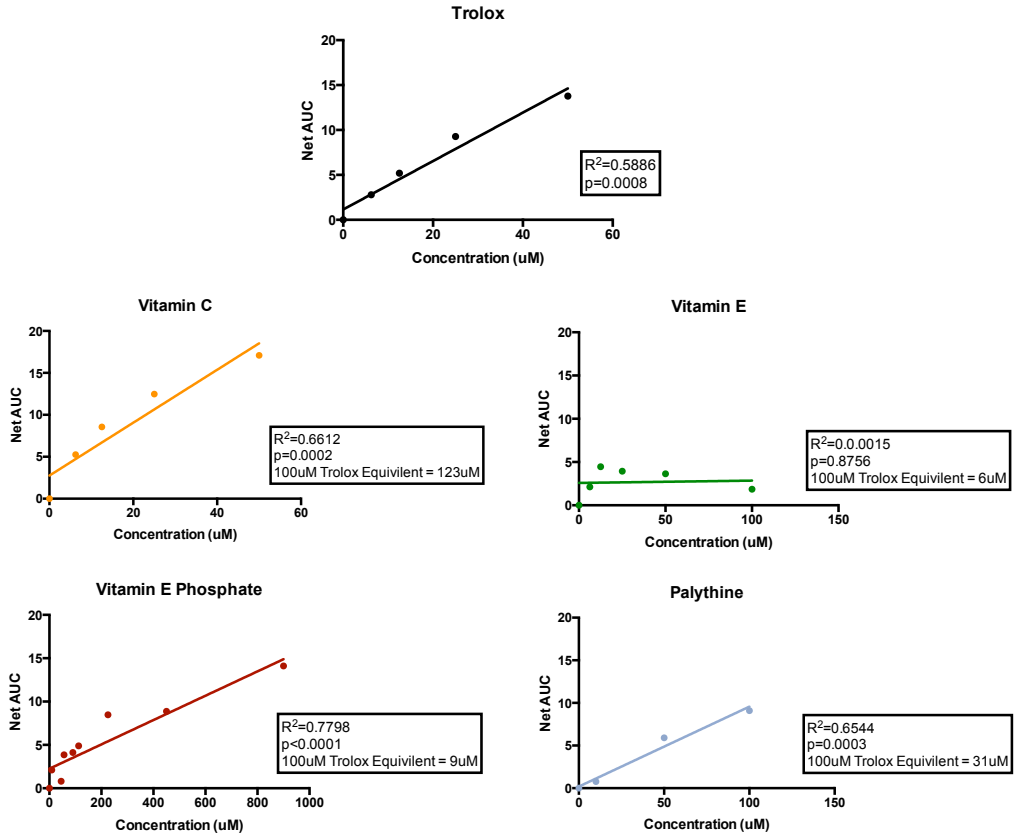

Figure 3.11: The oxygen radical scavenging ability of known anti-oxidant and palythine. Known antioxidants and palythine solutions of increasing concentration were analysed in their ability to quench the ROO• radical as a measure of anti-oxidant capability activity. All compounds demonstrated significant activity with the exception of vitamin E (Linear regression analysis). Each data point represents the mean (n=3).

3.1.6 Photoprotection Against Gene Expression Changes by Palythine

SSR induced gene expression changes in HaCat keratinocytes were assessed to identify suitable markers for photoprotection studies. Gene selection was based on previous human skin *in vivo* work in our group and to cover a range of different endpoints including inflammatory cytokines (IL-8, IL-6, IL-20), oxidative stress response (HMOX-1, PON-2) and matrix remodelling enzymes as markers of photoageing (MMP-1, MMP-3, MMP-12 – mostly expressed in the epidermis). These were measured by qPCR on SSR irradiated HaCat cells ($5J/cm^2$). This lower dose was used because it is important to maintain a cell viability of ≥ 80%. 12 hours post UVR exposure total RNA was extracted from the cells as described in the Materials and Methods. After checking the RNA quality by nanodrop, cDNA was synthesized and qPCR performed. GAPDH was used as the housekeeping gene. The ΔΔCT method was used to analyse the difference in fold change compared to the unirradiated samples (with a value of 1). Many of the genes were significantly upregulated 12 hours post-exposure, demonstrating good correlation with previous *in vitro* and *in vivo* studies and indicating the significant damage of SSR exposure (Figure 3.12).

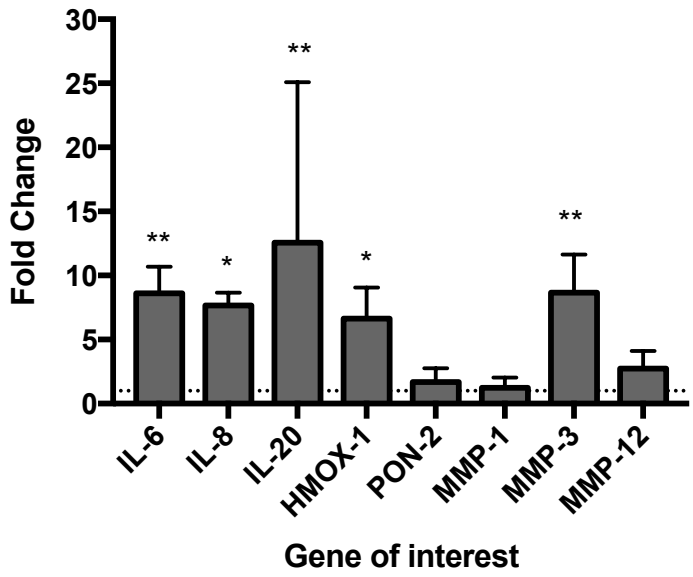

Figure 3.12: SSR induced gene changes in HaCaT keratinocytes. HaCaT keratinocytes were exposed to 5J/cm² of SSR. Gene expression was measured 12 hours post exposure by qPCR. Columns represent the mean ± SD (n≥3). There was a significant upregulation in many of the genes (ANOVA - p=0.0001, Multiple comparisons - IL-6: p=0.0016, IL-8: p=0.0459, IL-20: p=0.0014, HMOX-1: p=0.0014, PON-2: p>0.9999, MMP-1: p>0.9999, MMP-3; p=0.0050, MMP-12: p=0.8874 One-way ANOVA with Kruskal-Wallis multiple comparisons test).

The protection of palythine against UVR induced gene expression changes was investigated covering a range of endpoints from selected from the time course experiment shown in Figure 3.13. The genes selected were (IL-8, IL-6, IL-20) to represent inflammation/immunoregulation, HMOX-1 as an oxidative stress response marker, MMP-3 as a marker for photoageing. Cells were irradiated with and without palythine at different concentrations (0.3-10%). The results are expressed as mean fold change ± SD (n=5). All palythine concentrations showed significant protection against SSR-induced gene expression. The only exception was palythine at 0.3% w/v for the expression of

IL-8, which was reduced but not statistically significant. All other concentrations of palythine provided significant protection for IL-8. This indicates palythine has a significant effect in protecting against solar UVR-induced markers of inflammation, oxidative stress and photoageing.

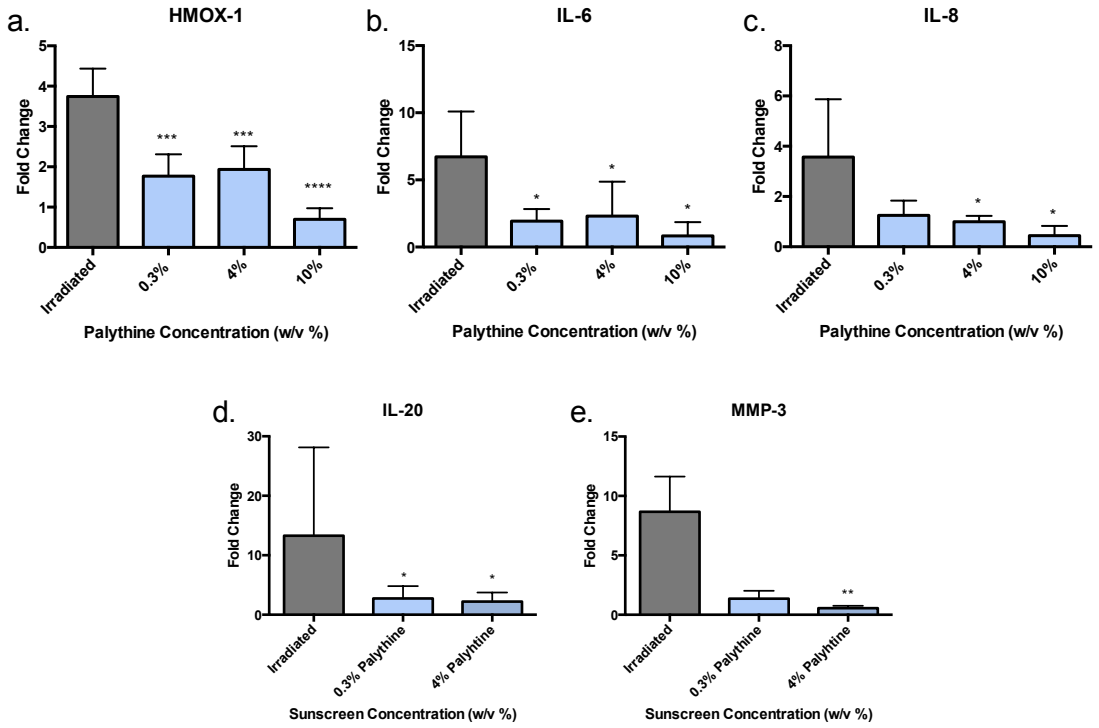

Figure 3.13: Palythine provided significant protection from SSR-induced gene changes in HaCaT keratinocytes. HaCaT keratinocytes were untreated, exposed to 5J/cm^2 of SSR with 0%, 0.3%, 4% and in some cases 10% of palythine. Gene expression was measured 12 hours post exposure by qPCR. Columns represent the mean ± SD (n=5). Palythine provided significant protection compared to irradiated cells for all genes tested at all concentrations with the exceptions of 0.3% palythine against IL-8. (HMOX-1 ($p<0.0001$; n=5), IL-6 ($p=0.0105$; n=5), IL-8 ($p=0.0126$; n=5), IL-20 ($p=0.0024$; n=5), MMP-3 ($p<0.0001$; n=5) One-way ANOVA with Tukey's multiple comparisons test).

3.1.7 Molar Extinction Coefficient, SPF, UVA-PF and Critical Wavelength Test of Palythine

The photoprotection of palythine was assessed by various *in vitro* methods based on the spectral profile of palythine between 290-400nm (Figure. 2.2). The first test is the calculation of the molar absorption coefficient ($\varepsilon^{(m)}$) at $\lambda_{max,}$ which for palythine is at 320nm (Figure 3.14). The calculated value is described in Table 3.2 (n=4, average ± SD).

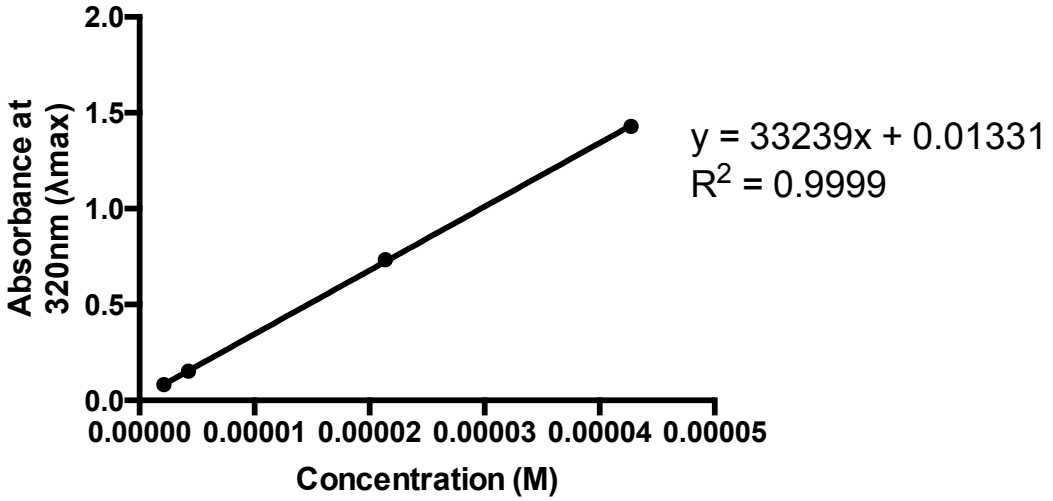

Figure 3.14: The absorbance of palythine at λ_{max} for a range of concentrations. The absorbance of palythine at a range of concentrations was measured using UV spectrophotometry and plotted. This was used to calculate ($\varepsilon^{(m)}$).

Molar Extinction Coefficient ($\varepsilon^{(m)}$) at λmax
36,947.7 ± 2238.6

Table 3.2: The molar extinction coefficient of palythine. The average molar extinction coefficient of palythine ± SD is displayed, calculated from Figure. 3.12. (n= 4).

The *in vitro* SPF and UVA-PF of palythine can be determined from its molar extinction coefficients in the method described by Herzog and Osterwalder (Herzog and Osterwalder, 2015). The calculated values of different palythine concentrations, which fall into the range approved for synthetic filters are displayed in Table 3.3. Palythine demonstrated good SPF values but poor UVA-PF values, in line with its spectral properties. The poor UVA/broad spectrum protection offered by palythine is further displayed using two other tests commonly used to assess sunscreen efficacy. Firstly, is the critical wavelength test, displayed in Table 3.4. This test requires a value of ≥370nm to pass. Palythine failed this test with a value of 337nm. Table 3.4 also shows the results of the Boots star-rating test. A result of ≥0.6 is required for the lowest 3* rating, for palythine a value of 0.34 was calculated indicating no rating.

Concentration of Palythine (% w/v)	***In Vitro* SPF**	***In Vitro* UVA-PF**
0.3%	1.9	1.1
1%	3.4	1.2
5%	10.9	1.4
10%	17.9	1.6
25%	30.2	2.1

Table 3.3: The *in vitro* SPF and UVA-PF of palythine. The *in vitro* SPF and UVA-PF of palythine was calculated as described in the methods from the absorption spectrum of palythine at a range of concentrations. The SPF values obtained are relatively high for a single molecule however a low UVA-PF is achieved.

Critical Wavelength Test		Boots Star Rating Test	
Critical Wavelength	Pass/Fail	UVA/UVB Ratio (Unirradiated)	Boots Star Rating
337nm	Fail	0.34	No Rating

Table 3.4: The critical wavelength test and Boots star rating result. The result of the critical wavelength test as described in the methods from the absorption spectrum of palythine. Palythine fails the test that requires a value of ≥370nm to pass. The result of the Boots star rating test result as described in the methods from the absorption spectrum of palythine. Palythine receives no rating; a value of ≥0.6 is required for the lowest approved rating of 3. These data indicate a lack of broad-spectrum protection.

3.2 Discussion

The absorption of UVR by skin chromophores initiates the formation of photoproducts that cause the acute and long-term effects of the sun on the skin. The CPD is one of the most important and is responsible for the C to T transition mutations, especially in p53, that initiate many skin cancers. Field studies show a UVB (~295 -320nm) dose-dependent increase in CPDs after a one-week holiday in the sun (Petersen *et al.*, 2014). Laboratory studies show that the stem cell containing basal layer of the epidermis is especially sensitive to UVA1-induced CPDs (Tewari *et al.*, 2013a). ROS can damage DNA resulting in mutations that play a role in skin cancer, and can also damage other important cellular components (McAdam *et al.*, 2016; Wolfle *et al.*, 2014). Solar UVR also induces gene transcription and protein synthesis that underpin its many adverse health effects. The molecular markers in this study were largely chosen to be representative of those that occur in human skin *in vivo* as well as being relevant to clinical outcomes (Marionnet *et al.*, 2014; Quan *et al.*, 2009).

Sunscreen use is important in the prevention of the acute and long-term effects of solar UVR. At present, the only regulatory requirement of a sunscreen is that it inhibits erythema as indicated by its sun protection factor (SPF) and that it has some measure of UVA protection, which is assessed by techniques that have no direct biological relevance. There are few data on the ability of sunscreens to prevent molecular photodamage, especially *in vivo* (Olsen et al., 2017). Current sunscreens approved by global regulatory bodies are either synthetic organic molecules or organic/inorganic pigments. There is increasing

concern (see introduction) that some of these agents may cause environmental harm (Danovaro *et al.*, 2008; Kunz and Fent, 2006b). In part, this has initiated the exploration of natural biocompatible sunscreens, many of which have evolved under conditions of extreme insolation over several hours every day. One such group of compounds is the MAA as described in detail in the introduction.

The aim of this work was to establish SSR-induced damage endpoints in HaCat keratinocytes, to confirm they correlate well with more complex models and reported effects in the literature, and then to assess the ability of MAAs to prevent this damage. All the studies reported in this chapter have been carried out with environmentally and physiologically relevant exposures of UVR. A dose of 20J/cm^2 SSR is equivalent to about an hour of peak UK summer sun (roughly the same for the UVA dose of 20J/cm^2 used) (Diffey, 2015) which is about 4-5 minimal erythema doses (MED) in a fair-skinned person (Harrison and Young, 2002).

For each of the end points investigated (cell viability (Figure 3.2), DNA damage (Figures 3.4 & 3.5), oxidative stress (Figure 3.8), differential gene expression (Figure 3.11) the first step was to confirm the effects as stated above and optimise the methods, doses and time points used in the photoprotection studies. For all of the end points there was clear UVR dose-response relationship, verifying the effects found in the literature. The gene expression results found many upregulated genes covering a range of endpoints to be used in

photoprotection studies. They also verified previous *in vivo* work, validating the use of this model (Tewari *et al.*, 2014; Tewari *et al.*, 2012a).

Palythine was selected as a model MAA for the photoprotection studies described above. There were several reasons for the selection of this compound rather than the other 20 or so other MAAs that have been discovered. Firstly MAAs are not available commercially and so require prior extraction from their natural sources. Palythine as a single MAA is easily obtained from highly farmed alga called *Chrondus yendoi*, which is widely consumed in Japan. Having a single MAA was important, as most studies have been carried out on MAA mixtures, usually shinorine, porphyra-334 and mycosporine-glycine so is difficult to attribute any effects to any one of these compounds. Finally, palythine has good absorption in the most damaging UVB spectral region, had been shown to posses good photostability and anti-oxidant ability in chemical assays. It was also much less investigated than other MAAs making it a good candidate for the studies.

One requirement of UVR filters and sunscreens is excellent photostability. Lack of photostability has been a concern with some synthetic sunscreens (Maier *et al.*, 2001) and there have been numerous studies to investigate the photostability of MAAs. Palythine has been found to be extremely photostable in air saturated aqueous solutions (Conde *et al.*, 2007) and in distilled and sea water in the presence of photosensitizers (Whitehead and Hedges, 2005). Figure 3.1 also demonstrates the photostability of palythine in response to SSR radiation. Even after irradiation of up to 50 SED, which is equivalent to around a full day of UK summer sun (a dose of 51J/cm^2) there is only a small reduction in

the total absorption of 3.63% (Table 3.1). This confirms the excellent photostability of palythine using an environmentally relevant dose and spectrum.

Figure 3.3 shows that exposure to an SSR dose of 20J/cm^2 reduced cell viability to 28% of unexposed control cells, and that palythine significantly protects against cell death across a range of concentrations from 0.3% to 10%. Complete protection at concentrations as low as 0.3% is advantageous because most sunscreens contain a combination of synthetic filters at concentrations between 1-10%. Palythine was also shown to have no effect on cell viability when incubated at 10% for 24 hours suggesting a lack of cytotoxicity.

The induction of ROS in the skin by UVR has been well documented (Bickers and Athar, 2006; Wolfle *et al.*, 2014). ROS cause oxidative damage to different cellular macromolecules – such as DNA, lipids and proteins, protein oxidation has become of particular interest recently as it was demonstrated that oxidation of proteins can lead to inhibition of DNA repair machinery, suggesting an increased risk of mutations (McAdam *et al.*, 2016). There is evidence that some MAAs are antioxidants, mainly demonstrated in non-biological chemical assays (Nazifi *et al.*, 2013; Rastogi *et al.*, 2015). The results displayed in Figure. 3.9 show that palythine significantly reduces ROS generation by SSR. *In vitro* studies in human keratinocytes have shown that ROS are generated for 15 minutes after UVR exposure (Valencia and Kochevar, 2008). Palythine was also added immediately after UVR exposure in order to distinguish between its UVR filtering and antioxidants properties. The data show that it is equally effective under both

conditions, demonstrating its antioxidant properties though not confirming its benefit as a UVR filter as expected by its absorption profile. These results support a recent study that showed pre-incubation for 24 hours with an MAA (porphyra-334) significantly reduced UVA-induced ROS in human skin fibroblasts (CCD-986sk) (Ryu *et al.*, 2014). The mechanism for this anti-oxidant activity was investigated further using two assays, the DPPH (Figure 3.10) and ORAC (Figure 3.11) assays. The results demonstrate that palythine acts by quenching radicals using electron transfer as well as hydrogen atom transfer mechanisms. The results of palythine were compared with other known anti-oxidants including vitamin C, vitamin E, vitamin E phosphate and Trolox in the ORAC assay. The efficacy of palythine was several orders of magnitude lower than with the known anti-oxidants (for example compared to vitamin C, palythine was 176x less potent with the DPPH assay and 4x for the ORAC assay). Although this is significantly lower, both vitamin C and E have been demonstrated a lack of photostability (e.g. vitamin C degrading 70x faster with exposure compared to unirradiated control (Ahmad *et al.*, 2011)) and provide only minimal absorption in the UVR region (Neunert *et al.*, 2016), properties which are established in palythine and other MAAs. There is also evidence that vitamin E has poor skin penetration properties, not diffusing beyond the *stratum corneum* into the viable epidermis or dermis (Zhao *et al.*, 2009). Vitamin E Phosphate is used with this in mind as it thought to have better penetration properties. This suggests limited efficacy with topical application of these widely used compounds, with palythine possessing properties that may be more effective in real world situations. The results also suggest the anti-oxidant effect

of palythine is primarily due to a hydrogen atom transfer mechanism, as demonstrated by its potency in the ORAC assay.

The immunohistological assessments for CPDs show that they are readily induced by 20J/cm^2 of SSR as shown in Figure 3.6. Palythine at all concentrations resulted in a highly significant reduction in CPD formation, comparable with the unirradiated control. The comet assay was also used to assess DNA damage and the photoprotective properties of palythine. The results (Figure 3.7) confirmed that palythine (0.3%) significantly reduced the formation of CPDs by SSR (5J/cm^2). Additionally, palythine significantly reduced the levels of SSB, ALS, CPDs and 8-oxoGua by UVA as well as SSR. Protection against UVA-induced DNA damage is particularly unexpected as the UVR absorption of palythine does not extend across the whole UVA range (shown in Figure 3.1) and demonstrated by its very modest UVA-PF (Table 3.3). This suggests that the shorter wavelengths of UVA, where palythine does absorb, is more important to protect against to prevent DNA damage, and/or that the anti-oxidant effect of palythine is significant enough to prevent damage across the whole UVA range. Although directly not investigated in this work, MAAs have been demonstrated previously to be triplet state quenchers, preventing the formation of CPDs in solution (Misonou *et al.*, 2003). This shows MAAs have additional potential in preventing damage post UVR exposure as recently the formation of delayed or 'dark' CPDs up to 6 hours after irradiation has been reported (Premi *et al.*, 2015). This study demonstrates this is due to chemiexcitation of melanin, and transfer of the triplet state electrons to thymine bases that results in CPD formation. Vitamin E was capable of preventing the formation of these lesions. MAA have previously

demonstrated triplet-quenching activity that could account for the prevention of CPDs at palythine concentrations as low as 0.3%. Overall these data are the first to show that an MAA can protect against UVA and SSR-induced DNA damage, and that it is protective against oxidative DNA damage (8-oxoGua), although the exact mechanism is unknown. They also conform previous work that an MAA (Collemin A) protects against UVB induced CPD formation in HaCaT keratinocytes (Torres *et al.*, 2004).

Figure 3.13 shows the results for gene expression for antioxidant activity (HMOX-1), cytokines associated with inflammation/immunoregulation (Il-6, IL-8, IL-20) and photoageing (MMP-3). There is a reduction in the expression of all genes, showing significant protection even at 0.3%, with the exception of IL-8, where significant protection is offered at higher concentrations of palythine. In general, there was no advantage with palythine at higher concentrations. The MMP-3 data support a role for protecting against photoageing that has also been reported for MAAs (porphyra-334) against MMP-1 after UVA exposure of skin fibroblasts (Ryu *et al.*, 2014).

The ability of palythine to inhibit UVR induced molecular damage is in part due to its very high molar extinction coefficient (Table 3.2), $\varepsilon^{(m)}$ = 36,947.7 ± 2238.6, confirming the work of Takano who found a value of 36,200 for palythine at its λ_{max} (Takano *et al.*, 1978). This is one of the most basic assessments and requirements of the efficacy of a UVR filter. A high $\varepsilon^{(m)}$ enables the use of the filter at a low concentration, reducing costs and potential side effects. Palythine has an $\varepsilon^{(m)}$ which is greater than commonly used filters, which

can range from $\varepsilon^{(m)}$ =4,900 for octyl salicylate to $\varepsilon^{(m)}$ = 120,000 for ethylhexyl Triazone at their respective λ_{max} (Lowe *et al.*, 1997; Shaath, 2010). The extinction coefficient is the basis for the *in vitro* SPF and UVA-PF test methods as described by Herzog and Osterwalder (Herzog and Osterwalder, 2015).

One limitation of this work is that there is a lack of palythine concentration – response relationship as the protection offered is saturated at the doses of UVR and concentrations of palythine used for many of the markers investigated. The palythine concentrations were selected to be in the range that sunscreen filters are typically used at, between 0.1 and 10% for the majority of filters. The lack of dose response even with concentrations as low at 0.3% demonstrates excellent photoprotection but also made it difficult to determine a protection factor. For this reason it was decided to calculate the *in vitro* SPF and UVA-PF using the method mentioned above (Table 3.3). Although the accuracy of these tests is not completely indicative of the *in vivo* outcome, this is the best indication that could be made. The results demonstrate a relatively high *in vitro* SPF for a single molecule. Most sunscreens contain a mixture of several filters, each in the range of 1-10% (most filters have an upper limit of 5-10% each), however palythine for example at 10% has an SPF of 17.9, despite only absorbing minimally in the UVA range. This is clearly demonstrated by the UVA-PF, which is extremely low (10% palythine = UVA-PF of 1.6). There are additional tests that demonstrate the poor level of UVA protection, which are newer regulatory requirements of sunscreens. One is the critical wavelength test that requires 90% of the integral of the absorbance of a formulation to be greater than ≥ 370nm. The value for palythine alone is shown in Table 3.4. With a value of 337nm, this is some way off passing

this measurement of protection. Another method used in the UK is the Boots star rating which recommends a UVA/UVB ratio of ≥0.9 for the highest 5* rating. Again palythine falls short of this with a value of only 0.34, which is also short of even the lowest possible 3* rating that requires a value of ≥0.6.

These results clearly demonstrate that using palythine, as a single molecule, is not enough to pass the stringent sunscreen requirements. This however does not take into account the anti-oxidant properties of palythine. This effect may compensate for its spectral shortcomings, and has been shown in Figure 3.7, which shows significant protection from UVA induced DNA damage. Furthermore, the spectral profile may be improved by the addition of another MAA compound that has better UVA absorption, such as palythene (with a peak absorbance of 360nm). Another benefit of adding a UVA absorber was demonstrated using the BASF sunscreen simulator, which uses the method described by Herzog and Osterwalder to simulate the spectral profile of different UVR filter combinations and determine the protection offered (*https://www.sunscreensimulator.basf.com/Sunscreen_Simulator/Login_show.action*) (Herzog and Osterwalder, 2015). The addition of a small amount of a photostable UVA absorber not only improved the UVA protection but also led to needing less palythine for a comparable SPF. A concentration of 25% palythine resulted in an SPF of 30.2, however if a low concentration (e.g. 2%) of a photostable UVA absorber was to be added, much less palythine was needed for the same SPF (10% palythine - personal communication with Professor Bernd Herzog – data not shown), decreasing the overall amount of compound from

25% to 12%, reducing potential costs to manufacturers and the chance of side effects.

A limitation of this work is that it was only carried out keratinocytes *in vitro.* This may not be representative of keratinocytes *in vivo* or of other cell types in the epidermis such as melanocytes. There are however other studies which demonstrate good correlation between *in vitro* results in HaCat keratinocytes and more complex models, such as between HaCats and mouse skin (Afaq *et al.*, 2007) and HaCats and primary keratinocytes (Kang *et al.*, 2007). Additionally a considerable amount of *in vivo* gene expression work has been carried out in our laboratory (Tewari *et al.*, 2014; Tewari *et al.*, 2012a). The genes displayed in Figure 3.12 were chosen based on this work and the majority showed good correlation. The genes used for subsequent photoprotection studies in this and the following chapters were only selected if they showed good correlation with the *in vivo* work. It is also impractical to measure many types of oxidative stress and oxidative damage *in vivo*. Tissue disruption is a significant cause of oxidation of biomolecules. At the protein level for example, cysteines and methionines would be expected to be quite sensitive to the procedure. Furthermore, assuming intact viable cells were acquired at the end of the procedure of disruption, ROS measurement would not be reliable due to the oxidative stress caused by this process. The same would hold true for DNA oxidation measurements. It is notable how few publications there are on oxidative damage to DNA *in vivo* due to the issue of inducing oxidative damage when processing samples. Our model allows us to measure oxidative and non-oxidative damage in the same experiments. This validates the use of HaCat keratinocytes as a suitable

model for assessing the ability of palythine, as a model MAA, to be photoprotective in human skin. This also validates the further development of palythine in more complex models.

Some issues may arise from developing MAA based sunscreens due to their physiochemical properties, requiring careful formulation. MAAs are highly water soluble, which makes it more difficult to formulate sunscreens intended for beach use, where their benefit on the environment would be greatest. Water-soluble filters do however have some advantages; one being they have better sensorial properties than those based on oils and so may be useful for daily-care products. This may improve compliance and therefore photoprotection. Also the majority of UV filters are oil based, meaning that when the water phase evaporates there are areas of the skin left unprotected without UV filters present. Water-soluble filters are currently used to fill these gaps however there are few available, so MAA may be good candidates for this role. A second issue is the potential for skin penetration of MAA. They are small (typically <500 kDa), charged molecules meaning they have high potential for penetrating the skin (Hadgraft and Lane, 2016). This is advantageous in some aspects, as it permits delivery of the MAA to the viable cells, allowing the antioxidant properties to have an effect. However, most sunscreens are designed to stay on the surface of the skin, preventing damage to even the unviable layer of cells, which is an important sensing and reporting matrix. Finally, it is important to note MAA photostability would also have to be assessed in sunscreen formulations because photostability may vary with solvent. Alcohol based formulations may be the most suitable for MAA based sunscreens.

In conclusion, the data presented show that UVR radiation induced several damaging effects to keratinocytes and that palythine, even at low concentrations, significantly reduces the most biologically relevant forms of solar UVR induced damage - cell death, DNA damage, ROS and gene expression in an *in vitro* skin model. Unlike current synthetic sunscreens, palythine combines UVR filtering and antioxidant properties in a single photostable molecule. Overall, these data suggest that MAAs have the potential to be developed as effective biocompatible UVR filters that may appeal to the public as natural products (Kim and Seock, 2009). This would require further studies on formulation, delivery and to assess the SPF of sunscreens containing palythine or other MAAs, as well as the ability to inhibit molecular damage *in vivo*. The data also suggest that MAAs may have a role in after-sun preparations. These results show that MAAs have the potential to be developed as effective, biocompatible environmentally friendly sunscreens that have abilities equal to and beyond currently available UVR filters. MAAs also have the potential to replace UVR filters that may be banned by the ECHA.

3.3 Summary of Chapter

- Solar UVR has many reported detrimental effects to the skin.
- These effects were demonstrated and extended in HaCat keratinocytes, and some were selected as relevant endpoints for photoprotection studies. These were cell viability, DNA damage, oxidative stress and differential gene expression covering different photobiological outcomes: inflammation/immunoregulation, photoageing and oxidative stress.
- The main way of preventing UVR induced damage to the skin is with the use of sunscreens, which contain a mix of synthetic organic and inorganic compounds.
- There is growing concern with the use of these compounds because they have been shown to accumulate in the marine environments in which they are used, cause hormonal changes to fish and the bleaching of corals, suggesting the need for a natural alternative.
- MAAs are a group of environmentally compatible photoprotective compounds that have potential to be used as an alternative to synthetic filters, but have been under researched in human applications.
- Palythine was selected as a model MAA for studies to investigate the potential of MAAs to prevent UVR induced damage to HaCat keratinocytes (as a model for human skin) using environmentally and physiologically relevant UVR doses.
- Palythine significantly prevented UVR induced damage across all endpoints and additionally displayed anti-oxidant ability, another significant benefit over current UVR filters.

- This data contained within this chapter was successfully submitted to the UK patent office (details in Appendix).

Chapter 4: The Cellular and Molecular Effects of the UV/visible Border Region (385-405nm) on Human Skin *in vitro* and *in vivo*

4.1 Results

4.1.1 Cell Viability Reduction *In Vitro*

HaCat keratinocytes were exposed to increasing doses (0-150J/cm^2) of 385nm or 405nm LED sources to assess the effects of the UV/visible radiation border region on cell viability. This was measured 24 hours post exposure using the Neutral Red and Alamar Blue methods (Figure 4.1). There was a significant dose dependent reduction in cell viability for both spectra with both assays. Doses of 50J/cm^2 and above significantly reduced viability for both sources using the Neutral Red assay (and doses of 100J/cm^2 for 385nm and 50J/cm^2 for 405nm when using the Alamar Blue assay). In the case of Neutral Red, there was no significant difference between both wavelengths however 385nm was significantly more lethal with the Alamar Blue assay.

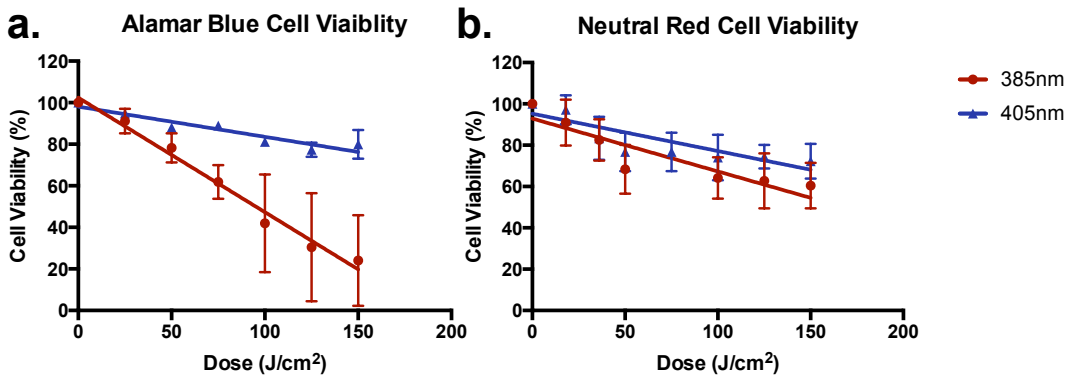

Figure 4.1: Wavelengths at the UV/visible border (385-405nm) significantly reduced cell viability *in vitro* in a dose dependent manner. HaCaT keratinocytes were exposed 0-150J/cm^2 of 385nm or 405nm radiation. Cell viability was assessed 24 hours post exposure using the (a) Alamar Blue and (b) Neutral Red assays. Data points represent the mean ± SD (n=3). The Neutral Red assay showed a significant dose dependent decrease in cell viability for both wavelengths (385nm - $p<0.0001$; 405nm $p<0.0001$; n=3 linear regression analysis) with no significant difference between both wavelengths ($p<0.1559$; n=3, linear regression analysis). For Alamar Blue there was a significant dose dependent decrease in cell viability for both wavelengths (385nm - $p<0.0001$; 405nm - $p<0.0001$; n=3 linear regression analysis). There was a significant difference between wavelengths ($p<0.0001$; n=3, linear regression analysis).

4.1.2 Reactive Oxygen Species Induction *In Vitro*

The ability of 385nm and 405nm to induce ROS was measured. HaCat keratinocytes were exposed to increasing doses of 385nm or 405nm radiation (0-150J/cm^2). Immediately after exposure, ROS levels were measured by staining with carboxy-H_2DCFDA (a ROS indicator) and the fluorescence measured by FACS, eliminating non-viable cells with the use of DAPI. For both 385nm and 405nm there was a significant dose dependent increase in ROS formation (Figure 4.2). Significance was achieved with doses of 36J/cm^2 and above with the 385nm source, however at 100J/cm^2 and above there was a drop in ROS production. At 405nm, the lowest significant dose was 50J/cm^2 with doses above 100J/cm^2 showing a plateau. It was for this reason that these higher doses were omitted from the analyses, and only the linear regions of the dose responses were used and compared by linear regression. There was a significant dose dependent increase in ROS production with both sources. The slopes of both lines were compared and it was shown there was a significant difference, with the 385nm slope being steeper than that at 405nm.

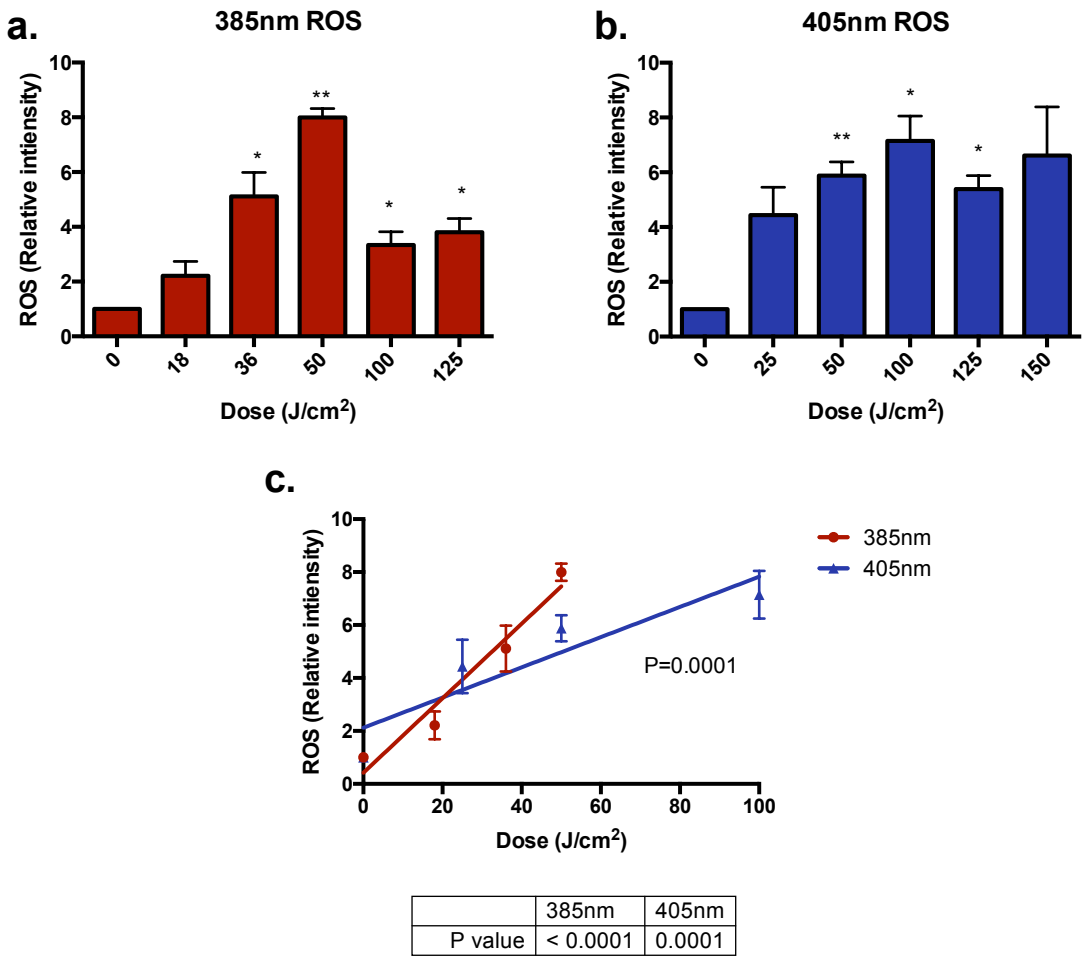

	385nm	405nm
P value	< 0.0001	0.0001

Figure 4.2: 385nm and 405nm significantly induced the formation of ROS in a dose dependent manner *in vitro* when measured with the H_2DCFDA assay. HaCaT keratinocytes were treated with 0-150J/cm^2 of either (a) 385nm or (b) 405nm radiation, and levels of ROS were assessed. Columns represent the mean ± SD (n=3). Both wavelengths induced a significant dose dependent increase in ROS (385nm: $p<0.001$, 405nm: $p=0.0244$ n=3, one-way ANOVA with Dunnett's multiple comparisons test). (c) For both sources there was a significant dose dependent increase in ROS production (385nm: $p<0.0001$, 405nm: $p=0.0001$; n=3; linear regression analysis) with a significant difference between the slopes of both wavelengths $p=0.0001$; n=3; linear regression analysis).

4.1.3 DNA Damage

UVR is well known to induce damage to DNA, particularly in the form of CPD lesions. The ability of 385nm and 405nm radiation to induce such lesions was investigated *in vitro* as well as over time *in vivo* to assess any potential formation of 'dark' CPDs (Premi *et al.*, 2015).

4.1.3.1 DNA Damage In Vitro

HaCat keratinocytes were exposed to increasing doses (0-150J/cm^2) of either source, and the production of CPD lesions was assessed by IHC-IF immediately post exposure. Columns represent mean ± SD (n=3). The 385nm source produced a significant increase in CPD induction at a dose of 150J/cm^2. There was no significant increase detected at any of the doses with the 405nm source. The results are displayed below in Figure 4.3.

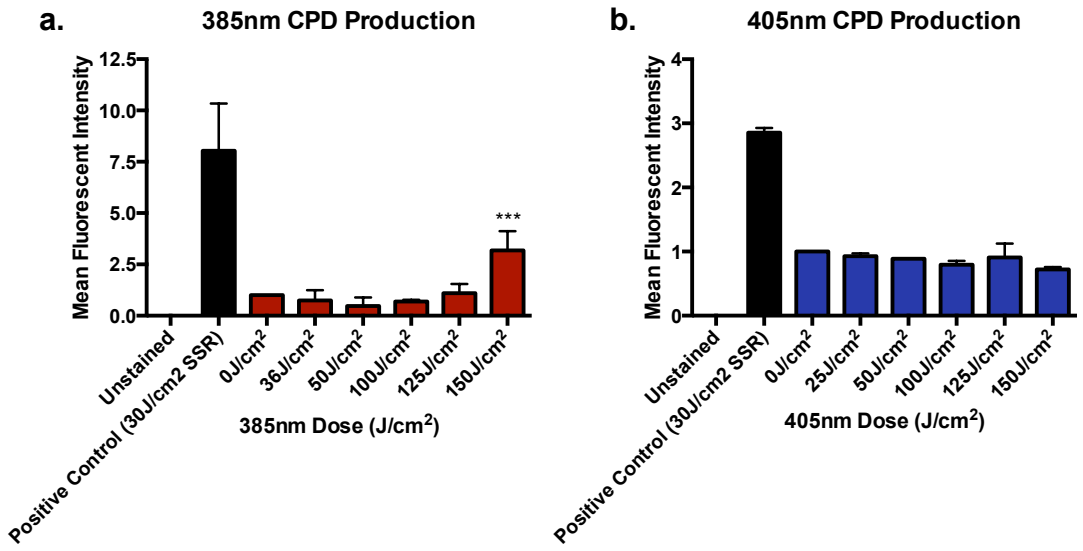

Figure 4.3: The ability of wavelengths at the UV/visible border (385-405nm) to induce CPDs *in vitro* when measured by IHC-IF. HaCaT keratinocytes were untreated, or exposed 0-150/cm^2 of (a) 385nm or (b) 405nm radiation. CPDs were measured immediately post exposure using IHC-IF. Columns represent mean ± SD (n=3). There was a significant increase in CPD formation at the highest dose of 385nm radiation ($p<0.0001$; n=3, one-way ANOVA with Dunnett's multiple comparisons test). There was no significant increase in CPD formation at any of the doses with the 405nm source.

4.1.3.2 DNA Damage In Vivo

The buttock skin of human volunteers (demographics described below in Table 4.1) was exposed to 150J/cm^2 of both 385 and 405nm, and the production of TT CPD lesions was assessed by HPLC-MS/MS 0-24 hours post exposure. An adjacent non-exposed site was also assessed. Columns represent mean ± SD (n=4, 8 volunteers in total). Details of volunteers are displayed in Table 4.1 There was an increase in the number of CPD lesions over 2 hours post exposure with the 385nm source that was maintained over a 24-hour period with no repair displayed (Figure 4.4). There was a slightly increase with the 405nm source but this was only detected in two samples. Each point represents the mean value (each time point n=4, total volunteers =8).

Volunteer ID	Age	Sex	Skin Type	Time Points (hours)
003	32	F	II	0, 6, 24
004	26	M	III	0, 6, 24
005	27	M	II	0, 6, 24
006	21	F	III	0, 6, 24
007	28	F	I	0, 2, 4
008	23	M	II	0, 2, 4
009	27	M	II	0, 2, 4
010	18	M	II	0, 2, 4

Table 4.1: Volunteer demographics for *in vivo* DNA damage studies.

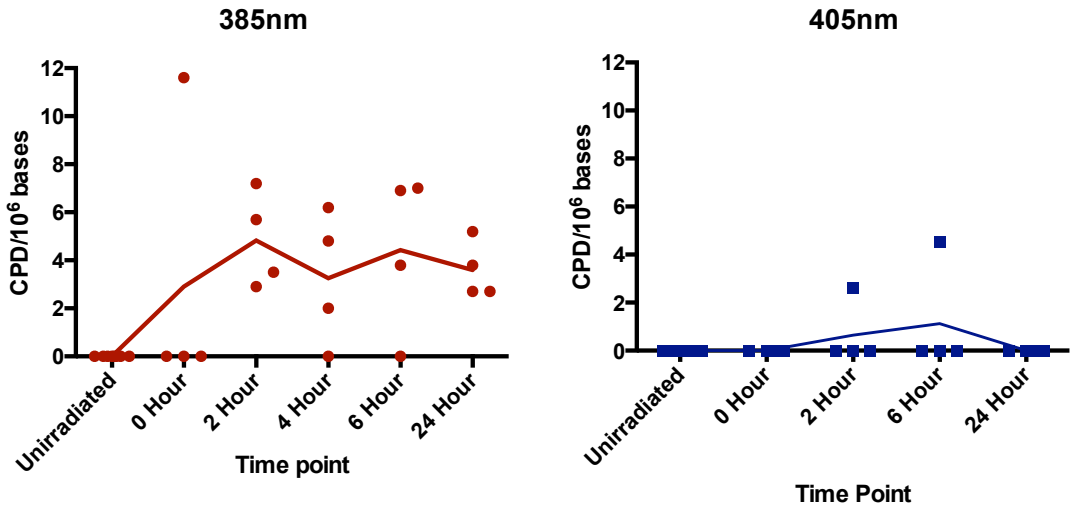

Figure 4.4: The ability of wavelengths at the UV/visible border (385-405nm) to induce CPDs over time *in vivo* assessed by HPLC-MS/MS. Human volunteers were unexposed, or exposed 0-150/cm^2 of (a) 385nm or (b) 405nm radiation. Biopsies were taken 0-24 hours post exposure. DNA was extracted and CPDs were assessed by HPLC MS/MS. Columns represent mean ± SD (n=4 per time point, 8 volunteers in total).

4.1.4 Gene Expression

4.1.4.1 Gene Expression In Vitro

The effect of the UV/visible border region on differential gene expression was assessed *in vitro*. This was measured by qPCR on HaCat keratinocytes irradiated with increasing doses of 385nm (0-105J/cm^2) and 405nm (0-150J/cm^2) radiation. These doses were selected to maintain a cell viability of ≥80%. Twelve 2 hours post exposure, total RNA was extracted from the cells as described in the Materials and Methods section. After checking the RNA quality by nanodrop, cDNA was synthesized. Finally qPCR was carried out. GAPDH was used as the housekeeping gene. The ΔΔCT method was used to analyse the difference in fold change compared to the unirradiated samples (with a value of 1). The results are displayed in Figure 4.5. The dose response relationships of all the genes were assessed using linear regression analysis and the difference in the slopes between 385nm and 405nm wavelengths subsequently assessed. The results of the statistical comparisons are displayed in Table 4.2.

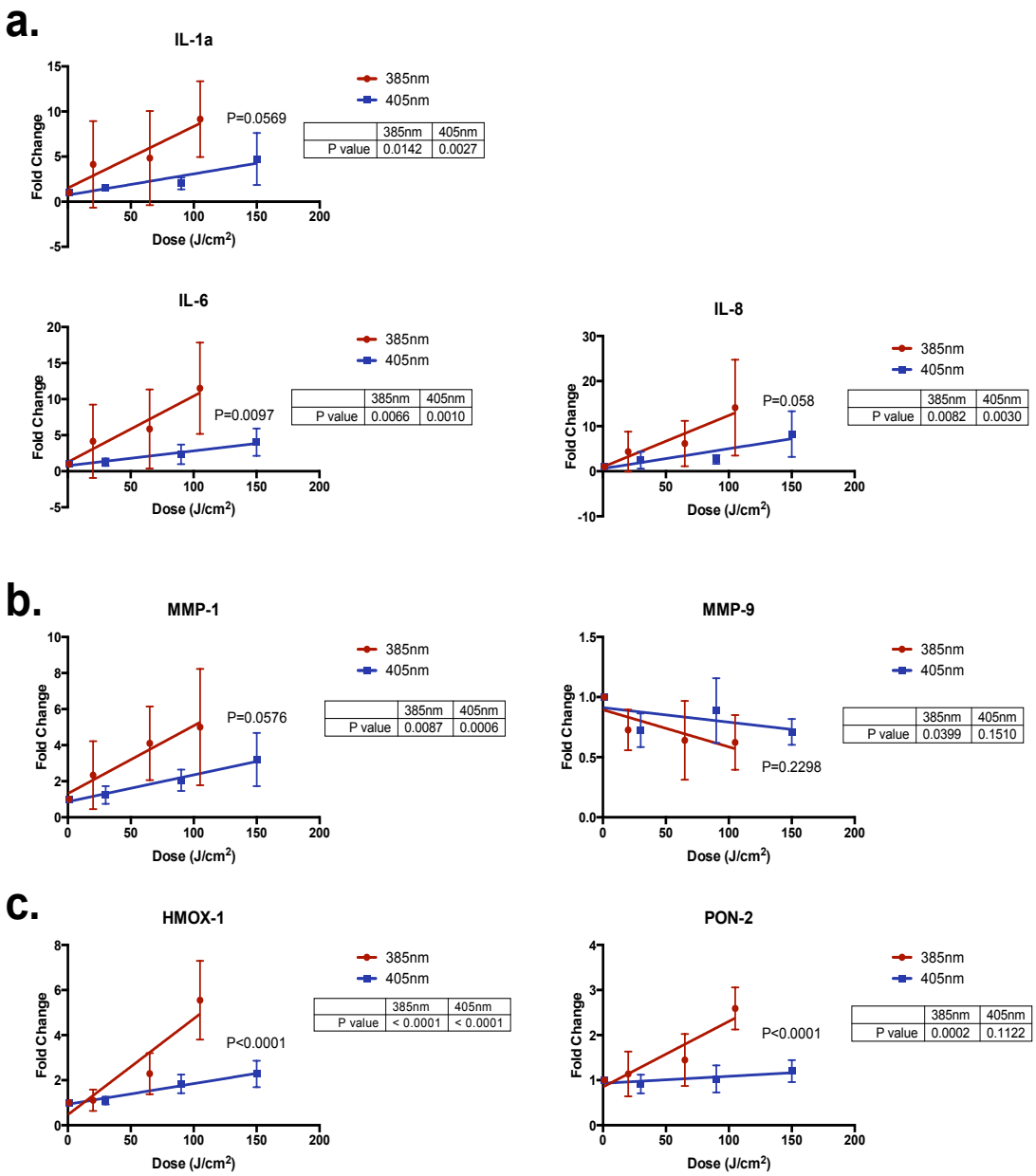

Figure 4.5: 385nm and 405nm induced gene expression changes *in vitro*. Genes were categorised based on (a) inflammation (b) photoageing or (c) oxidative stress. HaCaT keratinocytes were exposed to 0-105J/cm² of 385nm or 0-150J/cm² for 405nm radiation. Gene expression changes were measured 12 hours post exposure by qPCR. Columns represent the mean ± SD (n=4). There was a significant upregulation in many of the genes. The individual results are displayed in table 1.1. The slopes of both 385nm and 405nm response were compared and in general there was significant difference in responses with the exception of PON-2, HMOX-1 and IL-6. Results of statistical analysis are displayed in Table 4.2.

Gene	385nm p value	405nm p value	385nm vs. 405nm
IL-1a	0.0142	**0.0027**	0.0596
IL-6	**0.0066**	**0.0010**	**0.0097**
IL-8	**0.0082**	**0.0030**	0.0580
MMP-1	**0.0087**	**0.0006**	0.0576
MMP-9	**0.0399**	0.1510	0.2298
HMOX-1	**<0.0001**	**<0.0001**	**<0.0001**
PON-2	**0.0002**	0.1122	**<0.0001**

Table 4.2: Results of the statistical analysis of differential gene expression *in vitro*. 385nm was more effective in all comparisons. Displayed are the linear regression analyses for each gene and wavelength, and a comparison of the slopes between wavelengths.

In general there was a significant dose dependent upregulation in gene expression for the majority of genes tested for both the 385nm and 405nm sources. The 385nm source was more efficient at inducing an upregulation of gene expression for all genes tested in which there was an increase.

4.1.4.2 Gene Expression In Vivo

The effect of the UV/visible border region on differential gene expression was assessed *in vivo*. This was measured by qPCR on skin type II-III human volunteers irradiated with 150J/cm^2 doses of 385nm and 405nm radiation. The details of the volunteers are shown in Table 4.3. RNA extraction and gene expression was carried out as for *the in vitro* gene expression and explained in *Materials and Methods*. Many genes across all endpoints demonstrated an upregulation in response to both wavelengths. The results are displayed in Figure 4.6.

Volunteer ID	Age	Sex	Skin Type
002	21	M	II
003	32	F	II
004	26	M	III
005	27	M	II
006	21	F	III

Table 4.3: Volunteer demographics for *in vivo* gene expression studies.

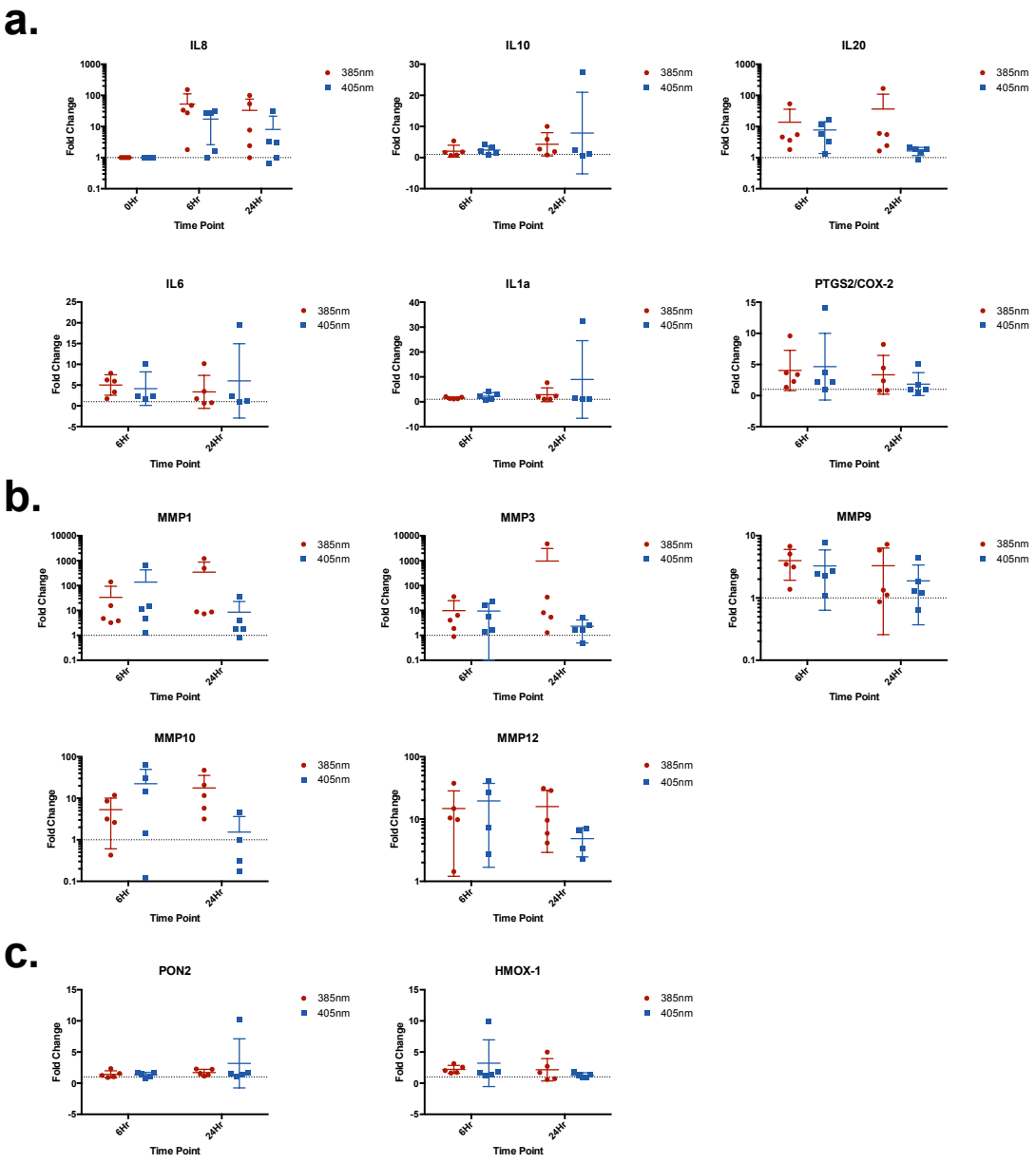

Figure 4.6: 385nm and 405nm induced gene changes *in vivo*. Volunteers were exposed to 0 or 150J/cm^2 of 385 or 405nm radiation. Biopsies were taken 0, 6 or 24 hours post exposure and gene expression changes were measured by qPCR and categorised based on (a) inflammation (b) photoageing and (c) oxidative stress. Columns represent the mean ± SD (n=5).

Many genes showed a large fold change, but when tested statistically this was not significant compared to the non-irradiated controls. The lack of statistical significance with individual genes was investigated by assessing the spread of all data for each person to evaluate if any volunteers had a greater or lesser

response that was responsible for skewing the data. All responses were plotted for each volunteer as well as pooled for specific endpoints. The results are displayed in Figure 4.7. The response of all volunteers was not significantly different when the fold changes of all genes tested were pooled together or when separated for photoageing genes. Genes associated with inflammation showed a difference between volunteers 003 and 006, and for oxidative stress response volunteer 006 responded significantly more than three of the other volunteers. The remaining volunteers showed good correlation in the level of gene expression for inflammation and oxidative stress response.

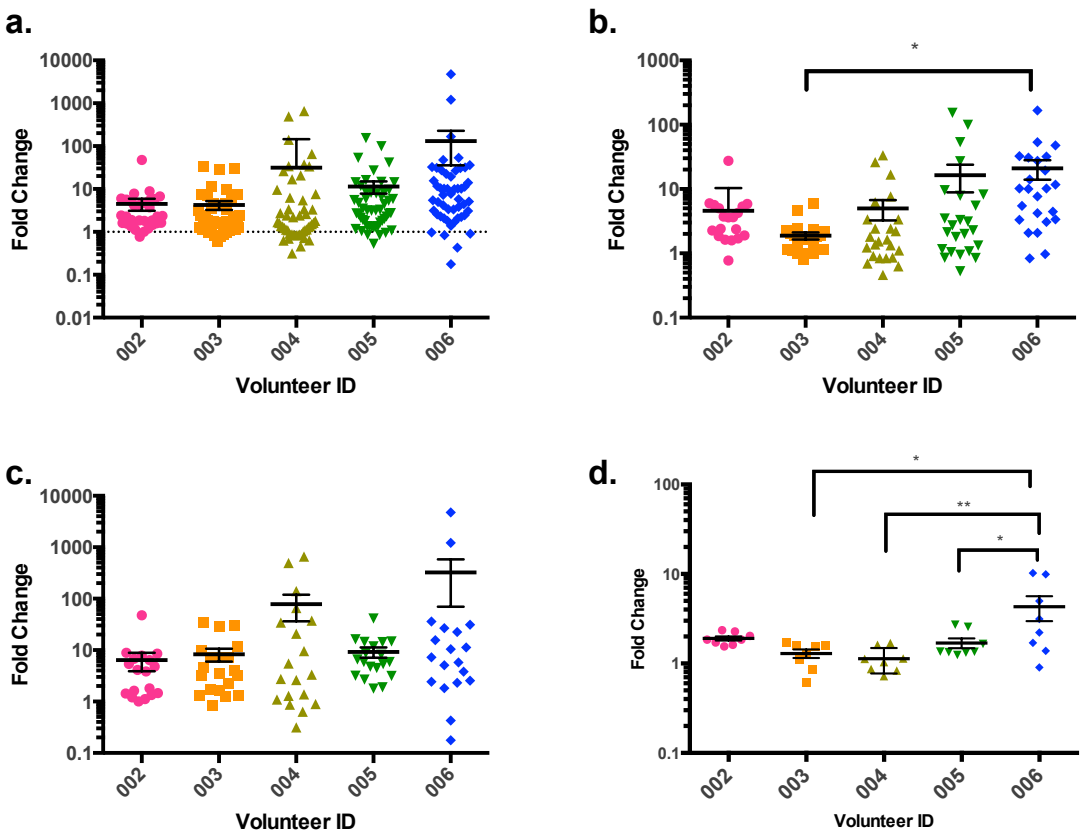

Figure 4.7: **Individual responses of 385nm and 405nm induced gene changes *in vivo*.** Gene expression responses were assessed on an individual-by-individual basis. All responses for all genes were pooled (a) as well as by end point for (b) inflammation, (c) photoageing and (d) oxidative stress. Data are displayed as mean ± SD. Average fold change between all volunteers was analysed using one-way ANOVA with Tukey's multiple comparisons test (All: p=0.0020, inflammation: p=0.0175, photoageing: p=0.2662, oxidative stress: p=0.0051).

Data were not normally distributed when assessed by the D'Agostino and Pearson test (p<0.0001) so the data were logged to normalise the data before further analysis. Genes with similar end points were pooled (for inflammation, photoageing and oxidative stress), and two-way ANOVA was performed. This approach led to statically significant responses for many of the endpoints that better matched the graphically expressed data. The data are displayed in Figure 4.8 and results of the statistical analyses described in Table 4.4.

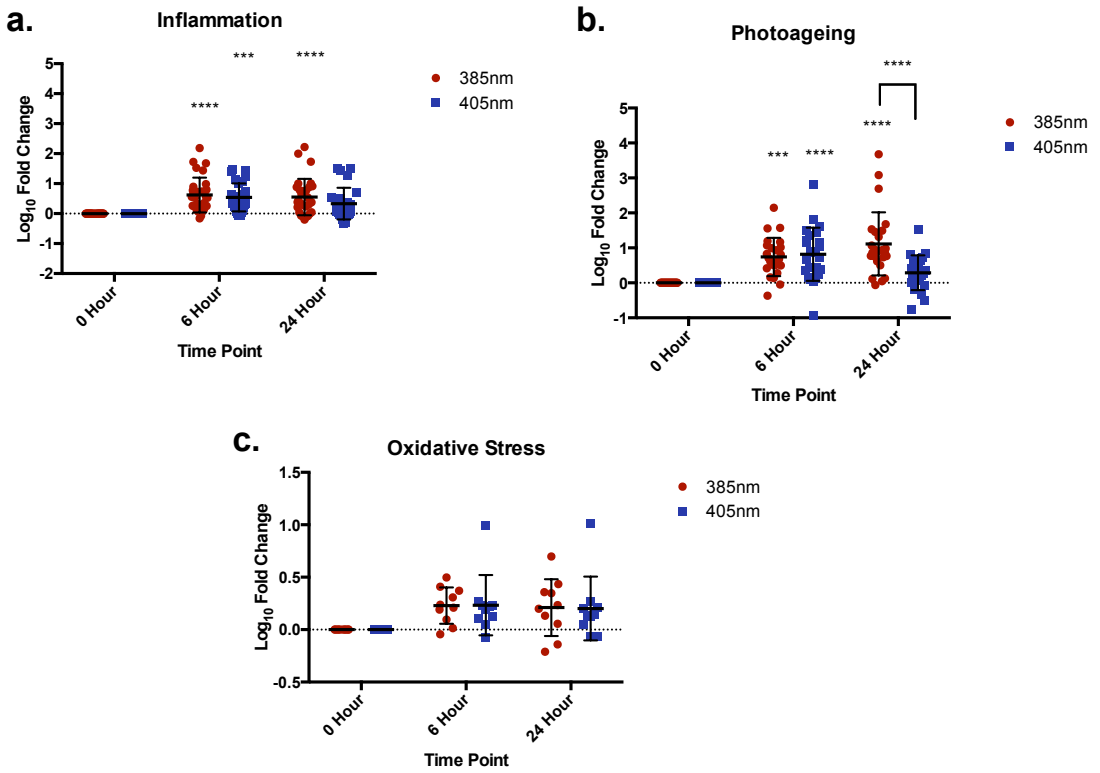

Figure 4.8: **Pooled response of 385nm and 405nm induced gene expression changes *in vivo*.** Genes were pooled based on endpoint: (a) inflammation, (b) photoageing and (c) oxidative stress. Data are displayed as mean ± SD with the responses of 5 volunteers pooled. Differences were analysed using two-way ANOVA with Sidak's multiple comparisons test with results displayed in Table 4.4.

			Inflammation	Photoageing	Oxidative Stress
ANOVA result	**Relationship**	**Interaction**	0.6129	**0.0001**	0.9950
		Time	0.2629	**< 0.0001**	**0.0021**
		Wavelength	0.9626	**0.0087**	0.9777

Table 4.4: The statistical analysis of pooled gene expression. Changes using two-way ANOVA with Sidak's multiple comparisons test.

When the logged data were pooled based on endpoint, more significance and clearer relationships were established. Genes associated with inflammation and photoageing were significantly upregulated compared to unirradiated control with both 385nm and 405nm sources. There was no significant increase in genes associated with oxidative stress with either source. In general there was no significant difference between sources with the exception of photoageing genes at 24 hours, where there was no significant increase in these genes at 24 hours with the 405nm source. There was however a significant increase at 6 hours. Without this exception there was generally no difference between the 6 and 24-hour responses.

4.1.4.3 In Vitro – In Vivo Comparisons

The *in vitro* and *in vivo* gene expression responses were compared Figure 4.9 to assess the validity of the *in vitro* model. The time points used for studies were different so direct time comparison was not possible but general responses were compared for genes that were measured using both methods.

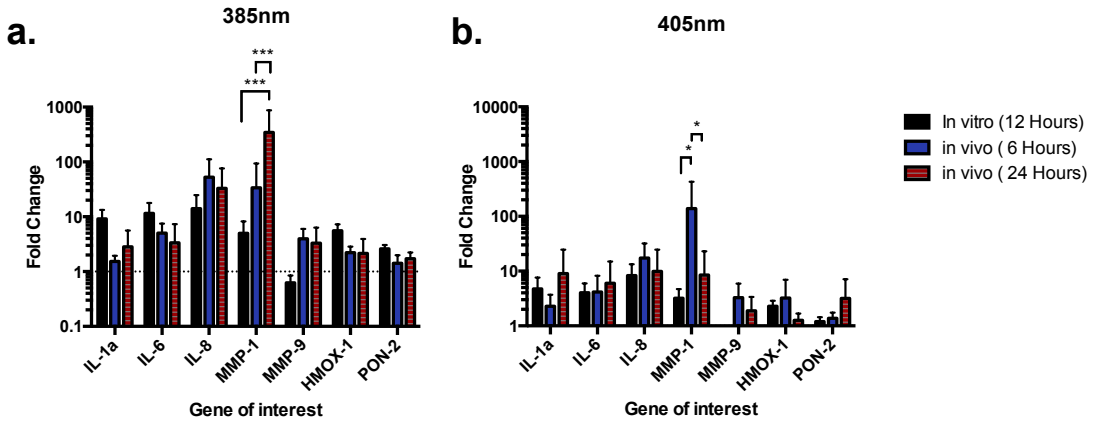

Figure 4.9. Comparison of *in vitro* and *in vivo* 385nm and 405nm induced gene changes. The *in vitro* and *in vivo* responses to 385nm and 405nm irradiation were compared to assess the validity of *in vitro* studies. Differences were analysed using two-way ANOVA with Sidak's multiple comparisons test, comparing the fold change differences between *in vitro* response at 12 hours with the *in vivo* response at 6 and 24 hours. There was no significant difference between methods used with the exception of MMP-1, which showed the same trend, but a different magnitude of response (385nm: p=0.0.0915, 405nm: p=0.6083). The response at 6 and 24 hours *in vivo* were also compared with the same outcome, in general there was no significant difference with the exception of MMP-1.. Columns represent the mean ± SD (*in vitro* n=4; *in vivo* n= 5)

In general, there was no significant difference in the magnitude of the responses of the genes after irradiation with either 385nm or 405nm between *in vitro* and *in vivo* experiments. The only exception was with the response of MMP-1 induction with both 385nm and 405nm, where MMP-1 was significantly more upregulated in *in vivo* compared to *in vitro*, however the trend was the same *in vitro,* just not to the same extent. These results validate the use of the *in vitro* HaCat keratinocyte model for gene expression studies, as overall there are similar responses *in vitro* and *in vivo*.

4.1.5 Pigmentation and Erythema Induction *In Vivo*

The effect of 385nm and 405nm radiation on the induction of skin pigmentation and/or erythema was measured in human volunteers across skin types (II-IV). Volunteers were exposed to increasing doses 0-150J/cm^2 of 385nm or 405nm radiation, and pigmentation and erythema were assessed at 0, 6 and 24 hours post-exposure, using three different methods: (i) visual assessment, (ii) the Minolta chromameter and (iii) the Optimize device. The site layout for the study is displayed in Figure 4.10. Photographs were taken at each time point and representative pictures for each skin type are displayed in Figure 4.11. The details of the volunteers studied are shown in Table 4.5. The average responses for each skin type are plotted in Figures 4.12 – 4.16 and described in Tables 4.6 – 4.10.

Volunteer ID	Age	Sex	Skin type
003	21	M	II
006	26	F	II
010	25	M	II
004	23	F	III
005	19	F	III
008	32	F	III
007	30	M	IV
009	31	F	IV
011	33	F	IV

Table 4.5: Volunteer demographics for *in vivo* pigmentation/erythema studies.

Figure 4.10: Study layout for pigmentation/erythema studies. The scheme for irradiation of volunteers to assess pigmentation and redness after exposure to 385 or 405nm radiation.

4.1.5.1 Representative Images

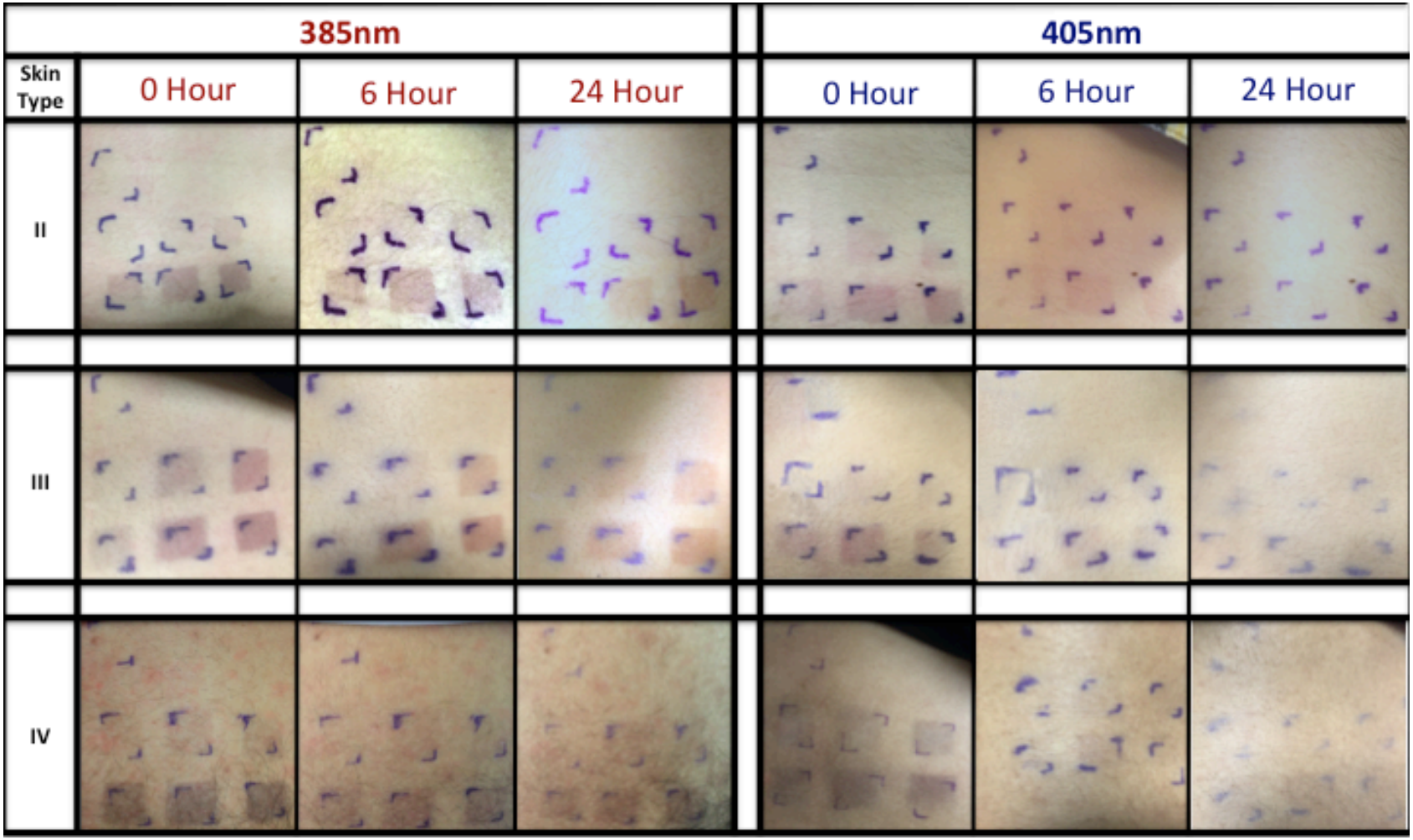

Figure 4.11: Images representing typical responses for each skin type and time point tested.

4.1.5.2 Visual Score

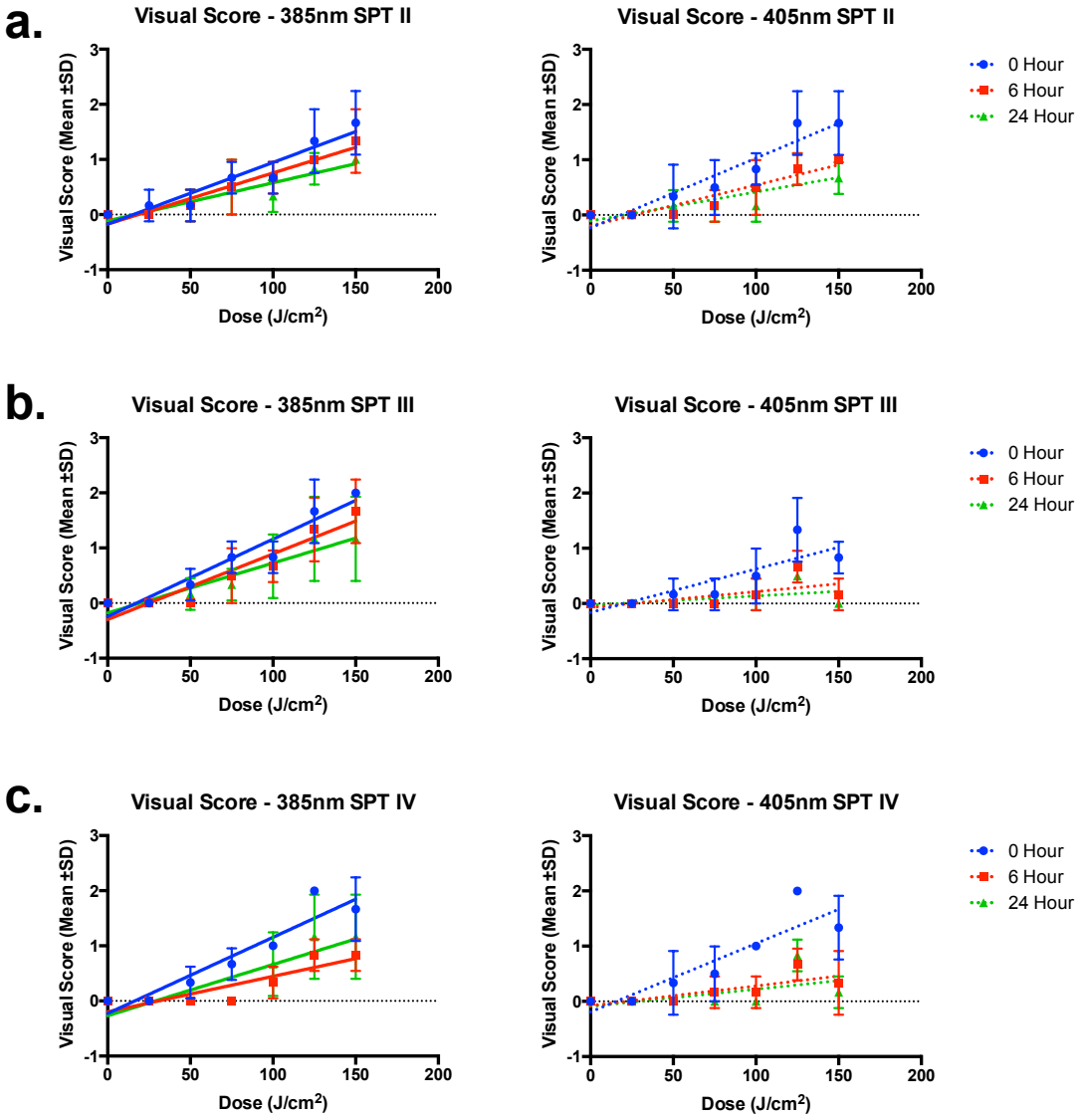

Figure 4.12: The effects of 385nm and 405nm wavelengths on skin pigmentation assessed visually. Volunteers of skin type (a) II (b) III and (c) IV were irradiated with increasing doses (0-150J/cm²) of 385nm and 405nm radiation and pigmentation was assessed visually immediately, 6 and 24 hours post irradiation. Data points represent the mean ± SD (n=3). Data were analysed using linear regression analysis and results are displayed in Table 4.6.

Visual Score slope p values				
Wavelength	**Skin Type**	**0 Hour**	**6 Hour**	**24 Hour**
385nm	**II**	**<0.0001**	**<0.0001**	**<0.0001**
	III	**<0.0001**	**<0.0001**	**0.0002**
	IV	**<0.0001**	**<0.0001**	**0.0002**
405nm	**II**	**<0.0001**	**<0.0001**	**0.0002**
	III	**0.0002**	**0.0152**	0.0551
	IV	**<0.0001**	**0.0103**	**0.0232**

Table 4.6: Linear regression analysis of pigmentation change scored visually. Slopes were analysed for significance and p values are displayed.

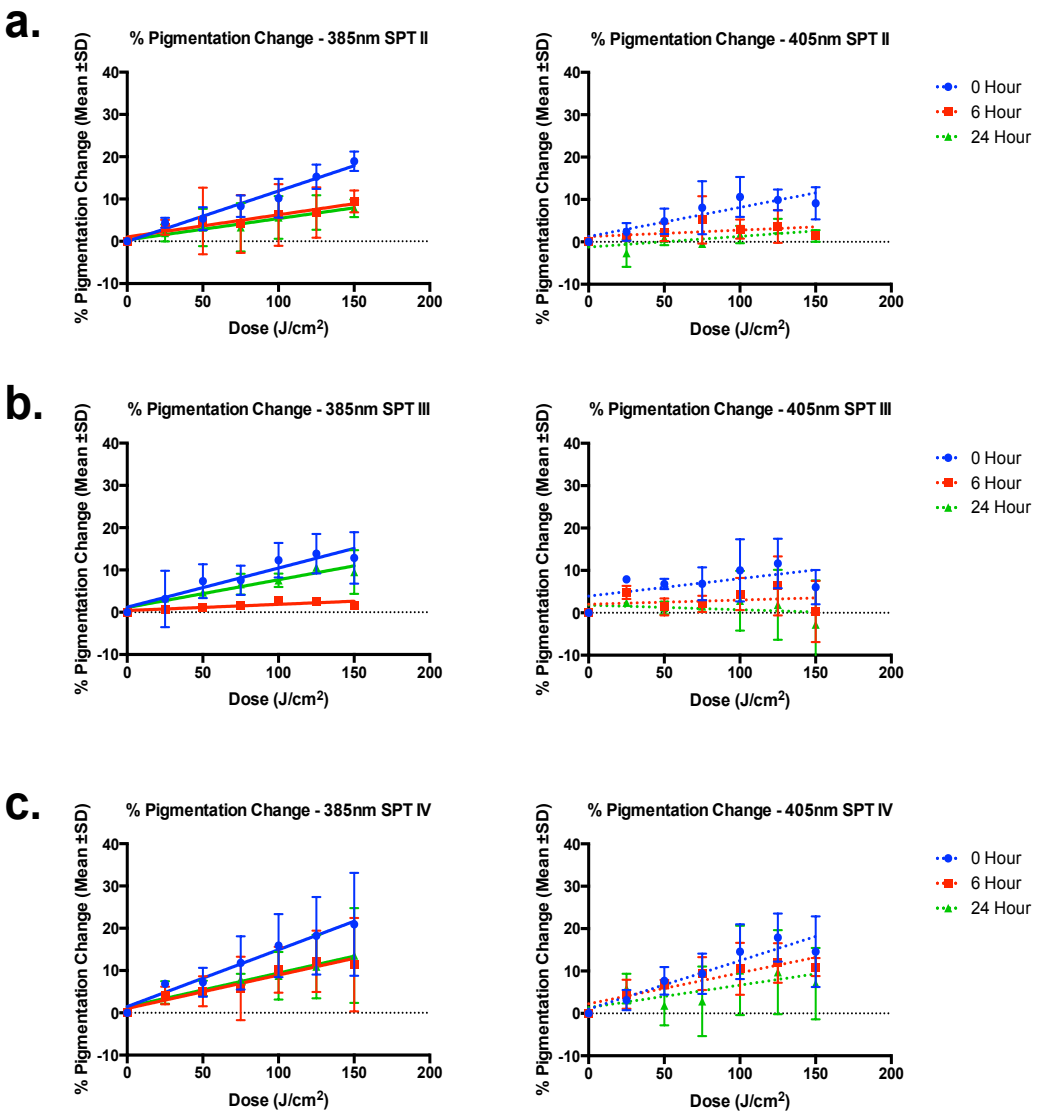

Figure 4.13: **The effects of 385nm and 405nm wavelengths on skin % pigmentation values measured using the Optimize device.** Volunteers of skin type (a) II (b) III and (c) IV were irradiated with increasing doses (0-150J/cm²) of 385nm and 405nm radiation and pigmentation was assessed using the Optimize device immediately, 6 and 24 hours post irradiation. Data points represent the mean ± SD (n=3). Data were analysed using linear regression analysis and results are displayed in Table 4.7.

Optimize - Change in Pigmentation slope p values				
Wavelength	**Skin Type**	**0 Hour**	**6 Hour**	**24 Hour**
385nm	**II**	**< 0.0001**	**0.0206**	**0.0024**
	III	**0.0007**	**0.0017**	**< 0.0001**
	IV	**< 0.0001**	**0.004**	**0.0015**
405nm	**II**	**0.0003**	0.2330	**0.0117**
	III	0.0997	0.6514	0.6751
	IV	**<0.0001**	**0.0001**	0.0928

Table 4.7: Linear regression analysis of pigmentation change scored with the Optimize device. Slopes were analysed for significance and p values are displayed.

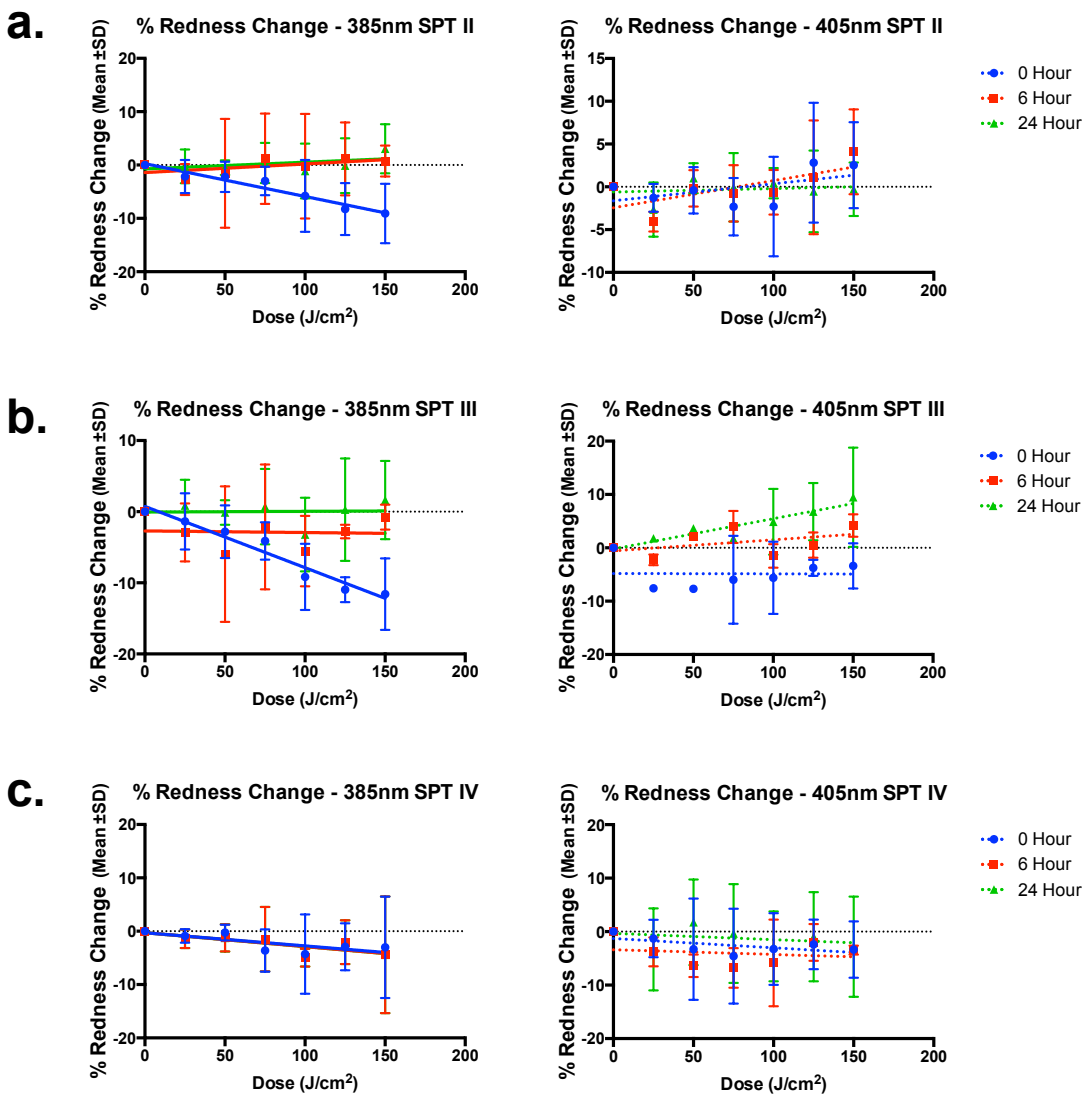

Figure 4.14: The effects of 385nm and 405nm wavelengths on skin % redness values measured using the Optimize device. Volunteers of skin type (a) II (b) III and (c) IV were irradiated with increasing doses (0-150J/cm²) of 385nm and 405nm radiation and redness was assessed using the Optimize device immediately, 6 and 24 hours post irradiation. Data points represent the mean ± SD (n=3). Data were analysed using linear regression analysis and results are displayed in Table 4.8.

Optimize - Change in Redness slope p values				
Wavelength	**Skin Type**	**0 Hour**	**6 Hour**	**24 Hour**
385nm	**II**	**0.0012**	0.4591	0.4145
	III	**0.0001**	0.9299	0.9603
	IV	0.2295	0.2055	0.2052
405nm	**II**	0.2792	0.0545	0.7482
	III	0.9782	0.1734	**0.0157**
	IV	0.4773	0.6217	0.6969

Table 4.8: Linear regression analysis of redness change scored with the Optimize device. Slopes were analysed for significance and p values are displayed.

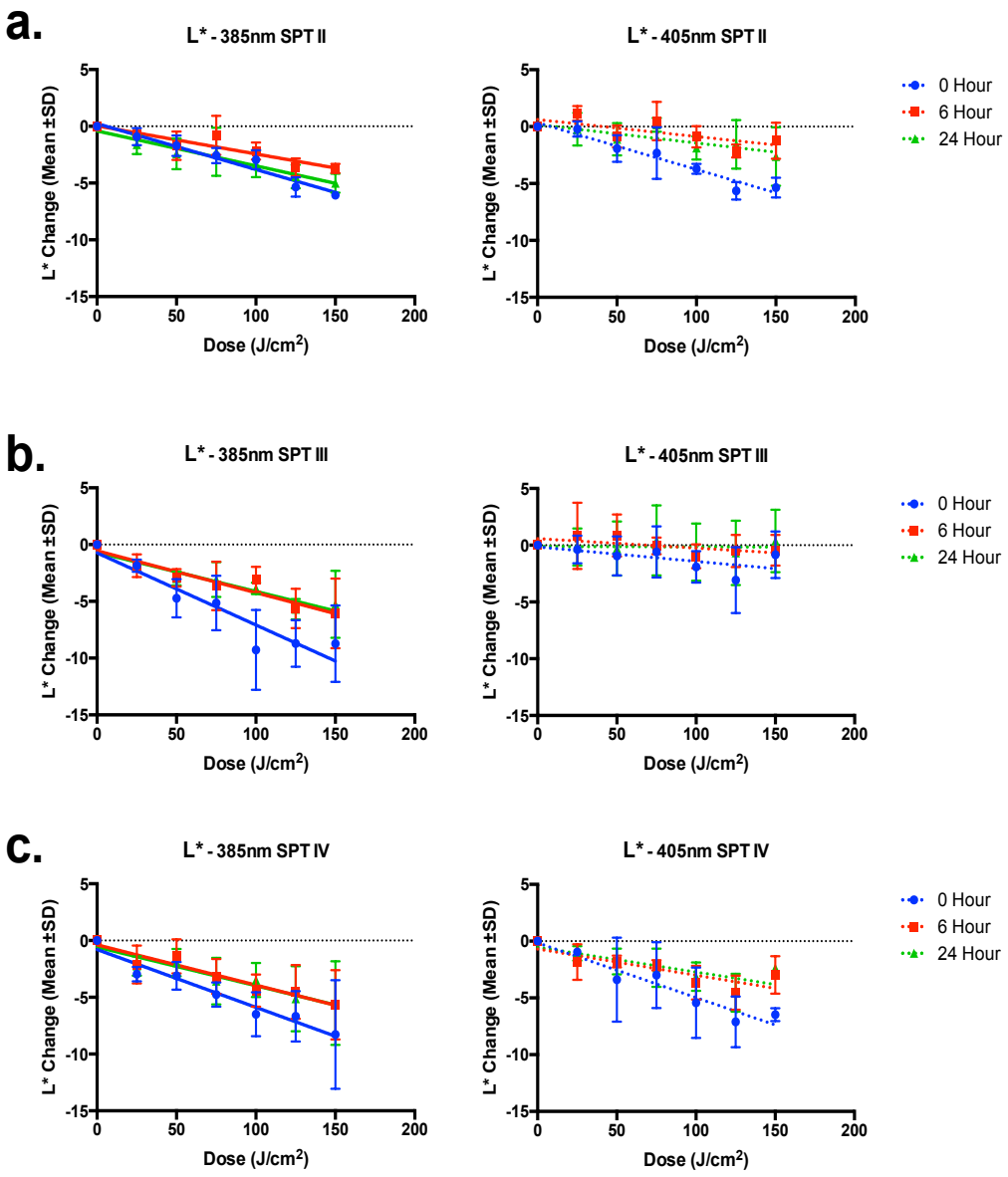

Figure 4.15: The effects of 385nm and 405nm wavelengths on skin L* values (pigmentation) measured using the Minolta device. Volunteers of skin type (a) II (b) III and (c) IV were irradiated with increasing doses (0-150J/cm²) of 385nm and 405nm radiation and pigmentation was assessed using the Minolta device immediately, 6 and 24 hours post irradiation. Data points represent the mean ± SD (n=3). Data were analysed using linear regression analysis and results are displayed in Table 4.9.

Minolta - Change in L* slope p values				
Wavelength	**Skin Type**	**0 Hour**	**6 Hour**	**24 Hour**
385nm	**II**	**<0.0001**	**<0.0001**	**<0.0001**
	III	**<0.0001**	**<0.0001**	**<0.0001**
	IV	**<0.0001**	**0.0001**	**0.0005**
405nm	**II**	**<0.0001**	**0.0099**	**0.0187**
	III	0.1161	0.2022	0.9719
	IV	**<0.0001**	**0.0006**	**0.0009**

Table 4.9: Linear regression analysis of pigmentation change scored with the Minolta device. Slopes were analysed for significance and p values are displayed.

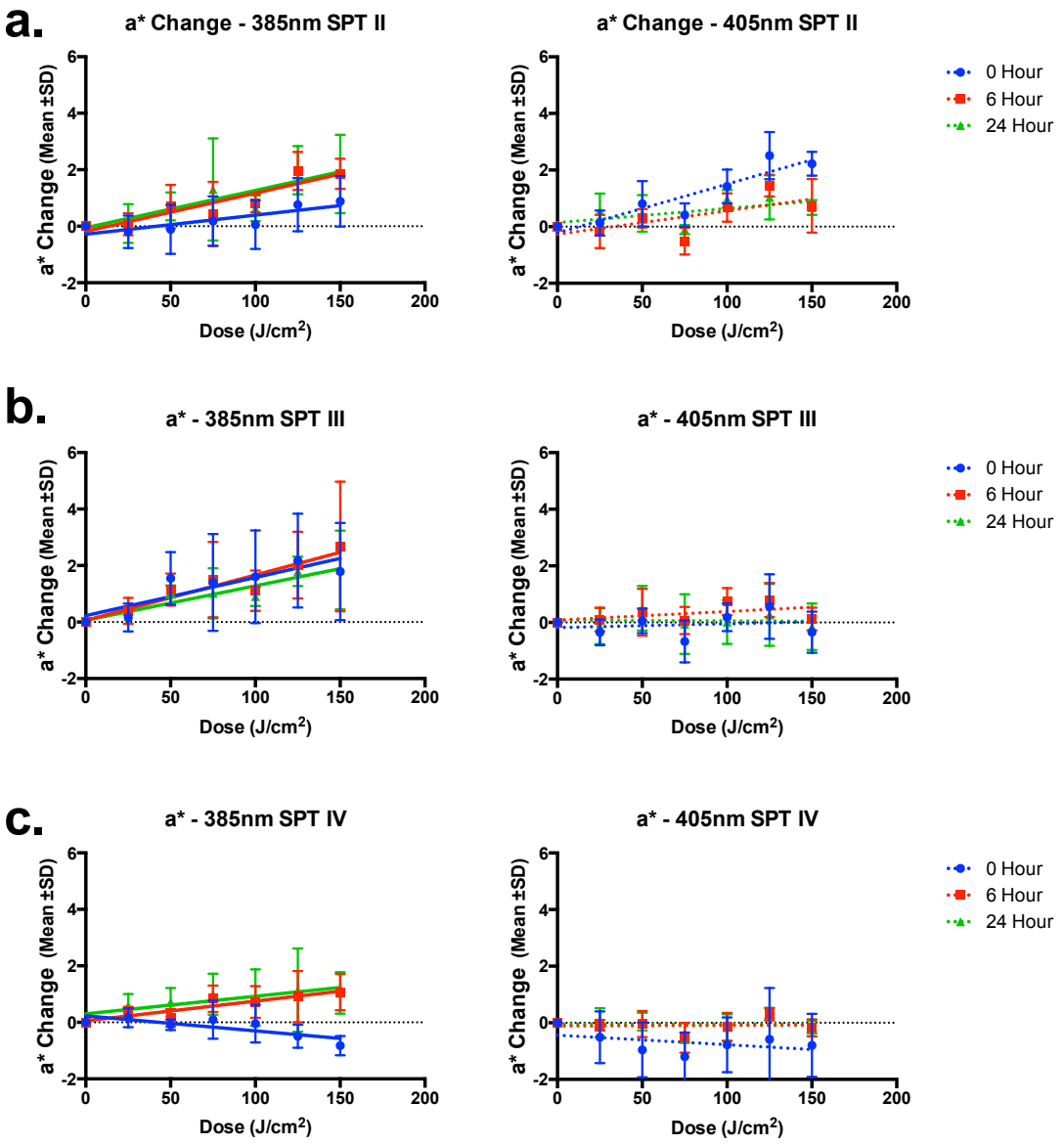

Figure 4.16: The effects of 385nm and 405nm wavelengths on skin a* values (redness) measured using the Minolta device. Volunteers of skin type (a) II (b) III and (c) IV were irradiated with increasing doses (0-150J/cm²) of 385nm and 405nm radiation and redness was assessed using the Minolta device immediately, 6 and 24 hours post irradiation. Data points represent the mean ± SD (n=3). Data were analysed using linear regression analysis and results are displayed in Table 4.10.

Minolta - Change in a* slope p values				
Wavelength	**Skin Type**	**0 Hour**	**6 Hour**	**24 Hour**
385nm	**II**	**0.0408**	**<0.0001**	**0.0036**
	III	**0.0193**	**0.0022**	**0.0003**
	IV	**0.0099**	**0.0031**	0.0640
405nm	**II**	**<0.0001**	**0.0090**	**0.0439**
	III	0.6641	0.1980	0.9486
	IV	0.4381	0.9187	0.9976

Table 4.10: Linear regression analysis of redness change scored with the Minolta device. Slopes were analysed for significance and p values are displayed.

Using all three assessment methods (visually and Optimize and Minolta devices), both 385nm and 405nm sources demonstrated an increase in pigmentation in a dose dependent manner across all skin types assessed. In general, the greatest change was seen immediately with a lessening of effect over time. As with other endpoints assessed, the 385nm source was more efficient in inducing pigmentation compared with the 405nm source. It was not possible to assess redness visually due to the lack of response as well as the masking effect of pigmentation so this was excluded. Redness was however assessed using the Optimize and Minolta reflectance devices, but this approach showed mostly no significant changes or trends, especially with 405nm wavelengths.

The Optimize device gave the results that most closely correlated with the visual assessments of pigmentation and redness and for this reason was selected for subsequent evaluation of source (Table 4.11) and skin type (Table 4.12) differences. However, as redness was largely insignificant and difficult to assess visually this was excluded from analysis. Comparison of slopes by linear regression analysis was used to determine the significance of these differences.

Overall, there were no significant differences in induction of pigmentation from either source used (although visually 385nm appeared to be more efficient). When comparing the response between skin types, for 385nm there were no significant differences between skin types II-IV, however for 405nm there was a difference between skin types at 0 and 6 hours.

385nm vs 405nm – Pigmentation comparison of slope p values			
Skin Type	**0 Hour**	**6 Hour**	**24 Hour**
II	**0.0116**	0.1329	0.1474
III	0.1092	0.8314	**0.0102**
IV	0.5535	0.8355	0.4696

Table 4.11: Comparison of wavelength differences in pigmentation induction. 385nm and 405nm sources compared by linear regression analysis in their ability to induce pigmentation assessed by Optimize device. Slopes were compared and p values are displayed.

Skin type II vs III vs IV – Pigmentation comparison of slope p values			
Skin Type	**0 Hour**	**6 Hour**	**24 Hour**
385nm	0.4041	0.1283	0.4643
405nm	**0.0447**	**0.0095**	0.1893

Table 4.12: Comparison of skin type differences in pigmentation induction. Skin types II, III and IV were compared by linear regression analysis in their ability to induce pigmentation from 385nm and 405nm wavelengths assessed by Optimize device. Slopes were compared and p values are displayed.

4.1.6 Spectral Dependence of Endpoints

The spectral dependencies of cell viability reduction, induction of ROS and CPD production for 385nm, 405nm and SSR were compared to determine the relative damage incurred. This was calculated for each response by calculating the dose required for an equivalent level of damage for each spectrum in the linear part of the response for each endpoint. The reciprocal of the corresponding dose required for this damage was then normalised against the SSR source to give the relative contribution of SSR, 385nm and 405nm wavelengths.

For cell viability, the data used are taken from the Neutral Red assay, as it was decided this was a better assay to assess cell viability (explained in discussion). The doses required for a cell viability reduction of 83% were calculated (Figure 4.17). There was no difference between 385nm and 405nm, but SSR was more efficient in reducing viability.

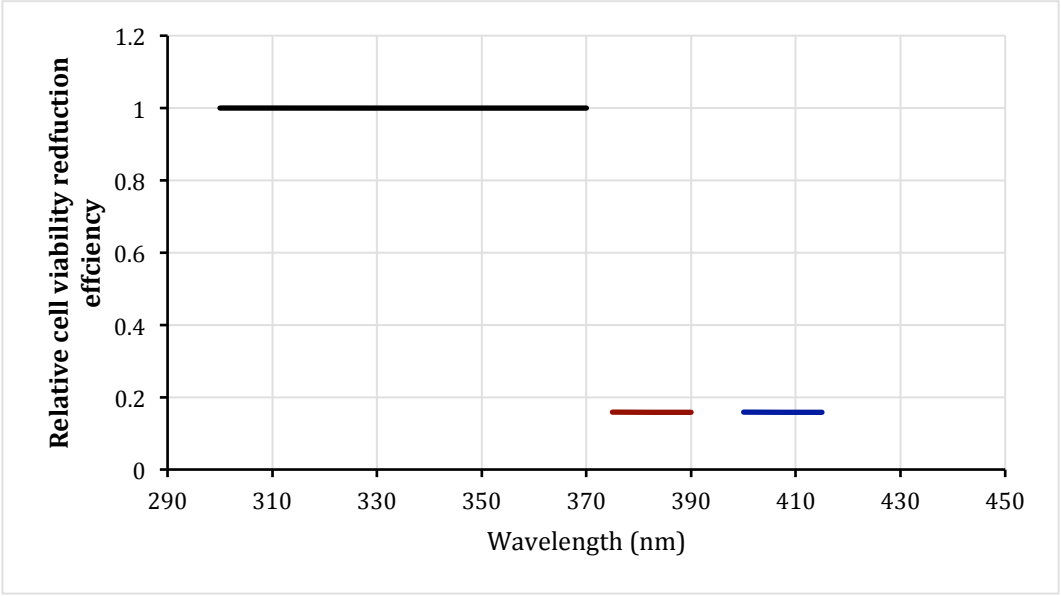

Figure 4.17: The spectral dependence of solar radiation induced cell viability reduction *in vitro*. The reduction of cell viability was measured by the Neutral Red assay in HaCaT keratinocytes after exposure to SSR, 385nm and 405nm, and relative efficiency of each spectrum was plotted (SSR source – 300-370nm, relative efficiency: 1; 385nm source - 375-390nm, relative efficiency: 0.16; 405nm - 400-415nm, relative efficiency: 0.16).

The dependence of ROS production for each wavelength was also compared. Doses required for a relative ROS production value of 7.1 across the range of each spectrum were calculated (Figure 4.18). The SSR source was most efficient in inducing ROS, followed by 385nm and 405nm (relative induction of 1 vs. 0.75 vs. 0.35). These data show that these wavelengths are extremely efficient in producing ROS.

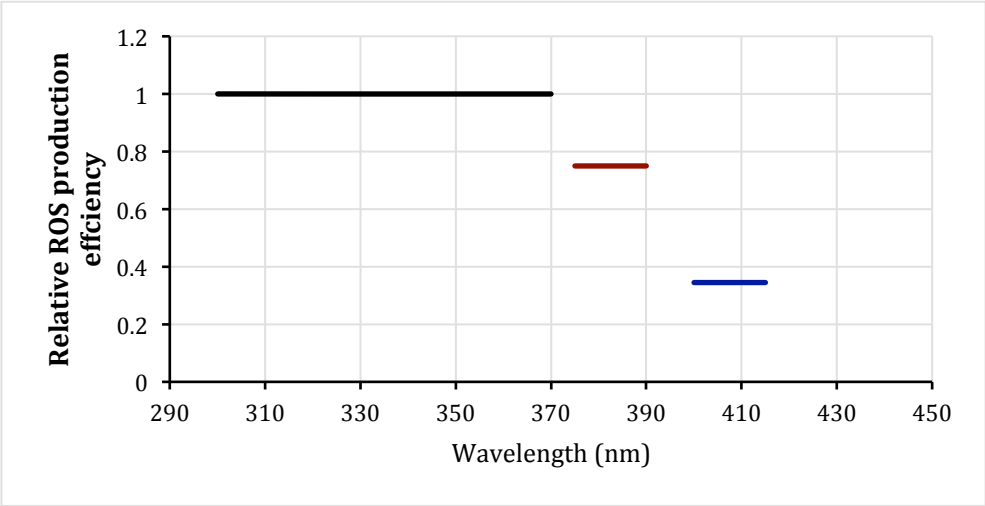

Figure 4.18: The spectral dependence of solar radiation induced ROS production *in vitro*. The spectral dependencies of ROS production *in vitro* by SSR, 385nm and 405nm wavelengths were calculated. (SSR source – 300-370nm, relative efficiency: 1; 385nm source - 375-390nm, relative efficiency: 0.75; 405nm - 400-415nm, relative efficiency: 0.35).

The effect of spectrum on CPD production *in vitro* for each waveband was compared. The doses required for a CPD production value of 3.2 were used (Figure 4.19). The SSR source was by far the most efficient in inducing CPDs. 405nm initiated no formation of ROS and the 385nm source was 50 times less efficient (value of 1 for SSR against 0.02 for 385nm). These data show that the wavelengths at the UV/visible border are extremely inefficient at producing CPDs.

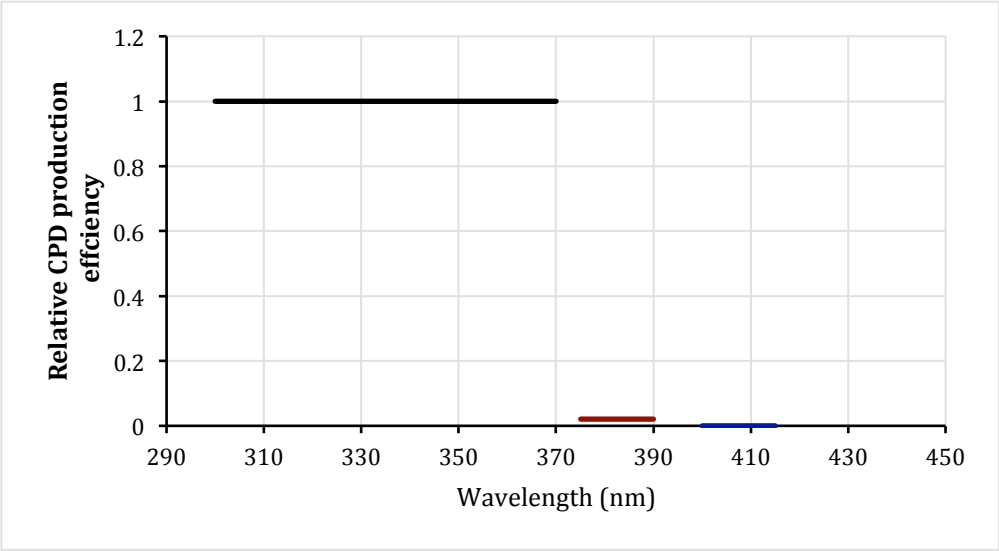

Figure 4.19: The spectral dependence of solar radiation induced CPD production *in vitro*. The production of CPDs was measured *in vitro* using IHC-IF immediately post exposure using SSR, 385nm and 405nm radiation and spectral dependence calculated. The dose required for a CPD induction of 3.2 was calculated and relative CPD production (SSR source – 300-370nm, relative efficiency: 1; 385nm source - 375-390nm, relative efficiency: 0.02; 405nm - 400-415nm, relative efficiency: 0.00).

4.2 Discussion

Terrestrial solar radiation comprises UV, visible and infrared wavebands. However, most photobiological studies on human skin have focussed on the UVR spectrum, with many studies concentrating on the shortwave UVB wavelengths. Scientists are beginning to realise the importance of UVA1, visible and IR parts of the spectrum with an increase in published studies investigating these regions in more recent times. One spectral region that is still largely neglected is the UV/visible border (375-415nm). This region is of particular interest because it is currently poorly protected against by sunscreens. The aim of this chapter was to investigate this region to determine if the skin incurs any significant damage, to compare this with the known effects of shorter wavelengths of the UVR spectrum and to determine damage markers for subsequent photoprotection studies.

All the experiments in this chapter were carried out with two high irradiance LED sources with peak emissions of 385nm and 405nm. LED technologies have undergone rapid advancements in recent years, allowing reproducible, stable narrowband spectra to be produced, which are extremely useful to determine the effects of small bandwidths of radiation. Displayed below in Table 4.13 is the spectral breakdown of solar radiation (London, UK; 12pm, 21st June (Diffey, 2015)). The region of interest (375-415nm) is responsible for only 3.9% of the total solar irradiance; however when this is compared to the UVR/visible boundary region including wavelengths up to 415nm (290-415nm) this accounts for 50.91%, showing the importance of investigating these wavelengths as the irradiance is much higher than for those of the shorter wavelength UVR.

	Wavelength (nm)		Irradiance (mW/m^2)	Percentage of total solar irradiance	Percentage of UVR (%)	Percentage of 290 - 415nm (%)
	From	To				
UVR	290	400	53.9	5.76	**100.00**	75.62
UVB	290	320	2.7	0.29	5.02	3.79
UVA2	320	340	10.3	1.10	19.17	14.50
UVA1	340	400	41.8	4.47	77.59	58.68
385nm	375	395	14.7	1.57	NR	20.61
405nm	395	415	22.4	2.40	NR	31.44
385+405nm	375	415	36.3	3.88	NR	50.91
290-415nm	290	415	71.3	7.62	NR	**100.00**
Visible	400	780	486.8	52.04	NR	NR
IR	780	3000	396.9	42.43	NR	NR
Total	**290**	**3000**	**935.4**	**100.00**	NR	NR

Table 4.13: The spectral breakdown of solar radiation. The spectral breakdown of solar radiation (12pm, 21st June, London, UK). The percentage of each component compared with total irradiance

It might be expected that the effects on the skin by this boundary region would be a continuation of those from broadband UVA, with a lower efficacy, but with a higher efficiency than the longer wavelength visible light. The boundary region has been mainly linked to oxidative damage, gene expression for genes linked with photoageing, and inflammation and pigmentation changes. Thus, earlier studies were the basis for investigation into this spectral region.

All the doses used in these studies are environmentally and biologically relevant, capable of being received by the skin on a summer sun holiday in a tropical climate, with the lower doses still achievable in the UK mid summer. The times taken to receive the relevant doses in the summer of cities of a variety of different latitudes are displayed in Table 4.14. The highest dose used in any

study for either source is 150J/cm^2, however many of the responses are significant at much lower doses.

Dose (J/cm^2)	Times for Doses (Hours)							
	385nm Source	London	Mexico City	Rio de Janeiro	405nm Source	London	Mexico City	Rio de Janeiro
0	0.00	0.00	0.00	0.00	0.00	0.00	0.00	0.00
25	0.23	2.04	1.75	1.64	0.08	1.56	1.34	1.25
50	0.46	4.08	3.50	3.29	0.15	3.12	2.68	2.50
100	0.92	8.16	7.01	6.57	0.31	6.23	5.36	5.01
150	1.38	12.24	10.51	9.86	0.46	9.35	8.04	7.51

Table 4.14: The time required for equivalent dose of 385nm or 405nm radiation in world cities of varying latitude. The times required to receive the doses used at various world cities in mid summer at midday, as calculated from simulated solar spectra (Diffey, 2015).

The results obtained from two cell viability assays informed the doses used for later studies. Both assays resulted in a significant dose dependent reduction for both wavelengths. Neutral Red showed no significant difference between the wavelengths, and in both cases, doses as low as 50J/cm^2 induced significant death. However, when using the Alamar Blue assay the 385nm source was significantly more potent than the 405nm source. This difference may be due to the way the assays measure cell viability. Briefly, Neutral Red is a measure of cell membrane integrity and Alamar Blue measures reduction potential. As is explained later in this chapter, both wavelengths induced oxidative stress, with 385nm being more efficient than 405nm. Because Alamar Blue measures reduction potential of the cell, the increased oxidative stress with 385nm may reduce this reduction potential, and so subsequently the rate at which the resazurin dye can be reduced to its fluorescent metabolite, rather than the cells viability *per se* being reduced.

Generation of ROS by UVA and visible wavelengths is well established *in vitro* (Liebel *et al.*, 2012; Wolfle *et al.*, 2014). This stress is most likely generated by the absorption of photons by cellular photosensitizers. The exact chromophores are unknown but protoporphyrin IX, beta-carotene and melanin have been proposed *in vivo*. This damage is particularly important as oxidative stress has been linked with oxidation of DNA, leading to mutations, and protein oxidation, reducing the efficacy of DNA repair enzymes (McAdam *et al.*, 2016; Ravanat *et al.*, 2001). Visible light exposure has also recently been linked to protein oxidation (Mizutani *et al.*, 2016). The relative ROS effects of 385nm and 405nm are shown in Figure 4.2. The lower dose range of each spectrum induced a clear linear dose-dependent increase in ROS. However the highest two doses at 385nm showed a marked reduction of ROS. One explanation for this unexpected result is that high doses cause so much damage that the fluorescent dye used to measure ROS leaks out of the cells giving spurious results (Radka, 2013). In contrast, the 405nm data suggest that a plateau is reached at 100J/cm^2. One explanation for this is that the putative chromophore(s) are completely depleted/saturated.

The wavelength dependence for CPDs has been studied in the UVR region. The *in vitro* and *in vivo* results are different because of competing chromophores *in vivo* (Young et al., 1998). The UVC region causes the maximal effect *in vitro* that reflects the absorption spectrum of DNA. It is widely accepted that, in skin, the UVB wavelengths are more important, with tapering into the UVA region. There are conflicting reports about CPD production in the UV/visible boundary region (Kvam and Tyrrell, 1997; Liebel *et al.*, 2012). No CPDs were detected *in*

vitro with the highest 405nm dose (150J/cm^2) but same dose of 385nm resulted in a low but significant increase, with none detected at lower doses. This supports data that show a slight increase in CPDs at long wave UVA in AS52 Chinese hamster cells but virtually none with visible radiation (Kielbassa *et al.*, 1997).

The *in vivo* CPD data demonstrated an increase in CPDs over 2 hours with the 385nm source which were persistent over 24 hours. The 405nm source showed very little effect. These results suggest the formation of 'dark CPDs' (Premi *et al.*, 2015). The role of melanin has also been demonstrated in DNA damage caused by visible light, although this was not linked to any particular lesion (Chiarelli-Neto *et al.*, 2014). This could explain the depth difference in CPD production by UVA found by Tewari *et al* that showed increasing CPDs with increased epidermal depth, with more melanin found in deeper layers (Tewari *et al.*, 2012b). The role of melanin has also been demonstrated in DNA damage caused by visible light, although this was not linked to any particular lesion (Chiarelli-Neto *et al.*, 2014). This shows that UVR/visible border region wavelengths may cause damage in melanin containing cells, particularly melanocytes. In the case of the *in vivo* CPD assessment contained within this chapter, the total epidermis was assessed so the observed effect cannot be attributed to a single cell type or compound. It could be expected that other endogenous skin chromophores might cause CPDs through similar mechanisms.

The CPD produced via 385nm irradiance seems to be delayed and persistent. Even at 24 hours post exposure there is no observable repair, which isn't the

case in studies of immediate CPD. There are a number of possible explanations for this. Firstly the levels of CPD are relatively low, so perhaps there is a threshold that must be reached before the DNA damage repair response is triggered. Another possible explanation is that there is so much oxidative stress induced that it damages the DNA repair enzymes and leads to a loss of function (as previously demonstrated by broadband UVA irradiation (McAdam *et al.*, 2016)) or there is a longer term production of CPD that masks the repair.

UVR has been widely implicated in differential gene and protein expression, with certain parts of the spectrum responsible for different effects. The effect of visible light is much less widely studied. The UVR effects found in previous human *in vivo* work in our laboratory were used as a starting point. These comprised three main categories: inflammation/immunoregulation, matrix metalloproteinases (as a marker of photoageing) and oxidative stress. Changes in gene expression were initially measured *in vitro* and later in *vivo.* The *in vitro* results demonstrate significant increases in many of the genes for all categories for both 385nm and 405nm. The exceptions were MMP-9 and PON-2. MMP-9 expression was slightly down regulated with 385nm with no effect with 405nm irradiation. For PON-2 there was a significant upregulation with 385nm that was not seen with 405nm. The difference in PON2 expression can be explained by the greater oxidative potency of 385nm compared to 405nm however the difference with MMP-9 need to be investigated further. Neither gene showed any effect at 405nm. These differences may reflect different chromophores for different genes. It is evident that both wavelengths significantly induce markers of

inflammation and photoageing at a cellular level, with the upregulation of HMOX-1 corroborating with the data from the ROS assay.

The *in vivo* data demonstrate a much greater increase and range of responses compared to the *in vitro* data, however the general trends are comparable and similar to UVR responses reported by others. As the data showed large variation (due to variability of the population) and the study was carried out on a relatively small sample size, the responses for individual genes had very large SDs despite the fold change differences being high for many of the genes. This is expected due to the large variation of the population and is in part influenced by several genetic determinants (Morley *et al.*, 2004). A large variation between volunteers has been found in similar studies with a larger number of volunteers (Tewari *et al.*, 2014). This led to difficulty with evaluating the statistically significantly increased genes and the most relevant time points and wavelengths for later studies. Firstly, the cause of this variation was investigated by determining if there were volunteer(s) that responded differently across endpoints, with the data displayed in Figure 4.7. The data were pooled for all endpoints as well as being split into markers of inflammation, photoageing and oxidative stress. Four of the five volunteers showed good comparable responses (002, 003, 004, 005) for all endpoints, with the remaining volunteer appearing to be more sensitive to the exposure. This is most likely due to the natural variation in the population, however it is important to note that the volunteer that differed the most (006) had the visibly darkest skin tone of the volunteers, which potentially had a an influence.

To overcome the issue of a large SD, it was decided to pool the genes based on the responses for inflammation, photoageing and oxidative stress. The data was not normally distributed so data was also logged to correct this. This largely solved the issue, with significant increase in gene expression associated with inflammation at both time points for both wavelengths, with no significant difference between wavelengths. With the photoageing genes, 6 hours post irradiation gave the greatest response for both wavelengths, with a significant difference between wavelengths at 24 hours. This does not corroborate with previous work in the group that found that UVA1 induced changes in MMP in genes linked to photoageing showed the greatest response after 24 hour, and may suggest a different mechanism for expression than with UVB (Tewari *et al.*, 2014; Tewari *et al.*, 2012a). There was no significant change in genes linked to oxidative stress, matching the previous studies by Tewari *et al* (unpublished) but not the *in vitro* gene expression experiments. The excellent correlation between *in vitro* and *in vivo* studies in the results for gene expression justifies the use of these models for further studies.

Combining the *in vitro* DNA damage and photoageing results is particularly interesting as there is some debate about the trigger for the expression of MMPs. The doses used in the gene expression studies induced no measurable CPDs but significantly increased MMP mRNA; suggesting independence from CPDs, but related to oxidative damage. The different time scales in MMP expression found *in vivo* with UVB/broadband UVA and the visible border region may be due to MMP expressed via differing mechanisms. There is evidence that has linked MMP expression to CPD production (Dong *et al.*, 2008) and also ROS induction (Cho S

Fau - Lee *et al.*; Kim *et al.*, 2006). As the UVR/visible border region induces no/few CPDs immediately the mechanism of MMP expression is most likely linked to ROS production, whereas CPDs are immediately induced with the other wavelengths tested. This suggests there mechanisms involved with both have different time scales.

Exposure of the skin to UVA radiation is well known to induce pigmentation, and this response is one of the endpoints used to assess the UVA protection offered by sunscreens. Furthermore, visible light induced skin pigmentation has been established, although the responses of the full range of skin types are yet to be reported. UVR causes erythema, with conflicting reports on the ability of visible radiation to induce this response. Both pigmentation and redness were assessed immediately, 6 hours and 24 hours post exposure, across different skin types using visual assessments and reflectance spectroscopy. The results demonstrate that there is a clear dose dependent increase in pigmentation across Fitzpatrick skin types II-IV. This affect was immediate, suggesting IPD (due to the oxidation of melanin and a marker of oxidative stress) as well as over 24 hours, indicating PPD. Although not assessed over a longer period than this, informal follow up with volunteers indicated that the pigmentation was visible for several months (8-10 months) after irradiation implicating a role for delayed tanning from these wavelengths. The relative contribution of 405nm wavelengths to induce pigmentation compared to the 385nm sources was in the range of 0.65-0.81 (depending on the skin type), showing both wavelengths are similarly effective for all skin types tested (SPT II-IV). This demonstrates the need for photoprotection in this region, which is particularly of interest to Asian

skin types who have a preference for lighter skins. There was generally no significant increase in erythema, with the exception of the data collected by the Minolta device – however there are reports of issues with the collection of erythema data from this device (Seo *et al.*, 2012; Stamatas *et al.*, 2008). Most of the redness picked up was at the immediate time point and most likely due to heat from the irradiation rather than a photobiological effect. The results described here largely corroborate with studies investigating visible light induced pigmentation, especially in darker skin types (Mahmoud Bh Fau - Ruvolo *et al.*, 2010; Randhawa *et al.*, 2015).

The spectral dependence of each endpoint was analysed comparing the 385nm, 405nm, and SSR responses from the previous chapter. SSR irradiation was much more efficient (x6.25) than either the 385nm or 405nm sources in reducing cell viability (which had identical values). The ability of both the 385nm and 405nm wavelengths to induce ROS were much closer to being as effective as SSR, with only a drop of 25% for 385nm and 65% for 405nm. This crude 'mini action spectrum' corroborates well with another study that more accurately investigates the spectral dependence across the UV/visible spectrum (Zastrow and Lademann, 2016). The ratio of SSR:385nm:405nm in this study is 1:0.75:0.35 compared to the action spectrum produced by Zastrow and Lademann which found a ratio of around 1:0.5:0.35. These results demonstrate the significant damage in this region, at a level almost as high as the rest of the UVR spectrum combined. Finally, the relative efficiency of 385nm to immediately induce CPDs *in vitro* was compared to SSR was only 2%, implying the CPD induction in this region is not significant. This however may not be the case for

delayed CPDs. The three endpoints assessed clearly have different spectral dependencies, suggesting different chromophores and mechanisms involved for each of the outcomes.

In conclusion, the data demonstrate that the UV/visible boundary wavelengths cause significant damage *in vitro* and *in vivo*, probably by oxidative stress. This has potential consequences for cell survival, inflammation, photoageing and pigmentation. These effects occur with environmentally relevant exposures and have many implications, especially for photoprotection in the normal population. They also support additional investigations into the effects of longer wave solar radiation, further into the visible and IR regions. The endpoints determined from this chapter are suitable for subsequent photoprotection studies.

4.3 Summary of Chapter

- Wavelengths at the UVR-visible border (385-405nm) are capable of inducing significant damage to the skin.
- These effects were determined in HaCat keratinocytes and confirmed with some endpoints *in vivo* in human volunteers. These were cell viability, DNA damage, oxidative stress, pigmentation induction and differential gene expression covering different photobiological outcomes: inflammation/immunoregulation, photoageing and oxidative stress.
- In most cases, the 385nm waveband was more efficient at inducing damage than 405nm.
- In some cases, the responses were compared to that of the SSR induced effects and the 'spectral dependence' of responses calculated. In all cases SSR was the most efficient in inducing damage followed by 385nm and 405nm. The relative contribution of each wavelength varied hugely depending on the endpoint assessed.
- There was good correlation between *in vitro* and *in vivo* endpoints.
- Endpoints determined in this chapter are suitable for sunscreen assessments in the following chapter.

Chapter 5: The Photoprotection of UV/visible Border Radiation Induced Damage of the Skin *In Vitro* and *in Vivo*

5.1 Results

5.1.1. Comparison of Spectra and Photostability of Sunscreen Formulations

The absorbance and transmission spectra of two sunscreen formulations (conventional and conventional + C1332 – see *Materials and Methods* for their chemical compositions) were calculated using the BASF sunscreen calculator (using the method described by Herzog and Osterwalder (Herzog and Osterwalder, 2015), and *in vitro* using spectroscopic methods as described in *Materials and Methods* (average of 15 readings). The absorbance results from two different methods were then compared and the differences plotted.

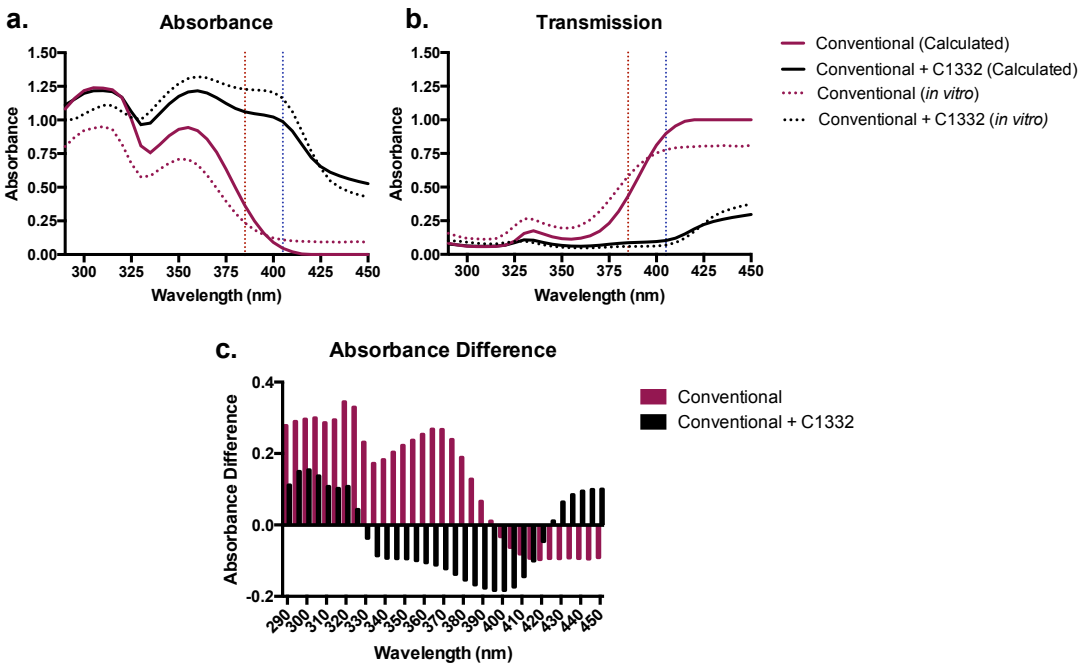

Figure 5.1: The spectral properties of the sunscreen formulations. The absorbance (a) and transmission (b) profiles of sunscreens used in the study as measured by computer simulation using the BASF sunscreen calculator (calculated mathematically) and *in vitro* (average, n=15). The difference in methods used to assess absorbance profiles, for both sunscreens, was calculated by subtracting the *in vitro* calculation from the calculated spectra and plotted (c). Vertical lines on graphs a and b indicate the peak absorbance of the two sources used in this chapter – at 385nm and 405nm.

5.1.2 Photoprotection Against Cell Viability Reduction *In Vitro*

It was previously established that both 385nm and 405nm radiation induce a significant reduction in cell viability *in vitro*. Different sunscreen formulations were investigated for their ability to prevent this endpoint in HaCat keratinocytes. The following combinations/formulations were used: unirradiated, positive (no PMMA plate) irradiated control, irradiated plates with glycerol, a vehicle base cream (used in the following formulations), a conventional sunscreen and a conventional sunscreen of the same SPF containing the experimental UVR filter C1332.

The different formulations were applied to PMMA plates at a concentration of 1.3mg/cm^2 and cells were irradiated through the plates with 385nm or 405nm radiation (150J/cm^2). Cell viability was assessed 24 hours post exposure using the Neutral Red assay. For the 385nm waveband (Figure 5.2a), there was a significant reduction in cell viability with all the treatments compared with unirradiated control, with the exception of the conventional filter + C1332. However, there was no significant difference between conventional and conventional + C1332. When using the 405nm wavelengths (Figure 5.2b) there was a similar relationship, all conditions allowed a significant reduction in cell viability with the exception of the conventional + C1332 formulation. There was however a significant difference between conventional and conventional + C1332 formulations. The data show controls and conventional sunscreen were not sufficiently protective from 385nm and 405nm induced cell viability

reduction, but the addition of C1332 prevented any significant increase of cell death.

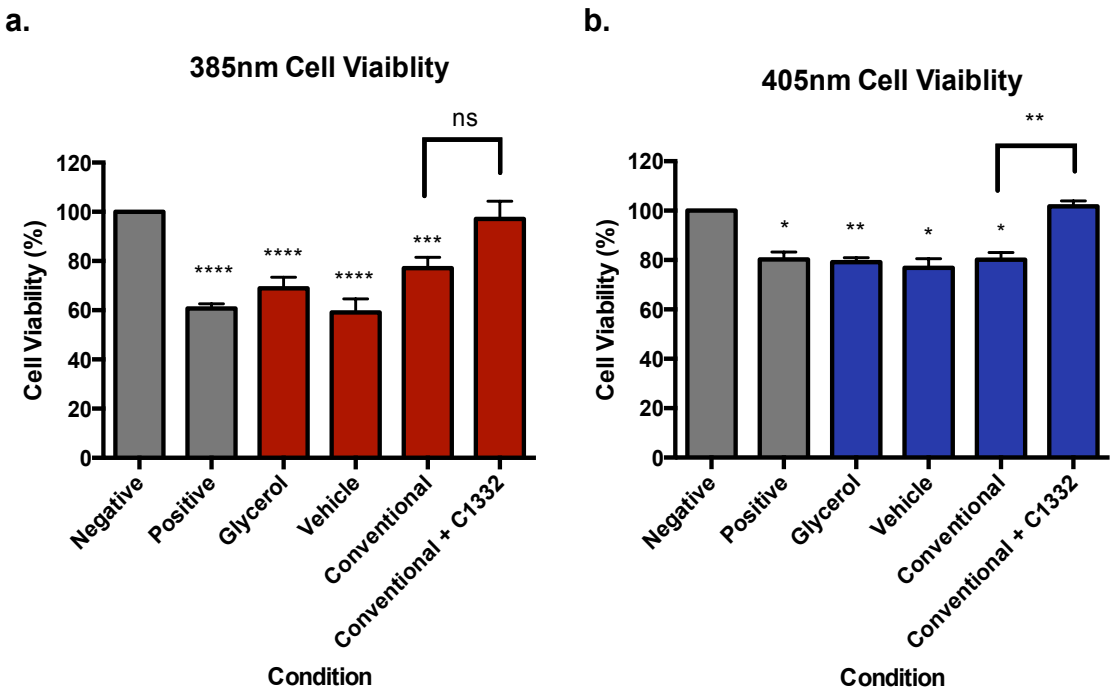

Figure 5.2: Sunscreen prevention of 385nm and 405nm induced cell viability reduction *in vitro*. HaCaT keratinocytes were untreated or exposed to 150J/cm^2 of (a) 385nm or (b) 405nm radiation through a range of test formulations. Cell viability was measured 24 hours later by the Neutral Red assay. Columns represent the mean ± SD (n=3). Cell viability was significantly reduced across all formulations with the exception of the conventional + C1332 sunscreen (385nm: $p<0.0001$, 405nm: $p=0.0002$; n=3, One-way ANOVA with Tukey's multiple comparisons test). There was a significant difference between the conventional and conventional + C1332 formulation for 385nm irradiation but this was significant for 405nm. (385nm: $p=0.0871$, 405nm: $p=0.0011$; n=3, paired t test).

5.1.3 Photoprotection Against Induction Reactive Oxygen Species *In Vitro*

In *Chapter 4*, it was demonstrated that irradiation with wavelengths of UV/visible border cause the generation of ROS displaying the importance of protecting against this region. The photoprotection offered by a range of sunscreen formulations was assessed. The different formulations were applied to PMMA plates at a concentration of 1.3mg/cm^2 and cells were irradiated through the plates with either 50J/cm^2 of 385nm (Figure 5.3a) or 100J/cm^2 405nm (Figure 5.3b) radiation based on the findings reported in *Chapter 4*. Immediately after exposure, ROS levels were measured by staining with carboxy-H_2DCFDA (a ROS indicator) and the fluorescence measured by FACS, eliminating unviable cells with the use of DAPI. Irradiation with both 385nm and 405nm wavelengths led to a significant increase in ROS for all formulations with the exception of the conventional + C1332 formulation. There was a significant difference between the conventional and conventional + C1332 formulations for both wavelengths, indicating that the addition of C1332 to a formulation significantly increases the protection offered.

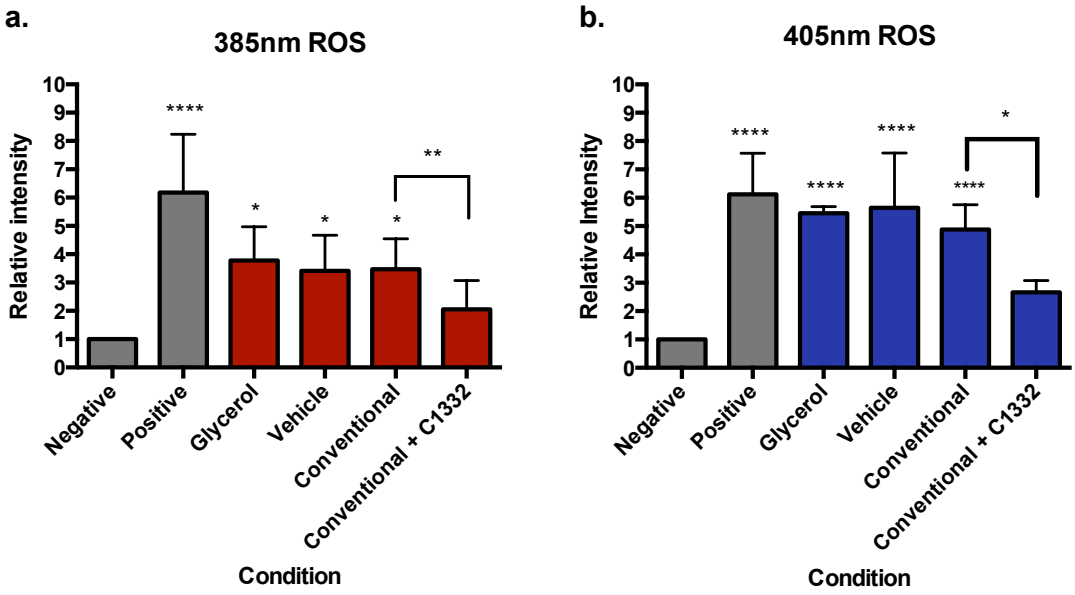

Figure 5.3: Sunscreen prevention of 385nm and 405nm induced ROS *in vitro*. HaCaT keratinocytes were untreated or exposed to (a) 50J/cm^2 of 385nm or (b) 100J/cm^2 405nm radiation through a range of sunscreen formulations. Columns represent the mean ± SD (n=4). There was a significant increase in ROS compared to the unirradiated control for all test conditions when irradiated with 385nm and 405nm radiation apart from the conventional + C1332 formulation (385nm: p=0.0004, 405nm: p<0.0001; n=3, One-way ANOVA with Holm-Sidak's multiple comparisons test). There was a significant difference reduction in ROS when using the conventional + C1332 formulation compared to the conventional formulation for both 385nm and 405nm wavelengths (385nm: p=0.0042, 405nm: p=0.0375; n=4, paired t test).

5.1.4 Photoprotection Against delayed CPD induction *In Vivo*

The 385nm source had previously been demonstrated to induce delayed CPD *in vivo* over a 2-24 hour period. There was no peak so a time point in the middle of the plateau of production was selected to assess photoprotection using the previously described formulations. Formulations were applied to human volunteers (details described in Table X) at a concentration of 2mg/cm^2 and allowed to dry for at least 10 minutes before irradiation with 150J/cm^2 of 385nm radiation. 4 hours post exposure, biopsies were taken and analysed by HPLC as previously described. There was an increase in CPD at the unprotected sitewith an even greater increase in CPD with the vehicle control. The conventional site provided some protection, with complete protection offered by the conventional + C1332 site. Each collumn represents mean ± SD (n=4).

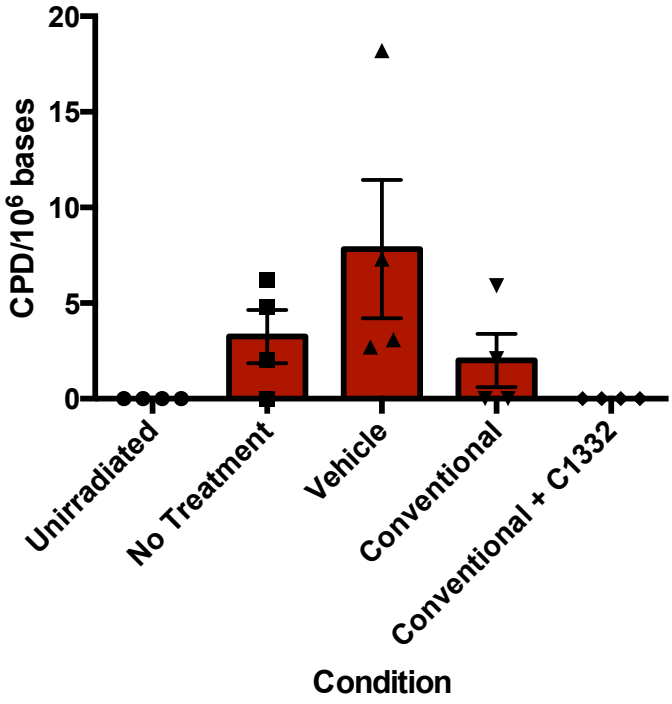

Figure 5.4: The photoprotection of 385nm induced delayed CPD *in vivo*. Human volunteers were unexposed, or exposed 150/cm^2 of 385nm radiation. Biopsies were taken 4 hours post exposure. DNA was extracted and CPDs were assessed by HPLC MS/MS. The increase in CPD for

all conditions was not statistically significant ($p=0.1771$; $n=4$, One-way ANOVA with Holm-Sidak's multiple comparisons test).

5.1.5 Photoprotection Against Gene Expression Changes

5.1.5.1 Photoprotection Against Gene Expression Changes In Vitro

A number of genes were found to be upregulated in the previous chapter (*Chapter 4*) in response to irradiation with the 385 and 405nm sources. The protection against the expression of these genes was investigated covering a range of adverse photobiological effects. The genes selected were IL-1a, IL-6 to cover inflammation/immunoregulation, HMOX-1 as an oxidative stress response marker and MMP-1, as a marker for photoageing. The gene expression changes were measured by qPCR on HaCat keratinocytes irradiated with 385nm (105J/cm^2) or 405nm (150J/cm^2) radiation with and without the different formulations. These doses were selected to maintain a cell viability of ≥ 80%. Twelve hours post-exposure total RNA was extracted from the cells and qPCR was carried out as in the *Materials and Methods*. The results are shown below (Figure. 5.5).

In general, with the 385nm source there was a significant increase in damage with the vehicle but no increase with either the conventional or conventional + C1332 formulations. When comparing these two formulations there was no statistically significant protection offered by the addition of C1332. The results for the 405nm source were slightly different. The overall trend was that irradiation through the vehicle and conventional formulations induced significant gene expression changes compared to the unirradiated control but the conventional + C1332 formulation showed no significant difference from

unirradiated control, indicating substantial protection. The comparison of the conventional against conventional + C1332 formulation showed that the addition of C1332 provided significant protection over the conventional sunscreen alone. The results are described in Table 5.1. When analysing the information for both wavelengths it can be concluded that adding the UV/visible filter C1332 to a formulation significantly increases the protection.

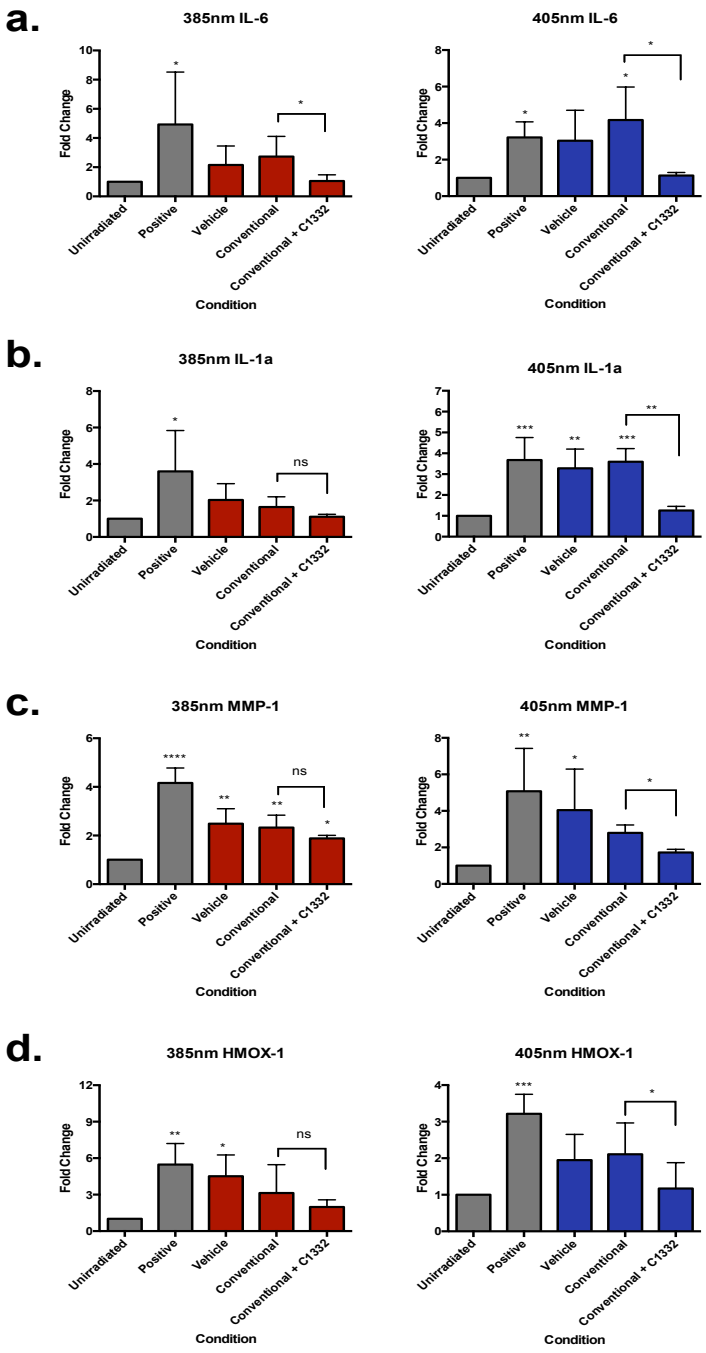

Figure 5.5: The photoprotection of 385nm and 405nm induced gene changes *in vitro*. HaCaT keratinocytes were unexposed, exposed to 105J/cm^2 of 385nm or 150J/cm^2 of 405nm radiation alone or with one of three of sunscreen formulations. Gene expression changes for (a) IL-6, (b) IL-1a, (c) MMP-1 and (d) HMOX-1 were measured 12 hours post exposure by qPCR. Columns represent the mean ± SD (n=4). For every gene studied, each condition was compared to the unirradiated control (n=4, One-way ANOVA with Dunnett's multiple comparisons test) and the conventional was compared with the conventional + C1332 formulation (n=3, paired t test). Results of the statistical tests are displayed below in Table 5.1.

Gene	385nm ANOVA p value	Conventional vs. Conventional + C1332 t test	405nm ANOVA p value	Conventional vs. Conventional + C1332 t test
IL-1a	0.0305	0.2290	<0.0001	0.0055
IL-6	0.0474	0.0428	0.0063	0.0431
MMP-1	<0.0001	0.1966	0.0084	0.0132
HMOX-1	0.0060	0.3008	0.0014	0.0226

Table 5.1: Statistical analysis for *in vitro* gene expression photoprotection studies. Displayed are the p values of the ANOVA test for each gene and wavelength and t test comparing the conventional against conventional + C1332 sunscreen formulations. The ANOVA result shows that there is a significant difference between the means of the test conditions. Results of the t-test show that for the 405nm wavelengths there is significant protection offered by the additional of C1332 compared to the conventional sunscreen alone. For 385nm only IL-6 expression is significantly down regulated with the addition of C1332.

5.1.5.2 Photoprotection Against Gene Expression Changes In Vivo

Chapter 4 demonstrated that a number of genes were also upregulated *in vivo* by irradiation at with wavelengths at the UV/visible border. The photoprotection offered by the sunscreens to prevent these changes was also investigated *in vivo*, with genes covering inflammation, photoageing and oxidative stress selected from previous studies. This was measured by qPCR on skin type II human volunteers irradiated with a dose of 150J/cm^2 of 385nm and 405nm radiation. Volunteers' details are displayed below in Table 5.2.

Volunteer ID	Age	Sex	Skin Type
001	27	M	II
002	27	F	II
003	27	M	II
004	25	F	II
005	28	M	II

Table 5.2: Volunteer Demographics for *in vivo* photoprotection gene expression studies.

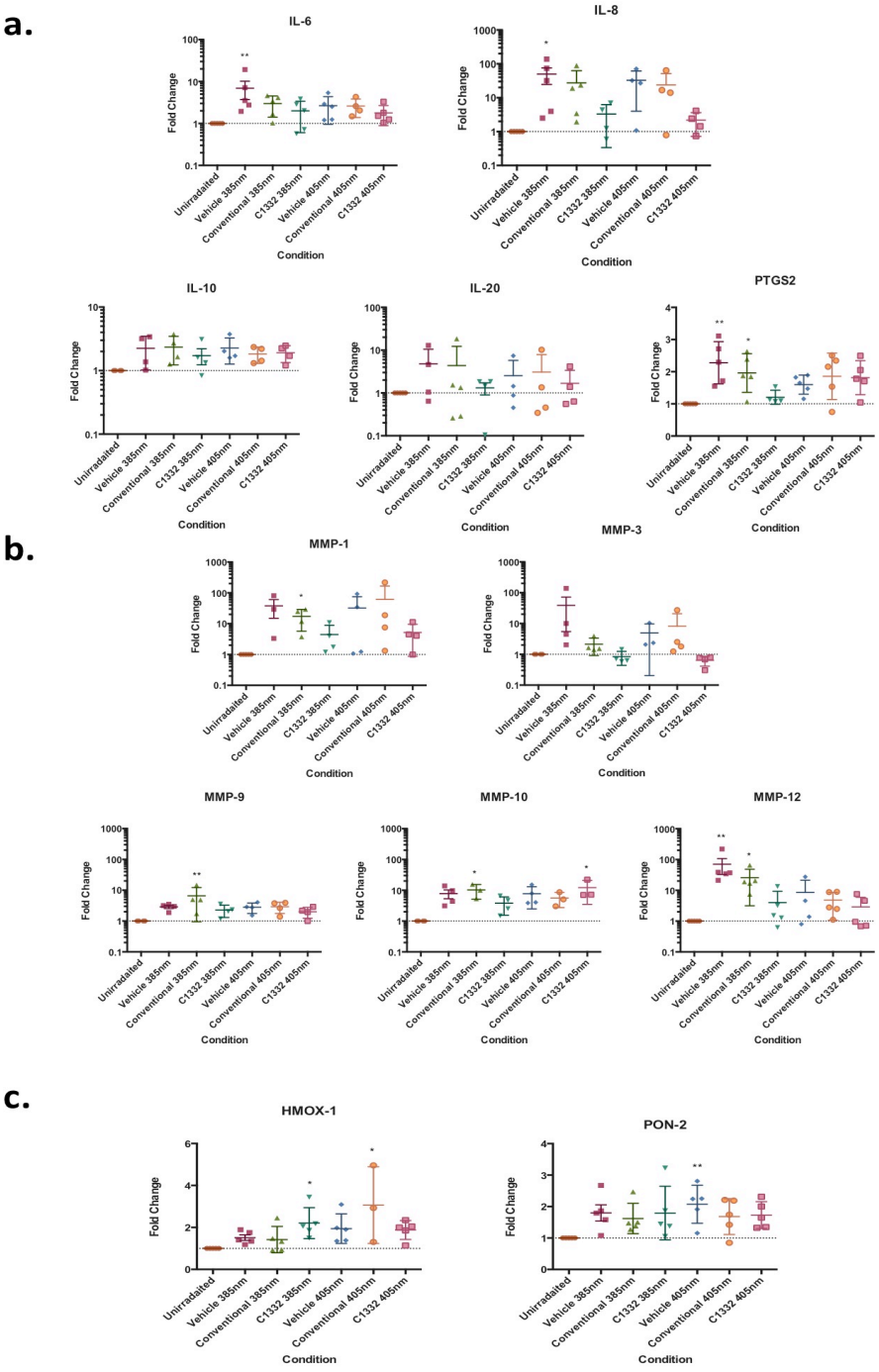

Figure 5.6: The photoprotection of 385nm and 405nm induced gene changes *in vivo* in human volunteers. Volunteers were unexposed, exposed to 150J/cm^2 of 385nm or 405nm radiation with one of three of sunscreen formulations. Biopsies were taken 24 hours post exposure and gene expression changes measured by qPCR. Genes are pooled based on (a) inflammation (b) photoageing and (c) oxidative stress Columns represent the mean ± SD (n=5). For every gene studied, each condition was compared to the unirradiated control (n=5, One-way ANOVA with Kruskal-Wallace's multiple comparisons test) and the conventional was compared with the conventional + C1332 formulation. Results of the statistical tests are displayed below in Table 5.3.

Endpoint	Gene	ANOVA p value
Inflammation	IL-6	**0.0256**
	IL-8	**0.0286**
	IL-10	0.1208
	IL-20	0.9379
	PTGS2	**0.0112**
Photoageing	MMP-1	**0.0387**
	MMP-3	**0.0020**
	MMP-9	**0.0290**
	MMP-10	**0.0250**
	MMP-12	**0.0015**
Oxidative Stress	HMOX-1	**0.0165**
	PON-2	**0.0489**

Table 5.3: Statistical analysis for *in vivo* gene expression photoprotection studies. Displayed are the p values of the ANOVA test for each gene. The ANOVA result shows that for the majority of genes there is a significant difference in the response between formulations.

The results largely reflected those found *in vitro* for both wavelengths. There was a large increase in fold change with the vehicle with both sources, suggesting very little protection. With the 385nm source there was a slight reduction compared to vehicle with the conventional formulation and much more protection with the addition of compound C1332. With the 405nm source there was almost no protection offered by the conventional formulation, however this was reduced with the addition of C1332.

As with *Chapter 4*, although there appeared to be a trend this was not statistically significant, due to the large variation and spread of results found with using volunteers. For this reason the approach of pooling data based on end point from the previous chapter was employed. Data was not normally distributed, so was logged to see asses if this produced normally distributed data as in the previous chapter. This was not the case so data was left unlogged and non-parametric analyses were employed. Genes were pooled to fit in three categories: inflammation, photoageing and oxidative stress. This produced more robust data with the same trends observed. Although there was still a significant increase with the C1332 formulation this increase was much less than for the other formulations tested.

5.1.5.3 Pooled Analysis

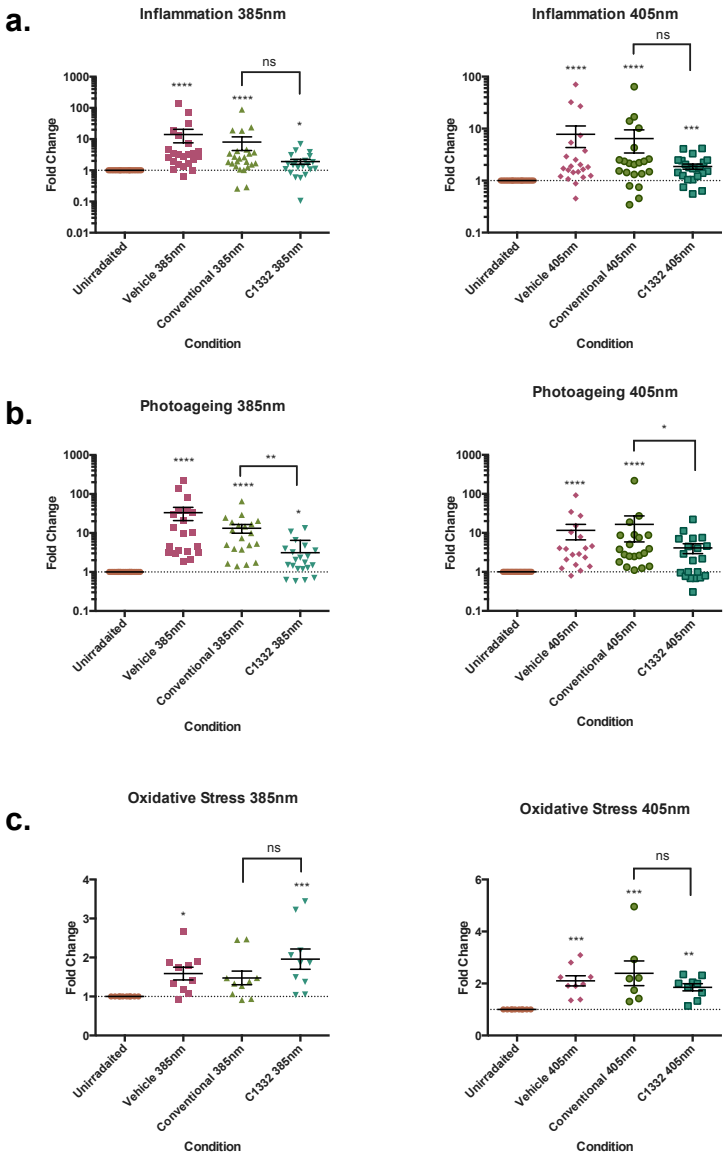

Figure 5.7: Pooled response of 385nm and 405nm induced gene changes *in vivo* with different formulations. Genes were pooled based on endpoint: (a) inflammation, (b) photoageing and (c) oxidative stress. Data are displayed as mean ± SD. Differences were analysed using one-way ANOVA with Kruskal-Wallis multiple comparisons test.

Endpoint	Genes Included	ANOVA 385nm p value	ANOVA 405nm p value
Inflammation	IL-6	<0.0001	<0.0001
	IL-8		
	IL-10		
	IL-20		
	PTGS2		
Photoageing	MMP-1	<0.0001	<0.0001
	MMP-3		
	MMP-9		
	MMP-10		
	MMP-12		
Oxidative Stress	HMOX-1	0.0008	<0.0001
	PON-2		

Table 5.4: Statistical analysis for pooled *in vivo* gene expression photoprotection studies. Displayed are the p values of the ANOVA test for each endpoint pooled. The ANOVA result shows that for the majority of genes there is a significant difference in the response between formulations.

5.1.6 Photoprotection Against Pigmentation Changes *In Vivo*

Photoprotection against of 385nm and 405nm radiation induced pigmentation was measured *in vivo* in human volunteers of skin type II-IV. Volunteers were exposed to increasing doses (0, 100, 125 and 150J/cm^2) of 385nm or 405nm radiation with either no sunscreen, vehicle, conventional or conventional + C1332 sunscreens, and pigmentation was assessed at 0, 6 and 24 hours post radiation exposure, using three different methods: visual assessment, Minolta chromometer and an Optimize device. Photographs were taken at each time point. Representative pictures for each skin type are displayed in Figure 5.9 (other photographs are contained within supplementary data). The details of the volunteers used are displayed in Table 5.5. The responses for each method are plotted in Figures 5.10, 5.11 and 5.12. Results are described in Tables 5.6, 5.7 and 5.8.

Volunteer ID	Age	Sex	Skin type
002	21	M	II
003	25	M	III
004	30	M	IV

Table 5.5: Volunteer Demographics for *in vivo* pigmentation/erythema photoprotection studies.

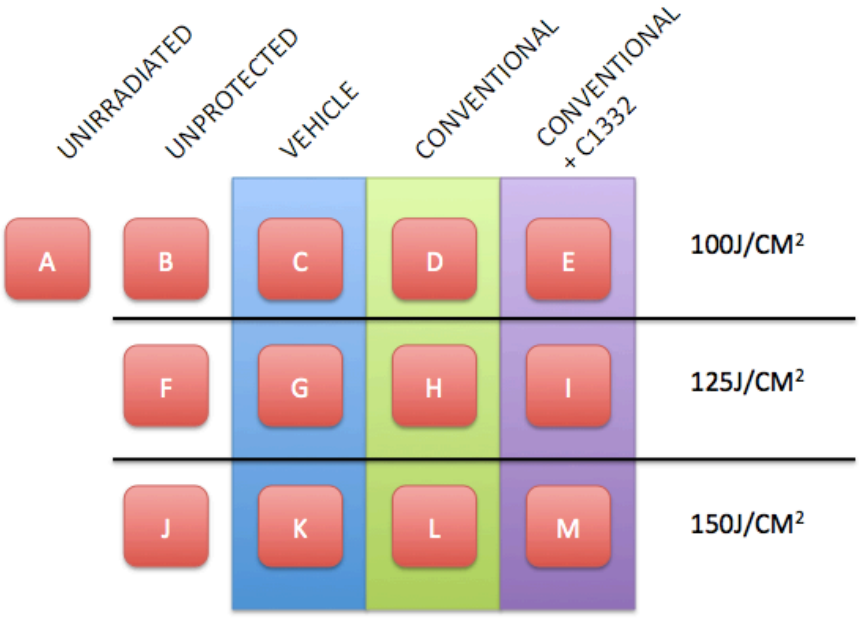

Figure 5.8: Study layout for pigmentation photoprotection studies. The scheme for irradiation of volunteers to assess protection offered by different formulation against 385nm and 405nm induced pigmentation.

5.1.6.1 Typical Responses

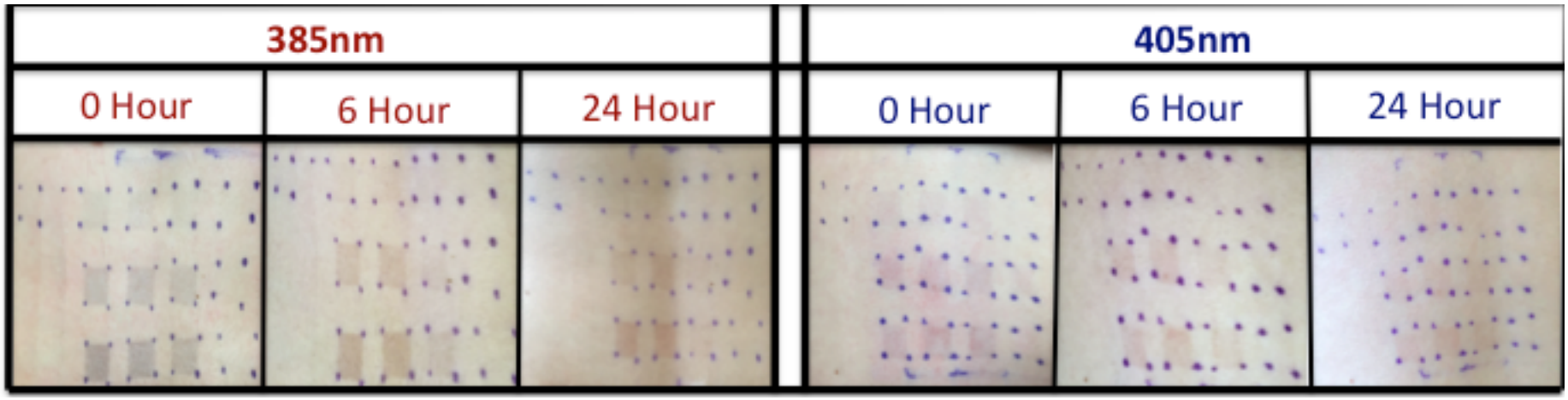

Figure 5.9: Typical response of one volunteer over time for pigmentation studies. The responses of one volunteer to both 385nm and 405nm over time. Photographs are solely for illustrative purposes – no data based on responses were determined from images. Differences in base colours are due to photographs being taken in different environments.

5.1.6.2 Visual Score of Pigmentation

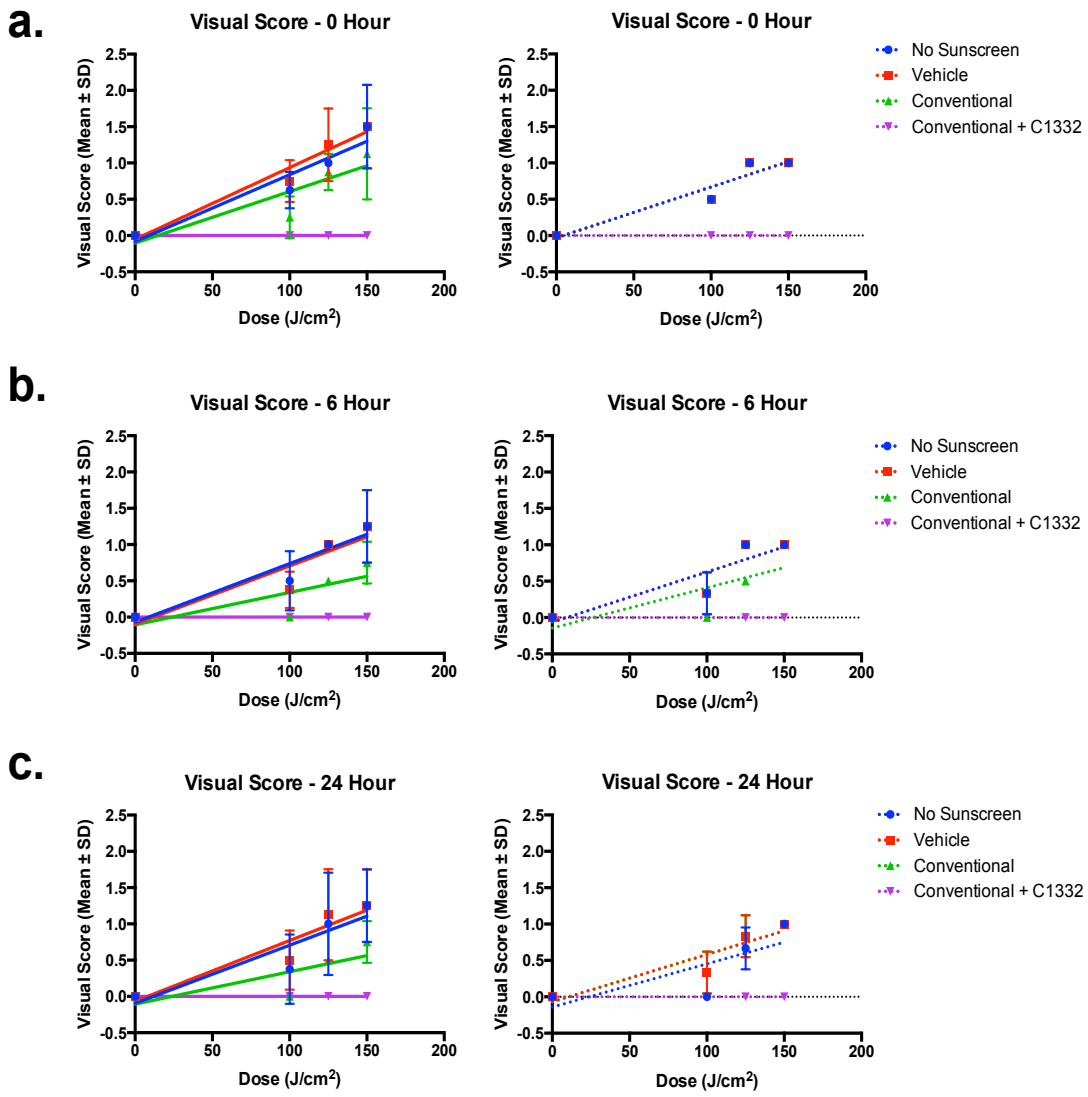

Figure 5.10: Photoprotection against pigmentation by different sunscreen formulations scored visually. The visual score of pigmentation with 385nm and 405nm sources at (a) 0, (b) 6 and (c) 24 hours was assessed for each condition: No sunscreen, vehicle control, conventional and conventional + C1332. The dose response relationship is plotted and linear regression analysis was calculated and displayed Table 5.6 (Mean ± SD; Linear regression analysis, n=3 skin types II-IV).

Wavelength	Formulation	Time point		
		0 Hour	6 Hour	24 Hour
385nm	No Sunscreen	**<0.0001**	**<0.0001**	**0.0027**
	Vehicle	**<0.0001**	**<0.0001**	**0.0008**
	Conventional	**0.0014**	**0.0013**	**0.0013**
	Conv. + C1332	N.S.	N.S.	N.S.
405nm	No Sunscreen	**<0.0001**	**0.0002**	**0.0046**
	Vehicle	**<0.0001**	**0.0002**	**0.0003**
	Conventional	**<0.0001**	**0.0040**	**0.0003**
	Conv. + C1332	N.S.	N.S.	N.S.

Table 5.6: Linear regression analysis of pigmentation photoprotection scored visually. (Mean ± SD; Linear regression analysis, n=3 skin types II-IV).

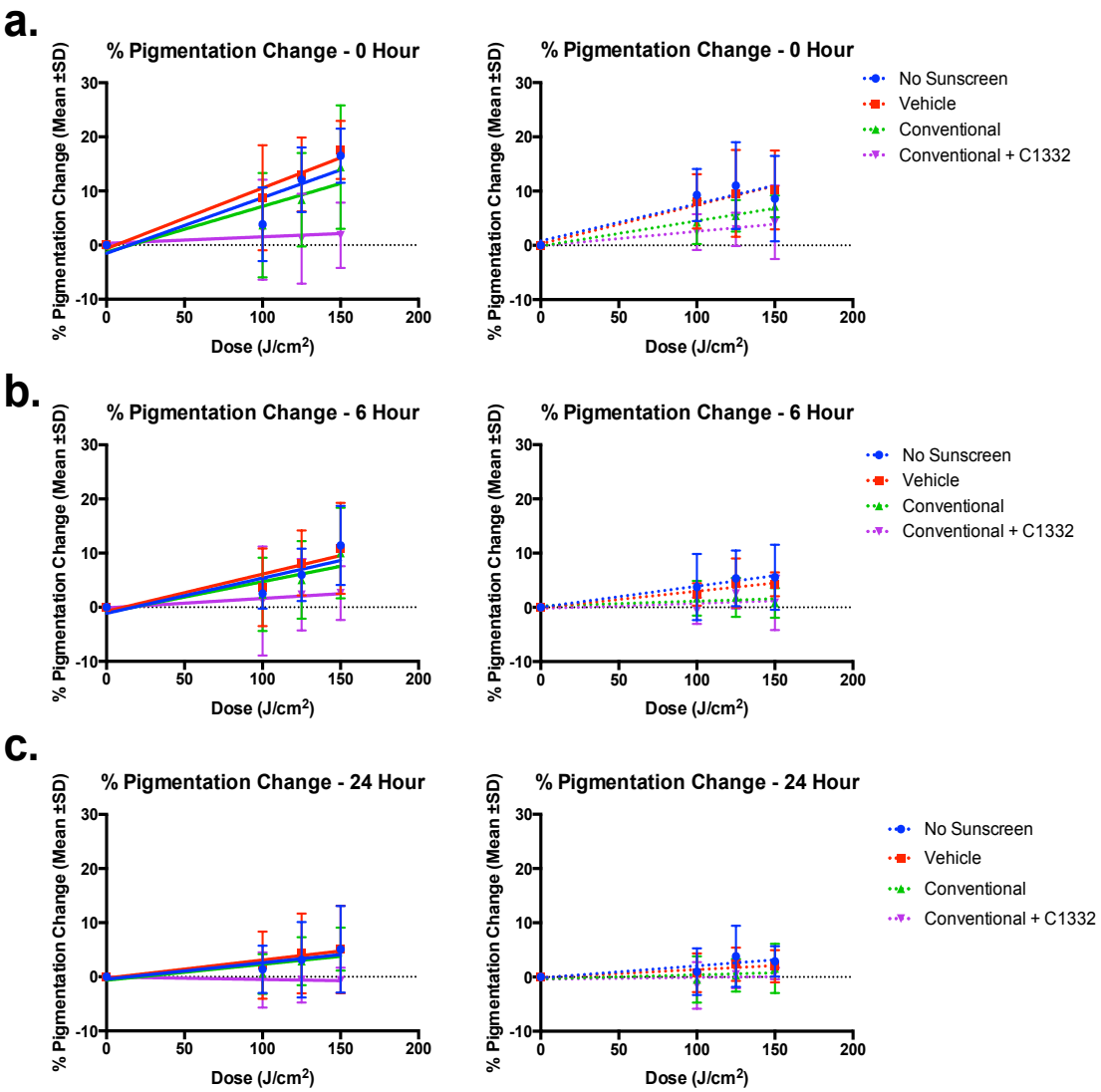

Figure 5.11: Photoprotection against pigmentation by different sunscreen formulations scored with the Optimize device. The Optimize % pigmentation score of pigmentation with 385nm and 405nm sources at (a) 0, (b) 6 and (c) 24 hours was assessed for each condition: No sunscreen, vehicle control, conventional and conventional + C1332. The dose response relationship is plotted and linear regression analysis was calculated and displayed Table 5.7 (Mean ± SD; Linear regression analysis, n=3 skin types II-IV).

Wavelength	Formulation	Time point		
		0 Hour	6 Hour	24 Hour
385nm	No Sunscreen	**0.0048**	**0.0216**	0.2205
	Vehicle	**0.0042**	**0.0428**	0.2146
	Conventional	0.0687	0.0976	0.0740
	Conv. + C1332	0.7108	0.5675	0.7553
405nm	No Sunscreen	**0.0424**	0.1183	0.2417
	Vehicle	**0.0259**	**0.0372**	0.2826
	Conventional	**0.0034**	0.5116	0.6556
	Conv. + C1332	0.1795	0.5537	0.0675

Table 5.7: Linear regression analysis of pigmentation photoprotection scored with the Optimize device. (Mean ± SD; Linear regression analysis, n=3 skin types II-IV).

5.1.6.4 Minolta Score of Pigmentation

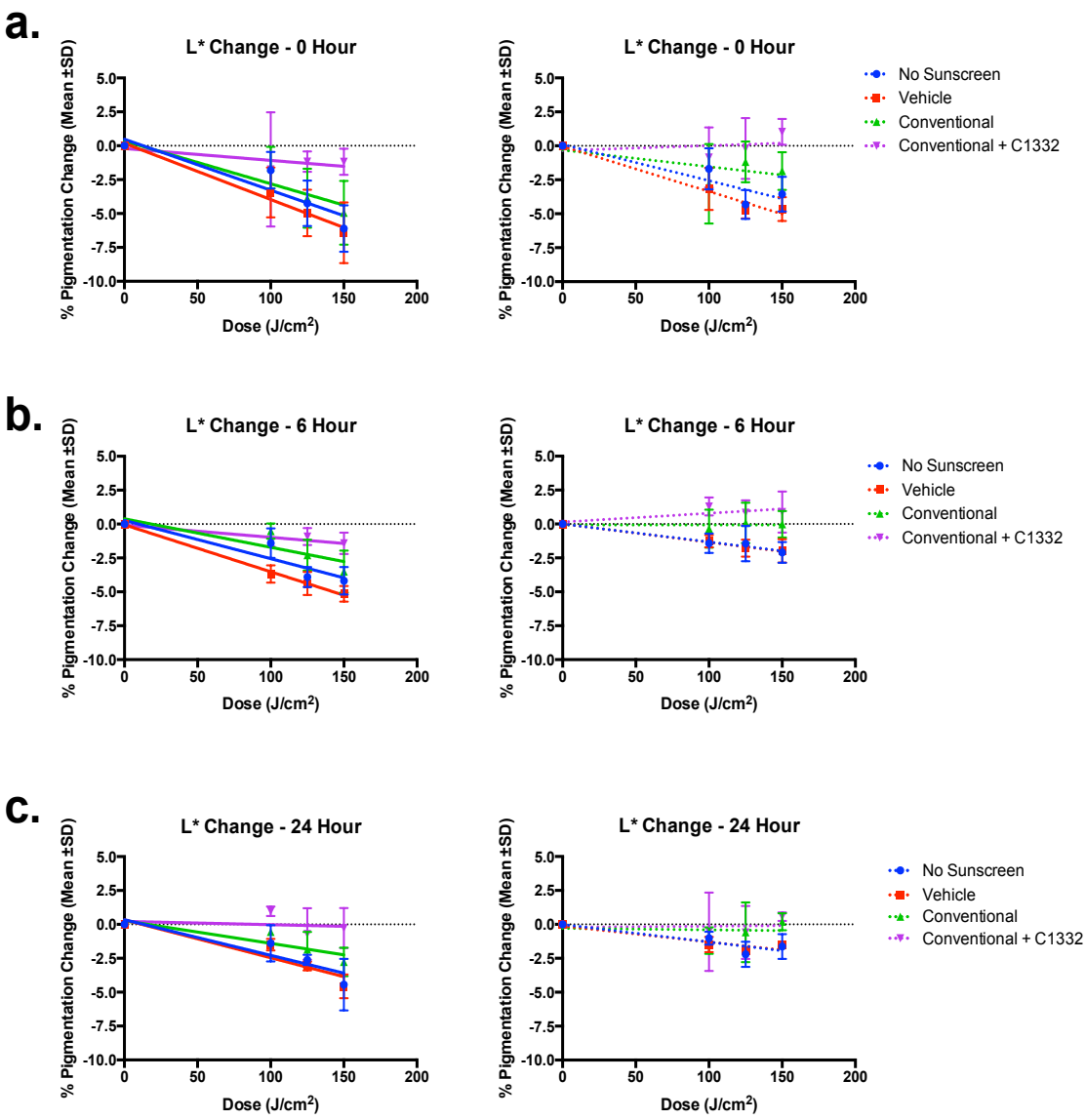

Figure 5.12: Photoprotection against pigmentation by different sunscreen formulations scored with the Minolta device. The Minolta L* score of pigmentation with 385nm and 405nm sources at (a) 0, (b) 6 and (c) 24 hours was assessed for each condition: No sunscreen, vehicle control, conventional and conventional + C1332. The dose response relationship is plotted and linear regression analysis was calculated and displayed Table x (Mean ± SD; Linear regression analysis, n=3 skin types II-IV).

Wavelength	Formulation	Time point		
		0 Hour	6 Hour	24 Hour
385nm	No Sunscreen	**0.0009**	**0.0004**	**0.0136**
	Vehicle	**0.0004**	**<0.0001**	**0.0017**
	Conventional	**0.0055**	**0.0063**	**0.0252**
	Conv. + C1332	0.4095	**0.0077**	0.7582
405nm	No Sunscreen	**0.0021**	**0.0063**	**0.0252**
	Vehicle	**<0.0001**	**0.0005**	**0.0034**
	Conventional	0.2062	0.9908	0.8836
	Conv. + C1332	0.6716	0.1895	0.9350

Table 5.8: Linear regression analysis of pigmentation photoprotection scored with the Minolta device. (Mean ± SD; Linear regression analysis, n=3 skin types II-IV).

In general the vehicle formulation induced more damage than control, with the conventional sunscreen providing more protection and the conventional + C1332 sunscreen providing almost complete protection. There was good corroboration between the three methods used to assess pigmentation indicating that any of methods employed are capable of accurately assessing pigmentation and its prevention. The protection offered for against both wavelengths was similar.

5.1.7 Transmitted Spectra and Photostability

The irradiance per nm transmitted through each formulation, as well as the photostability, was assessed for the 385 and 405nm sources. The irradiance of each source was measured with no plate, a PMMA plate alone, the PMMA plate with glycerol and vehicle, or with each formulation (at a concentration of 1.3mg/cm^2) using a spectrophotometer. Each formulation was also measured after an irradiation of 150J/cm^2 to assess photostability. The results are displayed in Figure 5.13. The percentage of maximum transmitted irradiance for each formulation was calculated for both sources along with the percentage degradation (Table 5.9). The conventional + C1332 formulation have the lowest transmittance in both cases and application of glycerol or vehicle to the PMAA plate resulted in an apparently increased transmittance.

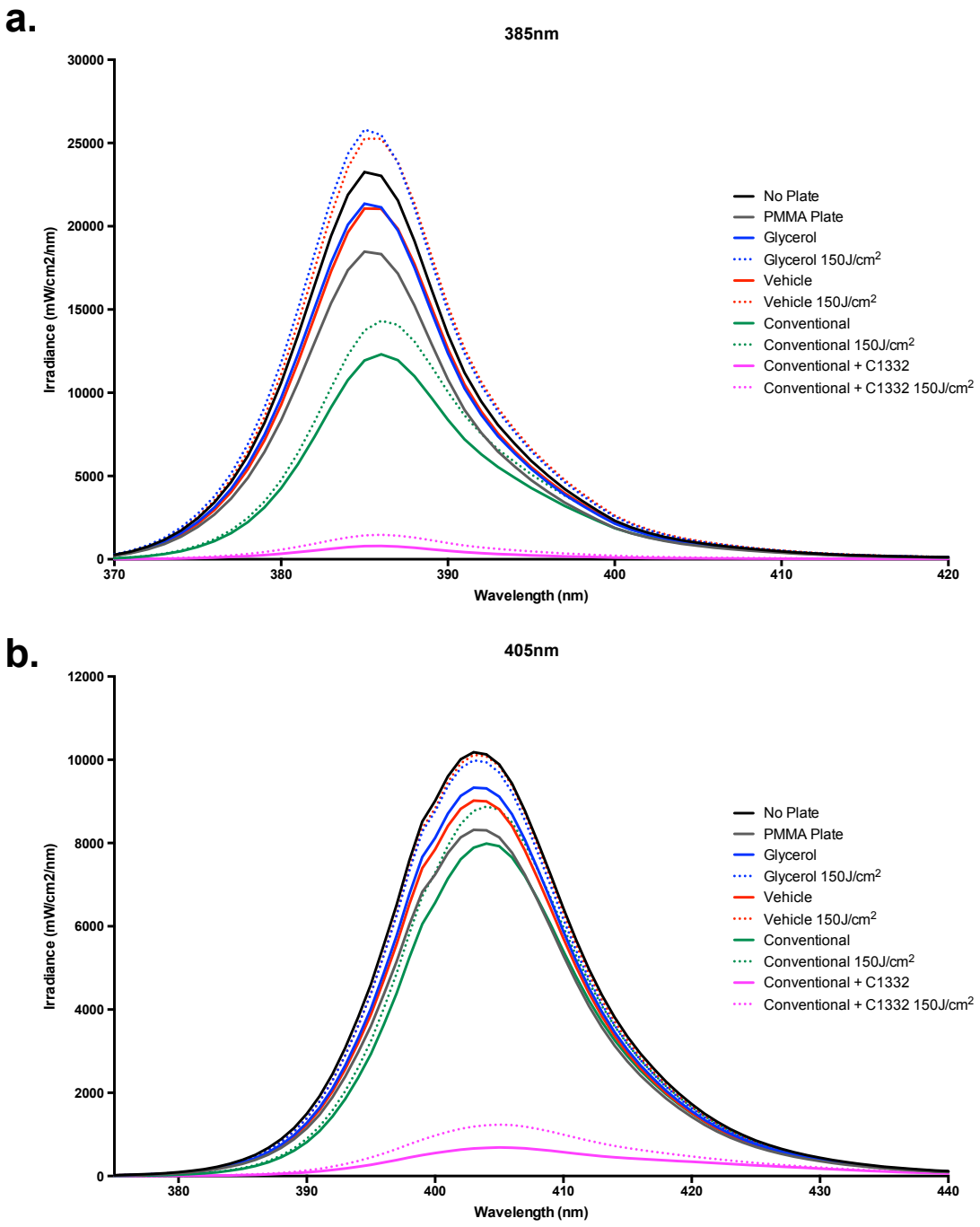

Figure 5.13: Spectral transmission through each formulation and their photodegradation for 385nm and 405nm sources. The sunscreen formulations were applied to PMMA plates and irradiated with (a) 385nm and (b) 405nm sources. The irradiance per nm for each source was measured for (, pre and post an exposure of 150J/cm^2 (mean, n=2).

Condition	Dose (J/cm²)	385nm			405nm		
		Irradiance (mW/m²)	% of Max	% Degradation	Irradiance (mW/m²)	% of Max	% Degradation
No Plate	0	301963.94	100.00		194808.96	100.00	
PMMA Plate	0	240552.14	79.66		157834.74	81.02	
Glycerol	0	276796.97	91.67		175905.88	90.30	
	150	334028.30	110.62	17.13	187455.28	96.23	6.16
Vehicle	0	275128.72	91.11		170328.67	87.43	
	150	329745.05	109.20	16.56	190192.47	97.63	10.44
Conventional	0	166748.19	55.22		149483.40	76.73	
	150	194586.69	64.44	14.31	165434.19	84.92	9.64
Conventional + C1332	0	11417.61	3.78		18389.71	9.44	
	150	20796.37	6.89	45.10	28938.63	14.85	36.45

Table 5.9: The total irradiance, percentage of maximum dose and percentage degradation of each treatment group. The total irradiance after transmittance of each test condition was calculated. From this, the percentage irradiance for each formulation compared to the maximum was calculated, along with the percentage degradation for each formulation. These were calculated for both the 385nm and 405nm sources.

5.2 Discussion

The absorbance/transmission spectra for the two sunscreen formulations used in this chapter were calculated using the BASF sunscreen simulator, and *in vitro* and the results from these methods were compared. The shapes of the spectra of each formulation were largely similar with the two techniques, particularly in the region of interest (375-420nm), with less correlation in the shortwave UVR spectrum, giving confidence in the spectra acquired. BASF's vast experience has shown that they value the results of the sunscreen calculator much more than *in vitro* measurements and, as such, these were used to calculate the protection indices such as SPF and UVA SPF (displayed in, *Materials and Methods*).

The results discussed in chapter 4 clearly demonstrate that wavelengths of radiation at the UV/visible border region (375-415nm) cause significant biological damage to the skin across a range of skin types. This damage is associated with skin cancer and photoageing. Sunscreens are the main way of protecting against UVR-induced damage. Displayed below in Figure 5.14 are the transmission spectra of two conventional sunscreens: one is a typical low SPF 15 sunscreen and one an SPF 50+ sunscreen. Overlaid is the solar spectrum and the 385nm and 405n radiation sources used in this chapter and *Chapter 4*.

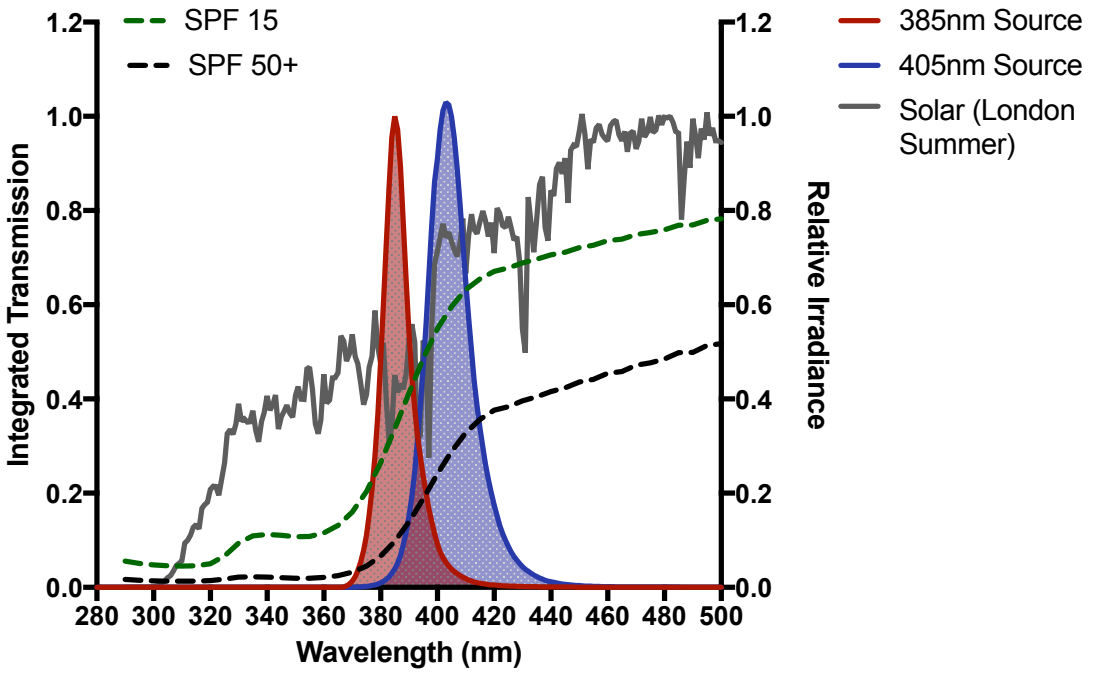

Figure 5.14: The transmission of radiation through conventional low SPF (SPF15) and high SPF (SPF 50+) sunscreens compared to the solar spectrum and the sources used in this study.

Figure 5.14 illustrates two main points: 1) – with increasing wavelength there is increasing solar irradiance and increasing transmission of this radiation through the conventional sunscreens and 2) – at the UVR/visible border region a low SPF sunscreen allows high transmission across the full range and a high SPF sunscreen may provide some protection in the UVR side of the border but there is still significant amounts of radiation allowed to pass through in the visible region. This suggests that current formulations do not provide adequate protection in this region. This is especially important in extreme phenotypes such as patients with the photosensitivity disease erythropoietic protoporphyria (EPP). These patients have a defective enzyme in the haem biosynthetic

pathway, leading to a build up of the intermediate protoporphyrin IX, which is a photosensitizer with peak absorbance in this region (λ_{max}= 406nm). Currently available sunscreens have demonstrated only minimal protection against the symptoms of this disease, with only one formulation known as the Dundee Cream providing any meaningful protection. Dundee Cream however is very thick and unpleasant to use as it takes advantage of the light scattering properties of inorganic filters, and appears visibly on the skin.

The aim of this chapter was to investigate if conventional sunscreens provide adequate protection in the UV/visible region and if the incorporation of a new filter in a formulation of a similar SPF could improve the protection offered.

The compound C1332 is a new UVR/visible radiation organic filter developed by BASF GmbH, Germany, and is currently in the latter stages of the European Commission (EC) and Scientific Committee on Consumer Safety (SCCS) regulatory approval processes. This filter has a peak absorbance in the UVR/visible boundary region (λ_{max}= 394nm) and was developed with the idea of being able to create better formulations to cover the entire UVR spectrum. This would also allow sunscreens to act more like neutral density filters i.e. allowing uniform UVR attenuation across the whole solar UVR spectrum (Diffey, 2016). These formulations were also compared to a vehicle base cream. Endpoints were determined from the results of *Chapter 4*.

The photoprotection offered by the formulations on preventing cell viability reduction was assessed. The Neutral Red assay was chosen from the results in

Chapter 4 after concluding it was a better test of cell viability than the Alamar Blue assay, which appears to measure a reduced reduction potential caused by oxidative stress, rather than viability. For all the formulations tested, with both radiation sources there was a significant decrease in cell viability, with the exception of the conventional + C1332 sunscreen, where there was no significant change compared to the unirradiated control for both sources. This demonstrates complete protection, even at extremely high doses, which also cause some photodegradation. Subsequently the difference between the conventional and conventional + C1332 was compared. For the 405nm source there was significant protection with the new formulation, however with 385nm there was no statically significant difference, although there appears to be some benefit.

The generation of oxidative stress has many serious consequences for skin health. ROS can cause damage to important macromolecules, leading to oxidation of lipid membranes, DNA and proteins. DNA oxidation has been associated with mutations and subsequent onset of cancer. Visible light exposure has recently been linked to protein oxidation (Mizutani *et al.*, 2016) which itself has been linked to impaired DNA repair capacity (McAdam *et al.*, 2016), and oxidative stress is thought to have implications for MMP expression and photoageing (Nishigori *et al.*, 2003). As such, adequate photoprotection against this damage is vital, with the addition of anti-oxidants to sunscreens viewed as one strategy, although the effectiveness of doing so *in vivo* has never been definitively proven. In *Chapter 4* the ability of the UV/visible border region to induce ROS was established. Irradiation of the cells with both 385nm and 405nm wavebands led

to an increase of ROS for all formulations, apart from the conventional + C1332 formulation. When the difference between conventional and conventional + C1332 was tested for both wavelengths there was significant protection acquired by adding C1332. This confirms results previous reports that a conventional broad-spectrum UVA/UVB sunscreen was unable prevent visible light induced ROS production (Liebel *et al.*, 2012).

The induction of delayed CPD by UVA is somewhat of a new phenomenon as CPD had always thought to be formed through direct absorption of DNA, so there are no studies currently investigating the ability of sunscreens to prevent such damage. In the first study that described them however the benefit of applying vitamin E was demonstrated (Premi *et al.*, 2015). The data (Figure 5.4) shows an increase in CPD with no treatment, which is even higher in the vehicle control group, although in none of the cases was the increase statistically significant due to the small samples size and large variation in responses seen in *in vivo* studies on human volunteers. This increased damage in the vehicle control over unprotected site is mainly due to an outlier in the data, but there is a small increase in the vehicle over the unprotected site of two further volunteers. This effect may not be real and within the margin of error or possibly due to a physical effect such as reduced scatter (this is discussed further later in the chapter). The conventional sunscreen provided some protection over the unprotected and vehicle control sites, however the conventional + C1332 formulation provided complete protection, with no detectable CPD present.

Previously, a study by Liebel *et al* demonstrated visible light induced expression of the cytokine IL-1 (linked to inflammation) and protein MMP-1 (linked to photoageing) was not prevented with the use of the sunscreen (Liebel *et al.*, 2012). Here, this is also confirmed to be the case for UV/visible border wavelength induced gene expression. Genes were selected to represent different photobiological responses covering inflammation (IL-1a, IL-6), photoageing (MMP-1) and oxidative stress (HMOX-1), as determined in chapter 4. Results are displayed in Figure 5.5 and described in Table 5.1. The general trend is that there is still significant upregulation of many of the genes with the use of the vehicle formulation, less damage with the conventional sunscreen and no significant increase in gene expression with the sunscreen containing C1332 when compared with unirradiated control. Comparing the conventional sunscreen with the conventional + C1332 formulation there is, in most cases, a significant increase in protection with the latter with both sources. As with the *in vivo* gene expression studies in *Chapter 4*, there was a large interpersonal variation in individual responses in gene expression in the photoprotection studies, resulting if difficulty analysing the results. Overall the general trend is the same as for *in vitro* results, however some genes varied. For this reason it was again decided to pool the responses based on endpoint: inflammation, photoageing and oxidative stress. This analysis provided much clearer results. For inflammation and photoageing genes, the trend again matched the *in vitro* work; the conventional provided some protection against 385nm wavelengths but was at levels similar to those of the vehicle control for 405nm. The formulation containing C1332 provided protection equivalent to the unirradiated control, however there was still a slight significant increase. For photoageing, the C1332 containing

formulation was significantly more protective than the conventional sunscreen. With photoageing this was not significantly different but the fold increase was much less. The results for oxidative damage show a clear relationship. This is most likely due to only measuring two oxidative damages genes and because the relatively low fold increase in these genes with irradiation. It can be concluded that conventional sunscreens do not provide adequate protection against gene expression changes induced by 385nm and 405nm wavelengths, but that this is improved with the addition of C1332.

Finally the ability of these formulations to prevent pigmentation in this region was investigated. This is important, as pigmentation is evidence of oxidation (particularly IPD) and is also particularly of interest to Asian populations for whom it is socially desirable to keep skin light. The pigmentation was measured using three methods: Visual assessment and two reflectance spectroscopy devices designed for this purpose: The Minolta chromameter and the Optimize device. Although there is not absolute agreement between the methods, in general the trends do correlate. The discrepancies however are minimal and are most likely due to how the different methods calculate the skin colour, with many confounding factors such as redness (erythema) and constitutive skin colour. The main difference between the two methods is that the Minolta uses reflectance values between 400-700nm whereas the Optimize device measures reflectance at a specific wavelength of 555nm to minimise the influence of competing chromophores. The new formulation (conventional + C1332) largely shows complete protection at both wavelengths and all doses and time points tested, with no significant increase in pigmentation. The

conventional sunscreen formulation appears to provide some protection but there is still a significant dose dependent increase in pigmentation.

The photodegradation and transmission of each formulation was assessed after irradiation at the highest dose used for each source of 150J/cm^2 which is an extreme test as this is slightly more than could be received from a whole day's exposure at low latitude. The percentage degradation was highest in formulations containing the C1332 filter, however the relative transmission compared to the maximum possible was still significantly lower than any other formulation.

The transmission through each sunscreen was calculated for both radiation sources and displayed in Figure 5.13 and described in Table 5.9. The conventional sunscreen transmitted 55% and 76% of the maximum for 385nm and 405nm sources respectively. The addition of the new filter reduced this for both sources with only 4% and 9% transmitted respectively, clearly demonstrating the benefit of adding this compound. The PMMA plate alone decreased transmission to 80% of maximum (i.e. no obstacle), which shows that the substrate absorbs or scatters radiation. However, transmission was enhanced with both sources to around 90% of the maximum output (no plate) with the vehicle alone and with glycerol. This may be due to a reduction of the scattering effect of the PMMA plate. This possibly has implications for human skin, as PMMA plates are moulded to mimic the texture of skin, suggesting perhaps that the use of skin products that do not contain UVR filters may increase the damage over untreated skin. This is demonstrated clearly in the

pigmentation and delayed CPD data. The use of the vehicle cream with both wavelengths seemed to slightly increase the level of DNA damage and pigmentation induced. For pigmentation, in one case there was no significant increase in pigmentation without the use of any treatments apart from with vehicle. Additionally, on many of the graphs the vehicle treatment appears to have a steeper curve than the untreated site. This phenomenon has been observed the past in mouse models investigating the effect of 8-methoxypsoralen on phototumorigenesis, although some potential causes were suggested, such as a stress response from application of the vehicle, this was not investigated further (Gibbs *et al.*, 1985; Young *et al.*, 1983). Calculated from the transmission values in Table 5.9, this effect could equate to an 11.45% for 385nm and 6.41% for 405nm percentage increase in the dose received. At the highest doses used in this study of 150J/cm^2, that leads to an increase in the dose by 17.18J/cm^2 and 9.62J/cm^2 respectively. This effect was not demonstrated with the *in vitro* studies possibly explained by the different spectral properties of the plate and skin (with the plates having a much harsher roughness). This suggests skin treatments, such as moisturisers, that do not contain any UVR filters may cause more damage to the skin than no treatment.

These findings give evidence to the argument of the 'ideal sunscreen' spectrum. Many argue that formulations should be designed to be UVB weighted, as these are the most energetic and damaging wavelengths, with protection across the rest of the range decreasing with wavelength (Cole, 2016). This concept is generally now disproved with most believing that a sunscreen acting as a neutral density filter is the ideal scenario (Diffey, 2016; Osterwalder and

Herzog, 2010). The results in this chapter support the latter hypothesis, showing the need to sufficiently protect at the shorter wavelengths as well as the UVR/visible boundary.

One criticism of this study could be that a relatively low SPF was chosen for the formulations and that a high SPF formulation may have demonstrated more protection. There is however a large body of evidence to demonstrate that sunscreens are typically used at a much lower application density that required for the labelled SPF of sunscreens (at 2mg/cm^2). Reports vary, but typically the applied amount is 0.75-1.5mg/cm^2, meaning an SPF 50 sunscreen is actually SPF 18-25, and for an SPF15 is as low as 5-7.5 (Petersen *et al.*, 2013). An SPF 15 sunscreen is therefore closer to the real world use than the unrealistic correct application of an SPF 50 sunscreen.

In conclusion, the results clearly demonstrate that currently available formulations do not provide adequate photoprotection against numerous biomarkers of damage to the skin by the UVR/visible boundary region. This suggests new methods of preventing this damage are required. One strategy is the development and addition of new UVR/visible light filters. The new compound C1332 currently under regulatory review is one such filter, which displayed significant protection with its addition at an equivalent SPF.

5.3 Summary of Chapter

- Wavelengths at the UVR-visible border cause a wide range of damage to the skin *in vitro* and *in vivo* as reported in chapter 4.
- This is a region in which there is very little/no protection provided by conventional UVR filters used in sunscreens.
- The ability of such formulations to prevent the damage induced by this region was assessed along with the addition of a new experimental filter called C1332 currently in development from BASF GmbH. Both formulations had an equivalent SPF of 15.
- The photoprotective properties of these formulations were assessed *in vitro* in HaCat keratinocytes and *in vivo* in human volunteers. Endpoints included cell viability, oxidative stress, pigmentation and differential gene expression covering different photobiological outcomes: inflammation/ immunoregulation, photoageing and oxidative stress.
- For almost all end points there was still significant damage to the skin despite the use of a conventional sunscreen formulation. This damage was largely reduced by the formulation containing the new filter, and in most cases was significantly more protective than the conventional formulation.

Overall Conclusions

Solar radiation, mainly UVR, has long been known to induce damage to the skin. The results contained within this thesis expand this knowledge and provide potential ways to improve photoprotection. Summarised below are the main findings from this thesis:

1. **Mycosporine-like amino acids are effective biocompatible UVR filters with anti-oxidant properties**. The results in *Chapter 3* show that one of the known MAA compounds, palythine, is an extremely potent photostable photoprotective agent, acting by filtering UVR and as an antioxidant. This indicates MAAs could potentially by used as an alternative to currently available synthetic UVR filters, potentially addressing the environmental concerns associated with their use.
2. **Wavelengths at the UV/visible border induce significant damage to the skin.** *Chapter 4* clearly demonstrates *in vitro* and *in vivo* that there is significant damage caused by wavelengths of the UV/visible border region. These include DNA damage, reduction of cell viability, upregulation of genes associated with inflammation, photoageing and oxidative stress, inducing ROS and the production of pigmentation.
3. **A new CPD action spectrum is needed which considers delayed CPD formation.** The production of delayed CPDs by both 385nm and 405nm wavelengths *in vivo* (shown in *Chapter 4*) demonstrates the need to produce an updated action spectrum for CPD production which takes into consideration this effect. Current action spectra

demonstrate little/no production in this region, which may be the case immediately after exposure but not in the subsequent hours.

4. **Conventional sunscreen formulations do not effectively prevent UVR/visible border region induced damage.** The main practice employed to prevent solar radiation induced damage to the skin is with the topical application of sunscreens. The results of *Chapter 5* demonstrate that currently available formulations do not provide adequate photoprotection against damage produced by the UV/visible border region.
5. **The addition of a new experimental filter, C1332, to formulations is capable of preventing this damage.** The experimental filter C1332, produced by BASF and currently going through the regulatory process, is effective in reducing the damage caused by the UVR/visible border region over that of currently available filters for all markers of damage tested.
6. **HaCat keratinocytes provide an adequate model for assessing solar radiation induced changes in the skin and their photoprotection.** The models used in this thesis include the use of both cell lines *in vitro* and human volunteers *in vivo*. When comparing the results of both strategies they largely corroborate each other. It was not possible during the course of these studies to translate the work from *Chapter 3* *in vivo*, however the reproducibility between methods in subsequent studies largely justifies these results.

Future Perspectives

In the future, each of the chapter contained in this thesis could be developed in many ways, with many of the results contained here providing the foundations for further work.

Development of Chapter 3: MAA Photoprotection

The MAA palythine was clearly demonstrated to be an effective photostable, UVR filtering and antioxidant compound *in vitro.* There at least 20 known MAAs which are yet to be fully investigated, each with different spectral, antioxidant and Nrf2 activation properties. Mixtures of these compounds could be developed to provide broad-spectrum protection from solar radiation induced damage. There is evidence that some of the MAAs are triplet state quenchers, and their ability to prevent delayed CPDs production is yet to be investigated. Also the evidence that MAAs are activators of the Nrf2 antioxidant pathway has yet to be applied to photoprotection.

Much of the work on MAAs has been focussed *in vitro* assays. Although it has been demonstrated within this thesis that HaCat keratinocytes are a good model for *in vivo* studies, the testing of these compounds *in vivo* is still needed. The marker at which all sunscreens efficacy is tested is by determining the SPF, which can only be determined effectively *in vivo*, and this is needed to compare to other available synthetic sunscreens. There are also other properties that only

in vivo testing will demonstrate such as the skin feel which is an important characteristic consumers consider when purchasing a product.

Development of Chapter 4: UVR/visible border region induced damage

The results contained in Chapter 4 provided many new insights into the damage caused at the UVR/visible border region of the electromagnetic spectrum, with much appearing to be oxidative in nature. The exact mechanisms and chromophores involved in the production of this damage are still not known and were not possible to determine in the timeframe of this studentship. Additionally, there are a number of other markers of damage linked to oxidative stress that came to light during the studentship that would be interesting to investigate. Oxidation of proteins and subsequent inhibition of DNA damage repair capacity was demonstrated for broadband UVA exposure by other groups, and could be expected in this region too (McAdam et al., 2016). Also, the production of oxidative DNA lesions and subsequent mutagenicity of this region would be interesting to investigate. This is something that was attempted, however despite multiple attempts with different protocols, antibody clones, and tissue/cell types was not possible, due to the well known issue of inducing oxidative damage during the processing of samples. Some attempt was made to determine the spectral dependence of the outputs measured, however this could be developed further using narrowband exposure across the entire UVR and visible range so the relative importance of the spectrum could be determined, better informing photoprotection needs and potential chromophores involved.

Development of Chapter 5: Photoprotection of UVR/visible border region induced damage

This chapter demonstrated one successful way in which to prevent damage at the UVR/visible border region. There are however a number of potential other mechanisms of protection that could be investigated. As the damage appears to be mainly oxidative in nature, the use of anti-oxidants and Nrf-2 activators could be investigated. The delayed CPD data suggests the use of triplet state quenchers may also be effective in preventing damage. One class of compounds that encompass all of these properties are the MAAs, so testing their ability to prevent damage in this region would be a logical next step.

References

Adams NL, Shick JM (1996) Mycosporine-like Amino Acids Provide Protection Against Ultraviolet Radiation in Eggs of the Green Sea Urchin Strongylocentrotus droebachiensis. *Photochemistry and photobiology* 64:149-58.

Adams NL, Shick JM (2001) Mycosporine-like amino acids prevent UVB-induced abnormalities during early development of the green sea urchin Strongylocentrotus droebachiensis. *Marine Biology* 138:267-80.

Afaq F, Syed DN, Malik A, *et al.* (2007) Delphinidin, an anthocyanidin in pigmented fruits and vegetables, protects human HaCaT keratinocytes and mouse skin against UVB-mediated oxidative stress and apoptosis. *The Journal of investigative dermatology* 127:222-32.

Ageeva NM, Markosov VA, Muzychenko GF, *et al.* (2015) [Antioxidant and antiradical properties of red grape wines]. *Voprosy pitaniia* 84:63-7.

Agostinis P, Berg K, Cengel KA, *et al.* (2011) Photodynamic therapy of cancer: an update. *CA: a cancer journal for clinicians* 61:250-81.

Agrapidis-Paloympis A, Nash R (1987) The effect of solvents on the ultraviolet absorbance of sunscreens. *J Soc Cosmet Chem* 38:209-21.

Ahmad I, Sheraz MA, Ahmed S, *et al.* (2011) Photostability and interaction of ascorbic acid in cream formulations. *AAPS PharmSciTech* 12:917-23.

Aldahan AS, Shah VV, Mlacker S, *et al.* (2015) The History of Sunscreen. *JAMA dermatology* 151:1316.

Andreguetti D, Stein EM, Pereira CM, *et al.* (2013) Antioxidant properties and UV absorbance pattern of mycosporine-like amino acids analogs synthesized in an environmentally friendly manner. *Journal of biochemical and molecular toxicology* 27:305-12.

Arndt S, Haag SF, Kleemann A, *et al.* (2013) Radical protection in the visible and infrared by a hyperforin-rich cream--in vivo versus ex vivo methods. *Experimental dermatology* 22:354-7.

Asamizu S, Xie P, Brumsted CJ, *et al.* (2012) Evolutionary divergence of sedoheptulose 7-phosphate cyclases leads to several distinct cyclic products. *Journal of the American Chemical Society* 134:12219-29.

Auletta M, Gange RW, Tan OT, *et al.* (1986) Effect of cutaneous hypoxia upon erythema and pigment responses to UVA, UVB, and PUVA (8-MOP + UVA) in human skin. *The Journal of investigative dermatology* 86:649-52.

Autier P (2016) Vitamin D status as a synthetic biomarker of health status. *Endocrine* 51:201-2.

Autier P, Dore JF, Negrier S, *et al.* (1999) Sunscreen use and duration of sun exposure: a double-blind, randomized trial. *Journal of the National Cancer Institute* 91:1304-9.

Bais AF, McKenzie RL, Bernhard G, *et al.* (2015) Ozone depletion and climate change: impacts on UV radiation. *Photochemical & Photobiological Sciences* 14:19-52.

Balmer ME, Buser HR, Muller MD, *et al.* (2005) Occurrence of some organic UV filters in wastewater, in surface waters, and in fish from Swiss Lakes. *Environmental science & technology* 39:953-62.

Balskus EP, Walsh CT (2010) The Genetic and Molecular Basis for Sunscreen Biosynthesis in Cyanobacteria. *Science* 329:1653-6.

Bentham (2014) A GUIDE TO SPECTRORADIOMETRY: Instruments & Applications for the Ultraviolet. <http://www.bentham.co.uk/pdf/UVGuide.pdf> Accessed 03.06.2016 2016.

Berardesca E, Bertona M, Altabas K, *et al.* (2012) Reduced ultraviolet-induced DNA damage and apoptosis in human skin with topical application of a photolyase-containing DNA repair enzyme cream: clues to skin cancer prevention. *Molecular medicine reports* 5:570-4.

Bhatia S, Garg A, Sharma K, *et al.* (2011) Mycosporine and mycosporine-like amino acids: A paramount tool against ultra violet irradiation. *Pharmacogn Rev* 5:138-46.

Bickers DR, Athar M (2006) Oxidative stress in the pathogenesis of skin disease. *The Journal of investigative dermatology* 126:2565-75.

Bissett DL, Chatterjee R, Hannon DP (1991) Chronic ultraviolet radiation-induced increase in skin iron and the photoprotective effect of topically applied iron chelators. *Photochemistry and photobiology* 54:215-23.

Bissett DL, Oelrich DM, Hannon DP (1994) Evaluation of a topical iron chelator in animals and in human beings: short-term photoprotection by 2-furildioxime. *Journal of the American Academy of Dermatology* 31:572-8.

Boyd AS, Naylor M, Cameron GS, *et al.* (1995) The effects of chronic sunscreen use on the histologic changes of dermatoheliosis. *Journal of the American Academy of Dermatology* 33:941-6.

Brash DE (2014) UV Signature Mutations. *Photochemistry and photobiology*.

Brash DE, Rudolph JA, Simon JA*, et al.* (1991) A role for sunlight in skin cancer: UV-induced p53 mutations in squamous cell carcinoma. *Proceedings of the National Academy of Sciences of the United States of America* 88:10124-8.

Brenner M, Hearing VJ (2008) The Protective Role of Melanin Against UV Damage in Human Skin. *Photochemistry and photobiology* 84:539-49.

Bruls WA, Slaper H, van der Leun JC*, et al.* (1984) Transmission of human epidermis and stratum corneum as a function of thickness in the ultraviolet and visible wavelengths. *Photochemistry and photobiology* 40:485-94.

Burnett ME, Wang SQ (2011) Current sunscreen controversies: a critical review. *Photodermatology, photoimmunology & photomedicine* 27:58-67.

Cardozo KH, Guaratini T, Barros MP*, et al.* (2007) Metabolites from algae with economical impact. *Comparative biochemistry and physiology Toxicology & pharmacology : CBP* 146:60-78.

Carducci M, Pavone PS, De Marco G*, et al.* (2015) Comparative Effects of Sunscreens Alone vs Sunscreens Plus DNA Repair Enzymes in Patients With Actinic Keratosis: Clinical and Molecular Findings from a 6-Month, Randomized, Clinical Study. *Journal of drugs in dermatology : JDD* 14:986-90.

Chalker BE, Dunlap WC, Oliver JK (1983) Bathymetric adaptations of reef-building corals at davies reef, great barrier reef, Australia. II. Light saturation curves for photosynthesis and respiration. *Journal of Experimental Marine Biology and Ecology* 73:37-56.

Chiarelli-Neto O, Ferreira AS, Martins WK*, et al.* (2014) Melanin photosensitization and the effect of visible light on epithelial cells. *PloS one* 9:e113266.

Chisvert A, Leon-Gonzalez Z, Tarazona I*, et al.* (2012) An overview of the analytical methods for the determination of organic ultraviolet filters in biological fluids and tissues. *Analytica chimica acta* 752:11-29.

Cho S Fau - Lee MJ, Lee Mj Fau - Kim MS, Kim Ms Fau - Lee S*, et al.* Infrared plus visible light and heat from natural sunlight participate in the expression of MMPs and type I procollagen as well as infiltration of inflammatory cell in human skin in vivo.

Choi Y-H, Yang D, Kulkarni A*, et al.* (2015) Mycosporine-Like Amino Acids Promote Wound Healing through Focal Adhesion Kinase (FAK) and Mitogen-Activated Protein Kinases (MAP Kinases) Signaling Pathway in Keratinocytes. *Marine drugs* 13:7056.

Chow HH, Cai Y, Hakim IA*, et al.* (2003) Pharmacokinetics and safety of green tea polyphenols after multiple-dose administration of epigallocatechin gallate and

polyphenon E in healthy individuals. *Clinical cancer research : an official journal of the American Association for Cancer Research* 9:3312-9.

Cleaver JE (1968) Defective repair replication of DNA in xeroderma pigmentosum. *Nature* 218:652-6.

Cleaver JE (2005) Cancer in xeroderma pigmentosum and related disorders of DNA repair. *Nat Rev Cancer* 5:564-73.

Cleaver JE, Lam ET, Revet I (2009) Disorders of nucleotide excision repair: the genetic and molecular basis of heterogeneity. *Nature reviews Genetics* 10:756-68.

Cole C (2016) Sunscreen formulation: optimizing efficacy of UVB and UVA protection. In: *Principles and Practice of Photoprotection* (Wang S, Lim HW, eds): Springer International Publishing, 275-87.

Cole C, Shyr T, Ou-Yang H (2015) Metal Oxide Sunscreens Protect Skin by Absorption, Not by Reflection or Scattering. *Photodermatology, photoimmunology & photomedicine*.

Conde FR, Churio MS, Previtali CM (2000) The photoprotector mechanism of mycosporine-like amino acids. Excited-state properties and photostability of porphyra-334 in aqueous solution. *Journal of photochemistry and photobiology B, Biology* 56:139-44.

Conde FR, Churio MS, Previtali CM (2004) The deactivation pathways of the excited-states of the mycosporine-like amino acids shinorine and porphyra-334 in aqueous solution. *Photochemical & photobiological sciences : Official journal of the European Photochemistry Association and the European Society for Photobiology* 3:960-7.

Conde FR, Churio MS, Previtali CM (2007) Experimental study of the excited-state properties and photostability of the mycosporine-like amino acid palythine in aqueous solution. *Photochemical & photobiological sciences : Official journal of the European Photochemistry Association and the European Society for Photobiology* 6:669-74.

Cooke MS, Evans MD, Dizdaroglu M*, et al.* (2003) Oxidative DNA damage: mechanisms, mutation, and disease. *FASEB journal : official publication of the Federation of American Societies for Experimental Biology* 17:1195-214.

Correa Mde P (2015) Solar ultraviolet radiation: properties, characteristics and amounts observed in Brazil and South America. *Anais brasileiros de dermatologia* 90:297-313.

Courdavault S, Baudouin C, Charveron M*, et al.* (2004) Larger yield of cyclobutane dimers than 8-oxo-7,8-dihydroguanine in the DNA of UVA-irradiated human skin cells. *Mutation research* 556:135-42.

D'Agostino PM, Javalkote VS, Mazmouz R*, et al.* (2016) Comparative profiling and discovery of novel glycosylated mycosporine-like amino acids in two strains of the cyanobacterium Scytonema cf. crispum. *Applied and environmental microbiology*.

Dale Wilson B, Moon S, Armstrong F (2012) Comprehensive Review of Ultraviolet Radiation and the Current Status on Sunscreens. *The Journal of clinical and aesthetic dermatology* 5:18-23.

Danovaro R, Bongiorni L, Corinaldesi C*, et al.* (2008) Sunscreens cause coral bleaching by promoting viral infections. *Environmental health perspectives* 116:441-17.

de Groot AC, Roberts DW (2014) Contact and photocontact allergy to octocrylene: a review. *Contact dermatitis* 70:193-204.

de la Coba F, Aguilera J, de Galvez MV*, et al.* (2009a) Prevention of the ultraviolet effects on clinical and histopathological changes, as well as the heat shock protein-70 expression in mouse skin by topical application of algal UV-absorbing compounds. *Journal of dermatological science* 55:161-9.

de la Coba F, Aguilera J, Figueroa FL*, et al.* (2009b) Antioxidant activity of mycosporine-like amino acids isolated from three red macroalgae and one marine lichen. *J Appl Phycol* 21:161-9.

Deleo V (2006) Sunscreen use in photodermatoses. *Dermatologic clinics* 24:27-33.

Denda M, Fuziwara S (2007) Visible Radiation Affects Epidermal Permeability Barrier Recovery: Selective Effects of Red and Blue Light. *The Journal of investigative dermatology* 128:1335-6.

Dennis LK, Beane Freeman LE, VanBeek MJ (2003) Sunscreen use and the risk for melanoma: a quantitative review. *Annals of internal medicine* 139:966-78.

Desotelle JA, Wilking MJ, Ahmad N (2012) The circadian control of skin and cutaneous photodamage. *Photochemistry and photobiology* 88:1037-47.

Diffey B (1982) *Ultraviolet Radiation In Medicine*. Adam Hilger Ltd, 163.

Diffey B (2015) Solar spectral irradiance and summary outputs using excel. *Photochemistry and photobiology* 91:553-7.

Diffey BL (2001) Chapter 27 Sunscreens: use and misuse. In: *Comprehensive Series in Photosciences* (Paolo UG, ed) Vol. Volume 3: Elsevier, 521-34.

Diffey BL (2016) Optimizing the spectral absorption profile of sunscreens. *International journal of cosmetic science*.

Diffey BL, Jansen CT, Urbach F*, et al.* (1997) The standard erythema dose: a new photobiological concept. *Photodermatology, photoimmunology & photomedicine* 13:64-6.

Dong KK, Damaghi N, Picart SD*, et al.* (2008) UV-induced DNA damage initiates release of MMP-1 in human skin. *Experimental dermatology* 17:1037-44.

Downs CA, Kramarsky-Winter E, Fauth JE*, et al.* (2014) Toxicological effects of the sunscreen UV filter, benzophenone-2, on planulae and in vitro cells of the coral, Stylophora pistillata. *Ecotoxicology (London, England)* 23:175-91.

Drobetsky EA, Grosovsky AJ, Glickman BW (1987) The specificity of UV-induced mutations at an endogenous locus in mammalian cells. *Proceedings of the National Academy of Sciences of the United States of America* 84:9103-7.

Dufour EK, Kumaravel T, Nohynek GJ*, et al.* (2006) Clastogenicity, photo-clastogenicity or pseudo-photo-clastogenicity: Genotoxic effects of zinc oxide in the dark, in pre-irradiated or simultaneously irradiated Chinese hamster ovary cells. *Mutation research* 607:215-24.

Dunlap WC, Chalker BE, Oliver JK (1986) Bathymetric adaptations of reef-building corals at Davies Reef, Great Barrier Reef, Australia. III. UV-B absorbing compounds. *Journal of Experimental Marine Biology and Ecology* 104:239-48.

Dunlap WC, Shick JM (1998) Ultraviolet radiation-absorbing mycosporine-like amino acids in coral reef oragnisms: a biochemical and environmental perspective. *Journal of Phycology* 34:418-30.

Duteil L, Cardot-Leccia N, Queille-Roussel C*, et al.* (2014) Differences in visible light induced-pigmentation according to wavelengths: a clinical and histological study in comparison with UVB exposure. *Pigment cell & melanoma research*.

Elmets CA, Singh D, Tubesing K*, et al.* (2001) Cutaneous photoprotection from ultraviolet injury by green tea polyphenols. *Journal of the American Academy of Dermatology* 44:425-32.

Emanuele E, Spencer JM, Braun M (2014) An experimental double-blind irradiation study of a novel topical product (TPF 50) compared to other topical products with DNA repair enzymes, antioxidants, and growth factors with sunscreens: implications for preventing skin aging and cancer. *Journal of drugs in dermatology : JDD* 13:309-14.

Faurschou A, Wulf HC (2008) Synergistic effect of broad-spectrum sunscreens and antihistamines in the control of idiopathic solar urticaria. *Archives of dermatology* 144:765-9.

Favre-Bonvin J, Bernillon J, Salin N*, et al.* (1987) Biosynthesis of mycosporines: Mycosporine glutaminol in Trichothecium roseum. *Phytochemistry* 26:2509-14.

Fedorow H, Tribl F, Halliday G, *et al.* (2005) Neuromelanin in human dopamine neurons: comparison with peripheral melanins and relevance to Parkinson's disease. *Progress in neurobiology* 75:109-24.

Feng YN, Zhang ZC, Feng JL, *et al.* (2012) Effects of UV-B radiation and periodic desiccation on the morphogenesis of the edible terrestrial cyanobacterium Nostoc flagelliforme. *Applied and environmental microbiology* 78:7075-81.

Fent K, Kunz PY, Gomez E (2008) UV filters in the aquatic environment induce hormonal effects and affect fertility and reproduction in fish. *Chimia* 62:368 - 75.

Fent K, Zenker A, Rapp M (2010) Widespread occurrence of estrogenic UV-filters in aquatic ecosystems in Switzerland. *Environmental pollution (Barking, Essex : 1987)* 158:1817-24.

Fernandes SCM, Alonso-Varona A, Palomares T, *et al.* (2015) Exploiting Mycosporines as Natural Molecular Sunscreens for the Fabrication of UV-Absorbing Green Materials. *ACS applied materials & interfaces* 7:16558-64.

Fernandez-Garcia E (2014) Skin protection against UV light by dietary antioxidants. *Food & function* 5:1994-2003.

Ferreyra GA, Mostajir B, Schloss IR, *et al.* (2006) Ultraviolet-B radiation effects on the structure and function of lower trophic levels of the marine planktonic food web. *Photochemistry and photobiology* 82:887-97.

Fisher GJ, Datta SC, Talwar HS, *et al.* (1996) Molecular basis of sun-induced premature skin ageing and retinoid antagonism. *Nature* 379:335-9.

Fitzpatrick TB (1988) The validity and practicality of sun-reactive skin types I through VI. *Archives of dermatology* 124:869-71.

Foley P, Nixon R, Marks R, *et al.* (1993) The frequency of reactions to sunscreens: results of a longitudinal population-based study on the regular use of sunscreens in Australia. *The British journal of dermatology* 128:512-8.

Freitas JV, Gaspar LR (2016) In vitro photosafety and efficacy screening of apigenin, chrysin and beta-carotene for UVA and VIS protection. *European journal of pharmaceutical sciences : official journal of the European Federation for Pharmaceutical Sciences* 89:146-53.

Fuchs J, Kern H (1998) Modulation of UV-light-induced skin inflammation by d-alpha-tocopherol and l-ascorbic acid: a clinical study using solar simulated radiation. *Free Radical Biology and Medicine* 25:1006-12.

Gacesa R, Dunlap WC, Long PF (2015) Bioinformatics analyses provide insight into distant homology of the Keap1-Nrf2 pathway. *Free radical biology & medicine* 88:373-80.

Gaddameedhi S, Selby CP, Kemp MG, *et al.* (2014) The Circadian Clock Controls Sunburn Apoptosis and Erythema in Mouse Skin. *The Journal of investigative dermatology*.

Gago-Ferrero P, Alonso MB, Bertozzi CP, *et al.* (2013a) First Determination of UV Filters in Marine Mammals. Octocrylene Levels in Franciscana Dolphins. *Environmental science & technology* 47:5619-25.

Gago-Ferrero P, Alonso MB, Bertozzi CP, *et al.* (2013b) First determination of UV filters in marine mammals. Octocrylene levels in Franciscana dolphins. *Environmental science & technology* 47:5619-25.

Gambichler T, Boms S, Stucker M, *et al.* (2005) Acute skin alterations following ultraviolet radiation investigated by optical coherence tomography and histology. *Archives of dermatological research* 297:218-25.

Gao Q, Garcia-Pichel F (2011) An ATP-grasp ligase involved in the last biosynthetic step of the iminomycosporine shinorine in Nostoc punctiforme ATCC 29133. *Journal of bacteriology* 193:5923-8.

Garcia-Pichel F, Castenholz RW (1993) Occurrence of UV-Absorbing, Mycosporine-Like Compounds among Cyanobacterial Isolates and an Estimate of Their Screening Capacity. *Applied and environmental microbiology* 59:163-9.

Ghiasvand R, Weiderpass E, Green AC, *et al.* (2016) Sunscreen Use and Subsequent Melanoma Risk: A Population-Based Cohort Study. *Journal of clinical oncology : official journal of the American Society of Clinical Oncology*.

Gibbs NK, Young AR, Magnus IA (1985) Failure of UVR dose reciprocity for skin tumorigenesis in hairless mice treated with 8-methoxypsoralen. *Photochemistry and photobiology* 42:39-42.

Gjersvik PJ (2001) [Etiology of non-melanoma skin cancer]. *Tidsskrift for den Norske laegeforening : tidsskrift for praktisk medicin, ny raekke* 121:2052-6.

Gniadecka M, Wulf HC, Mortensen NN, *et al.* (1996) Photoprotection in vitiligo and normal skin. A quantitative assessment of the role of stratum corneum, viable epidermis and pigmentation. *Acta dermato-venereologica* 76:429-32.

Goralczyk R, Wertz K (2009) Skin Photoprotection by Carotenoids. In: *Carotenoids: Volume 5: Nutrition and Health* (Britton G, Pfander H, Liaaen-Jensen S, eds), Basel: Birkhäuser Basel, 335-62.

Goyal RK (2015) Voriconazole-associated phototoxic dermatoses and skin cancer. *Expert review of anti-infective therapy* 13:1537-46.

Grampurohit VU, Dinesh US, Rao R (2011) Multiple cutaneous malignancies in a patient of xeroderma pigmentosum. *Journal of cancer research and therapeutics* 7:205-7.

Grant WB, Strange RC, Garland CF (2003) Sunshine is good medicine. The health benefits of ultraviolet-B induced vitamin D production. *Journal of cosmetic dermatology* 2:86-98.

Green A, Williams G, Neale R*, et al.* (1999) Daily sunscreen application and betacarotene supplementation in prevention of basal-cell and squamous-cell carcinomas of the skin: a randomised controlled trial. *Lancet* 354:723-9.

Green AC, Williams GM (2007) Point: sunscreen use is a safe and effective approach to skin cancer prevention. *Cancer epidemiology, biomarkers & prevention : a publication of the American Association for Cancer Research, cosponsored by the American Society of Preventive Oncology* 16:1921-2.

Green AC, Williams GM, Logan V*, et al.* (2011) Reduced melanoma after regular sunscreen use: randomized trial follow-up. *Journal of clinical oncology : official journal of the American Society of Clinical Oncology* 29:257-63.

Greul AK, Grundmann JU, Heinrich F*, et al.* (2002) Photoprotection of UV-irradiated human skin: an antioxidative combination of vitamins E and C, carotenoids, selenium and proanthocyanidins. *Skin pharmacology and applied skin physiology* 15:307-15.

Gueranger Q, Li F, Peacock M*, et al.* (2014) Protein oxidation and DNA repair inhibition by 6-thioguanine and UVA radiation. *The Journal of investigative dermatology* 134:1408-17.

Ha S-Y, Lee Y, Kim M-S*, et al.* (2015) Seasonal Changes in Mycosporine-Like Amino Acid Production Rate with Respect to Natural Phytoplankton Species Composition. *Marine drugs* 13:6740.

Hadgraft J, Lane ME (2016) Advanced topical formulations (ATF). *International Journal of Pharmaceutics* 514:52-7.

Haldar C, Ahmad R (2010) Photoimmunomodulation and melatonin. *Journal of photochemistry and photobiology B, Biology* 98:107-17.

Halliday GM, Rana S (2008) Waveband and dose dependency of sunlight-induced immunomodulation and cellular changes. *Photochemistry and photobiology* 84:35-46.

Harris SL, Levine AJ (2005) The p53 pathway: positive and negative feedback loops. *Oncogene* 24:2899-908.

Harrison GI, Young AR (2002) Ultraviolet radiation-induced erythema in human skin. *Methods (San Diego, Calif)* 28:14-9.

Hartmann A, Gostner J, Fuchs JE*, et al.* (2015a) Inhibition of Collagenase by Mycosporine-like Amino Acids from Marine Sources. *Planta medica*.

Hartmann A, Holzinger A, Ganzera M*, et al.* (2015b) Prasiolin, a new UV-sunscreen compound in the terrestrial green macroalga Prasiola calophylla (Carmichael ex Greville) Kutzing (Trebouxiophyceae, Chlorophyta). *Planta*.

Hayden CG, Roberts MS, Benson HA (1997) Systemic absorption of sunscreen after topical application. *Lancet* 350:863-4.

Haylett AK, Nie Z, Brownrigg M*, et al.* (2011) Systemic photoprotection in solar urticaria with alpha-melanocyte-stimulating hormone analogue [Nle4-D-Phe7]-alpha-MSH. *The British journal of dermatology* 164:407-14.

Heinrich U, Neukam K, Tronnier H*, et al.* (2006) Long-term ingestion of high flavanol cocoa provides photoprotection against UV-induced erythema and improves skin condition in women. *The Journal of nutrition* 136:1565-9.

Herzog B (2012) Photoprotection of human skin. In: *Photochemistry: Volume 40* (Vol. 40: The Royal Society of Chemistry, 245-73.

Herzog B, Osterwalder U (2015) Simulation of sunscreen performance. In: *Pure and Applied Chemistry* (937.

Heurung AR, Raju SI, Warshaw EM (2014) Adverse reactions to sunscreen agents: epidemiology, responsible irritants and allergens, clinical characteristics, and management. *Dermatitis : contact, atopic, occupational, drug* 25:289-326.

Hewison M (2011) Vitamin D and innate and adaptive immunity. *Vitam Horm* 86:23-62.

Honigsmann H (2003) Mechanisms of phototherapy and photochemotherapy for photodermatoses. *Dermatologic therapy* 16:23-7.

Honigsmann H, Schuler G, Aberer W*, et al.* (1986) Immediate pigment darkening phenomenon. A reevaluation of its mechanisms. *The Journal of investigative dermatology* 87:648-52.

Huang XX, Scolyer RA, Abubakar A*, et al.* (2012) Human 8-oxoguanine-DNA glycosylase-1 is downregulated in human basal cell carcinoma. *Molecular genetics and metabolism* 106:127-30.

Hughes MC, Williams GM, Baker P*, et al.* (2013) Sunscreen and prevention of skin aging: a randomized trial. *Annals of internal medicine* 158:781-90.

Iannacone MR, Hughes MC, Green AC (2014) Effects of sunscreen on skin cancer and photoaging. *Photodermatology, photoimmunology & photomedicine* 30:55-61.

Ichihashi M, Ueda M, Budiyanto A*, et al.* (2003) UV-induced skin damage. *Toxicology* 189:21-39.

Janjua NR, Mogensen B, Andersson AM, *et al.* (2004) Systemic absorption of the sunscreens benzophenone-3, octyl-methoxycinnamate, and 3-(4-methyl-benzylidene) camphor after whole-body topical application and reproductive hormone levels in humans. *The Journal of investigative dermatology* 123:57-61.

Jansen JG, Tsaalbi-Shtylik A, Hendriks G, *et al.* (2009) Mammalian polymerase zeta is essential for post-replication repair of UV-induced DNA lesions. *DNA repair* 8:1444-51.

Kang JS, Kim HN, Jung da J, *et al.* (2007) Regulation of UVB-induced IL-8 and MCP-1 production in skin keratinocytes by increasing vitamin C uptake via the redistribution of SVCT-1 from the cytosol to the membrane. *The Journal of investigative dermatology* 127:698-706.

Karlsson I, Vanden Broecke K, Martensson J, *et al.* (2011) Clinical and experimental studies of octocrylene's allergenic potency. *Contact dermatitis* 64:343-52.

Katoch M, Mazmouz R, Chau R, *et al.* (2016) Heterologous production of cyanobacterial mycosporine-like amino acids mycosporine-ornithine and mycosporine-lysine in E. coli. *Applied and environmental microbiology*.

Kielbassa C, Epe B (2000) DNA damage induced by ultraviolet and visible light and its wavelength dependence. *Methods in enzymology* 319:436-45.

Kielbassa C, Roza L, Epe B (1997) Wavelength dependence of oxidative DNA damage induced by UV and visible light. *Carcinogenesis* 18:811-6.

Kim HJ, Son ED, Jung JY, *et al.* (2013) Violet light down-regulates the expression of specific differentiation markers through Rhodopsin in normal human epidermal keratinocytes. *PloS one* 8:e73678.

Kim MS, Kim YK, Cho KH, *et al.* (2006) Regulation of type I procollagen and MMP-1 expression after single or repeated exposure to infrared radiation in human skin. *Mech Ageing Dev* 127:875-82.

Kim S, Seock Y-K (2009) Impacts of health and environmental consciousness on young female consumers' attitude towards and purchase of natural beauty products. *International Journal of Consumer Studies* 33:627-38.

Kim S, You DH, Han T, *et al.* (2014) Modulation of viability and apoptosis of UVB-exposed human keratinocyte HaCaT cells by aqueous methanol extract of laver (Porphyra yezoensis). *Journal of photochemistry and photobiology B, Biology* 141:301-7.

Kimeswenger S, Schwarz A, Fodinger D, *et al.* (2016) Infrared A radiation promotes survival of human melanocytes carrying ultraviolet radiation-induced DNA damage. *Experimental dermatology* 25:447-52.

Kitazawa M, Iwasaki K, Sakamoto K (2006) Iron chelators may help prevent photoaging. *Journal of cosmetic dermatology* 5:210-7.

Kleinpenning MM, Smits T, Frunt MH*, et al.* (2010) Clinical and histological effects of blue light on normal skin. *Photodermatology, photoimmunology & photomedicine* 26:16-21.

Kockott D, Herzog B, Reichrath J*, et al.* (2016) New Approach to Develop Optimized Sunscreens that Enable Cutaneous Vitamin D Formation with Minimal Erythema Risk. *PloS one* 11:e0145509.

Kogej T, Gostinčar C, Volkmann M*, et al.* (2006) Mycosporines in Extremophilic Fungi—Novel Complementary Osmolytes? *Environmental Chemistry* 3:105-10.

Kozmin S, Slezak G, Reynaud-Angelin A*, et al.* (2005) UVA radiation is highly mutagenic in cells that are unable to repair 7,8-dihydro-8-oxoguanine in Saccharomyces cerevisiae. *Proceedings of the National Academy of Sciences of the United States of America* 102:13538-43.

Kripke ML (1974) Antigenicity of Murine Skin Tumors Induced by Ultraviolet Light. *Journal of the National Cancer Institute* 53:1333-6.

Kuluncsics Z, Perdiz D, Brulay E*, et al.* (1999) Wavelength dependence of ultraviolet-induced DNA damage distribution: Involvement of direct or indirect mechanisms and possible artefacts. *Journal of Photochemistry and Photobiology B: Biology* 49:71-80.

Kunisada M, Sakumi K, Tominaga Y*, et al.* (2005) 8-Oxoguanine formation induced by chronic UVB exposure makes Ogg1 knockout mice susceptible to skin carcinogenesis. *Cancer research* 65:6006-10.

Kunz PY, Fent K (2006a) Estrogenic activity of UV filter mixtures. *Toxicology and applied pharmacology* 217:86-99.

Kunz PY, Fent K (2006b) Multiple hormonal activities of UV filters and comparison of in vivo and in vitro estrogenic activity of ethyl-4-aminobenzoate in fish. *Aquatic toxicology (Amsterdam, Netherlands)* 79:305-24.

Kunz PY, Fent K (2009) Estrogenic activity of ternary UV filter mixtures in fish (Pimephales promelas) - an analysis with nonlinear isobolograms. *Toxicology and applied pharmacology* 234:77-88.

Kunz PY, Gries T, Fent K (2006) The ultraviolet filter 3-benzylidene camphor adversely affects reproduction in fathead minnow (Pimephales promelas). *Toxicological sciences : an official journal of the Society of Toxicology* 93:311-21.

Kurlansik SL, Ibay AD (2012) Seasonal affective disorder. *Am Fam Physician* 86:1037-41.

Kushibiki T, Hirasawa T, Okawa S*, et al.* (2013) Blue laser irradiation generates intracellular reactive oxygen species in various types of cells. *Photomedicine and laser surgery* 31:95-104.

Kvam E, Tyrrell RM (1997) Induction of oxidative DNA base damage in human skin cells by UV and near visible radiation. *Carcinogenesis* 18:2379-84.

Landsberg JH (2002) The Effects of Harmful Algal Blooms on Aquatic Organisms. *Reviews in Fisheries Science* 10:113-390.

Lautenschlager S, Wulf HC, Pittelkow MR (2007) Photoprotection. *Lancet* 370:528-37.

Lavker RM, Kaidbey KH (1982) Redistribution of melanosomal complexes within keratinocytes following UV-A irradiation: a possible mechanism for cutaneous darkening in man. *Archives of dermatological research* 272:215-28.

Lea CS, Scotto JA, Buffler PA*, et al.* (2007) Ambient UVB and melanoma risk in the United States: a case-control analysis. *Annals of epidemiology* 17:447-53.

Leach CM (1965) Ultraviolet-absorbing substances associated with light-induced sporulation in fungi. *Canadian Journal of Botany* 43:185-200.

Lecha M, Puy H, Deybach JC (2009) Erythropoietic protoporphyria. *Orphanet J Rare Dis* 4:19.

Lee A, Garbutcheon-Singh KB, Dixit S*, et al.* (2015) The influence of age and gender in knowledge, behaviors and attitudes towards sun protection: a cross-sectional survey of Australian outpatient clinic attendees. *American journal of clinical dermatology* 16:47-54.

Leiter U, Garbe C (2008) Epidemiology of melanoma and nonmelanoma skin cancer--the role of sunlight. *Advances in experimental medicine and biology* 624:89-103.

Lenane P, Murphy GM (2001) Sunscreens and the photodermatoses. *The Journal of dermatological treatment* 12:53-7.

Liebel F, Kaur S, Ruvolo E*, et al.* (2012) Irradiation of skin with visible light induces reactive oxygen species and matrix-degrading enzymes. *The Journal of investigative dermatology* 132:1901-7.

Liebmann J, Born M, Kolb-Bachofen V (2010) Blue-light irradiation regulates proliferation and differentiation in human skin cells. *The Journal of investigative dermatology* 130:259-69.

Llewellyn CA, Airs RL (2010) Distribution and Abundance of MAAs in 33 Species of Microalgae across 13 Classes. *Marine drugs* 8:1273-91.

Lomnitski L, Grossman S, Bergman M*, et al.* (1997) In vitro and in vivo effects of beta-carotene on rat epidermal lipoxygenases. *International journal for vitamin and nutrition research Internationale Zeitschrift fur Vitamin- und Ernahrungsforschung Journal international de vitaminologie et de nutrition* 67:407-14.

Lowe N, Shaath N, Pathak M (1997) *Sunscreen: Development, Evaluation and Regulatory Aspects*, vol. 15. Marcel Dekker Inc.

Luger TA, Kock A, Danner M (1985) Characterization of immunoregulatory cytokines produced by epidermal cells. *Scandinavian journal of immunology* 21:455-62.

Lugovic Mihic L, Bulat V, Situm M*, et al.* (2008) Allergic hypersensitivity skin reactions following sun exposure. *Collegium antropologicum* 32 Suppl 2:153-7.

M. Bandaranayake W (1998) Mycosporines: are they nature's sunscreens? *Natural Product Reports* 15:159-72.

MacCormack MA (2008) Photodynamic therapy in dermatology: an update on applications and outcomes. *Seminars in cutaneous medicine and surgery* 27:52-62.

Maeda K, Hatao M (2004) Involvement of photooxidation of melanogenic precursors in prolonged pigmentation induced by ultraviolet A. *The Journal of investigative dermatology* 122:503-9.

Mahmoud Bh Fau - Ruvolo E, Ruvolo E Fau - Hexsel CL, Hexsel Cl Fau - Liu Y*, et al.* (2010) Impact of long-wavelength UVA and visible light on melanocompetent skin.

Maier H, Schauberger G, Brunnhofer K*, et al.* (2001) Change of ultraviolet absorbance of sunscreens by exposure to solar-simulated radiation. *The Journal of investigative dermatology* 117:256-62.

Marionnet C, Pierrard C, Golebiewski C*, et al.* (2014) Diversity of Biological Effects Induced by Longwave UVA Rays (UVA1) in Reconstructed Skin. *PloS one* 9:e105263.

Marks R, Foley PA, Jolley D*, et al.* (1995) The effect of regular sunscreen use on vitamin D levels in an Australian population. Results of a randomized controlled trial. *Archives of dermatology* 131:415-21.

Martino TA, Oudit GY, Herzenberg AM*, et al.* (2008) Circadian rhythm disorganization produces profound cardiovascular and renal disease in hamsters. *Am J Physiol Regul Integr Comp Physiol* 294:R1675-83.

Mason DS, Schafer F, Shick JM*, et al.* (1998) Ultraviolet radiation-absorbing mycosporine-like amino acids (MAAs) are acquired from their diet by medaka

fish (Oryzias latipes) but not by SKH-1 hairless mice. *Comp Biochem Physiol A Mol Integr Physiol* 120:587-98.

Matsui K, Nazifi E, Hirai Y, *et al.* (2012) The cyanobacterial UV-absorbing pigment scytonemin displays radical-scavenging activity. *The Journal of general and applied microbiology* 58:137-44.

Matsumura Y, Ananthaswamy HN (2002) Short-term and long-term cellular and molecular events following UV irradiation of skin: implications for molecular medicine. *Expert Rev Mol Med* 4:1-22.

Matsuoka LY, Ide L, Wortsman J, *et al.* (1987) Sunscreens suppress cutaneous vitamin D3 synthesis. *The Journal of clinical endocrinology and metabolism* 64:1165-8.

Matsuoka LY, Wortsman J, Hanifan N, *et al.* (1988) Chronic sunscreen use decreases circulating concentrations of 25-hydroxyvitamin D. A preliminary study. *Archives of dermatology* 124:1802-4.

McAdam E, Brem R, Karran P (2016) Oxidative stress-induced protein damage inhibits DNA repair and determines mutation risk and therapeutic efficacy. *Molecular cancer research : MCR*.

McKenzie RL, Aucamp PJ, Bais AF, *et al.* (2007) Changes in biologically-active ultraviolet radiation reaching the Earth's surface. *Photochemical & photobiological sciences : Official journal of the European Photochemistry Association and the European Society for Photobiology* 6:218-31.

McMicken B, Thomas RJ, Brancaleon L (2014) Photoinduced partial unfolding of tubulin bound to meso-tetrakis(sulfonatophenyl) porphyrin leads to inhibition of microtubule formation in vitro. *Journal of biophotonics* 7:874-88.

McMillan DC, Talwar D, Sattar N, *et al.* (2002) The relationship between reduced vitamin antioxidant concentrations and the systemic inflammatory response in patients with common solid tumours. *Clinical nutrition (Edinburgh, Scotland)* 21:161-4.

Misonou T, Saitoh J, Oshiba S, *et al.* (2003) UV-absorbing substance in the red alga Porphyra yezoensis (Bangiales, Rhodophyta) block thymine photodimer production. *Marine biotechnology (New York, NY)* 5:194-200.

Mitchell DL, Fernandez AA, Nairn RS, *et al.* (2010) Ultraviolet A does not induce melanomas in a Xiphophorus hybrid fish model. *Proceedings of the National Academy of Sciences of the United States of America* 107:9329-34.

Miyamura Y, Coelho SG, Wolber R, *et al.* (2007) Regulation of human skin pigmentation and responses to ultraviolet radiation. *Pigment cell research / sponsored by the European Society for Pigment Cell Research and the International Pigment Cell Society* 20:2-13.

Mizutani T, Sumida H, Sagawa Y, *et al.* (2016) Carbonylated proteins exposed to UVA and to blue light generate reactive oxygen species through a type I photosensitizing reaction. *Journal of dermatological science*.

Moriwaki S, Takahashi Y (2008) Photoaging and DNA repair. *Journal of dermatological science* 50:169-76.

Morley M, Molony CM, Weber TM, *et al.* (2004) Genetic analysis of genome-wide variation in human gene expression. *Nature* 430:743-7.

Mouret S, Leccia MT, Bourrain JL, *et al.* (2011) Individual photosensitivity of human skin and UVA-induced pyrimidine dimers in DNA. *The Journal of investigative dermatology* 131:1539-46.

Moyal DD, Fourtanier AM (2008) Broad-spectrum sunscreens provide better protection from solar ultraviolet-simulated radiation and natural sunlight-induced immunosuppression in human beings. *Journal of the American Academy of Dermatology* 58:S149-54.

Munch M, Bromundt V (2012) Light and chronobiology: implications for health and disease. *Dialogues Clin Neurosci* 14:448-53.

Navid F, Boniotto M, Walker C, *et al.* (2012) Induction of regulatory T cells by a murine beta-defensin. *Journal of immunology* 188:735-43.

Naylor EC, Watson REB, Sherratt MJ (2011) Molecular aspects of skin ageing. *Maturitas* 69:249-56.

Naylor MF, Boyd A, Smith DW, *et al.* (1995) High sun protection factor sunscreens in the suppression of actinic neoplasia. *Archives of dermatology* 131:170-5.

Nazifi E, Wada N, Yamaba M, *et al.* (2013) Glycosylated porphyra-334 and palythine-threonine from the terrestrial cyanobacterium Nostoc commune. *Marine drugs* 11:3124-54.

Nemazannikova N, Antonas K, Dass CR (2013) Role of vitamin D metabolism in cutaneous tumour formation and progression. *J Pharm Pharmacol* 65:2-10.

Neunert G, Szwengiel A, Walejko P, *et al.* (2016) Photostability of alpha-tocopherol ester derivatives in solutions and liposomes. Spectroscopic and LC-MS studies. *Journal of photochemistry and photobiology B, Biology* 160:121-7.

Nichols JA, Katiyar SK (2010) Skin photoprotection by natural polyphenols: anti-inflammatory, antioxidant and DNA repair mechanisms. *Archives of dermatological research* 302:71-83.

Nishigori C, Hattori Y, Arima Y, *et al.* (2003) Photoaging and oxidative stress. *Experimental dermatology* 12 Suppl 2:18-21.

Nishigori C, Yarosh DB, Ullrich SE, *et al.* (1996) Evidence that DNA damage triggers interleukin 10 cytokine production in UV-irradiated murine keratinocytes. *Proceedings of the National Academy of Sciences of the United States of America* 93:10354-9.

Norval M, Cullen AP, de Gruijl FR, *et al.* (2007) The effects on human health from stratospheric ozone depletion and its interactions with climate change. *Photochemical & photobiological sciences : Official journal of the European Photochemistry Association and the European Society for Photobiology* 6:232-51.

O'Connor I, O'Brien N (1998) Modulation of UVA light-induced oxidative stress by beta-carotene, lutein and astaxanthin in cultured fibroblasts. *Journal of dermatological science* 16:226-30.

Okereke CS, Abdel-Rhaman MS, Friedman MA (1994) Disposition of benzophenone-3 after dermal administration in male rats. *Toxicology letters* 73:113-22.

Olsen CM, Wilson LF, Green AC, *et al.* (2017) Prevention of DNA damage in human skin by topical sunscreens. *Photodermatology, photoimmunology & photomedicine*.

Olsson-Francis K, Watson JS, Cockell CS (2013) Cyanobacteria isolated from the high-intertidal zone: a model for studying the physiological prerequisites for survival in low Earth orbit. *Int J Astrobiol* 12:292-303.

Oplander C Fau - Hidding S, Hidding S Fau - Werners FB, Werners Fb Fau - Born M, *et al.* (2011) Effects of blue light irradiation on human dermal fibroblasts.

Oren A (1997) Mycosporine-like amino acids as osmotic solutes in a community of halophilic cyanobacteria. *Geomicrobiol J* 14:231-40.

Oren A, Gunde-Cimerman N (2007) Mycosporines and mycosporine-like amino acids: UV protectants or multipurpose secondary metabolites? *FEMS Microbiol Lett* 269:1-10.

Osmond-McLeod MJ, Oytam Y, Rowe A, *et al.* (2016) Long-term exposure to commercially available sunscreens containing nanoparticles of TiO2 and ZnO revealed no biological impact in a hairless mouse model. *Particle and fibre toxicology* 13:44.

Osterwalder U, Herzog B (2009) Sun protection factors: world wide confusion. *The British journal of dermatology* 161 Suppl 3:13-24.

Osterwalder U, Herzog B (2010) The long way towards the ideal sunscreen--where we stand and what still needs to be done. *Photochemical & photobiological*

sciences : Official journal of the European Photochemistry Association and the European Society for Photobiology 9:470-81.

Osterwalder U, Sohn M, Herzog B (2014) Global state of sunscreens. *Photodermatology, photoimmunology & photomedicine* 30:62-80.

Oyamada C, Kaneniwa M, Ebitani K*, et al.* (2008) Mycosporine-like amino acids extracted from scallop (Patinopecten yessoensis) ovaries: UV protection and growth stimulation activities on human cells. *Marine biotechnology (New York, NY)* 10:141-50.

Pail G, Huf W, Pjrek E*, et al.* (2011) Bright-light therapy in the treatment of mood disorders. *Neuropsychobiology* 64:152-62.

Pal A, Alam S, Mittal S*, et al.* (2016) UVB irradiation-enhanced zinc oxide nanoparticles-induced DNA damage and cell death in mouse skin. *Mutation research Genetic toxicology and environmental mutagenesis* 807:15-24.

Palczewski K (2012) Chemistry and biology of vision. *The Journal of biological chemistry* 287:1612-9.

Pandel R, Poljsak B, Godic A*, et al.* (2013) Skin photoaging and the role of antioxidants in its prevention. *ISRN dermatology* 2013:930164.

Parrish JA, Jaenicke KF, Anderson RR (1982) Erythema and melanogenesis action spectra of normal human skin. *Photochemistry and photobiology* 36:187-91.

Peinado NK, Abdala Díaz RT, Figueroa FL*, et al.* (2004) Ammonium and UV radiation stimulate the accumulation of mycosporine-like amino acids in porphyra Columbina (rhodophta) from Patagonia Argentina *Journal of Phycology* 40:248-59.

Petersen B, Datta P, Philipsen PA*, et al.* (2013) Sunscreen use and failures--on site observations on a sun-holiday. *Photochemical & photobiological sciences : Official journal of the European Photochemistry Association and the European Society for Photobiology* 12:190-6.

Petersen B, Wulf HC (2014) Application of sunscreen--theory and reality. *Photodermatology, photoimmunology & photomedicine* 30:96-101.

Petersen B, Wulf HC, Triguero-Mas M*, et al.* (2014) Sun and ski holidays improve vitamin D status, but are associated with high levels of DNA damage. *The Journal of investigative dermatology* 134:2806-13.

Pfeifer GP, Besaratinia A (2012) UV wavelength-dependent DNA damage and human non-melanoma and melanoma skin cancer. *Photochemical & photobiological sciences : Official journal of the European Photochemistry Association and the European Society for Photobiology* 11:90-7.

Pfeifer GP, You YH, Besaratinia A (2005) Mutations induced by ultraviolet light. *Mutation research* 571:19-31.

Pflaum M, Boiteux S, Epe B (1994) Visible light generates oxidative DNA base modifications in high excess of strand breaks in mammalian cells. *Carcinogenesis* 15:297-300.

Placzek M, Gaube S, Kerkmann U, *et al.* Ultraviolet B-Induced DNA Damage in Human Epidermis Is Modified by the Antioxidants Ascorbic Acid and D-α-Tocopherol. *Journal of Investigative Dermatology* 124:304-7.

Pope MA, Spence E, Seralvo V, *et al.* (2015) O-Methyltransferase is shared between the pentose phosphate and shikimate pathways and is essential for mycosporine-like amino acid biosynthesis in Anabaena variabilis ATCC 29413. *Chembiochem : a European journal of chemical biology* 16:320-7.

Porges SB, Kaidbey KH, Grove GL (1988) Quantification of visible light-induced melanogenesis in human skin. *Photo-dermatology* 5:197-200.

Portwich A, Garcia-Pichel F (1999) Ultraviolet and osmotic stresses induce and regulate the synthesis of mycosporines in the cyanobacterium chlorogloeopsis PCC 6912. *Archives of microbiology* 172:187-92.

Portwich A, Garcia-Pichel F (2003) Biosynthetic pathway of mycosporines (mycosporine-like amino acids) in the cyanobacterium Chlorogloeopsis sp. strain PCC 6912. *Phycologia* 42:384-92.

Premi S, Wallisch S, Mano CM, *et al.* (2015) Chemiexcitation of melanin derivatives induces DNA photoproducts long after UV exposure. *Science* 347:842-7.

Quan T, Qin Z, Xia W, *et al.* (2009) Matrix-degrading metalloproteinases in photoaging. *The journal of investigative dermatology Symposium proceedings / the Society for Investigative Dermatology, Inc [and] European Society for Dermatological Research* 14:20-4.

Radka T. (2013) Improving the efficiency of aminolevulinate-photodynamic therapy of skin cells by combining UVA irradiation and potent iron chelating agents. Doctor of Philosophy thesis, University of Bath.

Ranadive NS, Menon IA, Shirwadkar S, *et al.* Quantitation of cutaneous inflammation induced by reactive species generated by UV-visible irradiation of Rose bengal. *Inflammation* 13:483-94.

Randhawa M, Seo I, Liebel F, *et al.* (2015) Visible Light Induces Melanogenesis in Human Skin through a Photoadaptive Response. *PloS one* 10:e0130949.

Rastogi RP, Incharoensakdi A (2013) Characterization of UV-screening compounds, mycosporine-like amino acids, and scytonemin in the cyanobacterium Lyngbya sp. CU2555. *FEMS Microbiol Ecol*.

Rastogi RP, Madamwar D, Incharoensakdi A (2015) Sun-screening bioactive compounds mycosporine-like amino acids in naturally occurring cyanobacterial biofilms: Role in photoprotection. *Journal of applied microbiology*.

Ravanat JL, Di Mascio P, Martinez GR*, et al.* (2001) Singlet oxygen induces oxidation of cellular DNA. *The Journal of biological chemistry* 276:40601-4.

Repetto G, del Peso A, Zurita JL (2008) Neutral red uptake assay for the estimation of cell viability/cytotoxicity. *Nat Protocols* 3:1125-31.

Rosen CF, Jacques SL, Stuart ME*, et al.* (1990) Immediate pigment darkening: visual and reflectance spectrophotometric analysis of action spectrum. *Photochemistry and photobiology* 51:583-8.

Rosenstein BS, Mitchell DL (1987) Action spectra for the induction of pyrimidine(6-4)pyrimidone photoproducts and cyclobutane pyrimidine dimers in normal human skin fibroblasts. *Photochemistry and photobiology* 45:775-80.

Rosic NN (2012) Phylogenetic analysis of genes involved in mycosporine-like amino acid biosynthesis in symbiotic dinoflagellates. *Applied microbiology and biotechnology* 94:29-37.

Ryu J, Kwon MJ, Nam TJ (2015) Nrf2 and NF-kappaB Signaling Pathways Contribute to Porphyra-334-Mediated Inhibition of UVA-Induced Inflammation in Skin Fibroblasts. *Marine drugs* 13:4721-32.

Ryu J, Park SJ, Kim IH*, et al.* (2014) Protective effect of porphyra-334 on UVA-induced photoaging in human skin fibroblasts. *International journal of molecular medicine*.

Sambandan DR, Ratner D (2011) Sunscreens: an overview and update. *Journal of the American Academy of Dermatology* 64:748-58.

Sanchez-Quiles D, Tovar-Sanchez A (2014) Sunscreens as a source of hydrogen peroxide production in coastal waters. *Environmental science & technology* 48:9037-42.

Sander CS, Chang H, Salzmann S*, et al.* (2002) Photoaging is associated with protein oxidation in human skin in vivo. *The Journal of investigative dermatology* 118:618-25.

Saraswat A (2012) Contact allergy to topical corticosteroids and sunscreens. *Indian journal of dermatology, venereology and leprology* 78:552-9.

Sarkany RP (2002) Erythropoietic protoporphyria (EPP) at 40. Where are we now? *Photodermatology, photoimmunology & photomedicine* 18:147-52.

Saw CL, Huang MT, Liu Y*, et al.* (2011) Impact of Nrf2 on UVB-induced skin inflammation/photoprotection and photoprotective effect of sulforaphane. *Molecular carcinogenesis* 50:479-86.

Scharffetter-Kochanek K, Brenneisen P, Wenk J*, et al.* (2000) Photoaging of the skin from phenotype to mechanisms. *Experimental gerontology* 35:307-16.

Scheuer PJ (1990) Some marine ecological phenomena: chemical basis and biomedical potential. *Science* 248:173-7.

Schlumpf M, Cotton B, Conscience M*, et al.* (2001) In vitro and in vivo estrogenicity of UV screens. *Environmental health perspectives* 109:239-44.

Schmid D, Schürch C, Zülli F (2003) UV-A sunscreen from red algae for protection against premature skin aging. *Cosmetics and Toiletries Manufacture Worldwide*.

Schreurs RH, Sonneveld E, Jansen JH*, et al.* (2005) Interaction of polycyclic musks and UV filters with the estrogen receptor (ER), androgen receptor (AR), and progesterone receptor (PR) in reporter gene bioassays. *Toxicological sciences : an official journal of the Society of Toxicology* 83:264-72.

Schwarz A, Maeda A, Gan D*, et al.* (2008) Green tea phenol extracts reduce UVB-induced DNA damage in human cells via interleukin-12. *Photochemistry and photobiology* 84:350-5.

Schwarz T (2008) 25 years of UV-induced immunosuppression mediated by T cells-from disregarded T suppressor cells to highly respected regulatory T cells. *Photochemistry and photobiology* 84:10-8.

Seo I, Liu Y, Bargo PR*, et al.* Assessing human skin with diffuse reflectance spectroscopy and colorimetry. In: *Proceedings of the Conference Assessing human skin with diffuse reflectance spectroscopy and colorimetry;* 2012.

Setlow RB, Grist E, Thompson K*, et al.* (1993) Wavelengths effective in induction of malignant melanoma. *Proceedings of the National Academy of Sciences of the United States of America* 90:6666-70.

Shaath NA (2010) Ultraviolet filters. *Photochemical & photobiological sciences : Official journal of the European Photochemistry Association and the European Society for Photobiology* 9:464-9.

Shah P, He YY (2015) Molecular regulation of UV-induced DNA repair. *Photochemistry and photobiology* 91:254-64.

Shick JM, Dunlap WC (2002) Mycosporine-like amino acids and related Gadusols: biosynthesis, acumulation, and UV-protective functions in aquatic organisms. *Annual review of physiology* 64:223-62.

Shick JM, Romaine-Lioud S, Romaine-Lioud S*, et al.* (1999) Ultraviolet-B radiation stimulates shikimate pathway-dependent accumulation of mycosporine-like amino acids in the coral Stylophora pistillata despite decreases in its population of symbiotic dinoflagellates. *Limnology and Oceanography* 44:1667-82.

Shindo Y, Witt E, Packer L (1993) Antioxidant defense mechanisms in murine epidermis and dermis and their responses to ultraviolet light. *The Journal of investigative dermatology* 100:260-5.

Shore RM, Chesney RW (2013) Rickets: Part I. *Pediatr Radiol* 43:140-51.

Singh NP, McCoy MT, Tice RR*, et al.* (1988) A simple technique for quantitation of low levels of DNA damage in individual cells. *Experimental cell research* 175:184-91.

Singh SP, Klisch M, Sinha RP*, et al.* (2008a) Effects of abiotic stressors on synthesis of the mycosporine-like amino acid shinorine in the Cyanobacterium Anabaena variabilis PCC 7937. *Photochemistry and photobiology* 84:1500-5.

Singh SP, Klisch M, Sinha RP*, et al.* (2010) Genome mining of mycosporine-like amino acid (MAA) synthesizing and non-synthesizing cyanobacteria: A bioinformatics study. *Genomics* 95:120-8.

Singh SP, Kumari S, Rastogi RP*, et al.* (2008b) Mycosporine-like amino acids (MAAs): chemical structure, biosynthesis and significance as UV-absorbing/screening compounds. *Indian journal of experimental biology* 46:7-17.

Sinha RP, Ambasht NK, Sinha JP*, et al.* (2003) Wavelength-dependent induction of a mycosporine-like amino acid in a rice-field cyanobacterium, Nostoc commune: role of inhibitors and salt stress. *Photochemical & Photobiological Sciences* 2:171-6.

Sivalingam PM, Ikawa T, Nisizawa K (1976) Physiological roles of a substance 334 in algae. *Botanica Marina* 19:9-21.

Sklar LR, Almutawa F, Lim HW*, et al.* (2013) Effects of ultraviolet radiation, visible light, and infrared radiation on erythema and pigmentation: a review. *Photochemical & photobiological sciences : Official journal of the European Photochemistry Association and the European Society for Photobiology* 12:54-64.

Spector SA (2011) Vitamin D and HIV: letting the sun shine in. *Top Antivir Med* 19:6-10.

Spence E, Dunlap WC, Shick JM, *et al.* (2012) Redundant pathways of sunscreen biosynthesis in a cyanobacterium. *Chembiochem : a European journal of chemical biology* 13:531-3.

Stahl W, Heinrich U, Jungmann H, *et al.* (2000) Carotenoids and carotenoids plus vitamin E protect against ultraviolet light-induced erythema in humans. *The American journal of clinical nutrition* 71:795-8.

Stahl W, Heinrich U, Wiseman S, *et al.* (2001) Dietary tomato paste protects against ultraviolet light-induced erythema in humans. *The Journal of nutrition* 131:1449-51.

Stamatas GN, Zmudzka BZ, Kollias N, *et al.* (2008) In vivo measurement of skin erythema and pigmentation: new means of implementation of diffuse reflectance spectroscopy with a commercial instrument. *The British journal of dermatology* 159:683-90.

Starcevic A, Akthar S, Dunlap WC, *et al.* (2008) Enzymes of the shikimic acid pathway encoded in the genome of a basal metazoan, Nematostella vectensis, have microbial origins. *Proceedings of the National Academy of Sciences of the United States of America* 105:2533-7.

Starcevic A, Dunlap WC, Cullum J, *et al.* (2010) Gene expression in the scleractinian Acropora microphthalma exposed to high solar irradiance reveals elements of photoprotection and coral bleaching. *PloS one* 5:e13975.

Starcher B, O'Neal P, Granstein RD, *et al.* (1996) Inhibition of neutrophil elastase suppresses the development of skin tumors in hairless mice. *The Journal of investigative dermatology* 107:159-63.

Stewart MS, Cameron GS, Pence BC (1996) Antioxidant nutrients protect against UVB-induced oxidative damage to DNA of mouse keratinocytes in culture. *The Journal of investigative dermatology* 106:1086-9.

Stojic L, Brun R, Jiricny J (2004) Mismatch repair and DNA damage signalling. *DNA repair* 3:1091-101.

Straif K, Baan R, Grosse Y, *et al.* (2007) Carcinogenicity of shift-work, painting, and fire-fighting. *Lancet Oncol* 8:1065-6.

Stubbins RE, Hakeem A, Nunez NP (2012) Using components of the vitamin D pathway to prevent and treat colon cancer. *Nutr Rev* 70:721-9.

Suh S-S, Hwang J, Park M, *et al.* (2014) Anti-Inflammation Activities of Mycosporine-Like Amino Acids (MAAs) in Response to UV Radiation Suggest Potential Anti-Skin Aging Activity. *Marine drugs* 12:5174-87.

Takamatsu S, Hodges TW, Rajbhandari I, *et al.* (2003) Marine natural products as novel antioxidant prototypes. *Journal of natural products* 66:605-8.

Takano S, Uemura D, Hirata Y (1978) Isolation and structure of a new amino acid, palythine, from the zoanthid Palythoa tuberculosa. *Tetrahedron Letters* 26:2299-300.

Tao S, Justiniano R, Zhang DD, *et al.* (2013) The Nrf2-inducers tanshinone I and dihydrotanshinone protect human skin cells and reconstructed human skin against solar simulated UV. *Redox biology* 1:532-41.

Tartarotti B, Laurion I, Sommaruga R (2001) Large variability in the concentration of mycosporine-like amino acids among zooplankton from lakes located across an altitude gradient. *Limnology and Oceanography* 46:1546-52.

Tartarotti B, Sommaruga R (2006) Seasonal and ontogenetic changes of mycosporine-like amino acids in planktonic organisms from an alpine lake. *Limnol Oceanogr* 51:1530-41.

Tebbe B, Wu S, Geilen CC, *et al.* (1997) L-ascorbic acid inhibits UVA-induced lipid peroxidation and secretion of IL-1alpha and IL-6 in cultured human keratinocytes in vitro. *The Journal of investigative dermatology* 108:302-6.

Tedetti M, Sempere R (2006) Penetration of ultraviolet radiation in the marine environment. A review. *Photochemistry and photobiology* 82:389-97.

Tewari A, Grage MM, Harrison GI, *et al.* (2013a) UVA1 is skin deep: molecular and clinical implications. *Photochemical & photobiological sciences : Official journal of the European Photochemistry Association and the European Society for Photobiology* 12:95-103.

Tewari A, Grys K, Kollet J, *et al.* (2014) Upregulation of MMP12 and its activity by UVA1 in human skin: potential implications for photoaging. *The Journal of investigative dermatology* 134:2598-609.

Tewari A, Grys K, Sarkany R, *et al.* (2013b) up-regulation of MMP12, and its activity, by ultraviolet A1 (UVA1) irradiation in human skin: Potential implications for photoageing. *Unpublished*.

Tewari A, Lahmann C, Sarkany R, *et al.* (2012a) Human erythema and matrix metalloproteinase-1 mRNA induction, in vivo, share an action spectrum which suggests common chromophores. *Photochemical & photobiological sciences : Official journal of the European Photochemistry Association and the European Society for Photobiology* 11:216-23.

Tewari A, Sarkany RP, Young AR (2012b) UVA1 induces cyclobutane pyrimidine dimers but not 6-4 photoproducts in human skin in vivo. *The Journal of investigative dermatology* 132:394-400.

Thieden E, Philipsen PA, Sandby-Moller J, *et al.* (2005) Sunscreen use related to UV exposure, age, sex, and occupation based on personal dosimeter readings and sun-exposure behavior diaries. *Archives of dermatology* 141:967-73.

Thody AJ, Higgins EM, Wakamatsu K, *et al.* (1991) Pheomelanin as well as eumelanin is present in human epidermis. *The Journal of investigative dermatology* 97:340-4.

Thompson SC, Jolley D, Marks R (1993) Reduction of solar keratoses by regular sunscreen use. *The New England journal of medicine* 329:1147-51.

Torregiani JH, Lesser MP (2007) The effects of short-term exposures to ultraviolet radiation in the Hawaiian Coral Montipora verrucosa. *Journal of Experimental Marine Biology and Ecology* 340:194-203.

Torres A, Enk CD, Hochberg M, *et al.* (2006) Porphyra-334, a potential natural source for UVA protective sunscreens. *Photochemical & photobiological sciences : Official journal of the European Photochemistry Association and the European Society for Photobiology* 5:432-5.

Torres A, Hochberg M, Pergament I, *et al.* (2004) A new UV-B absorbing mycosporine with photo protective activity from the lichenized ascomycete Collema cristatum. *European journal of biochemistry / FEBS* 271:780-4.

Tosato MG, Orallo DE, Churio MS, *et al.* (2014) Influence of mycosporine-like amino acids and gadusol on the rheology and Raman spectroscopy of polymer gels. *Biorheology* 51:315-28.

Tovar-Sanchez A, Sanchez-Quiles D, Basterretxea G, *et al.* (2013) Sunscreen products as emerging pollutants to coastal waters. *PloS one* 8:e65451.

Tran TT, Schulman J, Fisher DE (2008) UV and pigmentation: molecular mechanisms and social controversies. *Pigment cell & melanoma research* 21:509-16.

Tsujino T, Yabe K, Sekikawa I, *et al.* (1978) Isolation and structure of a mycosporine from the red alga chondrus yendoi. *Tetrahedron Letters* 16:1401-2.

Tuchinda C, Lim HW, Osterwalder U, *et al.* (2006) Novel emerging sunscreen technologies. *Dermatologic clinics* 24:105-17.

United Nations Environment Programme EEAP (2017) Environmental effects of ozone depletion and its interactions with climate change: Progress report, 10 2016. *Photochemical & photobiological sciences : Official journal of the European Photochemistry Association and the European Society for Photobiology*.

Urbach F (2001) The historical aspects of sunscreens. *Journal of photochemistry and photobiology B, Biology* 64:99-104.

Valavanidis A, Vlachogianni T, Fiotakis K*, et al.* (2013) Pulmonary Oxidative Stress, Inflammation and Cancer: Respirable Particulate Matter, Fibrous Dusts and Ozone as Major Causes of Lung Carcinogenesis through Reactive Oxygen Species Mechanisms. *International Journal of Environmental Research and Public Health* 10:3886-907.

Valencia A, Kochevar IE (2008) Nox1-based NADPH oxidase is the major source of UVA-induced reactive oxygen species in human keratinocytes. *The Journal of investigative dermatology* 128:214-22.

van der Pols JC, Williams GM, Pandeya N*, et al.* (2006) Prolonged prevention of squamous cell carcinoma of the skin by regular sunscreen use. *Cancer epidemiology, biomarkers & prevention : a publication of the American Association for Cancer Research, cosponsored by the American Society of Preventive Oncology* 15:2546-8.

Vincensi MR, d'Ischia M, Napolitano A*, et al.* (1998) Phaeomelanin versus eumelanin as a chemical indicator of ultraviolet sensitivity in fair-skinned subjects at high risk for melanoma: a pilot study. *Melanoma research* 8:53-8.

Wada N, Sakamoto T, Matsugo S (2015) Mycosporine-Like Amino Acids and Their Derivatives as Natural Antioxidants. *Antioxidants* 4:603-46.

Waditee-Sirisattha R, Kageyama H, Sopun W*, et al.* (2014) Identification and upregulation of biosynthetic genes required for accumulation of Mycosporine-2-glycine under salt stress conditions in the halotolerant cyanobacterium Aphanothece halophytica. *Applied and environmental microbiology* 80:1763-9.

Wang SQ, Dusza SW (2009) Assessment of sunscreen knowledge: a pilot survey. *The British journal of dermatology* 161 Suppl 3:28-32.

Wang SQ, Tooley IR (2011) Photoprotection in the era of nanotechnology. *Seminars in cutaneous medicine and surgery* 30:210-3.

Watanabe Y, Kojima H, Takeuchi S*, et al.* (2014) Metabolism of UV-filter benzophenone-3 by rat and human liver microsomes and its effect on endocrine-disrupting activity. *Toxicology and applied pharmacology* 282:119-28.

Webb AR, Holick MF (1988) The role of sunlight in the cutaneous production of vitamin D3. *Annual review of nutrition* 8:375-99.

Weber S (2005) Light-driven enzymatic catalysis of DNA repair: a review of recent biophysical studies on photolyase. *Biochimica et biophysica acta* 1707:1-23.

Weisbrod CJ, Kunz PY, Zenker AK*, et al.* (2007) Effects of the UV filter benzophenone-2 on reproduction in fish. *Toxicology and applied pharmacology* 225:255-66.

Weller RB (2016) Sunlight Has Cardiovascular Benefits Independently of Vitamin D. *Blood purification* 41:130-4.

Werninghaus K, Meydani M, Bhawan J, *et al.* (1994) Evaluation of the photoprotective effect of oral vitamin E supplementation. *Archives of dermatology* 130:1257-61.

Whitehead K, Hedges JI (2005) Photodegradation and photosensitization of mycosporine-like amino acids. *Journal of photochemistry and photobiology B, Biology* 80:115-21.

Wolfle U, Seelinger G, Bauer G, *et al.* (2014) Reactive molecule species and antioxidative mechanisms in normal skin and skin aging. *Skin pharmacology and physiology* 27:316-32.

Wood SR, Berwick M, Ley RD, *et al.* (2006) UV causation of melanoma in Xiphophorus is dominated by melanin photosensitized oxidant production. *Proceedings of the National Academy of Sciences of the United States of America* 103:4111-5.

Wright DJ, Smith SC, Joardar V, *et al.* (2005) UV irradiation and desiccation modulate the three-dimensional extracellular matrix of Nostoc commune (Cyanobacteria). *The Journal of biological chemistry* 280:40271-81.

Wulf HC, Sandby-Moller J, Kobayasi T, *et al.* (2004) Skin aging and natural photoprotection. *Micron (Oxford, England : 1993)* 35:185-91.

Wysong A, Gladstone H, Kim D, *et al.* (2012) Sunscreen use in NCAA collegiate athletes: identifying targets for intervention and barriers to use. *Preventive medicine* 55:493-6.

Yaar M, Gilchrest BA (2007) Photoageing: mechanism, prevention and therapy. *The British journal of dermatology* 157:874-87.

Yarosh D, Klein J, O'Connor A, *et al.* (2001) Effect of topically applied T4 endonuclease V in liposomes on skin cancer in xeroderma pigmentosum: a randomised study. Xeroderma Pigmentosum Study Group. *Lancet* 357:926-9.

Yiakouvaki A, Savovic J, Al-Qenaei A, *et al.* (2006) Caged-iron chelators a novel approach towards protecting skin cells against UVA-induced necrotic cell death. *The Journal of investigative dermatology* 126:2287-95.

Young AR (1990) Senescence and sunscreens. *The British journal of dermatology* 122 Suppl 35:111-4.

Young AR, Boles J, Herzog B, *et al.* (2010) A sunscreen's labeled sun protection factor may overestimate protection at temperate latitudes: a human in vivo study. *The Journal of investigative dermatology* 130:2457-62.

Young AR, Chadwick CA, Harrison GI*, et al.* (1996) The in situ repair kinetics of epidermal thymine dimers and 6-4 photoproducts in human skin types I and II. *The Journal of investigative dermatology* 106:1307-13.

Young AR, Chadwick CA, Harrison GI*, et al.* (1998) The similarity of action spectra for thymine dimers in human epidermis and erythema suggests that DNA is the chromophore for erythema. *The Journal of investigative dermatology* 111:982-8.

Young AR, Magnus IA, Davies AC*, et al.* (1983) A comparison of the phototumorgenic potential of 8-MOP and 5-MOP in hairless albino mice exposed to solar simulated radiation. *BJD* 108:507-108.

Zahid S, Brownell I (2008) Repairing DNA damage in xeroderma pigmentosum: T4N5 lotion and gene therapy. *Journal of drugs in dermatology : JDD* 7:405-8.

Zastrow L, Groth N, Klein F*, et al.* (2009) The missing link--light-induced (280-1,600 nm) free radical formation in human skin. *Skin pharmacology and physiology* 22:31-44.

Zastrow L, Lademann J (2016) Light - Instead of UV Protection: New Requirements for Skin Cancer Prevention. *Anticancer research* 36:1389-93.

Zenker A, Schmutz H, Fent K (2008) Simultaneous trace determination of nine organic UV-absorbing compounds (UV filters) in environmental samples. *Journal of Chromatography A* 1202:64-74.

Zepp RG, Erickson DJ, 3rd, Paul ND*, et al.* (2007) Interactive effects of solar UV radiation and climate change on biogeochemical cycling. *Photochemical & photobiological sciences : Official journal of the European Photochemistry Association and the European Society for Photobiology* 6:286-300.

Zhang L, Li L, Wu Q (2007) Protective effects of mycosporine-like amino acids of Synechocystis sp. PCC 6803 and their partial characterization. *Journal of photochemistry and photobiology B, Biology* 86:240-5.

Zhao Y, Moddaresi M, Jones SA*, et al.* (2009) A dynamic topical hydrofluoroalkane foam to induce nanoparticle modification and drug release in situ. *European Journal of Pharmaceutics and Biopharmaceutics* 72:521-8.

Appendix

Presentations arising from work in this thesis:

Lawrence, KP; Long, PF; Young, AR (2015) '*Molecular photoprotection by the naturally occurring mycosporine-like amino acid (MAA) palythine in a human in vitro skin model.'* **16th Congress of the European Society for Photobiology**; Aveiro, Portugal.

Lawrence, KP; Long, PF; Young, AR (2016) *'Molecular photoprotection by the naturally occurring mycosporine-like amino acid (MAA) palythine in a human in vitro skin model.'* **ASP Congress 2016, American Society for Photobiology**; Tampa, Florida, USA.

Lawrence, KP; Sarkany RPE; Acker, S; Herzog, B; Young, AR (2016) *'Wavelengths from 385-405nm cause photodamage to skin cells.'* **ASP Congress 2016, American Society for Photobiology**; Tampa, Florida, USA.

Lawrence, KP; Long, PF; Young, AR (July 2017) '*Mycosporine-like amino acids (MAA) - biocompatible sunscreens from nature.* **Naturals in Cosmetic Science Annual Conference**; London, UK. (Invited presentation).

Lawrence, KP; Sarkany RPE; Douki, T; Acker, S; Herzog, B; Young, AR (July 2017) *'Wavelengths from 385-405nm cause photodamage to skin cells.'* **British Association of Dermatologists Annual Meeting**, Liverpool, UK .

Lawrence, KP; Sarkany RPE; Douki, T; Acker, S; Herzog, B; Young, AR (September 2017) *'Wavelengths from 385-405nm cause photodamage to skin cells.'* **European Society for Photobiology**, Pisa, Italy.

Publications arising from work in this thesis:

Lawrence, KP., Long, PF., Young, AR**.** (2017) '*Mycosporine-like Amino Acids for Skin Photoprotection'* ***Current Medicinal Chemistry*** (Invited review - Published)

Lawrence, KP., Long, PF., Young, AR**.** (2017) *'Molecular photoprotection by the naturally occurring mycosporine-like amino acid (MAA) palythine in a human in vitro skin model*'. ***British Journal of Dermatology*** (Accepted)

Lawrence, KP; Sarkany RPE; Douki, T; Acker, S; Herzog, B; Young, AR (2017) *'Wavelengths from 385-405nm cause photodamage to skin cells.'* (In preparation)

Patents arising from work in this thesis:

'COMPOSITIONS AND METHODS USING PALYTHINE' (PCT/GB2016/052227– UK Patent office)

Second patent submitted (in collaboration with BASF) (PENDING – Confidential)

Send Orders for Reprints to reprints@benthamscience.ae

Current Medicinal Chemistry, **2017**, *24*, **1-16**

REVIEW ARTICLE

Mycosporine-Like Amino Acids for Skin Photoprotection

Karl P. Lawrence[a], Paul F. Long[b], and Antony R. Young[a,*]

[a]*St. John's Institute of Dermatology, Faculty of Life Sciences and Medicine, King's College London, London, United Kingdom;* [b]*Institute of Pharmaceutical Science, Faculty of Life Sciences and Medicine, King's College London, London, United Kingdom*

ARTICLE HISTORY

Received: March 12, 2017
Revised: May 15, 2017
Accepted: May 15, 2017

DOI:
10.2174/0929867324666170529124237

Abstract: Excessive human exposure to solar ultraviolet radiation (UVR) continues to be a major public health concern, with skin cancer rates increasing year on year. The major protective measure is the use of synthetic UVR filters formulated into sunscreens, but there is a growing concern that some of these chemicals cause damage to delicate marine ecosystems. One alternative is the use of biocompatible mycosporine-like amino acids (MAA), which occur naturally and are found predominantly in a wide range of marine species. Their role within nature is mainly thought to be photoprotective. This is a consequence of their optical properties but there is an increasing evidence that they are also antioxidants at a chemical level, as well by activation of endogenous cell antioxidant defence mechanisms. However, their potential for human photoprotection is largely understudied. This review explores the role of MAA in nature and considers the literature available on the use of MAA within human models for photoprotection.

Keywords: Photoprotection, mycosporine-like amino acids, skin, natural products, mechanisms, solar radiation.

1. INTRODUCTION

Exposure to terrestrial solar ultraviolet (~295-400nm) and visible (400-700nm) radiation has profound effects on all living systems. Photon energy absorbed by cellular chromophores may have beneficial or detrimental effects. The wavelength dependence (action spectrum) of a given photobiological outcome is primarily dependent on the absorption spectrum of the chromophore. The skin is the major organ exposed to solar radiation. The molecular effects of this exposure are well defined, causing either direct damage to DNA, proteins or lipids, such as in the formation of DNA photoproducts [1], and indirect damage via the generation of reactive oxygen species (ROS) [2, 3] that attack a range of molecular and cellular targets. It was initially thought that direct damage was mainly responsible for the most damage; however in recent years the importance of indirect and oxidative damage has been realised, with the generation of oxidative [4] and photosensitised [5] DNA damage, and the oxidation of proteins leading to inhibition of the DNA repair machinery [6]. The main established beneficial effect of ultraviolet radiation (UVR) exposure is the production of vitamin D in the skin.

The molecular effects of sunlight are summarised in Fig. (**1**). These effects can lead to sunburn in the short term, and skin cancer [7] and photoageing [8, 9] in the long term. Public health advice to prevent this damage mainly advocates the use of sunscreens, along with clothing cover and avoiding the sun at the time when exposure is strongest. Modern sunscreens are formulations that are applied to the skin [10]. They contain a range of different synthetic organic and inorganic UVR filters with different absorbance profiles to provide broad-spectrum protection across the solar UVR spectrum.

The organic chemical filters contain a chromophore, which is typically an aromatic molecule conjugated to carbonyl groups. In general, increasing the number of conjugated double bonds and number of resonance structures stabilizes the excited state and shifts the absorption spectrum to longer wavelengths and a larger

*Address correspondence to this author at the St. John's Institute of Dermatology, Faculty of Life Sciences and Medicine, King's College London, London, United Kingdom;
E-mail: antony.young@kcl.ac.uk

0929-8673/17 $58.00+.00

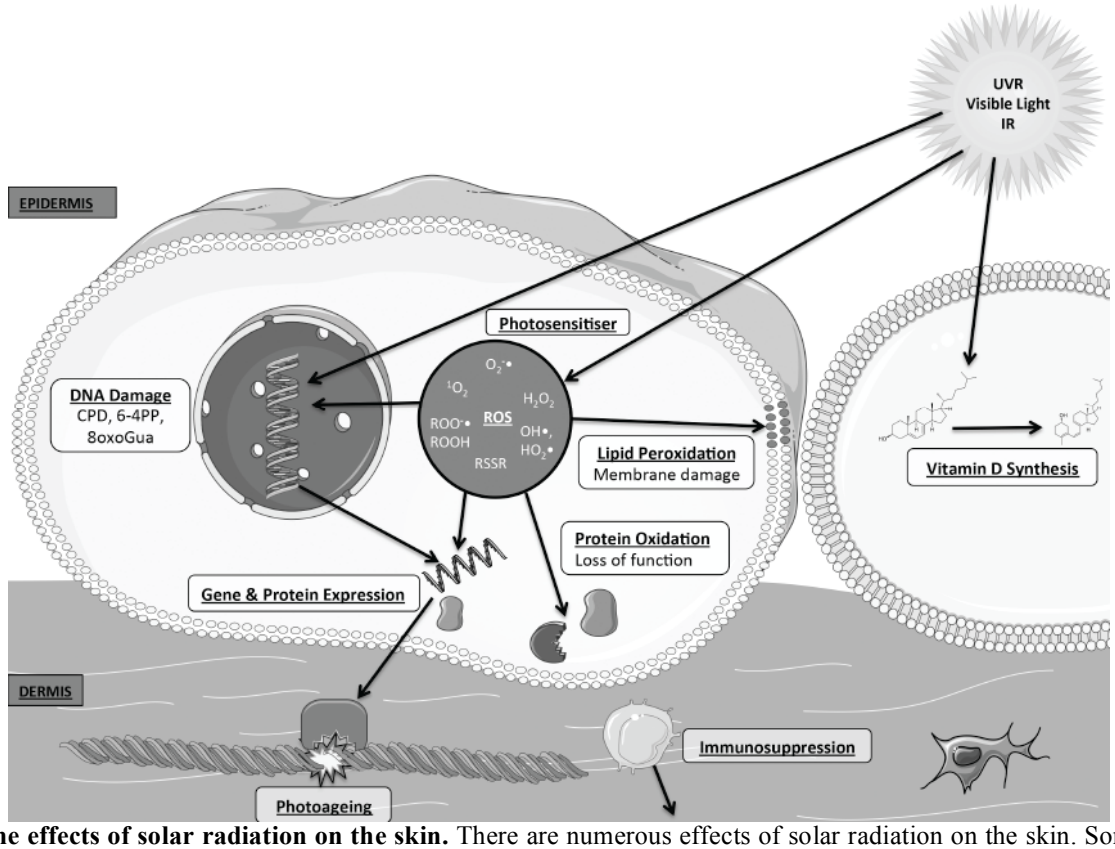

Fig. (1). The effects of solar radiation on the skin. There are numerous effects of solar radiation on the skin. Some of these are positive such as the production of vitamin D, however the vast majority of these is negative. The negative effects include direct damage to molecules such as DNA and the formation of cyclobutane pyrimidine dimers (CPD) and indirect damage through photosensitisation reactions resulting in the production of reactive oxygen species (ROS). Both these routes of damage induction cause secondary effects such as DNA, protein and lipid oxidation (resulting in reduced function), differential gene and protein expression (leading to photoageing, inflammation and melanogenesis) and immunosuppression. Damage to DNA can lead to mutations and eventually cancer [13].

absorption cross section – leading to UVB (280-315nm) absorbers having typically smaller molecular weights compared to UVA (315-400nm) and broad spectrum (UVB + UVA) filters [11, 12].

The energy of UVR photons lies in the same magnitude as the energy of the filters' electrons, and allows for the absorption of the photons. Once absorbed, this causes a photochemical excitation of the electrons to a higher energy (π*) state (excited singlet state), the electrons then return to the ground state emitting the excess energy, which can occur by a number of different processes shown in Fig. (**2**). The preferred route, to dissipate the energy returning the excited molecule to the ground state, is by internal conversion (IC), leading to dissipation by heat, or reversible isomerisation. When this is not possible, the remaining energy can be converted into photons as fluorescence, corresponding to the difference in energy between the two levels. This energy can be emitted in either the visible, infrared or long wave UVR region. Through intersystem crossing (ISC), the singlet excited state can cross to the triplet state, which can lead to phosphorescence or photosensitisation reactions. These reactions can result in the transfer of the excess energy to oxygen molecules to form ROS, or cause bonds to break [11]. This is highly undesirable for a sunscreen molecule; as the molecules need to be stable enough to prevent further damage rather than enhance damage.

The inorganic filters that are commonly used in sunscreen formulations are titanium dioxide (TiO_2) and zinc oxide (ZnO), and despite popular belief also act by absorption of UVR, with only a minimal effect by reflection or scattering. A recent study demonstrated that the average reflection range of UVR by TiO_2 and ZnO was around 4-5%, equating to a sun protection factor (SPF) of less than 2 [14]. The UVR is absorbed by excitation of the electrons from the valence band to the conduction band. These molecules do not absorb in the visible range but their particulate nature results in scattering and reflecting, which accounts for the white appearance on the skin. Clearly this is highly undesirable

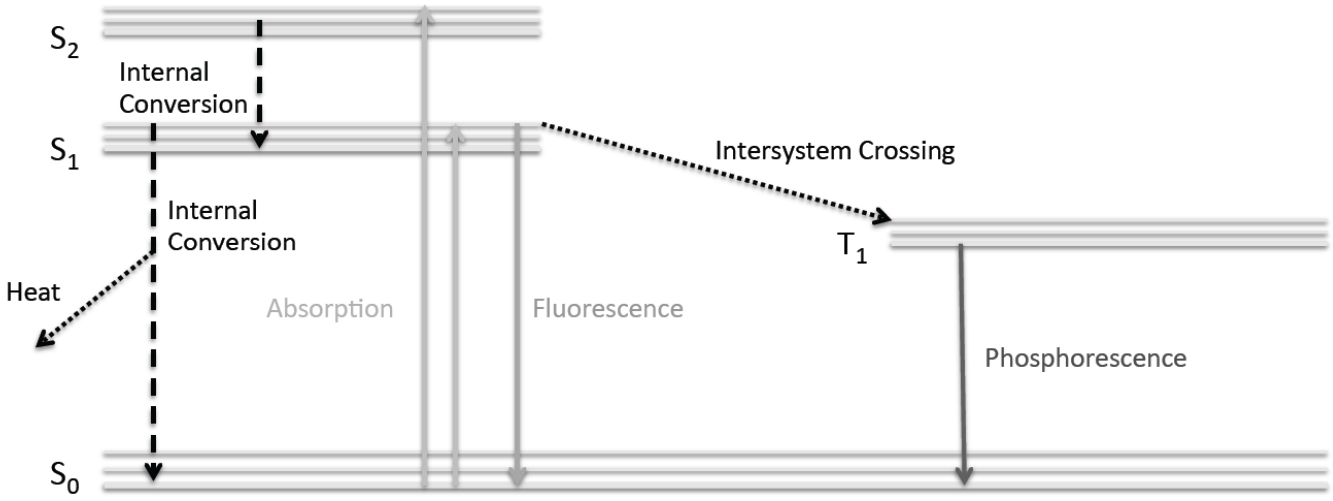

Fig. (2). Routes of excitation and dissipation of photochemical excitation of electrons.

for a sunscreen, so these molecules are increasingly micronized to improve their cosmetic properties [11].

There is evidence that suggests sunscreens may prevent a range of UVR-induced clinical outcomes including erythema (sunburn), squamous cell carcinoma (SCC), basal cell carcinoma (BCC) [15] and photoageing [16], however this is contested [17] and their ability to prevent malignant melanoma (MM) is yet to be fully established [18, 19].

In recent years there has been a shift in consumer trends to prefer more natural products, rather than their synthetic equivalents, as they are perceived to be safer and better [20]. Additionally, in the case of sunscreens there is a growing body of evidence that suggests that the synthetic UVR filters such as octocrylene (OCT), benzophenone-4 (BP-4), ethyl 4-aminobenzoate (Et-PABA), 3-benzylidene camphor (3BC) and TiO2 nanoparticles may cause damage to the marine environment in which they are widely used. Several negative effects have been reported, including the bioaccumulation of filters in many different species [21, 22], hormonal changes and endocrine disruption in fish [23, 24], production of hydrogen peroxide [25] and the bleaching of corals [26]. The Environmental Effects Assessment Panel (EEAP), that answers to the United Nations Environment Programme (UNEP), recently expressed concern about sunscreen damage to fragile marine ecosystems [27].

2. MYCOSPORINE-LIKE AMINO ACIDS

One class of such natural compounds is the mycosporines and mycosporine-like amino acids (MAA), which are thought to provide photoprotection to marine species and terrestrial fungi. Many marine species are exposed to very high levels of solar radiation, particularly in shallow clear waters. Solar UVR can penetrate to depths of between 0.5-47m depending on the water clarity. DNA is very susceptible to UVR-induced damage and wavelengths that readily damage DNA can reach depths of 16.4m [28]. Organisms of all classes have evolved complex DNA repair mechanisms, but some have also evolved other strategies, one of which is by the biosynthesis and accumulation of UVR absorbing molecules such as MAA. These are compounds that are synthesized or acquired by the diet in a taxonomically diverse range of marine organisms, including protozoa, algae, seaweed, corals, other invertebrates and fish [29]. The first MAA were discovered in fungi species in 1965 [30] and a recent study found a terrestrial alga containing MAA [31].

The cellular concentration and type of MAA vary with species, geographical location and environment (*e.g.* nitrate concentration) in which they are found. There are also ways to increase the MAA content such as with irradiation with different visible light/UVR sources, and treatment with nitrate compounds. Table **1** shows some examples of the different MAA and their concentrations produced by different species, and some treatments used to increase the yield of MAA [32-39].

Research on the photoprotective potential of these compounds has largely been focused on the species in which they are produced or found, but more recently there has been more work investigating their possible role as photoprotective agents in human skin models.

Table 1. The reported MAA and total content of different species and treatments to induce production of MAA. (DW= Dry weight, PAR= Photosynthetically active radiation).

Species	Reported MAA	Total MAA DW Content [ref]	MAA DW Content after Treatment
Ulva lactuca	Porphyra-334	0.005 mg/g [39]	-
Gymnogongrus antatcticus	Shinorine	0.1 mg/g [38]	PAR + UVA + UVB > 0.9 mg/g
Pilayella Littoralis	Porphyra-334	0.177 mg/g [39]	-
Kallymenia antartica	Shinorine, Palythine, Asterina-330	0.3 mg/g [38]	PAR + UVA + UVB > 1.6 mg/g
Palmaria decipiens	Shinorine, Porphyra-334 Palythine, Asterina-330	0.4 mg/g [38]	PAR + UVA + UVB > 0.9 mg/g
Chondrus crispus	Palythine, Palythinol	0.470 mg/g [39]	-
Gracilaria tenuis-tipitata	Information not available	0.6 mg/g [33, 34]	NO_3^- 0.5mM + PAR + UVR > 4.29 mg/g
Hydropuntia cornea	Shinorine, Porphyra-334, Palythine	1.3 mg/g [32]	Increase in nitrate availability > 2.25 mg/g
Porphyra leucosticta	Shinorine, Palythine, Porphyra-334, Asterina	6.99 mg/g [35]	300uM ammonium > 9.67 mg/g
Devaleraea ramen-tacea	Mycosporine-glycine, Shinorine, Porphyra-334, Palythine, Asterina, Palythinol, Palythene	3.552mg/g [39]	-
Porphyra endiviifo-lium	Shinorine, Porphyra-334	4.2 mg/g [38]	PAR + UVA > 8 mg/g
Pophyra columbina	Mycosporine-glycine, Shinorine, Porphyra-334, Palythine, Asterina,	5.5 mg/ g [36] (7.2 - 10.6 mg/g [37])	PAR + UVA + UVB + NH_4Cl > 0.9 mg/g
Gelidium pusillum	Shinorine, Porphyra-334, Palythine, Asterina, Palythinol	6.506 mg/g [39]	-
Gymnogongrus griffithsiae	Shinorine, Porphyra-334, Palythine, Asterina,	7.786 mg/g [39]	-

In addition to their UVR absorption characteristics, MAA appear to have other properties, such as antioxidant activity. This review reports on the mechanisms involved with the photoprotective role of MAA in nature and potential application to skin photoprotection.

2.1. MAA Structure and Biosynthesis

MAA are typically small (<400 Da) colourless, water-soluble compounds, of which over 20 are currently known. They have a similar general structure based on 4-deoxygadusol, containing cyclohexenone or cyclohexenimine rings conjugated to the nitrogen substituent of an amino acid or imino alcohol. These can undergo further carboxylation or demethylation, which changes their UVR absorption properties [40]. The general structures for mycosporines and MAA are displayed in Fig. (**3**).

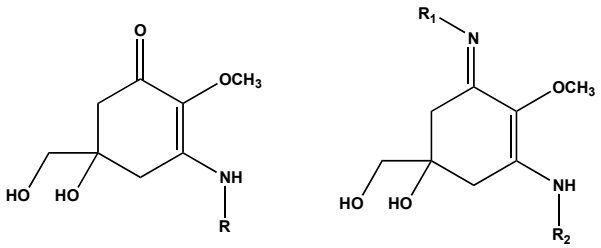

Fig. (3). The general structures of mycosporines and MAA.

The route of MAA biosynthesis is a contentious area. Historically it was believed that MAA were synthesised via the shikimate pathway. This pathway is found in many microorganisms including bacteria, algae, fungi and plants and is responsible for the biosynthesis of the essential aromatic amino acids phenylalanine, tyrosine and tryptophan. This pathway is not found in animals and these amino acids must be ac-

quired by diet. It was first implicated because the addition of the radiolabeled precursor [U-^{14}C]3-dehydroquinate to the fungus *Trichothecium roseu* produced labelled glutamicol. Furthermore, the *cyanobacterium* species *Chlorogloeopsis* successfully synthesised the MAA shinorine and mycosporine-glycine when ^{14}C-pyruvate was added to the culture [41, 42]. The use of the shikimate pathway inhibitors glyphosate and tyrosine has also demonstrated the ability to inhibit the production of MAA in the cyanobacteria *Nostoc commune* and the coral *Stylophora pistillata* [43, 44].

Further investigation has also implicated the pentose phosphate pathway in MAA biosynthesis. A four-gene cluster, linked to the pentose phosphate pathway in *Anabaena variabilis* ATCC 29413, was able to produce the MAA shinorine when inserted in to the heterologous host *E.coli* [45]. The genes in this cluster have been identified as shown in Table **2**.

Table 2. The four-gene cluster found in *Anabaena variabilis* ATCC 29413 linked to the pentose phosphate pathway synthesis of MAA.

Designation	Name	Product
Ava_3858	2-epi-5-epi-valiolone synthase (EVS)	2-epi-5-epi-valiolone
Ava_3857	*0*-methyltransferase (OMT)	4-deoxygadusol
Ava_3856	ATP-grasp amino acid ligase	Mycosporine-glycine
Ava_3855	NRP-like synthase	Shinorine

This finding has also been confirmed in another cyanobacterium *N. punctiforme*, which shares homologues of the first three genes found in *A. variabilis* (NpR5600, NpR5599 and NpR5598), and produced mycosporine-glycine after treatment with the 2-epi-5-epi-valiolone precursor sedoheptulose 7-phosphate (SH-7P) [46]. The incubation of the first two proteins of this cluster (NpR5600 and NpR5599) with SH-7P has also demonstrated the production of 4-deoxygadusol [46]. Typically the EVS gene is found in genome mining of species that produce MAA and is absent in those without this ability [47, 48]. There is however one known exception, in *Synechocystis sp.* PCC6803, which lacks EVS but produces three novel MAA after exposure to UVR. These are mycosporine-tau, dehydroxylusujirene and M-343 [49] and suggests an alternative pathway to MAA in this cyanobacterium.

Despite experimental data that support the pentose phosphate pathway, there is an evidence that this is not the major route of MAA synthesis. *A. variabillis* ATCC 29413 still produced shinorine, at levels equivalent to the wild type exposed to UVR, after a deletion of the gene encoding the enzyme EVS. This eliminates the role of the pentose phosphate pathway as the only mechanism for MAA synthesis [50]. Another proteomic study of the same cyanobacterium found that UVA exposure led to an increase in expression of the enzymes DAHPS and DHQS (part of the shikimate pathway) after irradiation. There was no increase in any enzymes associated with the pentose phosphate pathway, and when shikimate inhibitors were used there was only minimal shinorine produced, suggesting any activity from the pentose phosphate pathways was minimal. Overall, this implies the shikimate route of production as the most predominant for MAA synthesis in sufficient quantities to provide photoprotection. This is confirmed in studies with shikimate inhibitors, which found expression of shinorine after UVR exposure was very low, at levels equivalent to no exposure [51]. Quantities of MAA produced by the pentose phosphate pathway are likely to have other biological functions, for example in *Anabaena* there is evidence of a possible phycobillosome trimming role [50].

There are however clear links between the pentose phosphate and shikimate pathways. SH-7P, an intermediate of the pentose phosphate pathway is easily converted to the shikimate intermediate erythrose-4-phosphate by a transaldolase enzyme. The enzymes 3-dehydroquinate synthase (DHQS), from the shikimate pathway, and EVS, from the pentose phosphate pathway, are both part of the sugar phosphate cyclase family of enzymes. These enzymes have also remarkably similar amino acid sequences and carry out very similar reactions [52]. A knockout of the gene encoding the enzyme O-methyltransferase (OMT) (linked to the pentose phosphate pathway) in *A. variabillis* ATCC 29413 completely prevented shinorine synthesis [51] implying that both pathways must be linked at this point.

Evaluating this evidence, one proposed scheme for MAA synthesis is that SH-7P of the pentose phosphate pathway is fed into the shikimate pathway to form erythrose-4-phosphate (which is also formed from the earlier stages of the shikimate pathway). This then reacts with phosphoenolpyruvate (PEP) to form 3-deoxy-D-arabinoheptulosinate phosphate (DAHP) and 3-deyhdroquinate (DHQ). This explains the upregulation of the enzymes DAHPS and DHQS. The involvement of OMT implies that DHQ cannot be the direct precursor of 4-deoxygadusol, and it must feed back into the pentose phosphate pathway and undergo conversion to

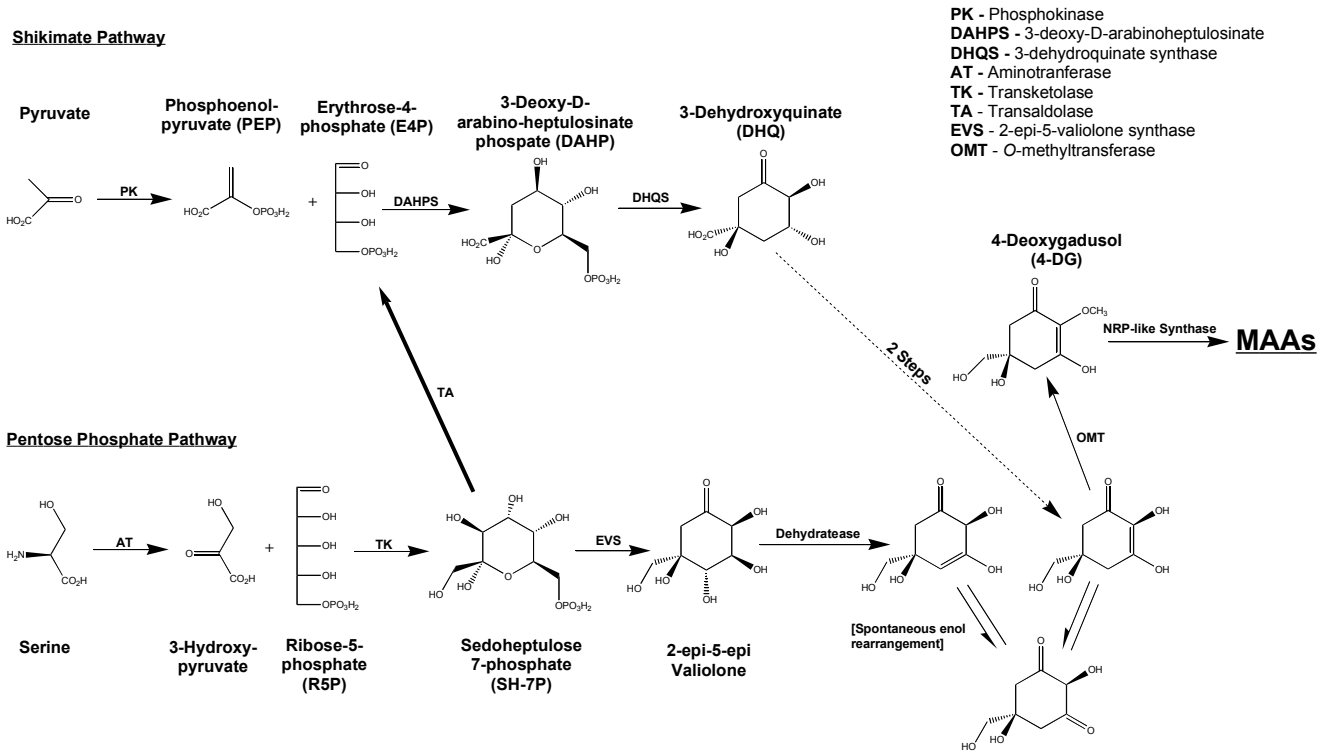

Fig. (4). The proposed route of MAA biosynthesis.

an intermediate (by an unidentified enzyme(s)), which is then converted by OMT into 4-deoxygadusol. A suggested biosynthesis scheme is depicted in (Fig. **4**), which incorporates both pathways.

The synthesis of mycosporine-glycine from 4–deoxygadusol has been shown to occur via ligase, and shinorine through NRP-like synthase of mycosporine-glycine. The biosynthesis routes of many other MAA are yet to be established [53]. However, a new five-gene cluster has recently been discovered in the soil dwelling cyanobacteria *Cylindrospermum stagnale sp*. PCC 7417, which when cloned into *E. coli* produced mycosporine-ornithine and mycosporine-lysine, giving insight into the synthesis of other MAA and a possible route to large scale production [54].

3. PHOTOPROTECTIVE ROLE OF MAA IN NATURE

3.1. Structural Evidence for Photoprotection

The UVR protective properties of MAA are largely inferred from their absorption spectra and high molar extinction coefficients. Typically they have a peak absorption wavelength (λ_{max}) between 268-362nm, covering much of the spectral range of UVR (~295-400nm) that reaches the earth's surface [29].

The photochemistry of MAA is poorly understood, with only a select few compounds having been investigated. The MAA that have been most studied are porphyra-334, shinorine and mycosporine-glycine. The photo-excited states of these molecules have been shown to relax by intersystem crossing from the singlet excited state to the triplet excited state and by subsequent non-radiative decay, resulting in a controlled dissipation of the energy as heat without the production of ROS [55]. Porphyra-334 and shinorine dissipate 96-98% of absorbed energy in this way [56, 57]. This pathway is consistent with the strong photostability of MAA. Palythine in particular has been shown to be extremely photostable in a saturated aqueous solutions [55], as well in the presence of seawater and the strong photosensitising agents riboflavin and rose Bengal [58]. The increased photostability of palythine over other MAA (such as shinorine and asterina-330) has been attributed to the substitution of the nitrogen atom R group (R_1=H), in relation to the geometrical isomerisation around the C=N double bond [55]. Displayed in (Fig. **5**) are data generated demonstrating the photostability of MAA as (a) a mixture and (b) palythine as a single molecule. Both examples demonstrate excellent photostability, with palythine as a single molecule demonstrating only a 3% degradation after an exposure of 40 standard erythema doses (SED) of solar simulated radiation (SSR), equivalent to around a full day of UK summer sun on an unshaded surface (a dose of around 60J/cm^2). Many synthetic filters rely upon addi-

tional filters to provide photostability; this demonstrates that this is not necessary with MAA.

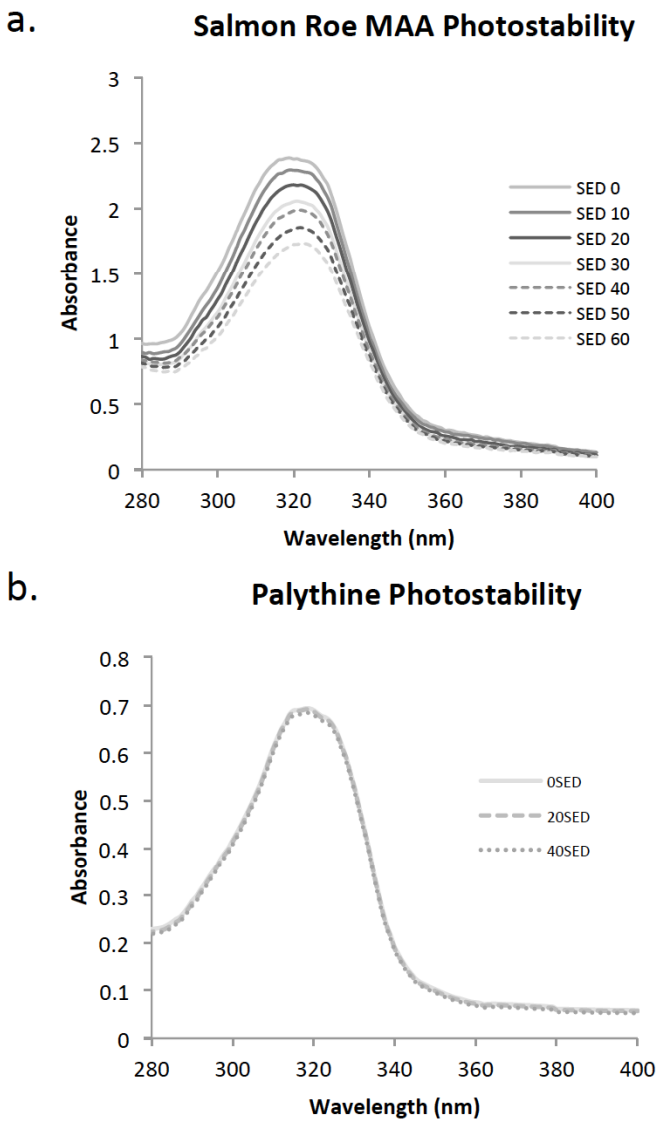

Fig. (5). The photostability of MAA. (a) MAA extracted from salmon roe (0.06%w/v and of (b) of palythine as a single molecule at a concentration of 0.001% w/v in PBS was exposed to increasing doses of SSR and the absorbance subsequently measured by UV spectrometry between 280-400nm.

3.2. Circumstantial Evidence for Photoprotection

In addition to the optical properties of MAA, there is also a large body of circumstantial evidence to suggest a photprotective role in their natural environments. This has been extensively reviewed by Shick and Dunlap [29], but the key conclusions are summarised below.

MAA appear to be preferentially accumulated in tissues that receive the greatest UVR exposure – the epidermis of coral reef holothuroids, sea urchin eggs and the eggs and lenses of freshwater and marine teleosts [29, 59, 60]. In other circumstances, such as with corals, the MAA are transferred through symbiosis with algae (*e.g.* zooanthellae). In this relationship, the host also receives organic carbon in the form of carbohydrates, lipids and amino acids and the symbiont is nourished by the host's waste products such as nitrogen, phosphorus, sulphur and carbon dioxide for photosynthesis [61, 62].

The MAA concentration of a species is directly related with its UVR exposure level that is dependent on latitude and altitude. Zooplankton sampled from lakes at different altitudes showed increasing MAA concentration with increasing altitude [63]. Species found in tropical waters have a greater concentration of MAA than those found in cooler climates. High levels of MAA are also found in species in the Antarctic Ocean, possibly due to high irradiances from the ozone layer hole [64]. Species show seasonal variation in MAA concentration. In winter months, they have a lower concentration compared to summer months when UVR exposure is highest as demonstrated in plankton growing in lake environments [65, 66]. There is also a strong negative correlation between the coral depth and MAA concentration that reflects the attenuation of UVR by water. This has been demonstrated experimentally by Dunlap *et al*, who relocated corals, with low MAA concentration, from deep to shallow waters [67]. This resulted in an increased in MAA content that supports a role in photoprotection. An increase in extracellular nitrogen concentration has also demonstrated an increase in MAA production, suggesting a potential role in intracellular nitrogen storage [68].

3.3. Biological Evidence for Photoprotection

The role of MAA in protecting marine species from UVR damage is a widely researched area. One study has shown an inverse relationship between the production of DNA photolesions, especially the cyclobutane pyrimidine dimer (CPD), and total MAA concentration in the coral *Montipora verrucosa* (found in Kaneohe Bay, Oahu, Hawaii) which contains mycosporine-glycine, shinorine and porpyra-334 [69]. Reduction of CPD and 6,4 pyrimidine-pyrimidone photoproducts by MAA has also been demonstrated, acting by attenuating the UVR before it reaches critical cellular targets in addition to their quenching effects (discussed in DNA Damage section) the photo-excited state thymine base [70]. Photoprotection has also been demonstrated in green sea urchin embryos by preventing UVB induced abnormalities [71, 72]. There are numerous studies investigating the effect of increased MAA content on

UVR resistance for a range of species and environmental stressors such as UVR and desiccation [73-77].

Initially it was thought that MAA acted solely by absorbing UVR before it could reach the critical cellular targets, but they also appear to have antioxidant properties. This is an extremely desirable characteristic for a photoprotective molecule, as much of the damaging effect of UVR is due to ROS. This has been demonstrated with different MAA from a large variety of species [78-81]. MAA have also been shown to block specific consequences of oxidative damage preventing lipid peroxidation and superoxide radicals [82]. An extensive review of MAA antioxidant abilities has been carried out by Wada *et al* [83].

3.4 Additional Protective Roles of MAA in Nature

Apart from their photoprotective properties, MAA exhibit additional protective effects, particularly to other environmental stressors. These roles are summarised below and are reviewed in more detail by Oren and Gunde-Cimerman [77].

3.4.1. Osmotic Stress

One such stressor the MAA appear to have an action against is osmotic stress, where a change in the solute concentration surrounding an organism, causes a loss or gain of cellular solvents. One halotolerant unicellular cyanobacterium, inhabiting in a gypsum crust in a hypersaline saltern pond, has an extremely high concentration of MAA (≥98mM), accounting for >3% of its mass. A reduction of the salinity of its surroundings was accompanied with a rapid expulsion of MAA, suggesting a role in osmotic stabilisation [84]. This hypothesis has since been investigated and the role of MAA in prevention from osmotic stress supported [77, 85-88].

3.4.2. Desiccation Stress

There is also evidence that MAA can protect against desiccation. Cyanobacteria under desiccation stress contain high concentrations of water stress protein (WSpA) and MAA in a 1:1 ratio (around 4-5% of dry mass each), along with other compounds including scytonemin (another UVR filter), superoxide dismutase and glycan. This group of compounds is thought to act by modifying the structure of the extracellular matrix. Upon rehydration there is an expulsion of MAA. Overall, this supports a role for MAA comparable to that for osmotic stress [76]. Another study found that cyanobacteria experimentally stressed by desiccation increased their total MAA content. When these pre-stressed cells were placed under desiccation conditions, they had better viability compared to control cyanobacteria (with a lower MAA content) [73]. Many different bacteria have shown this property in a range of environments [77].

3.4.3. Thermal Stress

In the above mentioned desiccation study, cyanobacterium survival was also measured under different temperatures. Pre-stressed cells had a higher survival rate than the controls between -20^{o}C and 40^{o}C but this difference was lost at 50^{o}C [73]. There are also other examples of thermal stress protection by an increase in MAA production in a range of species [77].

3.4.4. Photosynthesis Accessory Pigments

There are other reported properties of MAA but these are much less researched. There is evidence that porphyra-334 may act as a photosynthetic accessory pigment due its UVA absorption and subsequent production of small amounts of fluorescence in the Soret band of chlorophyll. This has been debated due to the relatively low amount of fluorescence that is produced in this way and that MAA are produced in environments of significant irradiance, suggesting photosynthetic wavelengths are in abundance [77, 89].

4. PHOTOPROTECTION OF THE SKIN

Despite the evidence that MAA are prime candidates for use as biocompatible photoprotective molecules for human use, there has been surprisingly little work carried out in skin models to demonstrate potential for human use. The reported effects in skin models are described below.

4.1. Cell Viability/Proliferation

Cell viability and toxicity are critical endpoints for MAA assessment. One study, done according to the International Organization for Standardization (ISO) 'extracted media' recommended short-term toxicity assay (ISO 10993-12), showed no toxicity of MAA including shinorine, porphyra-334 and mycosporine-glycine in murine fibroblasts. This was confirmed in a second longer-term direct incubation assay in the same cell line. After 14 and 21 days of incubation, with the different MAA, there was no significant toxicity and only minor effects on cell morphology for some of the MAA tested [90]. The same three MAA were shown to be non-toxic in human TIG-114 lung fibroblast cells at concentrations between 0-100μM at 48 hours, and actually increased cell proliferation [91]; an effect con-

firmed in by Kim *et al* studying cell viability [92]. Porphyra-334 has also shown have no effect on cell viability of human skin fibroblasts at concentrations up to 200μM [93]. In contrast with these findings, is work by Choi *et al* who found shinorine, porphyra-334 and mycosporine-glycine all significantly reduced cell viability in HaCaT keratinocytes, to differing extents, at concentrations from 0.1-mg/ml (around 0.301mM for shinorine) and above [94]. As mentioned MAA have demonstrated cell proliferation properties and have potential wound healing applications [94].

There are several studies that show that MAA prevent UVR induced toxicity. This protective effect has also been demonstrated in other MAA such as collemin A (a compound with a structure related to MAA), where UVB exposure of HaCat keratinocytes through a collemin A coated quartz plate produced an increase in cell viability, demonstrating a filtering effect [95]. Post 20J/cm^2 UVA exposure, application of poryhyra-334 at concentrations 10-40μM to skin fibroblasts also prevented reduction in cell viability and induction of senescence [93], confirmed with UVB irradiation with a greater effect with increasing MAA concentration [91]. Application of MAA post exposure contributing to increased cell viability compared to control suggests a significant effect outside of UVR filtering.

4.2. Oxidative Stress

Oxidative stress is a major consequence of UVR exposure [2, 3]. This results from photosensitization reactions, which can produce highly reactive molecules (such ROS). UVR-induced ROS may also be generated post-UVR exposure [96]. As previously mentioned, oxidative DNA damage can lead to mutations, and recently oxidative damage to proteins has shown to inhibit DNA repair, exacerbating the effect of UVR induced DNA damage [6].

Many studies using non-biological chemical assays have shown that MAA are antioxidants [78, 81, 97, 98]. A DPPH radical scavenging assay demonstrated that mycosporine-glycine had significant, dose dependent radical scavenging ability, but that porphyra-334 and shinorine had no effect. The authors concluded that this was because mycosporine-glycine has an oxocarbonyl structure whereas porphyra-334 and shinorine have an imino structure [99]. However, many other chemical and biological studies have reported that porphyra-334 and shinorine have antioxidant properties, and it is possible that MAA act in multiple ways.

Studies have also been carried out in biological models. Porphyra-334, the most widely studied MAA, has also demonstrated a dose dependent reduction in oxidative stress in skin fibroblasts, when added post exposure, again suggesting antioxidant capability [93]. These studies measured oxidative stress immediately post irradiation suggesting a ROS quenching role of MAA. The results from the biological and chemical assays are not always in agreement suggesting the further investigation is required to elucidate the mechanism of the anti-oxidant effects. Catalase and superoxide dismutase (SOD) showed reduced post-irradiation activity over time in unprotected mouse skin. However, the application of a reference sunscreen, or a porphyra-334 and shinorine formulation offered complete protection, along with a decrease in the expression of 70 kilodalton heat shock (stress) protein (Hsp70) [100]. For the most part, studies demonstrate that MAA efficiently prevent oxidative stress though filtering, direct and indirect quenching mechanisms, however the exact mechanism are yet to be elucidated.

4.3. NRF-2 Activation

Closely linked to prevention of environmental damage to the skin is the Kelch-like ECH-associated protein 1 (Keap1) and nuclear factor erythroid-2-related factor 2 (Nrf2) complex. Under conditions of stress (particularly oxidative stress), this complex dissociates to release Nrf-2 which subsequently binds to the antioxidant response element (ARE), leading to the transcription of over 200 cytoprotective genes linked to DNA repair, inflammation anti-oxidant response (among others). This is an area of emerging interest for photoprotection, using Nrf2 activators to boost the skin's natural responses to UVR damage [101, 102].

Recently, a bioinformatics based protein modelling and virtual screening approach has been applied to investigate potential compounds that interact with Keap1-Nrf2 complex. This approach identified 75 promising compounds that activated Nrf2, of which 25 were experimentally known to be potent activators. Eleven of these compounds were known to have antioxidant activities but had not been previously linked to Nrf2 activation, of which three were MAA: mycosporine-glycine, mycosporine-glycine-valine and porphyra-334 [103]. This *in silico* approach has been confirmed experimentally with porphyra-334, which demonstrated potent Nrf2 activation activity through the prevention of UVA induced markers of inflammation and cell death. Skin fibroblasts were incubated with increasing concentrations of porphyra-334 (0-40μM) after UVA irradiation. This resulted in a significant reduction of gene and protein expression of IL-6, IL-

1β, TNF-α and nuclear expression of NF-κB. In addition there was sustained Nrf2 activation, leading to the expression of a number of cytoprotective genes such as (HMOX-1), glutathione (GSH) and NAD(P)H dehydrogenase [quinone] 1 (NQO1) and the direct scavenging of reactive oxidative entities and their conversion to less harmful and inert products [104].

4.4. Accumulation in Human Skin Models

A key property of MAA is their accumulation in the food chain in marine species. This is a poorly researched area in non-marine species. In one study, investigators fed SKH-1 hairless mice a standard daily diet or the same diet with a freeze-dried red alga that contained a mixture of MAA that was known to accumulate in medaka fish. They found no MAA accumulation in the eyes, skin or liver after 14-130 days, apart from small amounts in the small intestine, suggesting no route for accumulation in mammals [60]. As part of the same study, the uptake of the MAA shinorine by human skin cancer A431 cells was also investigated. A dose dependent increase in shinorine (1-1.5mM) was observed after 48 hours of incubation, but saturation occurred at concentrations from 1.5-2.5mM. Raman confocal spectroscopy has shown that MAA incorporated into polymer gels applied to the skin *in vivo* penetrate and accumulate at depths of 2μm in the *Stratum corneum* at a concentration 103.4% higher than at the surface. These results suggest that MAA may accumulate in the skin, if not through the diet but further research is needed [105].

4.5. DNA Damage/Erythema

It is generally accepted that the most damaging consequence of UVR exposure to the skin is the formation of DNA photoproducts, which can subsequently lead to genomic mutations [106]. The CPD is the predominant and most important photoproduct induced by both UVA and UVB radiation, however oxidative photoproducts such as 8-oxo-7,8-dihydroguanine (8-oxoGua) are proving to be of increasing importance [107]. Closely related to the formation of DNA photoproducts, particularly the CPD, is the development of erythema in the skin, with DNA absorption and erythema sharing very similar action spectra [1].

In terms of photoprotection, the most widely used metric of the efficacy of sunscreen products is the is the SPF, which is a measure of their ability to prevent erythema (and presumed causal DNA damage). Despite this, the investigation of MAA to prevent DNA damage and/or erythema in human models is hugely under researched.

Collemin A significantly reduced UVB-induced CPD in HaCat human keratinocytes cells *in vitro* compared to an irradiated control [95]. In the same study, a crude formation of collemin A was made by mixing with olive oil and then applied to the skin (6μg/cm^2) of one volunteer. This formulation was estimated to have an SPF of at least 4. Little can be concluded from this pilot study other than it requires confirmation [95]. A more robust study in SKH-1 hairless mice, with a galenic formulation of 2% porphyra-334 and shinorine (ratio of 88:12) applied to the dorsal skin, prevented solar simulated UVR induced erythema, *stratum corneum* thickening, edema and sun burn cell formation (apoptosis) comparable with a reference sunscreen (the reference sunscreen is the standard used in sunscreen testing according to COLIPA guidelines). The calculated SPF was 3.71±0.78 [100]. One criticism of this study is the formulation was applied at a thickness of 4mg/cm^2, double the thickness at which sunscreens are tested suggesting that the real SPF would be at least half of this value, and used at a concentration significantly thicker than sunscreens are typically applied in real life situations [108].

Studies in a chemical model have shown that UVR-induced CPD can be inhibited by an MAA extract containing porphyra-334, shinorine and palythine. Thymine monomers were irradiated through the MAA extract with, no direct contact (in manner similar to a sunscreen application to the surface of the skin), and also irradiated with the extract and monomers mixed together. There was a greater protective effect in the mixed samples than those with no contact, suggesting an effect beyond the absorption properties of MAA. Further investigation established this was through quenching of the triplet state of UVR-excited thymine [70]. This shows that MAA may have even greater potential for photoprotection over current filters, especially with the recent discovery of delayed (also know as 'dark') CPD formation, which suggests that CPD can form for hours after exposure through a triplet photoexcitation mechanism [5].

4.6. Inflammation

The ability of MAA to inhibit biomarkers of skin inflammation is poorly studied. Over expression of these markers is linked to a range of inflammatory skin conditions such as psoriasis. Expression of cyclooxygenase-2 (COX-2) mRNA, widely associated with inflammation, was also prevented by topical application

of mycosporine-glycine to HaCat keratinocytes at the highest concentration tested (0.3mM) and with only at the lowest concentration of shinorine (0.03mM) having a statistically significant effect (questioning the validity of the result), and with porphyra-334 having no effect [99]. This used a broad-spectrum UVR source and the results could possibly be explained by the peak absorbance of each of the MAA, with mycosporine-glycine (λmax =310nm) and shinorine (λmax =334nm) absorbing in shorter wavelengths and porphyra-334 (λmax =344nm) absorbing at slightly longer wavelengths, suggesting COX-2 expression is linked to shorter wave UVR, however the lack of dose-response relationship is unclear.

4.7. Photoageing

Skin photoageing is a consequence of long-term solar UVR exposure. This is different from chronological skin ageing and is associated with deep wrinkles and sagging. It is generally accepted that photoageing is the consequence of UVR induced activation of a group of proteins known as the matrix metalloproteinases (MMPs), which degrade the structural extracellular matrix proteins of the dermis such as elastins and collagens [9].

The incubation of fibroblasts with porphyra-334 (0-40μM) after UVA exposure inhibited MMP-1 and MMP-8 gene expression, but had no effect on MMP-13. Elastase activity was dose dependently reduced by porphyra-334, with an increase in collagen and elastin mRNA and protein expression, and procollagen secretion [93]. Shinorine, porphyra-334, and palythine significantly inhibited MMP-2 activity in an *in vitro* fluorogenic assay, which was hypothesised to be due to competitive inhibition by binding to the active site determined using computer modelling [109].

In addition to their photoprotective properties, mycosporine-glycine, porphyra-334 and shinorine have been shown to be procollagen C proteinase enhancers (PCOLCE) and induced elastin mRNA upregulation in a largely dose dependent manner after UVA exposure, whereas only porphyra-334 showed an upregulation of involucrin, another skin protein [99].

Overall, relatively limited data suggest that MAA have multiple actions in the prevention of photoageing.

4.8. Potential Human Use of MAA

The evidence reviewed above demonstrates that MAA have huge photoprotection potential in traditional optical ways as well as in with new photomolecular strategies. Many studies have suggested the widespread use of MAA as sunscreens [110-113], however they have yet to been be exploited on a large scale, with only a few products currently available. One MAA product currently available called Helioguard 365, which contains MAA porphyra-334 and shinorine (11.5:1 ratio) extracted from the red alga P*orphyra umbilicalis* [114]. This product however mainly provides protection in UVA region with minimal protection in the more damaging UVB range, and the final concentration of MAA in the product is extremely small when compared to the concentration of UVR filters in most sunscreen products. One product contains a final MAA concentration of 0.0005%, whereas most sunscreen formulations contain filters at 0.5-10% w/v. This suggests the addition of a very low MAA concentration to a formulation will have a negligible influence on the SPF claims of the product.

There are numerous reasons for the lack of widespread use of MAA, one of which is the poor understanding of biosynthesis pathways involved to make specific MAA in an industrially economic manner. This makes the production process more complex, for example the need to farm vast amounts of seaweed. Further understanding of these pathways could lead to easier large-scale commercial biosynthesis, for example in a heterologous bacterial host *e.g. E. coli,* which is easier to cultivate. The chiral centres of MAA compounds make them highly difficult to synthesis chemically; again meaning large-scale synthesis is difficult, with unrealistic costs associated to production. One way that has been proposed to overcome this issue is via the synthesis of 'MAA-like' compounds, which are structurally similar and retain the chromophore of MAAs, but are simpler and cheaper to synthesize [115].

MAAs are highly water soluble, which makes it more difficult to formulate sunscreens intended for beach use. Water-soluble filters would however be much better for day-care products, because aqueous formulations have better sensorial properties than those based on oils. These properties improve compliance and therefore photoprotection. It is important to note MAA photostability would also have to be assessed in sunscreen formulations because photostability may vary with solvent.

Finally, the European Chemicals Agency (ECHA) has recently responded to environmental and human health concerns about some sunscreen filters by adding them to its Community Rolling Action Plan (CoRAP) list that includes 8/16 UVR filters that are commonly

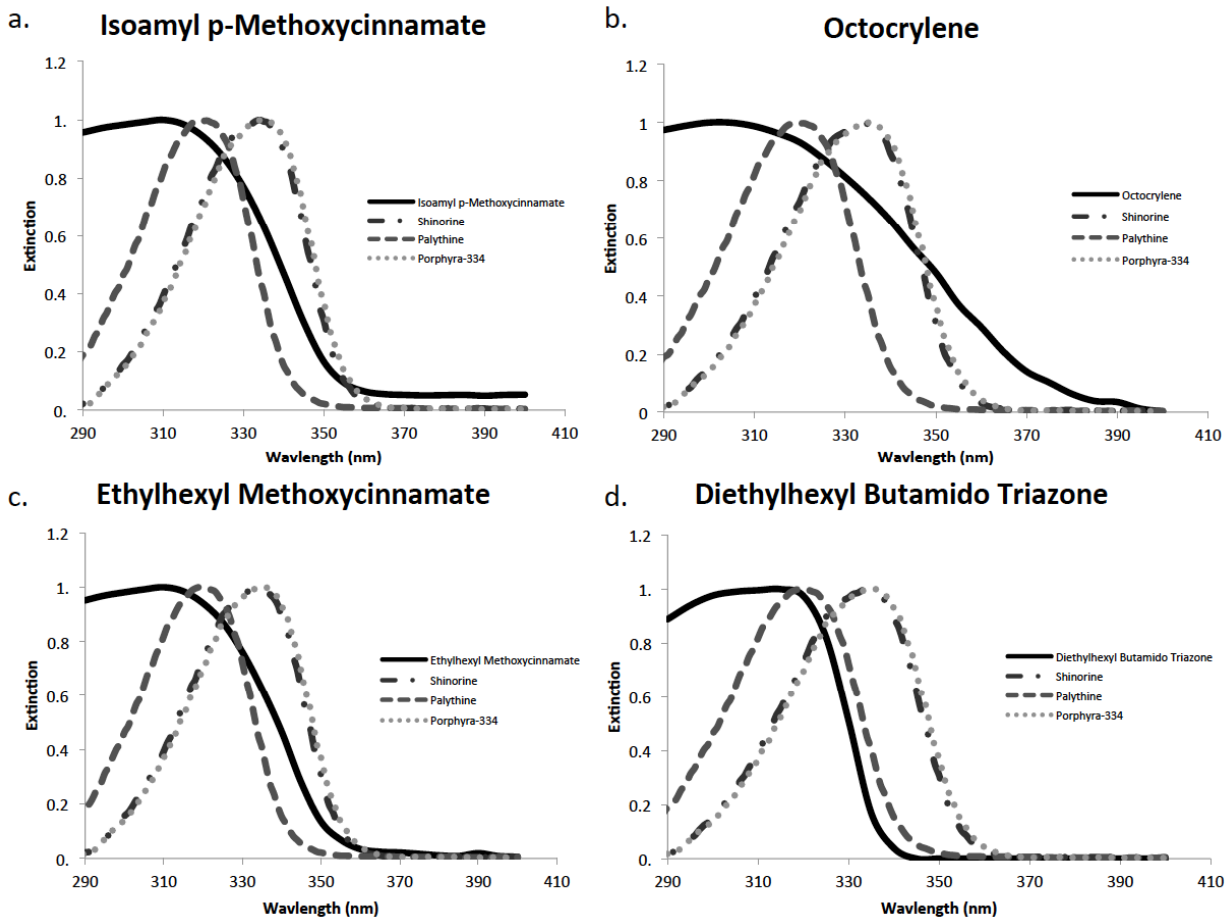

Fig. (6). The UVR absorbance spectra of CoRAP listed filters compared to MAAs. The relative UVR spectra of four CoRAP listers filters (a) isoamyl p-methoxycinnimate, (b) octocrylene, (c) ethylhexyl methoxycinnamate and (d) diethylhexyl butamido triazone were generated using the BASF sunscreen calculator [117] and compared to the spectra of the MAAs palythine, shinorine and porphyra-334.

used in European sunscreen formulations [116]. These concerns, especially for marine environments, support the development of spectrally equivalent MAA as alternative biocompatable sunscreens. Fig. (**6**) shows the similarity of the relative UVR absorbance spectra of 4 four CoRAP filters: (a) isoamyl p-methoxycinnimate, (b) octocrylene, (c) ethylhexyl methoxycinnamate and (d) diethylhexyl butamido triazone with those of palythine, shinorine and porphyra-334.

CONCLUSION

MAA are natural compounds that are thought to offer photoprotection to marine species. Initially thought of as protective based on their absorption properties in the solar UVR region, it is clear that they have additional activities, some of which may be also useful after exposure to UVR, such as anti-oxidant capacity and Nrf2 activation. This suggests that MAA offer a novel approach to photoprotection, which is usually focused on attenuation of UVR before it reaches cellular targets. Most MAA studies have been *in vitro* and concentrated on porphyra-334, shinorine and mycosporine-glycine, as these are some of the most abundant in nature, but systematic *in silico* and *in vitro* screening of all MAA may identify other compounds. Current *in vitro* data strongly suggest that MAA have potential for the protection of human skin from a diverse range of adverse effects of solar UVR.

CONSENT FOR PUBLICATION

Not applicable.

CONFLICT OF INTEREST

The authors declare the following interests: The results of our research into MAA compounds are subject of a patent application by King's College London, UK (PCT/GB2016/052227).

The sponsor or funding organization had no role in the design or conduct of this research.

ACKNOWLEDGEMENTS

Karl Lawrence is supported by a PhD studentship from BASF (BASF SE; Ludwigshafen, Germany). We also acknowledge the support of the National Institute for Health Research (NIHR) Clinical Research Facility at Guy's & St Thomas' NHS Foundation Trust and NIHR Biomedical Research Centre based at Guy's and St Thomas' NHS Foundation Trust and King's College London. The views expressed are those of the author(s) and not necessarily those of the NHS, the NIHR or the Department of Health. We thank Fatimah Hameer for her contribution to the photostability work. Open access for this article was funded by King's College London.

REFERENCES

[1] Young, A.R.; Chadwick, C.A.; Harrison, G.I.; Nikaido, O.; Ramsden, J.; Potten, C.S. The similarity of action spectra for thymine dimers in human epidermis and erythema suggests that DNA is the chromophore for erythema. *J. Invest. Dermatol.,* **1998**, *111*(6), 982-988.

[2] Bickers, D.R.; Athar, M. Oxidative stress in the pathogenesis of skin disease. *J. Invest. Dermatol.,* **2006**, *126*(12), 2565-2575.

[3] Wölfle, U.; Seelinger, G.; Bauer, G.; Meinke, M.C.; Lademann, J.; Schempp, C.M. Reactive molecule species and antioxidative mechanisms in normal skin and skin aging. *Skin Pharmacol. Physiol.,* **2014**, *27*(6), 316-332.

[4] Courdavault, S.; Baudouin, C.; Charveron, M.; Favier, A.; Cadet, J.; Douki, T. Larger yield of cyclobutane dimers than 8-oxo-7,8-dihydroguanine in the DNA of UVA-irradiated human skin cells. *Mutat. Res.,* **2004**, *556*(1-2), 135-142.

[5] Premi, S.; Wallisch, S.; Mano, C.M.; Weiner, A.B.; Bacchiocchi, A.; Wakamatsu, K.; Bechara, E.J.; Halaban, R.; Douki, T.; Brash, D.E. Photochemistry. Chemiexcitation of melanin derivatives induces DNA photoproducts long after UV exposure. *Science,* **2015**, *347*(6224), 842-847.

[6] McAdam, E.; Brem, R.; Karran, P. Oxidative stress-induced protein damage inhibits DNA repair and determines mutation risk and therapeutic efficacy. *Mol. Cancer Res.,* **2016**, *14*(7), 612-22.

[7] Armstrong, B.K.; Kricker, A. The epidemiology of UV induced skin cancer. *J. Photochem. Photobiol. B,* **2001**, *63*(1-3), 8-18.

[8] Fisher, G.J.; Datta, S.C.; Talwar, H.S.; Wang, Z.Q.; Varani, J.; Kang, S.; Voorhees, J.J. Molecular basis of sun-induced premature skin ageing and retinoid antagonism. *Nature,* **1996**, *379*(6563), 335-339.

[9] Quan, T.; Qin, Z.; Xia, W.; Shao, Y.; Voorhees, J.J.; Fisher, G.J. **2009**.

[10] Young, A.R.; Claveau, J.; Rossi, A.B. Ultraviolet radiation and the skin: Photobiology and sunscreen photoprotection. *J. Am. Acad. Dermatol.,* **2016**.

[11] Herzog, B. In Photochemistry: Volume 40. Royal Society of Chemistry, **2012**, 40, 245-273.

[12] Osterwalder, U.; Sohn, M.; Herzog, B. Global state of sunscreens. *Photodermatol. Photoimmunol. Photomed.,* **2014**, *30*(2-3), 62-80.

[13] Art, S.M. Servier. *Med. Art,* **2016**.

[14] Cole, C.; Shyr, T.; Ou-Yang, H. Metal Oxide Sunscreens Protect Skin by Absorption, Not by Reflection or Scattering. *Photodermatol. Photoimmunol. Photomed.,* **2015**.

[15] Green, A.C.; Williams, G.M. Point: sunscreen use is a safe and effective approach to skin cancer prevention. *Cancer Epidemiol. Biomarkers Prev.,* **2007**, *16*(10), 1921-1922.

[16] Iannacone, M.R.; Hughes, M.C.; Green, A.C. Effects of sunscreen on skin cancer and photoaging. *Photodermatol. Photoimmunol. Photomed.,* **2014**, *30*(2-3), 55-61.

[17] Sánchez, G.; Nova, J.; Rodriguez-Hernandez, A.E.; Medina, R.D.; Solorzano-Restrepo, C.; Gonzalez, J.; Olmos, M.; Godfrey, K.; Arevalo-Rodriguez, I. Sun protection for preventing basal cell and squamous cell skin cancers. *Cochrane Database Syst. Rev.,* **2016**, *7*, CD011161.

[18] Green, A.C.; Williams, G.M.; Logan, V.; Strutton, G.M. Reduced melanoma after regular sunscreen use: randomized trial follow-up. *J. Clin. Oncol.,* **2011**, *29*(3), 257-263.

[19] Ghiasvand, R.; Weiderpass, E.; Green, A.C.; Lund, E.; Veierød, M.B. Sunscreen Use and Subsequent Melanoma Risk: A Population-Based Cohort Study. *J. Clin. Oncol.,* **2016**, JCO675934.

[20] Kim, S.; Seock, Y-K. Impacts of health and environmental consciousness on young female consumers' attitude towards and purchase of natural beauty products. *Int. J. Consum. Stud.,* **2009**, *33*(6), 627-638.

[21] Gago-Ferrero, P.; Alonso, M.B.; Bertozzi, C.P.; Marigo, J.; Barbosa, L.; Cremer, M.; Secchi, E.R.; Domit, C.; Azevedo, A.; Lailson-Brito, J., Jr; Torres, J.P.; Malm, O.; Eljarrat, E.; Díaz-Cruz, M.S.; Barceló, D. First determination of UV filters in marine mammals. Octocrylene levels in Franciscana dolphins. *Environ. Sci. Technol.,* **2013**, *47*(11), 5619-5625.

[22] Gago-Ferrero, P.; Díaz-Cruz, M.S.; Barceló, D. An overview of UV-absorbing compounds (organic UV filters) in aquatic biota. *Anal. Bioanal. Chem.,* **2012**, *404*(9), 2597-2610.

[23] Kunz, P.Y.; Gries, T.; Fent, K. The ultraviolet filter 3-benzylidene camphor adversely affects reproduction in fathead minnow (Pimephales promelas). *Toxicol. Sci.,* **2006**, *93*(2), 311-321.

[24] Weisbrod, C.J.; Kunz, P.Y.; Zenker, A.K.; Fent, K. Effects of the UV filter benzophenone-2 on reproduction in fish. *Toxicol. Appl. Pharmacol.,* **2007**, *225*(3), 255-266.

[25] Sánchez-Quiles, D.; Tovar-Sánchez, A. Sunscreens as a source of hydrogen peroxide production in coastal waters. *Environ. Sci. Technol.,* **2014**, *48*(16), 9037-9042.

[26] Danovaro, R.; Bongiorni, L.; Corinaldesi, C.; Giovannelli, D.; Damiani, E.; Astolfi, P.; Greci, L.; Pusceddu, A. Sunscreens cause coral bleaching by promoting viral infections. *Environ. Health Perspect.,* **2008**, *116*(4), 441-447.

[27] E.E.A.P., Environmental effects of ozone depletion and its interactions with climate change: Progress report, 10 2016. *Photochem. Photobiol. Sci.,* **2017**.

[28] Tedetti, M.; Sempéré, R. Penetration of ultraviolet radiation in the marine environment. A review. *Photochem. Photobiol.,* **2006**, *82*(2), 389-397.

[29] Shick, J.M.; Dunlap, W.C. Mycosporine-like amino acids and related Gadusols: biosynthesis, acumulation, and UV-protective functions in aquatic organisms. *Annu. Rev. Physiol.,* **2002**, *64*, 223-262.

[30] Leach, C.M. Ultraviolet-absorbing substances associated with light-induced sporulation in fungi. *Can. J. Bot.,* **1965**, *43*(2), 185-200.

[31] Hartmann, A.; Holzinger, A.; Ganzera, M.; Karsten, U. Prasiolin, a new UV-sunscreen compound in the terrestrial green macroalga Prasiola calophylla (Carmichael ex Greville) Kutzing (Trebouxiophyceae, Chlorophyta). *Planta,* **2015**.

[32] Figueroa, F.L.; Korbee, N.; Abdala, R.; Jerez, C.G.; López-de la Torre, M.; Güenaga, L.; Larrubia, M.A.; Gómez-Pinchetti, J.L. Biofiltration of fishpond effluents and accumulation of N-compounds (phycobiliproteins and myco-

sporine-like amino acids) versus C-compounds (polysaccharides) in Hydropuntia cornea (Rhodophyta). *Mar. Pollut. Bull.,* **2012**, *64*(2), 310-318.

[33] Barufi, J.B.; Mata, M.T.; Oliveira, M.C.; Figueroa, F.L. Nitrate reduces the negative effect of UV radiation on photosynthesis and pigmentation in Gracilaria tenuistipitata (Rhodophyta): the photoprotection role of mycosporine-like amino acids. *Phycologia,* **2012**, *51*(6), 636-648.

[34] Barufi, J.B.; Korbee, N.; Oliveira, M.C.; Figueroa, F.L. Effects of N supply on the accumulation of photosynthetic pigments and photoprotectors in Gracilaria tenuistipitata (Rhodophyta) cultured under UV radiation. *J. Appl. Phycol.,* **2011**, *23*(3), 457-466.

[35] Korbee, N.; Huovinen, P.; Figueroa, F.L.; Aguilera, J.; Karsten, U. Availability of ammonium influences photosynthesis and the accumulation of mycosporine-like amino acids in two Porphyra species (Bangiales, Rhodophyta). *Mar. Biol.,* **2005**, *146*(4), 645-654.

[36] Peinado, N.K.; Diaz, R.T.; Figueroa, F.L.; Helbling, E.W. Ammonium and UV radiation stimulate the accumulation of mycosporine-like amino acids in Porphyra columbina (Rhodophyta) from Patagonia, Argentina. *J. Phycol.,* **2004**, *40*(2), 248-259.

[37] Huovinen, P.; Gomez, I.; Figueroa, F.L.; Ulloa, N.; Morales, V.; Lovengreen, C. Ultraviolet-absorbing mycosporine-like amino acids in red macroalgae from Chile. *Bot. Mar.,* **2004**, *47*(1), 21-29.

[38] Hoyer, K.; Karsten, U.; Wiencke, C. Induction of sunscreen compounds in Antarctic macroalgae by different radiation conditions. *Mar. Biol.,* **2002**, *141*(4), 619-627.

[39] Karsten, U.; Sawall, T.; Hanelt, D.; Bischof, K.; Figueroa, F.L.; Flores-Moya, A.; Wiencke, C. An inventory of UV-absorbing mycosporine-like amino acids in macroalgae from polar to warm-temperate regions. *Bot. Mar.,* **1998**, *41*(5), 443-453.

[40] Singh, S.P.; Kumari, S.; Rastogi, R.P.; Singh, K.L.; Sinha, R.P. Mycosporine-like amino acids (MAAs): chemical structure, biosynthesis and significance as UV-absorbing/screening compounds. *Indian J. Exp. Biol.,* **2008**, *46*(1), 7-17.

[41] Portwich, A.; Garcia-Pichel, F. Biosynthetic pathway of mycosporines (mycosporine-like amino acids) in the cyanobacterium Chlorogloeopsis sp. strain PCC 6912. *Phycologia,* **2003**, *42*(4), 384-392.

[42] Favre-Bonvin, J.; Bernillon, J.; Salin, N.; Arpin, N. Biosynthesis of mycosporines: Mycosporine glutaminol in Trichothecium roseum. *Phytochemistry,* **1987**, *26*(9), 2509-2514.

[43] Sinha, R.P.; Ambasht, N.K.; Sinha, J.P.; Häder, D-P. Wavelength-dependent induction of a mycosporine-like amino acid in a rice-field cyanobacterium, Nostoc commune: role of inhibitors and salt stress. *Photochem. Photobiol. Sci.,* **2003**, *2*(2), 171-176.

[44] Shick, J.M.; Romaine-Lioud, S.; Romaine-Lioud, S.; Ferrier-Pagès, C.; Gattuso, J.P. Ultraviolet-B radiation stimulates shikimate pathway-dependent accumulation of mycosporine-like amino acids in the coral Stylophora pistillata despite decreases in its population of symbiotic dinoflagellates. *Limnol. Oceanogr.,* **1999**, *44*(7), 1667-1682.

[45] Balskus, E.P.; Walsh, C.T. The genetic and molecular basis for sunscreen biosynthesis in cyanobacteria. *Science,* **2010**, *329*(5999), 1653-1656.

[46] Gao, Q.; Garcia-Pichel, F. An ATP-grasp ligase involved in the last biosynthetic step of the iminomycosporine shinorine in Nostoc punctiforme ATCC 29133. *J. Bacteriol.,* **2011**, *193*(21), 5923-5928.

[47] Singh, S.P.; Klisch, M.; Sinha, R.P.; Häder, D.P. Genome mining of mycosporine-like amino acid (MAA) synthesizing and non-synthesizing cyanobacteria: A bioinformatics study. *Genomics,* **2010**, *95*(2), 120-128.

[48] Rosic, N.N. Phylogenetic analysis of genes involved in mycosporine-like amino acid biosynthesis in symbiotic dinoflagellates. *Appl. Microbiol. Biotechnol.,* **2012**, *94*(1), 29-37.

[49] Zhang, L.; Li, L.; Wu, Q. Protective effects of mycosporine-like amino acids of Synechocystis sp. PCC 6803 and their partial characterization. *J. Photochem. Photobiol. B,* **2007**, *86*(3), 240-245.

[50] Spence, E.; Dunlap, W.C.; Shick, J.M.; Long, P.F. Redundant pathways of sunscreen biosynthesis in a cyanobacterium. *ChemBioChem,* **2012**, *13*(4), 531-533.

[51] Pope, M.A.; Spence, E.; Seralvo, V.; Gacesa, R.; Heidelberger, S.; Weston, A.J.; Dunlap, W.C.; Shick, J.M.; Long, P.F. O-Methyltransferase is shared between the pentose phosphate and shikimate pathways and is essential for mycosporine-like amino acid biosynthesis in Anabaena variabilis ATCC 29413. *ChemBioChem,* **2015**, *16*(2), 320-327.

[52] Asamizu, S.; Xie, P.; Brumsted, C.J.; Flatt, P.M.; Mahmud, T. Evolutionary divergence of sedoheptulose 7-phosphate cyclases leads to several distinct cyclic products. *J. Am. Chem. Soc.,* **2012**, *134*(29), 12219-12229.

[53] D'Agostino, P.M.; Javalkote, V.S.; Mazmouz, R.; Pickford, R.; Puranik, P.R.; Neilan, B.A. Comparative profiling and discovery of novel glycosylated mycosporine-like amino acids in two strains of the cyanobacterium Scytonema cf. crispum. *Appl. Environ. Microbiol.,* **2016**, *82*(19), 5951-5959.

[54] Katoch, M.; Mazmouz, R.; Chau, R.; Pearson, L.A.; Pickford, R.; Neilan, B.A. Heterologous production of cyanobacterial mycosporine-like amino acids mycosporine-ornithine and mycosporine-lysine in E. coli. *Appl. Environ. Microbiol.,* **2016**, *82*(20), 6167-6173.

[55] Conde, F.R.; Churio, M.S.; Previtali, C.M. Experimental study of the excited-state properties and photostability of the mycosporine-like amino acid palythine in aqueous solution. *Photochem. Photobiol. Sci.,* **2007**, *6*(6), 669-674.

[56] Conde, F.R.; Churio, M.S.; Previtali, C.M. The deactivation pathways of the excited-states of the mycosporine-like amino acids shinorine and porphyra-334 in aqueous solution. *Photochem. Photobiol. Sci.,* **2004**, *3*(10), 960-967.

[57] Conde, F.R.; Churio, M.S.; Previtali, C.M. The photoprotector mechanism of mycosporine-like amino acids. Excited-state properties and photostability of porphyra-334 in aqueous solution. *J. Photochem. Photobiol. B,* **2000**, *56*(2-3), 139-144.

[58] Whitehead, K.; Hedges, J.I. Photodegradation and photosensitization of mycosporine-like amino acids. *J. Photochem. Photobiol. B,* **2005**, *80*(2), 115-121.

[59] Chalker, B.E.; Dunlap, W.C.; Oliver, J.K. Bathymetric adaptations of reef-building corals at davies reef, great barrier reef, Australia. II. Light saturation curves for photosynthesis and respiration. *J. Exp. Mar. Biol. Ecol.,* **1983**, *73*(1), 37-56.

[60] Mason, D.S.; Schafer, F.; Shick, J.M.; Dunlap, W.C. Ultraviolet radiation-absorbing mycosporine-like amino acids (MAAs) are acquired from their diet by medaka fish (Oryzias latipes) but not by SKH-1 hairless mice. *Comp. Biochem. Physiol. A Mol. Integr. Physiol.,* **1998**, *120*(4), 587-598.

[61] Starcevic, A.; Akthar, S.; Dunlap, W.C.; Shick, J.M.; Hranueli, D.; Cullum, J.; Long, P.F. Enzymes of the shikimic acid pathway encoded in the genome of a basal metazoan, Nematostella vectensis, have microbial origins. *Proc. Natl. Acad. Sci. USA,* **2008**, *105*(7), 2533-2537.

[62] Starcevic, A.; Dunlap, W.C.; Cullum, J.; Shick, J.M.; Hranueli, D.; Long, P.F. Gene expression in the scleractin-

ian Acropora microphthalma exposed to high solar irradiance reveals elements of photoprotection and coral bleaching. *PLoS One,* **2010**, *5*(11), e13975.

[63] Tartarotti, B.; Laurion, I.; Sommaruga, R. Large variability in the concentration of mycosporine-like amino acids among zooplankton from lakes located across an altitude gradient. *Limnology and Oceanography,* 2001 Sep;*46*(6), 1546-1552.

[64] Dunlap, W.C.; Shick, J.M. Ultraviolet radiation-absorbing mycosporine-like amino acids in coral reef oragnisms: a biochemical and environmental perspective. *J. Phycol.,* **1998**, *34*(3), 418-430.

[65] Tartarotti, B.; Sommaruga, R. Seasonal and ontogenetic changes of mycosporine-like amino acids in planktonic organisms from an alpine lake. *Limnol. Oceanogr.,* **2006**, *51*(3), 1530-1541.

[66] Ha, S-Y.; Lee, Y.; Kim, M-S.; Kumar, K.S.; Shin, K-H. Seasonal Changes in Mycosporine-Like Amino Acid Production Rate with Respect to Natural Phytoplankton Species Composition. *Mar. Drugs,* **2015**, *13*(11), 6740-6758.

[67] Dunlap, W.C.; Chalker, B.E.; Oliver, J.K. Bathymetric adaptations of reef-building corals at Davies Reef, Great Barrier Reef, Australia. III. UV-B absorbing compounds. *J. Exp. Mar. Biol. Ecol.,* **1986**, *104*(1), 239-248.

[68] Peinado, N.K.; Abdala Díaz, R.T.; Figueroa, F.L.; Helbling, E.W. Ammonium and UV radiation stimulate the accumulation of mycosporine-like amino acids in porphyra Columbina (rhodophta) from Patagonia Argentina. *J. Phycol.,* **2004**, *40*(2), 248-259.

[69] Torregiani, J.H.; Lesser, M.P. The effects of short-term exposures to ultraviolet radiation in the Hawaiian Coral Montipora verrucosa. *J. Exp. Mar. Biol. Ecol.,* **2007**, *340*(2), 194-203.

[70] Misonou, T.; Saitoh, J.; Oshiba, S.; Tokitomo, Y.; Maegawa, M.; Inoue, Y.; Hori, H.; Sakurai, T. UV-absorbing substance in the red alga Porphyra yezoensis (Bangiales, Rhodophyta) block thymine photodimer production. *Mar. Biotechnol. (NY),* **2003**, *5*(2), 194-200.

[71] Adams, N.L.; Shick, J.M. Mycosporine-like amino acids prevent UVB-induced abnormalities during early development of the green sea urchin Strongylocentrotus droebachiensis. *Mar. Biol.,* **2001**, *138*(2), 267-280.

[72] Adams, N.L.; Shick, J.M. Mycosporine-like Amino Acids Provide Protection Against Ultraviolet Radiation in Eggs of the Green Sea Urchin Strongylocentrotus droebachiensis. *Photochem. Photobiol.,* **1996**, *64*(1), 149-158.

[73] Olsson-Francis, K.; Watson, J.S.; Cockell, C.S. Cyanobacteria isolated from the high-intertidal zone: a model for studying the physiological prerequisites for survival in low Earth orbit. *Int. J. Astrobiol.,* **2013**, *12*(4), 292-303.

[74] Feng, Y.N.; Zhang, Z.C.; Feng, J.L.; Qiu, B.S. Effects of UV-B radiation and periodic desiccation on the morphogenesis of the edible terrestrial cyanobacterium Nostoc flagelliforme. *Appl. Environ. Microbiol.,* **2012**, *78*(19), 7075-7081.

[75] Bhatia, S.; Garg, A.; Sharma, K.; Kumar, S.; Sharma, A.; Purohit, A.P. Mycosporine and mycosporine-like amino acids: A paramount tool against ultra violet irradiation. *Pharmacogn. Rev.,* **2011**, *5*(10), 138-146.

[76] Wright, D.J.; Smith, S.C.; Joardar, V.; Scherer, S.; Jervis, J.; Warren, A.; Helm, R.F.; Potts, M. UV irradiation and desiccation modulate the three-dimensional extracellular matrix of Nostoc commune (Cyanobacteria). *J. Biol. Chem.,* **2005**, *280*(48), 40271-40281.

[77] Oren, A.; Gunde-Cimerman, N. Mycosporines and mycosporine-like amino acids: UV protectants or multipurpose secondary metabolites? *FEMS Microbiol. Lett.,* **2007**, *269*(1), 1-10.

[78] Rastogi, R.P.; Incharoensakdi, A. Characterization of UV-screening compounds, mycosporine-like amino acids, and scytonemin in the cyanobacterium Lyngbya sp. CU2555. *FEMS Microbiol. Ecol.,* **2013**.

[79] Takamatsu, S.; Hodges, T.W.; Rajbhandari, I.; Gerwick, W.H.; Hamann, M.T.; Nagle, D.G. Marine natural products as novel antioxidant prototypes. *J. Nat. Prod.,* **2003**, *66*(5), 605-608.

[80] Matsui, K.; Nazifi, E.; Hirai, Y.; Wada, N.; Matsugo, S.; Sakamoto, T. The cyanobacterial UV-absorbing pigment scytonemin displays radical-scavenging activity. *J. Gen. Appl. Microbiol.,* **2012**, *58*(2), 137-144.

[81] Nazifi, E.; Wada, N.; Yamaba, M.; Asano, T.; Nishiuchi, T.; Matsugo, S.; Sakamoto, T. Glycosylated porphyra-334 and palythine-threonine from the terrestrial cyanobacterium Nostoc commune. *Mar. Drugs,* **2013**, *11*(9), 3124-3154.

[82] de la Coba, F.; Aguilera, J.; Figueroa, F.L.; de Galvez, M.V.; Herrera, E. Antioxidant activity of mycosporine-like amino acids isolated from three red macroalgae and one marine lichen. *J. Appl. Phycol.,* **2009**, *21*(2), 161-169.

[83] Wada, N.; Sakamoto, T.; Matsugo, S. Mycosporine-Like Amino Acids and Their Derivatives as Natural Antioxidants. *Antioxidants,* **2015**, *4*(3), 603-646.

[84] Oren, A. Mycosporine-like amino acids as osmotic solutes in a community of halophilic cyanobacteria. *Geomicrobiol. J.,* **1997**, *14*(3), 231-240.

[85] Portwich, A.; Garcia-Pichel, F. Ultraviolet and osmotic stresses induce and regulate the synthesis of mycosporines in the cyanobacterium chlorogloeopsis PCC 6912. *Arch. Microbiol.,* **1999**, *172*(4), 187-192.

[86] Kogej, T.; Gostinčar, C.; Volkmann, M.; Gorbushina, A.A.; Gunde-Cimerman, N. Mycosporines in Extremophilic Fungi—Novel Complementary Osmolytes? *Environ. Chem.,* **2006**, *3*(2), 105-110.

[87] Singh, S.P.; Klisch, M.; Sinha, R.P.; Häder, D.P. Effects of abiotic stressors on synthesis of the mycosporine-like amino acid shinorine in the Cyanobacterium Anabaena variabilis PCC 7937. *Photochem. Photobiol.,* **2008**, *84*(6), 1500-1505.

[88] Waditee-Sirisattha, R.; Kageyama, H.; Sopun, W.; Tanaka, Y.; Takabe, T. Identification and upregulation of biosynthetic genes required for accumulation of Mycosporine-2-glycine under salt stress conditions in the halotolerant cyanobacterium Aphanothece halophytica. *Appl. Environ. Microbiol.,* **2014**, *80*(5), 1763-1769.

[89] Sivalingam, P.M.; Ikawa, T.; Nisizawa, K. Physiological roles of a substance 334 in algae. *Bot. Mar.,* **1976**, *19*, 9-21.

[90] Fernandes, S.C.; Alonso-Varona, A.; Palomares, T.; Zubillaga, V.; Labidi, J.; Bulone, V. Exploiting Mycosporines as Natural Molecular Sunscreens for the Fabrication of UV-Absorbing Green Materials. *ACS Appl. Mater. Interfaces,* **2015**, *7*(30), 16558-16564.

[91] Oyamada, C.; Kaneniwa, M.; Ebitani, K.; Murata, M.; Ishihara, K. Mycosporine-like amino acids extracted from scallop (Patinopecten yessoensis) ovaries: UV protection and growth stimulation activities on human cells. *Mar. Biotechnol. (NY),* **2008**, *10*(2), 141-150.

[92] Kim, S.; You, D.H.; Han, T.; Choi, E.M. Modulation of viability and apoptosis of UVB-exposed human keratinocyte HaCaT cells by aqueous methanol extract of laver (Porphyra yezoensis). *J. Photochem. Photobiol. B,* **2014**, *141*, 301-307.

[93] Ryu, J.; Park, S.J.; Kim, I.H.; Choi, Y.H.; Nam, T.J. Protective effect of porphyra-334 on UVA-induced photoaging in human skin fibroblasts. *Int. J. Mol. Med.,* **2014**, *34*(3), 796-803.

[94] Choi, Y-H.; Yang, D.J.; Kulkarni, A.; Moh, S.H.; Kim, K.W. Mycosporine-Like Amino Acids Promote Wound Healing through Focal Adhesion Kinase (FAK) and Mito-

gen-Activated Protein Kinases (MAP Kinases) Signaling Pathway in Keratinocytes. *Mar. Drugs,* **2015**, *13*(12), 7055-7066.

[95] Torres, A.; Hochberg, M.; Pergament, I.; Smoum, R.; Niddam, V.; Dembitsky, V.M.; Temina, M.; Dor, I.; Lev, O.; Srebnik, M.; Enk, C.D. A new UV-B absorbing mycosporine with photo protective activity from the lichenized ascomycete Collema cristatum. *European Journal of Biochemistry / FEBS,* **2004**, *271*(4), 780-784.

[96] Valencia, A.; Kochevar, I.E. Nox1-based NADPH oxidase is the major source of UVA-induced reactive oxygen species in human keratinocytes. *J. Invest. Dermatol.,* **2008**, *128*(1), 214-222.

[97] Rastogi, R.P.; Madamwar, D.; Incharoensakdi, A. Sunscreening bioactive compounds mycosporine-like amino acids in naturally occurring cyanobacterial biofilms: role in photoprotection. *J. Appl. Microbiol.,* **2015**, *119*(3), 753-762.

[98] Andreguetti, D.; Stein, E.M.; Pereira, C.M.; Pinto, E.; Colepicolo, P. Antioxidant properties and UV absorbance pattern of mycosporine-like amino acids analogs synthesized in an environmentally friendly manner. *J. Biochem. Mol. Toxicol.,* **2013**, *27*(6), 305-312.

[99] Suh, S-S.; Hwang, J.; Park, M.; Seo, H.H.; Kim, H-S.; Lee, J.H.; Moh, S.H.; Lee, T-K. Anti-inflammation activities of mycosporine-like amino acids (MAAs) in response to UV radiation suggest potential anti-skin aging activity. *Mar. Drugs,* **2014**, *12*(10), 5174-5187.

[100] de la Coba, F.; Aguilera, J.; de Gálvez, M.V.; Alvarez, M.; Gallego, E.; Figueroa, F.L.; Herrera, E. Prevention of the ultraviolet effects on clinical and histopathological changes, as well as the heat shock protein-70 expression in mouse skin by topical application of algal UV-absorbing compounds. *J. Dermatol. Sci.,* **2009**, *55*(3), 161-169.

[101] Saw, C.L.; Huang, M.T.; Liu, Y.; Khor, T.O.; Conney, A.H.; Kong, A.N. Impact of Nrf2 on UVB-induced skin inflammation/photoprotection and photoprotective effect of sulforaphane. *Mol. Carcinog.,* **2011**, *50*(6), 479-486.

[102] Tao, S.; Justiniano, R.; Zhang, D.D.; Wondrak, G.T. The Nrf2-inducers tanshinone I and dihydrotanshinone protect human skin cells and reconstructed human skin against solar simulated UV. *Redox Biol.,* **2013**, *1*, 532-541.

[103] Gacesa, R.; Dunlap, W.C.; Long, P.F. Bioinformatics analyses provide insight into distant homology of the Keap1-Nrf2 pathway. *Free Radical Biology & Medicine,* **2015**, *88*(Pt B), 373-380.

[104] Ryu, J.; Kwon, M.J.; Nam, T.J. Nrf2 and NF-κB Signaling Pathways Contribute to Porphyra-334-Mediated Inhibition of UVA-Induced Inflammation in Skin Fibroblasts. *Mar. Drugs,* **2015**, *13*(8), 4721-4732.

[105] Tosato, M.G.; Orallo, D.E.; Churio, M.S.; Martin, A.A.; Soto, C.A.; Dicelio, L.E. Influence of mycosporine-like amino acids and gadusol on the rheology and Raman spectroscopy of polymer gels. *Biorheology,* **2014**, *51*(4-5), 315-328.

[106] Pfeifer, G.P.; Besaratinia, A. UV wavelength-dependent DNA damage and human non-melanoma and melanoma skin cancer. Photochemical & photobiological sciences : Official journal of the European Photochemistry Association and the European Society for Photobiology, **2012**, 11(1), 90-97.

[107] Huang, X.X.; Scolyer, R.A.; Abubakar, A.; Halliday, G.M. Human 8-oxoguanine-DNA glycosylase-1 is downregulated in human basal cell carcinoma. *Mol. Genet. Metab.,* **2012**, *106*(1), 127-130.

[108] Petersen, B.; Datta, P.; Philipsen, P.A.; Wulf, H.C. Sunscreen use and failures--on site observations on a sunholiday. *Photochem. Photobiol. Sci.,* **2013**, *12*(1), 190-196.

[109] Hartmann, A.; Gostner, J.; Fuchs, J.E.; Chaita, E.; Aligiannis, N.; Skaltsounis, L.; Ganzera, M. Inhibition of Collagenase by Mycosporine-like Amino Acids from Marine Sources. *Planta Med.,* **2015**, *81*(10), 813-820.

[110] Bandaranayake, W.M. Mycosporines: are they nature's sunscreens? *Nat. Prod. Rep.,* **1998**, *15*(2), 159-172.

[111] Cardozo, K.H.; Guaratini, T.; Barros, M.P.; Falcão, V.R.; Tonon, A.P.; Lopes, N.P.; Campos, S.; Torres, M.A.; Souza, A.O.; Colepicolo, P.; Pinto, E. Metabolites from algae with economical impact. *Comp. Biochem. Physiol. C Toxicol. Pharmacol.,* **2007**, *146*(1-2), 60-78.

[112] Torres, A.; Enk, C.D.; Hochberg, M.; Srebnik, M. Porphyra-334, a potential natural source for UVA protective sunscreens. *Photochem. Photobiol. Sci.,* **2006**, *5*(4), 432-435.

[113] Scheuer, P.J. Some marine ecological phenomena: chemical basis and biomedical potential. *Science,* **1990**, *248*(4952), 173-177.

[114] Schmid, D.; Schürch, C.; Zülli, F. *UV-A sunscreen from red algae for protection against premature skin aging*; Cosmetics and Toiletries Manufacture Worldwide, **2003**.

[115] Losantos, R.; Funes-Ardoiz, I.; Aguilera, J.; Herrera-Ceballos, E.; Garcia-Iriepa, C.; Campos, P.J.; Sampedro, D. *Rational Design and Synthesis of Efficient Sunscreens To Boost the Solar Protection Factor,* International ed.; Angewandte Chemie, **2017**. in English

[116] Agency, E.C. Community Rolling Action Plan (CoRAP) List. Available at: https://echa.europa.eu/information-on-chemicals/evaluation/community-rolling-action-plan/coraptable [Accessed date: 10th May 2017].

[117] BASF BASF Sunscreen Simulator. Available at: https://www.sunscreensimulator.basf.com/Sunscreen_Simulator/Login_show.action [Accessed date: 10th May 2017],

PMID: 28554325

(12) INTERNATIONAL APPLICATION PUBLISHED UNDER THE PATENT COOPERATION TREATY (PCT)

(19) World Intellectual Property Organization
International Bureau

(43) International Publication Date
26 January 2017 (26.01.2017)

WIPO | PCT

(10) International Publication Number
WO 2017/013441 A1

(51) International Patent Classification:
A61K 8/44 (2006.01) *A61Q 17/04* (2006.01)

(21) International Application Number:
PCT/GB2016/052227

(22) International Filing Date:
22 July 2016 (22.07.2016)

(25) Filing Language: English

(26) Publication Language: English

(30) Priority Data:
1512996.8 23 July 2015 (23.07.2015) GB

(71) Applicant: **KING'S COLLEGE LONDON** [GB/GB]; Strand, London WC2R 2LS (GB).

(72) Inventors: **LONG, Paul F.**; King's College London, Franklin-Wilkins Building, 150 Stamford Street, London SE1 9NH (GB). **YOUNG, Antony R.**; St John's Institute of Dermatology, 9th Floor, Tower Wing, Guy's Hospital, London SE1 9RT (GB). **LAWRENCE, Karl**; St John's Institute of Dermatology, 9th Floor, Tower Wing, Guy's Hospital, London SE1 9RT (GB).

(74) Agents: **SCRIPT IP LIMITED** et al.; Turnpike House, 18 Bridge Street, Frome, Somerset, BA11 1BB (GB).

(81) Designated States *(unless otherwise indicated, for every kind of national protection available)*: AE, AG, AL, AM, AO, AT, AU, AZ, BA, BB, BG, BH, BN, BR, BW, BY, BZ, CA, CH, CL, CN, CO, CR, CU, CZ, DE, DK, DM, DO, DZ, EC, EE, EG, ES, FI, GB, GD, GE, GH, GM, GT, HN, HR, HU, ID, IL, IN, IR, IS, JP, KE, KG, KN, KP, KR, KZ, LA, LC, LK, LR, LS, LU, LY, MA, MD, ME, MG, MK, MN, MW, MX, MY, MZ, NA, NG, NI, NO, NZ, OM, PA, PE, PG, PH, PL, PT, QA, RO, RS, RU, RW, SA, SC, SD, SE, SG, SK, SL, SM, ST, SV, SY, TH, TJ, TM, TN, TR, TT, TZ, UA, UG, US, UZ, VC, VN, ZA, ZM, ZW.

(84) Designated States *(unless otherwise indicated, for every kind of regional protection available)*: ARIPO (BW, GH, GM, KE, LR, LS, MW, MZ, NA, RW, SD, SL, ST, SZ, TZ, UG, ZM, ZW), Eurasian (AM, AZ, BY, KG, KZ, RU, TJ, TM), European (AL, AT, BE, BG, CH, CY, CZ, DE, DK, EE, ES, FI, FR, GB, GR, HR, HU, IE, IS, IT, LT, LU, LV, MC, MK, MT, NL, NO, PL, PT, RO, RS, SE, SI, SK, SM, TR), OAPI (BF, BJ, CF, CG, CI, CM, GA, GN, GQ, GW, KM, ML, MR, NE, SN, TD, TG).

Published:

— *with international search report (Art. 21(3))*

WO 2017/013441 A1

(54) **Title**: COMPOSITIONS AND METHODS USING PALYTHINE

(57) **Abstract**: The invention relates to a composition comprising palythine, or salts thereof, in an amount of 0.3% to 25% by weight, wherein palythine, or salts thereof, is the sole active ingredient. The invention also relates to said composition formulated for application to skin. The invention also relates to said composition formulated as a moisturiser. The invention also relates to a method of protecting a subject against skin damage, and/or against UVA damage, and/or against skin aging, and/or against UVB damage, and/or against reactive oxygen species generated by UVR, said method comprising applying said composition to the skin of said subject. The invention also relates to a cosmetic method of maintaining skin appearance of a subject, said method comprising applying said composition to the skin of said subject. The invention also relates to use of palythine, or salts thereof, as a sun filter.

(12) INTERNATIONAL APPLICATION PUBLISHED UNDER THE PATENT COOPERATION TREATY (PCT)

(19) World Intellectual Property Organization
International Bureau

(43) International Publication Date
23 November 2017 (23.11.2017)

WIPO | PCT

(10) International Publication Number
WO 2017/198806 A1

(51) International Patent Classification:
A61Q 17/04 (2006.01) *A61K 8/64* (2006.01)
A61K 8/06 (2006.01) *A61K 8/365* (2006.01)
A61K 8/49 (2006.01) *A61K 8/46* (2006.01)
A61K 8/42 (2006.01) *A61K 8/58* (2006.01)
A61K 8/81 (2006.01) *A61K 8/25* (2006.01)
A61K 8/44 (2006.01)

(21) International Application Number:
PCT/EP2017/062075

(22) International Filing Date:
19 May 2017 (19.05.2017)

(25) Filing Language: English

(26) Publication Language: English

(30) Priority Data:
16170307.9 19 May 2016 (19.05.2016) EP

(71) Applicant: **BASF SE** [DE/DE]; Carl-Bosch-Strasse 38, 67056 Ludwigshafen am Rhein (DE).

(72) Inventors: **FLOESSER-MUELLER, Heike**; De Borrekenslei 153, 2930Z BRASSCHAAT (BE). **ACKER, Stephanie**; 13, Rue De La Pierre Bleue, 68440 Dietwiller (FR). **DANOUX, Louis**; RUE DE BRETAGNE 12, 54420 SAULXURES LES NANCY (FR). **URCH, Henning**; Erich-Schug-Strasse 1, 67071 Ludwigshafen (DE). **GRUMELARD, Julie**; rue de Belfort 35, 68128 Village-Neuf (FR). **EHLIS, Thomas**; Harriet-Straub-Strasse 23, Freiburg Freiburg (DE). **HERZOG, Bernd**; Hornrain 21, 79639 Grenzach-Wyhlen (DE). **MENGE, Ullrich**; Erlenweg 6, 79639 Grenzach (DE). **YOUNG, Antony**; 209 New King's Road, London SW6 4XD (GB). **LAWRENCE, Karl**; 121 Fallowfield, Cambridge CB4 1PG (GB).

(74) Agent: **BASF IP ASSOCIATION**; BASF SE, G-FLP - C006, 67056 Ludwigshafen (DE).

(81) Designated States *(unless otherwise indicated, for every kind of national protection available)*: AE, AG, AL, AM, AO, AT, AU, AZ, BA, BB, BG, BH, BN, BR, BW, BY, BZ, CA, CH, CL, CN, CO, CR, CU, CZ, DE, DJ, DK, DM, DO, DZ, EC, EE, EG, ES, FI, GB, GD, GE, GH, GM, GT, HN,

(54) Title: MICRO-PARTICULATE ORGANIC UV ABSORBER COMPOSITION

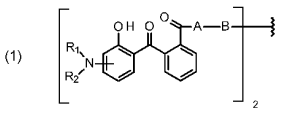

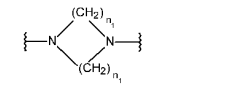

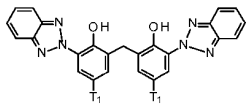

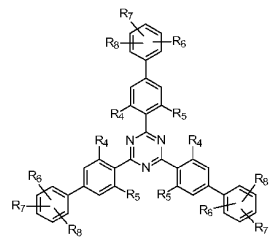

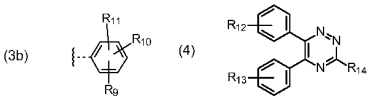

(57) Abstract: Disclosed are aqueous dispersions (A), comprising a micronized organic UV filter (a) selected from (a_1) the micronized compound of formula (1), wherein R_1 and R_2 independently from each other are C_1-C_{20}alkyl; C_2-C_{20}alkenyl; C_3-C_{10}cycloalkyl; C_3-C_{10}cycloalkenyl; or R_1 and R_2 together with the linking nitrogen atom form a 5- or 6-membered heterocyclic ring; A is— $N(R_3)$-; −O-; or the direct bond; B is a bivalent radical selected from alkylene, cycloalkylene alkenylene or phenylene radical which is optionally substituted by a carbonyl- or carboxy group; a radical of formula *— CH_2— C≡=C— CH_2—*; or the divalent radical *-B-* corresponds to the formula (1a), wherein n_1 is a number from 1 to 3; A is — $N(R_3)$-; or −O-; and R_3 is hydrogen; C_1-C_5alkyl; or hydroxy-C_1-C_5alkyl; (a_2) the micronized compound of formula (2), wherein T_1 is hydrogen; C_1-C_{12}alkyl; preferably iso-octyl, or C_1-C_4alkyl substituted by phenyl; (a_3) the micronized compound of formula (3a); wherein R_4 and R_5 independently from each other are hydrogen; C_1-C_{18}alkyl; or C_6-C_{12}acryl; R_6, R_7 and R_8 independently from each other, are hydrogen; C_1-C_{18}alkyl; or a radical of formula (3b); wherein R_9, R_{10} and R_{11} independently from each other, are hydrogen; or C_1-C_{18}alkyl; (a_4) the micronized compound of formula (4); wherein R_{12} and R_{13}, independently from each other, represent hydrogen; halogen; C_1-C_{12}alkyl: C_1-C_{18}hydroxy; C_1-C_{18}alkoxy; poly(ethoxy)-alkoxy with a C_1-C_4 alkyl fragment and an ethoxy number ranging from 1 to 4; C_1-C_4mono- or dialkyl amino, R_{14} represents halogen; hydroxy; amino; phenyl which is optionally substituted 1 to 3 times by a hydroxy radical situated at least in a para or phenyl position, possibly 1 to 3 times substituted in an ortho, meta or para position by a C_1-C_{12}alkoxy or cyano or C_1-C_7alkyl-amino group; and (b) a vinylpyrrolidone copolymer or homopolymer.

[Continued on next page]

WO 2017/198806 A1

HR, HU, ID, IL, IN, IR, IS, JP, KE, KG, KH, KN, KP, KR, KW, KZ, LA, LC, LK, LR, LS, LU, LY, MA, MD, ME, MG, MK, MN, MW, MX, MY, MZ, NA, NG, NI, NO, NZ, OM, PA, PE, PG, PH, PL, PT, QA, RO, RS, RU, RW, SA, SC, SD, SE, SG, SK, SL, SM, ST, SV, SY, TH, TJ, TM, TN, TR, TT, TZ, UA, UG, US, UZ, VC, VN, ZA, ZM, ZW.

(84) Designated States *(unless otherwise indicated, for every kind of regional protection available)*: ARIPO (BW, GH, GM, KE, LR, LS, MW, MZ, NA, RW, SD, SL, ST, SZ, TZ, UG, ZM, ZW), Eurasian (AM, AZ, BY, KG, KZ, RU, TJ, TM), European (AL, AT, BE, BG, CH, CY, CZ, DE, DK, EE, ES, FI, FR, GB, GR, HR, HU, IE, IS, IT, LT, LU, LV, MC, MK, MT, NL, NO, PL, PT, RO, RS, SE, SI, SK, SM, TR), OAPI (BF, BJ, CF, CG, CI, CM, GA, GN, GQ, GW, KM, ML, MR, NE, SN, TD, TG).

Published:

— *with international search report (Art. 21(3))*